The role of axonal transport disruption in the development of axonal mechanical sensitivity in intact C-fibre neurons

George Goodwin

A thesis submitted in full fulfilment of the requirements of the University of Brighton and University of Sussex for the degree of Doctorate of Philosophy

2018

Abstract

People suffering from chronic widespread pain, which include those diagnosed with non-specific arm pain, whiplash associated disorder, fibromyalgia and complex regional pain syndrome type 1, often complain of neuropathic pain like symptoms in the absence of obvious nerve injury upon routine clinical examination. Many of these patients shown signs of nerve trunk mechanical sensitivity (Tinel's sign), which can also be detected following a positive response to a neurodynamic test that stretches the peripheral nerve (i.e. movement-evoked pain). Although it is not clear what causes nerve trunk mechanical sensitivity in patients, it is hypothesised that localised nerve inflammation (neuritis) might contribute towards its development. Consistent with this hypothesis, modelling neuritis in the rat causes the development of axonal mechanical sensitivity (AMS) in nociceptive neurons. Previously, our laboratory has inferred a role for inflammatory-induced axonal transport disruption in the development of AMS. Axonal transport disruption is hypothesised to cause an accumulation of anterogradely transported mechanically sensitive ion channels, which are locally inserted into the axonal membrane thereby causing mechanical sensitivity. To examine the contribution of axonal transport to the development of AMS in the absence of inflammation, low doses of vinblastine (0.1mM) can be applied to the rat sciatic nerve. The main aim of this study was to investigate the role of axonal transport disruption in the development of AMS. Specific aims included: investigation of the time course of the development of AMS following vinblastine-induced axonal transport disruption, examination of the properties of mechanically sensitive axons and identification of the mechanically sensitive ion channels hypothesised to be responsible for AMS.

Following vinblastine-treatment, AMS developed rapidly in C-fibre neurons, reached a peak between days 4-5 and had resolved by days 14-15. These changes occurred in the absence of an increase in the development of ongoing activity. Following vinblastine treatment and neuritis, mechanically sensitive hotspots had relatively low firing thresholds and produced graded responses to changes in force. Mechanically sensitive ion channel blockers ruthenium red and FM1-43 attenuated AMS following vinblastine treatment and neuritis, indicating that mechanically sensitive ion

channels contribute towards AMS. The anterograde transport of the transient receptor potential channels vaniloid 1 and ankyrin 1 (TPRV1 and TRPA1 respectively) and acid sensing ion channel 3 (ASIC3) were disrupted following vinblastine-treatment and neuritis. Additionally, intraneural injection of OLDA and cinnamaldehyde (TRPV1 and TRPA1 agonists respectively) onto mechanically sensitive hotspots initiated responses in a proportion of neurons with AMS following neuritis. These results indicate an increased presence of functional TRPV1 and TRPA1 ion channels in neurons with AMS following neuritis, which suggests that they are involved in the development of mechanical sensitivity. However, a proportion of neurons that did not have AMS, but were ongoing, responded to cinnamaldehyde following neuritis, suggesting that TRPA1 may also be increased in these neurons and might contribute towards ongoing activity. In contrast, intraneural injections of the same agonists did not cause a response in the majority of neurons with AMS following vinblastine treatment, indicating that there is not an increased presence of functional TRPV1 and TRPA1 in these neurons. This finding suggests that TRPV1 and TRPA1 are not involved in the development of AMS following vinblastine treatment and that other ion channels play a role. In summary, data from this study supports the role of axonal transport disruption in the development of AMS and strongly infers that mechanically sensitive ion channels contribute towards AMS. Whereas the ion channels responsible for AMS following vinblastine treatment were not characterised, this study has revealed that TRPV1 and TRPA1 might contribute towards AMS following neuritis.

Table of contents

List of Tables

List of Figures

Abbreviations

AMS	axonal mechanical sensitivity
ANOVA	analysis of variance
ASIC	acid sensing ion channel
BDNF	brain-derived neurotrophic factor
BSA	bovine serum albumin
CCI	chronic constriction injury
CCL	chemokine (C-C motif) ligand
CIPN	chemotherapy induced peripheral neuropathy
CFA	complete Freund's adjuvant
CGRP	calcitonin gene related peptide
CNS	central nervous system
CRPS	complex regional pain syndrome
DNA	deoxyribonucleic acid
DRG	dorsal root ganglion
ERK	extracellular signal related kinase
HCN	hyperpolarisation-activated cyclic nucleotide-gated
HIV	human immunodeficiency virus
IASP	International Association for the Study of Pain
IB4	isolectin B 4
IL	Interleukin
IQR	interquartile range
K2P	two pore potassium channels
MAPK	mitogen activated protein kinase
MRI	magnetic resonance imaging
mRNA	messenger ribonucleic acid
NGF	nerve growth factor
NSAP	non-specific arm pain

OLDA	N-Oleoyldopamine
PBS	phosphate buffered saline
PIEZO	piezoelectric
PG	prostaglandin
PKC	protein kinase c
PSL	partial sciatic ligation
RNA	ribonucleic acid
SEM	standard error of the mean
SIF	synthetic interstitial fluid
SNI	spared nerve injury
SNL	spinal nerve ligation
TNF	tumour necrosis factor
TRP	transient receptor potential
WAD	whiplash associated disorder

Acknowledgements

I would like to express my utmost gratitude to Dr Andrew Dilley for his expert knowledge, supervision and support throughout the duration of this project. I would also like to express appreciation to Dr Manuela Mengozzi for her supervision and guidance. Thank you to my lab partner Ieva Satkevičiūtė for her help and friendship. I am also very grateful to Dr Chris Jones (BSMS Statistician) for his useful statistical advice and support.

I am forever grateful to my parents, who have supported and believed in me all the way throughout my academic studies. In addition, I am thankful to my brother and sisters for keeping me calm when times were tough.

A special mention to Rich Goodyear, Ben Alberts, Sonia Ingram and all the other colleagues who worked in the medical research building, for their friendship and guidance.

Finally, I would like to thank Marina for her consistent support and motivation, and putting up with me during the latter stages of completing this thesis.

Declaration

I declare that the research contained in this thesis, unless otherwise formally indicated within the text, is the original work of the author. The thesis has not been previously submitted to this or any other university for a degree, and does not incorporate any material already submitted for a degree.

Signed:……

Date:……

Chapter 1

Introduction

1.1 Chronic pain

Pain is an unpleasant sensory or emotional experience usually associated with physical triggers, which involve actual or potential tissue damage (IASP, 1986). A stimulus that is potentially harmful to our tissues (e.g. extreme temperatures, strong pressure) is known as noxious and causes the activation of nociceptors located on specialised fibres of the somatosensory nervous system (see **1.2**). This provides an early warning signal to prevent us from damaging our tissues. In the event of tissue injury, numerous inflammatory mediators can be released from the damaged area, which can result in inflammatory pain. Some of the mediators may activate nociceptors directly, others may sensitise sensory afferents, which in turn lowers the threshold for activation of pain pathways. This provides a degree of protection (reduces contact) to the damaged area whilst the wound takes time to repair (Scholz and Woolf, 2002). In some instances pain is thought to be triggered in a non-physical way. This is known as psychogenic pain, which is defined as pain that is caused or enhanced by psychological factors.

Pain that persists for a duration of 3 months or more, which can be continuous or interrupted by pain free intervals, is termed chronic (IASP, 1986). Chronic pain is an ongoing problem and it is estimated that about one in five adult Europeans are suffering from some form chronic pain of moderate to severe intensity (Breivik et al., 2006). It severely impairs quality of life and has a great socio-economic impact on the western world (Breivik et al., 2006; Dagenais et al., 2008; Juniper et al., 2009). Moreover, chronic pain conditions have been associated with psychological comorbidities (e.g. depression and sleep deprivation) (Breivik et al., 2006; Elliott et al., 2003). Chronic pain can be caused by nociceptive (e.g. osteoarthritis), inflammatory (e.g. rheumatoid arthritis) or neuropathic (see **1.1.1**) mechanisms.

1.1.1 Neuropathic pain

Pain is defined as neuropathic when it is caused by a lesion or disease of the somatosensory nervous system (IASP, 1986). In the western world it is estimated that between 7-10 percent of the general population are suffering from neuropathic pain (van Hecke et al., 2013).

Signs and Symptoms

Patients suffering from neuropathic pain often suffer from spontaneous pain (stimulus independent) and describe shooting, stabbing, burning, aching sensations. Patients may also suffer from evoked pain (stimulus dependent) such as radiating pain on limb movements, allodynia and hyperalgesia (see **Table 1.1** for a list of clinical definitions) (Backonja and Stacey, 2004; Bennett, 2001; Birklein et al., 2000).

Nerve trunk mechanical sensitivity is a prominent feature of neuropathic pain conditions such as whiplash associated disorder (WAD), carpal tunnel syndrome and non-specific arm pain (NSAP). In patients with such disorders, Tinel's sign or applying moderate pressure to nerve trunks in the periphery can cause pain, which is thought to be an indicator of nerve trunk mechanical sensitivity (Greening et al., 2005; Ide et al., 2001; Sterling et al., 2002). Tinel's sign or the Hoffman-Tinel sign, which was first described separately by Jules Tinel and Paul Hoffman in 1915 (Hoffmann et al., 1993), is the tingling sensation produced upon tapping over a nerve trunk. Nerve trunk mechanical sensitivity can also be detected following a positive response to neurodynamic tests that stretch peripheral nerves (i.e. movement evoked pain). Examples of neurodynamic tests include the upper limb abduction tests or straight leg raise.

The upper limb tension test

The upper limb tension test, also known as the brachial plexus tension test or 'Elvey test', was first described by Elvey in 1979. The test involves arm movements that cause increased stretch of the nerves innervating the upper limb. If there is damage to the nerves that are being stretched, there is an exacerbation of painful symptoms in the upper arm, back and neck (Elvey and Idczak, 1979; Quintner, 1989).

The straight leg raise

The straight leg raise test or 'Lasègue's sign' was recognised by Charles Lasègue in 1864, but not documented until 1880 by Lazerevi. The test, which involves lifting of the extended leg of a patient whilst in the supine position, causes stretching of the sciatic nerve; a positive result for the test is pain in the lower back (Lazarevic, 1880). The resultant pain is an indication that there is damage to the lumbar nerve roots.

Movement-evoked radiating pain is likely to be extremely uncomfortable to an individual and may limit the range of limb movements that are required to complete day-to-day tasks. Hence, it is important to understand the underlying mechanisms that lead to its development.

Clinical Term	Definition
Allodynia	Painful response to a stimulus that would normally be regarded as innocuous
Hyperalgesia	An Increased response to a painful stimulus
Hypoalgesia	A diminished response to a painful stimulus
Paraesthesia	An unusual sensation (e.g. pins and needles) which can be evoked or happens spontaneously
Hyperesthesia	Increased sensitivity to stimulation (tactile or thermal; both rare)
Hypoesthesia	Decreased sensitivity to stimulation (tactile/thermal; both frequent)
Dysesthesia	An unpleasant sensation that can be spontaneous or evoked.

Table 1.1 A list of clinical features that are common in patients with neuropathic pain. From IASP diagnosis and classification of chronic pain 2010

Causes

Neuropathic pain can arise in a number of different ways. A summary of the causes is provided in **Table 1.2.** Patients with frank nerve injury (nerve trauma) either have severed, crushed or stretched nerves, in which the cause of pain is normally a direct result of injury to the nerve fibres. However, pain can also develop in patients who do not always have an obvious nerve lesion. In these patients the reasons behind the development of neuropathic pain symptoms is not always clear. Inflammation of nerve fibres plays a major role in the underlying mechanisms of neuropathic pain, especially in those patients diagnosed with neuropathies such a Guillain-Barré syndrome (Press et al., 2001; Pritchard and Hughes, 2004), human immunodeficiency virus (HIV) neuropathy (Jones et al., 2005a; Nagano et al., 1996) and herpes zoster infection (Choi et al., 2009; Watson et al., 1991). Further to this, inflammation may also play a role in the development of neuropathic pain symptoms in patients with chronic widespread pain, who lack evidence of a frank nerve injury on routine clinical examination. Examples of these conditions are detailed below.

Cause of neuropathic pain	Examples
Traumatic	phantom limb pain, post-traumatic neuralgia, post-surgical neuroma, spinal cord injury
Metabolic	diabetic neuropathy, alcoholic neuropathy
Chemical	chemotherapy induced peripheral neuropathy, anti-retroviral induced neuropathy
Immune-mediated	complex regional pain syndrome type 1, non-specific arm pain, Guillain-Barré syndrome, multiple sclerosis
Cancer	osteosarcoma, carcinoma-associated paraneoplastic peripheral neuropathy
Hereditary	amyloid neuropathy, Charcot-Marie-tooth disease
Infectious	post-herpetic neuralgia, HIV induced pain

Table 1.2 A list of common causes of neuropathic pain conditions.
Adapted from (Baron et al., 2010)

Neuropathic pain without frank nerve injury

Non-specific arm pain

Non-specific arm pain (NSAP) (more commonly known as repetitive strain injury or cumulative trauma disorder) is caused by high repetition activities (e.g. typing on a keyboard, production line work) and it is the most common work-related injury (Fogleman and Brogmus, 1995; Silverstein et al., 1998). Sensory symptoms include diffuse pain, which can be present in the wrist, arm and neck, movement-evoked radiating pain, hyperalgesia and allodynia (Greening et al., 2005; Moloney et al., 2010). The mechanisms that cause NSAP are unknown; however ischaemia and inflammation are thought to play important roles in the development of the sensory symptoms. Evidence from magnetic resonance imaging (MRI) studies indicate possible inflammation in the nerves of patients with NSAP (Dilley et al., 2011). Moreover, patients with upper-extremity overuse disorders have been shown to have a raised systemic concentration of pro- inflammatory cytokines (e.g. tumour necrosis factor [TNF] and interleukin-1β [IL-1β]) (Carp et al., 2007).

Complex regional pain syndrome type 1

Most patients suffering from complex regional pain syndrome type 1 (CRPS-1), also known as reflex sympathetic dystrophy, have had a previous history of peripheral trauma (e.g. sprains, fractures or contusions) or nerve compression in the distal part of an extremity. Patients often describe a 'tearing' or 'burning' pain that is normally located deep in the distal part of the affected limb. Stimulus-evoked pain (hyperalgesia and allodynia) and autonomic abnormalities that can include changes to the skin temperature, sweating and oedema, are also common (Birklein et al., 2000). The mechanisms that cause the development of painful sensory symptoms are strongly linked with inflammation. Higher levels of pro inflammatory cytokines, such as IL-6, IL-1 beta and TNF, as well as neuropeptides such as substance P, have been found in affected patients (Huygen et al., 2002; Schinkel et al., 2006). Inflammation is thought to play a key role in the transition of CRPS-1 from an acute to chronic phase (Birklein et al., 2001; Maihofner et al., 2005).

Whiplash associated disorder

Whiplash associated disorder (WAD) is a condition which is associated with individuals who have been involved in motor vehicle collision. Approximately 50% of people will still experience painful symptoms one year following initiation of the injury (Gargan and Bannister, 1994). Symptoms of whiplash injury can include pain in the cervical spine, head, and upper limb. Tinel's sign may be present in the neck, elbow or arm and abduction of the arm can cause radiating pain in the neck (Ide et al., 2001). Some patients also experience pressure hypersensitivity of the neck muscles and over nerve trunks in the periphery (Gerdle et al., 2008; Sterling et al., 2002). The mechanisms that cause the development of painful symptoms are not fully understood. It is thought that a sudden acceleration/deceleration of the head in relation the neck causes nerve compression/traction. Additionally, soft tissue damage may also be present in the neck/shoulder region, which causes inflammation. In patients, there is evidence to suggest that the nerves in the shoulder and arm are inflamed (Greening et al., 2017). Moreover, systemic levels of the inflammatory cytokine IL-6 is increased in the acute phase of the injury (Kivioja et al., 2001).

Chemotherapy induced peripheral neuropathy

As part of this study, we have used the vinca-alkaloid drug vinblastine that is used to treat many different types of cancer (Garewal et al., 1983; Jelliffe, 1969; Stoter et al., 1984). However, the use of vinca-alkaloid drugs over a prolonged period is associated with sensory symptoms that indicate the development of a peripheral neuropathy (DeAngelis et al., 1991; Holland et al., 1973).

Chemotherapy induced peripheral neuropathy (CIPN) is the most common cause of dose limiting toxicity in cancer patients undergoing treatment (Windebank and Grisold, 2008). Drugs that can cause CIPN include the mitotic spindle inhibitors, platinum and DNA alkylating compounds. Examples of the mitotic spindle inhibitors include taxane or vinca-alkaloid compounds. These drugs are used to treat a range of different malignancies including breast, ovarian, prostate and lung carcinomas (Windebank and Grisold, 2008). Symptoms tend to develop weeks to months after

treatment has begun and the severity is largely dependent on the drug dose. Sensory symptoms, which are usually more prominent in the periphery, include paraesthesia, numbness, radiating pain, mechanical and cold allodynia (Dougherty et al., 2004; Forsyth et al., 1997; Holland et al., 1973). There are likely to be numerous mechanisms that cause the development of sensory symptoms in patients (See Windebank and Grisold, 2008 for review). As many of these drugs interfere with microtubules, which are important for normal axonal transport (see **1.2.3**), it seems that axonal transport disruption might contribute towards the development of sensory symptoms.

Treatment of neuropathic pain

Treating neuropathic pain has become a real challenge for clinicians. There are a limited number of treatments that can effectively control/ease painful symptoms in patients suffering from neuropathic pain (Finnerup et al., 2005; Finnerup et al., 2010; Kingery, 1997). Treatments that are currently available include the anti-convulsants (e.g. Pregabalin), anti-depressants (e.g. Amitriptyline) and opioids (e.g. Tramadol) (**Table 1.3**). These treatments are only effective in certain sub groups of patients and often have unwanted adverse effects, which can limit their use (Finnerup et al., 2005; Finnerup et al., 2010). Many of these drug treatments (e.g. morphine) only provide symptomatic pain relief, hence there is a requirement for drugs that treat the underlying mechanisms which cause pain in these patients.

Drug class	Examples	Mechanism of action	Problems associated with drug class
Anti-convulsants	Carbamazepine	Sodium channel blocker	Dizziness, drowsiness, nausea, blurred vision, fatigue, weight gain
	Pregabalin /Gabapentin	Binds to the auxiliary subunit of presynaptic voltage gated calcium channels	
Anti-depressants	TCA's (e.g. amitriptyline)	Monoamine uptake inhibitor	Nausea, weight gain, fatigue, drowsiness, GI disturbances
	SSRI's (e.g. duloxetine)	Serotonin selective reuptake inhibitor	
	SNRI's	Serotonin noradrenaline reuptake inhibitor	
Opioids	Morphine	μ-opioid receptor agonist	Constipation, drowsiness, dizziness. Patients become desensitised after long-term use/potential for addiction.
	Tramadol	μ-opioid receptor agonist	

Table 1.3 Summary of the major drug classes used to treat neuropathic pain.
SSRI's - Serotonin selective reuptake inhibitors, SNRI's – Serotonin noradrenaline reuptake inhibitors, TCA's - Tri-cyclic anti-depressants

1.2 Introduction to the somatosensory nervous system

To understand how neuropathic pain conditions can develop, it is essential to understand the normal physiology of the somatosensory nervous system.

The somatosensory nervous system, which forms part of the peripheral nervous system (motor, sensory and sympathetic neurons), allows us to sense changes in the surrounding environment (touch, pressure, vibration, movement, temperature and pain). Primary sensory neurons, which are pseudounipolar, are responsible for transmitting electrical impulses that encode sensory information to the central nervous system. One part of the axon terminates in the dorsal horn of the spinal cord or the brainstem, whilst the other typically extends all the way to the periphery (e.g. muscle, joints, and skin). However, there are a group of axons that innervate the nerve itself, which are known as the nervi nervorum (See Bove and Light, 1997 for review). The presence of sodium and potassium channels along axons allows electrical impulses to be conveyed in the form of action potentials. The cell body of the axon, which is located in the dorsal root ganglion, contains the nucleus and the machinery used to synthesise and process ion channels and other proteins.

Although glial cells (Schwann cells and satellite glial cells), immune cells (mast cells) and fibroblasts are important in maintaining the normal physiology of the somatosensory nervous system, this section will focus on the physiology of neuronal cells.

1.2.1 Sensory nerve fibre classification

Axons of primary sensory neurons can be classified into A- and C-fibre types. A-fibre neurons are subdivided based upon conduction velocity into Aα-, Aβ- and Aδ-fibre neurons. The thickly myelinated Aα/β-fibre neurons are large in diameter (1.5-12.5 μM) and have rapid conduction velocities (>14m/s) (Harper and Lawson, 1985; Vejsada et al., 1985). Aδ-fibre neurons are thinly myelinated, have a medium diameter (2-5 μM) and have conduction velocities that range between 2-8 m/s) (Harper and Lawson, 1985). The unmyelinated C-fibre neurons have small diameters (0.1-0.8 μM) and have slower conduction velocities (< 1.4 m/s) (Harper and Lawson,

1985; Suh et al., 1984). While A-fibre neurons are typically associated with specialised endings in the skin, muscle and joints, C-fibre and some Aδ-fibre neurons terminate as free nerve endings. Each type of nerve ending decodes information about different stimulus modalities to allow us to sense changes in our environment (**Table 1.4**).

A-alpha fibre neurons

The rapidly conducting Aα-fibre neurons convey information from the golgi tendon and muscle spindles (proprioceptors). Type 1 fibres respond to changes in muscle length and the rate of the change in length, whereas type 2 fibres only detect changes to muscle length (Loeb, 1981) The type 1a fibres (Golgi tendon organs) are activated during muscle contraction and are sensitive to changes in tension and changes in the rate of tension (McCloskey, 1978).

A-beta fibre neurons

Rapidly adapting A-beta fibre neurons

Aβ-fibre afferents terminate in glabrous (non-hairy) and hairy skin. In glabrous skin, rapidly adapting Aβ-fibre neurons are also associated with Meissners and Pacinian corpuscles. Meissner corpuscles are located on the edge of the dermis and are responsible for detection of skin motion/vibration (low frequency; 20-40Hz). Each corpuscle is connected to a single Aβ-fibre neuron and responds to low threshold stimulation in a rapidly adapting manner (Torebjork and Ochoa, 1980). The Pacinian corpuscles are also innervated by single Aβ-fibre neurons but are located slightly deeper in the dermis. They detect pressure changes and higher frequency vibrations (150-300Hz). These low threshold mechanoreceptors are very sensitive and rapidly adapt to stimuli (Lynn, 1971; Mendelson and Lowenstein, 1964). In the hairy skin, Aβ-fibre neurons may innervate low threshold mechanoreceptors present in hair follicles. These fibres respond in a rapidly adapting manner in response to hair follicle deflection (Brown and Iggo, 1967).

Slowly adapting A-beta fibre neurons

Aβ-fibre neurons that innervate Merkel cell complexes in the skin are classed as slowly adapting type 1. Merkel cells contain low threshold mechanosensitive receptors, which are able to transduce information about indentation of the skin. The slowly adapting type 1 fibres give a graded pattern of firing in response to the rate and depth of indentation. These fibres have no spontaneous activity and have clearly defined receptive fields (Coleman et al., 2001; Tapper, 1965). Unlike Meissner's and Pacinian's corpuscles, a number of different Merkel cell complexes in the skin can be innervated by a single Aβ-fibre neuron (Pare et al., 2002). Type 2 slowly adapting Aβ-fibre neurons are associated with Ruffini endings, which detect skin stretch. These neurons also produce a sustained response to skin indentation but have a more regular firing pattern in comparison to type 1 Aβ-fibre neurons (Chambers et al., 1972).

A-delta fibre neurons

Aδ-fibre neurons that terminate as free nerve endings in the skin are nociceptive. The majority of these nociceptive neurons are 'polymodal', which means they can be activated by multiple types of noxious stimuli. Every nociceptive Aδ-fibre neuron responds to noxious mechanical stimuli. There are a proportion (18%) of neurons that respond to noxious mechanical and cold stimuli (0 ˚C), of which the threshold is normally <16˚C (Cain et al., 2001; Simone and Kajander, 1997). Additionally, there are a population that respond to noxious mechanical and heat stimuli (15%). All of these neurons respond to extreme cold (when the stimulus < 0 ˚C) (Simone and Kajander, 1997). Nociceptive Aδ-neurons produce a graded response that encodes the intensity of the stimulus being applied (Cain et al., 2001). Not all of the Aδ-neurons are classed as nociceptive, there are a number that respond to lower threshold mechanical stimuli (e.g. D-hair afferents) (Millard and Woolf, 1988).

C-fibre neurons

There are two different populations of C-fibre neurons, which are distinguished based upon their binding to isolectin B4 (IB4). Non-peptidergic fibres bind to IB4 and express FRAP and P2X3 receptors, whereas peptidergic fibres express neurotransmitters and

neuropeptides (e.g. substance P and calcitonin gene-related peptide [CGRP]) (Bradbury et al., 1998; Nagy and Hunt, 1982; Silverman and Kruger, 1990). The latter are related to the transmission of pain.

C-fibre neurons terminate as free nerve endings in cutaneous and deep structures (Group IV). Many of these, approximately 90%, respond to potentially damaging stimuli and are therefore classed as nociceptive (Fang et al., 2005). The majority of nociceptive C-fibre neurons are 'polymodal' (Bessou and Perl, 1969; Cain et al., 2001). Most nociceptive C-fibres respond to both noxious mechanical stimuli and noxious temperatures (C mechano-thermal), however there are approximately 10% that only respond to noxious mechanical stimuli (CM) (Cain et al., 2001; Georgopoulos, 1976). The majority of neurons responding to noxious mechanical stimuli also respond to noxious heat (>43 ˚C), but approximately half of these also respond to noxious cold (10˚C) (Cain et al., 2001). Not many of these neurons respond to mechanical and cold stimuli alone. A low proportion (4%) of C-fibre neurons are thought to respond to temperature only (either just heat or cold or both heat and cold) (Georgopoulos, 1976). The responses to hot, cold and mechanical stimuli are graded, i.e. discharge increases as the stimulus intensity increases (Andrew and Greenspan, 1999; Cain et al., 2001; Hoffmann et al., 2008). A proportion of C-fibre nociceptors (10-20%), which were previously unresponsive to noxious mechanical stimulation, become responsive due to the effects of mediators released by tissue injury and inflammation; these fibres are referred to as 'silent' (Schmidt et al., 1995). Not all C-fibres show optimal responses to noxious stimuli. Some of these fibres have been shown to respond to gentle cooling and warming of the skin (Bessou and Perl, 1969). Moreover, there is a group found only in hairy skin, that have been shown to respond to low threshold mechanical stimuli (Vallbo et al., 1993).

Fibre type	Classification	Location	Stimulus
A_α	1a Muscle spindle	Deep	Muscle length (phasic discharge)
	1b Golgi tendon	Deep	Muscle tension
A_β	Muscle spindle	Deep	Muscle length (static discharge)
	Type 1 slowly adapting; Low threshold mechanical (Merkel disc)	Cutaneous (Glabrous/Hairy)	Indentation
	Type 2 slowly adapting; Low threshold mechanical (Ruffini ending)	Cutaneous (Glabrous/Hairy)	Stretch
	Rapidly adapting; Low threshold mechanical (Pacinian corpuscle)	Cutaneous (Glaborous)	High frequency vibration
	Rapidly adapting; Low threshold mechanical (Meissner's corpuscle)	Cutaneous (Glabrous)	Low frequency vibration
A_δ	Hair follicle	Cutaneous (Hairy)	Hair follicle deflection
	High threshold mechanical	Cutaneous (Glabrous/Hairy)	Strong pressure
	Cold receptors	Cutaneous (Glabrous/Hairy)	Cold
	Polymodal nociceptor	Cutaneous (Glabrous/Hairy)	Strong pressure/thermal
C	Polymodal nociceptors	Cutaneous (Glabrous/Hairy)	Strong pressure/thermal /irritant chemical
	Warm + Cold Thermoreceptor	Cutaneous (Glabrous/Hairy)	Hot/Cold temperatures
	C- mechanoreceptor	Cutaneous (Hairy)	Stroking
	High threshold mechanoreceptor	Cutaneous (Glabrous/Hairy)	Strong pressure
	Silent	Cutaneous (Glabrous/Hairy)	Irritant chemicals
	Group IV	Deep	Strong pressure

Table 1.4 Classification of the different sensory receptors found in the somatosensory nervous system. Adapted from (Abraira and Ginty, 2013).

1.3 Axonal transport

The axon of a neuron extends out an extremely long distance from the cell body where the majority of the protein machinery is located. Therefore, an elaborate transport system is required to ensure the delivery and removal of proteins, which include sensory ion channels and other macromolecules, from the periphery. This bi-directional transport network is powered by the motor proteins kinesin, which transports cargos in the anterograde direction, and dynein, which transports cargos in the retrograde direction (Hirokawa et al., 1991; Schnapp and Reese, 1989) (**Figure 1.1**). These motor proteins attach to their cargo via various adaptor and linker proteins (Karcher et al., 2002), and use microtubule tracks to travel up and down the axon. Microtubule tracks are in a constant state of dynamic instability. At the growth end (+), beta-tubulin monomers are added, while at the opposite end (-), they are removed (depolymerised).

There are two rate components of microtubule-based axonal transport, namely fast and slow axonal transport. The slow component only exists in the anterograde direction, whilst the fast component is present bi-directionally (Black and Lasek, 1980; Lorenz and Willard, 1978; Stockel et al., 1975). Membrane proteins, mitochondria and enzymes typically move rapidly via fast axonal transport, whereas sub-cellular organelles and cytoskeletal polymers are transported via the slow component of axonal transport (**Table 1.5**).

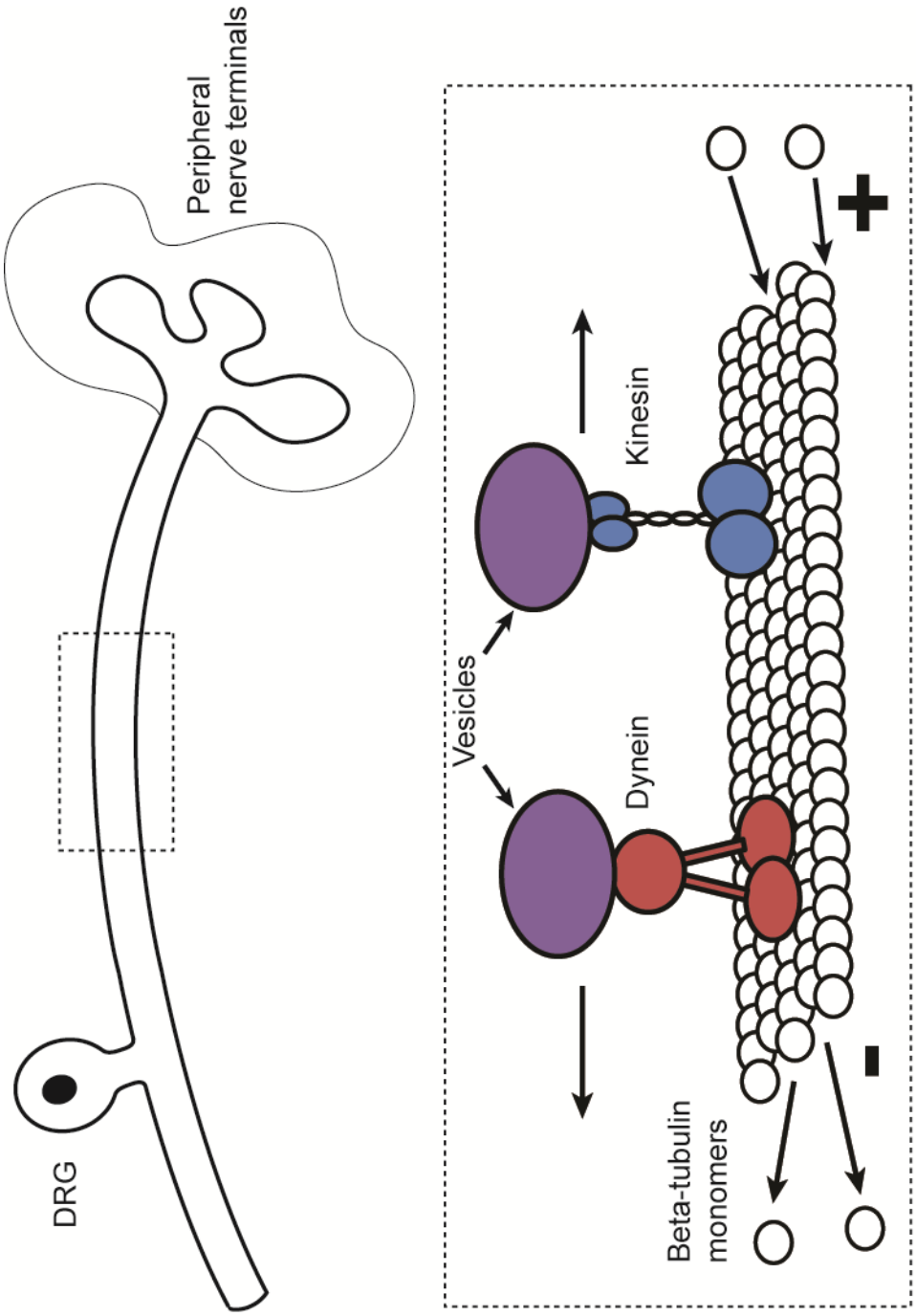

Figure 1.1 The mechanisms of axonal transport.
Kinesin motors predominantly transport vesicles containing proteins and other macromolecules in the anterograde direction (towards peripheral terminals). Dynein motor proteins transport is responsible for the retrograde transport signalling factors and proteins targeted to be recycled/degraded. These motor proteins use microtubule tracks that are in a dynamic state of instability. Polymerisation of Beta-tubulin monomers occurs at the growing end (+), whereas they are depolymerised at the opposite end (-).

	Type	Speed (mm/day)	Macromolecules	References
FAST TRANSPORT	Anterograde	200-400	Membrane proteins, lipids and neurotransmitters	(Forman et al., 1977; Lorenz and Willard, 1978; Ochs, 1972; Stockel et al., 1975)
	Mitochondria	34-68	Mitochondria	(Lorenz and Willard, 1978)
	Retrograde	100-250	Lysosomal vesicles, trophic factors and enzymes	(Forman et al., 1977; Hollenbeck, 1993; Stockel et al., 1975)
SLOW TRANSPORT	SCa	0.2-1	Neurofilaments, Tubulin	(Black and Lasek, 1980; Hoffman and Lasek, 1975)
	SCb	2-8	Microfilaments, actin, clathrin, calmodulin	(Black and Lasek, 1980; Gower and Tytell, 1987)

Table 1.5 Different components of axonal transport with their corresponding rates and compositions. SCa – slow component-a, SCb – slow component-b

1.3.1 Fast axonal transport

Anterograde transport

The maximum rate of anterograde transport in mammals is between 200-400 mm/day (Anderson and McClure, 1973; Lorenz and Willard, 1978; Ochs, 1972; Schonback and Cuenod, 1971). Vesicles containing proteins are thought to move continuously along the axon, seldom pausing as they travel towards the periphery (Reis et al., 2012). Membrane proteins (e.g. ion channels), lipids and neurotransmitters have all been reported to travel within the fast component of anterograde transport (Gilbert et al., 1980; Grafstein et al., 1975; Koschorke et al., 1994). The fast component of anterograde transport is required for the rapid delivery of materials to the periphery, to ensure the growth and maintenance of the axon.

Retrograde transport

The average rate of retrograde transport (150 mm/day) is slightly slower than anterograde transport (Stockel et al., 1975). Retrograde transport is important for the retrieval of materials, such as lysosomal vesicles and trophic factors, from the periphery back to the cell body (Hollenbeck, 1993; Stockel et al., 1975). Trophic factors have the ability to enter nuclear compartments and regulate gene expression (see Chowdary et al., 2012 for review). Vesicles targeted for degradation are sent to the lysosomes, whereas others are sent back to the golgi complex for recycling.

1.3.2 Slow axonal transport

Cytoplasmic materials such as microfilaments and neurofilaments are transported at slower rates, in which there are two different rate components. The slow component-a has a rate of 0.2-1mm/day and this group is mainly composed of proteins that form microtubules and neurofilaments. Slow component-b has a slightly faster rate of 2-8 mm/day and transports microfilament proteins such as actin, clathrin and spectrin (Black and Lasek, 1980; Gower and Tytell, 1987; Levine and Willard, 1981).

1.4 Signal transduction in sensory neurons

Sensory nerve terminals contain specialised transducers that are typically ion channels, such as transient receptor potential (TRP) channels and acid sensing ion channels (ASICs). These ion channels are responsible for transducing energy from a stimulus into an electrical signal, which is conveyed along axons in the form of an action potential. The two main ion channels responsible for action potential propagation are voltage-gated sodium (Na_v) and potassium ion channels (K_v). There are a variety of sub-types of these ion channels that are expressed in sensory neurons (See Du and Gamper, 2013 and Rush et al., 2007 for reviews). Nociceptive neurons predominantly express the $Na_v1.8$, $Na_v1.9$, $K_v1.4$, $K_v3.4$ and $K_v4.3$ subtypes (Chien et al., 2007; Djouhri et al., 2003; Fang et al., 2002; Rasband et al., 2001).

1.4.1 Mechanically sensitive ion channels

This section focuses on ion channels that are postulated to be involved in mechanotransduction, because it is hypothesised that these channels contribute towards the development of nerve trunk mechanical sensitivity in patients.

Mechanically sensitive ion channels may open or close in response to mechanical stimulation of the cell membrane. These channels play a role in the function of many different cell types in the body. For instance, mechanically sensitive channels are important in touch, hearing, osmoregulation and controlling blood pressure (Alessandri-Haber et al., 2003; Lu et al., 2009; Meyers et al., 2003; Woo et al., 2014). There are two theoretical models of how mechanically sensitive channels can open directly in response to a force applied to the membrane (Kung, 2005). The bilayer model proposes that changes in lipid tension are adequate enough to open mechanically sensitive channels (see **Figure 1.2 A**). For example, tension is proposed to cause the membrane to become thinner (Perozo et al., 2002). This is believed to cause a mismatch between the length of the hydrophobic interface of the channel and the hydrophobic section of the lipid bilayer, which is energetically unfavourable. To avoid this mismatch, the channel changes its confirmation, causing it to open. The second model, which materialised from studies on auditory hair cells (LeMasurier and Gillespie, 2005), involves a tether between the channel and the cytoskeleton or

extracellular matrix. The tether is proposed to transmit a change in tension, which results in the channel opening upon mechanical stimulation of the membrane (see **Figure 1.2 B**). The opening of mechanically sensitive channels in sensory neurons may be dependent on tethers, as cytoskeletal disrupting agents have been demonstrated to reduce the responsiveness of channels (Cho et al., 2002).

The mechanically sensitive ion channels that are postulated to be involved in mechanotransduction in the somatosensory nervous system are reviewed below (see **Table 1.6**). Although many of the mechanically sensitive ion channels involved the detection of low threshold mechanical stimuli have been formerly identified, the identity of the channel that responds to high threshold (noxious) mechanical stimuli remains unknown.

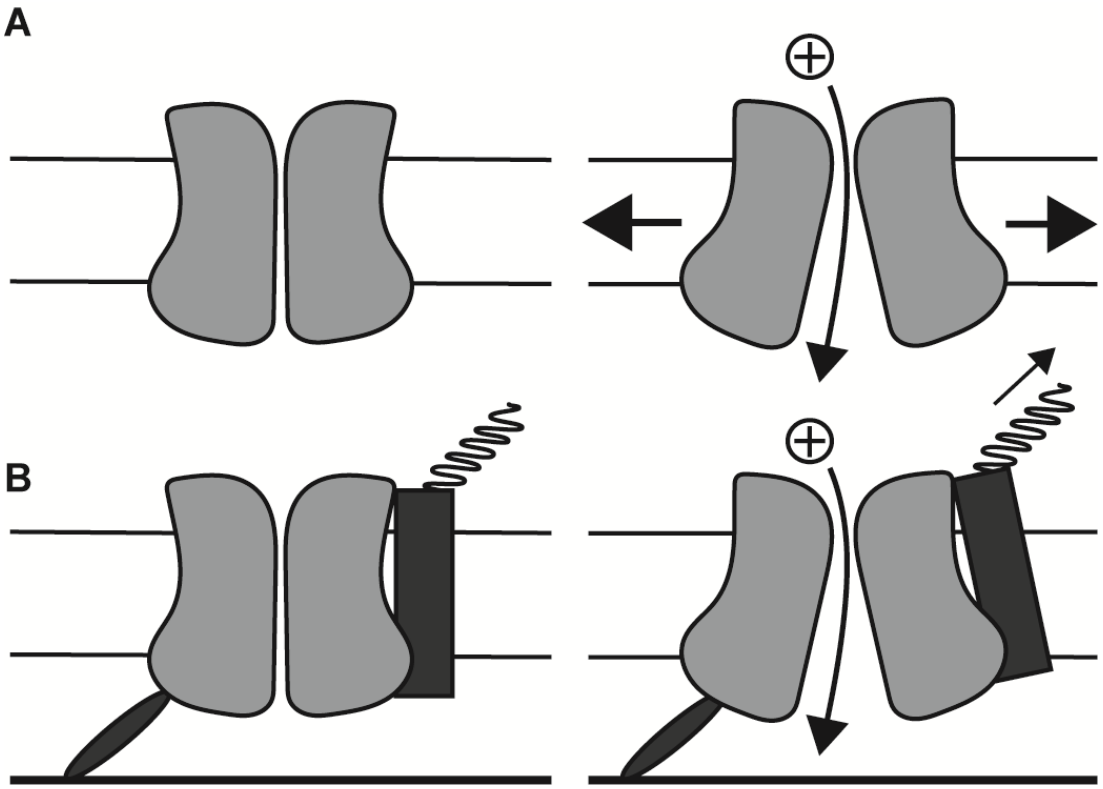

Figure 1.1 Models of mechanically sensitive channel opening in direct response to a force applied to the membrane. A) Gating mechanism in which channels are opened via changes in membrane tension. B) Gating mechanism in which channels open due to forces transmitted through tethers to the extracellular matrix or intracellular cytoskeletal proteins. Adapted from (Lin and Corey, 2005)

Transient receptor potential channels

Transient receptor potential channels are cation selective channels which are more permeable to calcium ions compared to sodium ions (Owsianik et al., 2006). These channels share a similar structure that consists of six transmembrane domains and a pore-forming loop between the last two domains (Liao et al., 2013; Paulsen et al., 2015). Both the carboxyl and amino terminals are on the inside of the cell membrane and contain a variety of different domains and motifs depending on the TRP subfamily. There are seven TRP channel families namely; TRPC, TRPM, TRPV, TRPN, TRPA, TRPP and TRPML, within which there are individual sub-types (Montell, 2005). The sub-types that are reported to be involved in mechanotransduction in the mammalian somatosensory nervous system are reviewed below.

Transient receptor potential ankyrin 1

Transient receptor potential ankyrin 1 (TRPA1) shares a similar structure to other TRP channels, specifics include an amino terminal that contains several ankyrin repeats (Paulsen et al., 2015). The channel is expressed in a variety of different location within the body, which include the inner ear, brain, skin, vasculature, bladder and gastrointestinal tract (Anand et al., 2008; Corey et al., 2004; Earley et al., 2009; Kwan et al., 2009; Nozawa et al., 2009; Streng et al., 2008). In the somatosensory nervous system, TRPA1 is predominantly expressed in a proportion of Aδ- and C-fibre neurons and is also expressed within auditory hair cells (Nagata et al., 2005; Story et al., 2003). It is a non-selective cation channel that can be opened when temperatures are lowered below 17 ˚C, or upon application of noxious chemicals such as mustard oil (Jordt et al., 2004; Story et al., 2003). As a putative mechanosensitive ion channel, it is thought that the N terminal domain ankyrin repeats act as gating springs (tethers) to facilitate channel opening, as they are assumed to do in hair cells (Corey et al., 2004). There is a body of evidence to suggest that TRPA1 is involved in mechanotransduction in sensory neurons. The gene that encodes a TRPA homologue in drosophila, is responsible for the transduction of noxious heat and mechanical stimuli (Tracey et al., 2003). In vertebrates, inhibiting the TRPA1 channel in both zebrafish and mice reduced the transduction currents produced in hair cells (Corey

et al., 2004). As a putative mechanotransduction channel in sensory neurons, in-vitro and ex vivo electrophysiological studies in mice have suggested that the channel is responsible for mechanotransduction in a population of C-fibre neurons (Brierley et al., 2011; Kerstein et al., 2009; Vilceanu and Stucky, 2010). TRPA1 knockout mice have deficits in sensing noxious mechanical stimuli, further supporting a role for the channel in mechanotransduction in C-fibre neurons (Kwan et al., 2006).

Transient receptor potential vaniloid 1

Similarly to TRPA1 the structure of TRPV1 has an N-terminal domain that contains ankyrin repeats (Liao et al., 2013). Transient receptor potential vanilloid channels can assemble in homotetramers or heterotetrameric complexes (Kuzhikandathil et al., 2001; Rutter et al., 2005). Within the body, the channel is expressed similar locations to TRPA1, which include the vasculature, bladder, skin, gastrointestinal tract and brain (Birder et al., 2002; Caterina et al., 1997; Deering-Rice et al., 2012; Golech et al., 2004; Inoue et al., 2002; Kark et al., 2008). In the somatosensory nervous system, TRPV1 is expressed in a proportion of Aδ- and C-fibre neurons of the trigeminal and dorsal route ganglia (Caterina et al., 1997; Guo et al., 1999). In these neurons, the channel has been specifically localised to the cell body, the peripheral terminals and is thought to be present along axons (Bernardini et al., 2004; Tominaga et al., 1998). It is a cation selective ion channel that can be activated by noxious heat (>40˚C), capsaicin and protons (Caterina et al., 1997). There is mixed evidence as to whether TRPV channels are able to respond to mechanical stimulation. The TRPV channels homologues in Caenorhabditis Elegens that are encoded by the OSM 9 and OCR-2 genes, were found to be essential for mechanosensation and detection of various other forms of sensory stimuli (Tobin et al., 2002). However, it currently remains to be determined whether mammalian TRPV1 channels open in response to mechanical stimulation. TRPV1 is not thought to be essential for noxious mechanotransduction in sensory nerve fibres which innervate the skin (Caterina et al., 2000). However, it has been found to be essential for mechanically evoked adenosine tri-phosphate (ATP) release in the bladder and has also been suggested to have a mechanosensory function in visceral afferents of the colon (Birder et al., 2002; Jones et al., 2005b).

Transient receptor potential vanilloid 4

Transient receptor potential vanilloid (TRPV4) is a non-selective cation channel that shares the same structure of TRPV1 channel (Shigematsu et al., 2010). The channel is expressed within various different organ systems, which include the inner ear, kidney, liver, heart, skin and brain (Liedtke et al., 2000; Strotmann et al., 2000). The channel is expressed in A- and C-fibre neurones and has been identified in the DRG, nerve trunk and the periphery; specifically the terminals of cutaneous mechanosensitive neurons (Alessandri-Haber et al., 2003; Suzuki et al., 2003). Similarly to TRPV1, the channel is activated by heat, but the channel opens at a temperature threshold that isn't noxious (>27˚C) (Guler et al., 2002). In C. Elegens the channel has been demonstrated to have an osmosensitive and mechanosensitive function (Liedtke et al., 2003). In rodents, there is evidence to suggest the channel is involved in the transduction of noxious mechanical stimuli in sensory neurons (Suzuki et al., 2003). However, the channel may not to be directly sensitive to mechanical stimulation, as removal of the ankyrin domain from the amino terminus had no effect on channel opening caused by osmotic stress or membrane stretch (Liedtke et al., 2000; Strotmann et al., 2000). It has been proposed that the channel opens indirectly via cytochrome p450 and phospholipase A2 production (Vriens et al., 2004).

Transient receptor potential canonical channels 1, 3 and 6

Transient receptor potential canonical (TRPC) channels are calcium permeable non-selective cation channels. In mammals there are seven homologues of the channel (Vazquez et al., 2004). Like the TRPV4 and TRPA1 ion channels, TRPC channels also have ankyrin repeats on their amino terminal domains (Lussier et al., 2005). However, they are different to other TRP channels in that the C-terminal domain contains specialised domains, such as the CIRB domain (calmodulin/Inositol tri-phosphate receptor binding), important in mediating channel activation via intracellular messengers (Tang et al., 2001; Wedel et al., 2003). The mRNA of the TRPC channels are expressed in several different areas of the central nervous system and variety of other locations within the body (Riccio et al., 2002). Channels are expressed within organs and tissues that contain mechanosensory complexes; examples include the

kidney and the vasculature (Huber et al., 2006; Reading et al., 2005). Accordingly, there is a body of evidence for the involvement of TRPC channels in mechanotransduction (reviewed in Hamill and Maroto, 2007). In the somatosensory nervous system there is evidence that all channels are expressed within DRG neurons, with TRPC1, TRPC3 and TRPC6 being most prominent (Elg et al., 2007). Transient receptor potential canonical 1 is expressed in A-fibre neurons and a proportion of C-fibre neurons and may play a role in the mechanotransduction processes involved in light touch (Elg et al., 2007; Garrison et al., 2012). The TRPC3 and TRPC6 channels are expressed alongside each other within C- and A-fibre neurons (Elg et al., 2007; Kress et al., 2008; Quick et al., 2012). There are suggestions that both of these channels are involved in mechanotransduction processes important in touch and hearing (Quick et al., 2012; Sexton et al., 2016). In nociceptive neurons, TRPC channels do not appear to play a role in mechanotransduction mechanisms (Garrison et al., 2012; Quick et al., 2012; Sexton et al., 2016). It is thought that TRPC channels are able to respond to mechanical stimuli through changes in membrane tension; both TRPC1 and TRPC6 open in response to stretch of the membrane (Maroto et al., 2005; Spassova et al., 2006)

Acid sensing ion channels

There are six known types of acid sensing ion channels (ASICs), which are encoded by four separate genes. ASIC 1α and ASIC 1β are splice variants of the ASIC1 gene (Chen et al., 1998; Garcia-Anoveros et al., 1997). Similarly, ASIC2a and ASIC2b are two variants of the ASIC2 gene (Garcia-Anoveros et al., 1997; Lingueglia et al., 1997). ASIC3 and ASIC4 channels are each encoded by the ASIC3 and ASIC4 gene respectively (Grunder et al., 2000; Waldmann et al., 1997b). Channels are composed of three subunits that each have a large extracellular domain and two transmembrane domains. The extracellular domains from different subunits form a hydrogen ion binding pocket and each of the three sets of transmembrane domains group together to form an ion selective pore (Jasti et al., 2007). Subunits from the same sub-type form homomeric channels, alternatively subunits from different sub-types can assemble to form heteromers (Benson et al., 2002). A decrease in extracellular pH causes most ASICs to open, resulting in the influx of cations which causes

depolarisation (Krishtal and Pidoplichko, 1980). However, ASIC4 does not respond to decreases in extracellular pH (Grunder et al., 2000). These channels are responsible for evoking pain behaviour in response to moderate acidosis (Deval et al., 2008; Dube et al., 2005; Voilley et al., 2001). Currently there is no evidence that these channels are directly sensitive to mechanical stimulation and hence possible gating mechanisms are unknown. However, evidence from immunohistochemical studies have shown that ASIC channels are expressed within specialised mechanosensory organs in the skin, bladder and cardiovascular system, suggesting that they may be involved in the mechanotransduction process (Calavia et al., 2010; Corrow et al., 2010; Lu et al., 2009).

Acid sensing ion channel 1

In the sensory nervous system, ASIC1 is expressed in A- and C-fibre neurons and has been identified along the sciatic nerve (Alvarez de la Rosa et al., 2002; Bohlen et al., 2011). Although ASIC1 is expressed within specialised mechanosensory Pacinian corpuscles in the skin and baroreceptors in the vasculature, it is not reported to be involved in mechanotransduction in these areas (Calavia et al., 2010; Lu et al., 2009; Page et al., 2004). However, ASIC1 is suggested to play a role in the mechanosensory mechanisms in the gastrointestinal tract, because knockout mice have colonic afferents that display an increased sensitivity to mechanical stimulation (Page et al., 2004).

Acid sensing ion channel 2

The ASIC2 channel is expressed within A-fibre neurons, in addition to some C-fibre neurons (Alvarez de la Rosa et al., 2002). In the periphery, the channel is expressed in the specialised mechanosensitive terminals, namely Meissner and Pacinian corpuscles, as well as some myelinated free nerve endings (Alvarez de la Rosa et al., 2002; Cabo et al., 2012; Garcia-Anoveros et al., 2001). Evidence from behavioural studies suggests that the channel is important in the mechanotransduction processes for low threshold touch sensation, but not for noxious mechanical stimuli (Price et al., 2000; Staniland and McMahon, 2009). However, in vitro evidence indicates that the channel does not contribute to the mechanotransduction process in the somata

of cultured sensory neurons (Drew et al., 2004). In the cardiovascular system, ASIC2 is thought to have a mechanosensory role in medaiting the barorecpetor reflex to changes in blood pressure (Lu et al., 2009). Similiar to ASIC1 knockout mice, ASIC2 knockouts have altered mechanosensory processing in the gastrointestinal tract, suggesting that it is involved in the mechantransduction in colonic afferents (Page et al., 2005).

Acid sensing ion channel 3

The ASIC3 channel is expressed within A- and C-fibre sensory neurones (Alvarez de la Rosa et al., 2002; Price et al., 2001). It has been localised to specialised mechanosensory structures near surface of skin, specifically Meissners corpuscles and Merkel cells, but is also present some cutaneous unmyelinated/myelinated free nerve endings and muscle afferents (Alvarez de la Rosa et al., 2002; Molliver et al., 2005; Price et al., 2001; Waldmann et al., 1997a). Although ASIC3 is reported to be involved in mechanotransduction in proprioreceptors (Lin et al., 2016), it is not clear whether ASIC3 participates in mechanotransduction in cutaneous afferents. Similarily to ASIC2, ASIC3 knockdown did not alter mechanosensitive currents in the somata of cultured sensory neurons (Drew 2004). In vitro skin-nerve data suggests that blocking ASIC3 function, either by pharmacological or genetic means, causes increased sensitivity to low threshold mechanical stimuli in rapidly adapting mechanosensitive neurons and reduces the sensitivity of population of mechanosensitive C-fibre neurons (Moshourab et al., 2013; Price et al., 2001). However behaviourally, ASIC3 knockouts do not show increased sensitivity to light touch and in addition to this do not show altered sensitivity to noxious mechanical stimulation (Chen et al., 2002). Acid sensing ion channel 3 is reported to play an important role in visceral nociception. Knockout mice have colonic afferents that show reduced sensitivity to colon distension, suggesting that the channel may function as a mechanotransducer in the gastrointestinal tract (Jones et al., 2005b; Page et al., 2005). Within the vasculature, ASIC3 is expressed on afferent terminals and may function as a mechanosensor important in the regulation of blood volume (Lee et al., 2011; Molliver et al., 2005).

Piezo channels

Piezo channels have a structure that contains between 24 and 36 transmembrane domains. Currently, there are only two channels that have been identified; namely Piezo1 and Piezo2. These channels are expressed in similar locations to other mechanically sensitive ion channels, such as the bladder, colon, kidney and skin (Coste et al., 2010). In sensory neurons, Piezo1 is reported to be expressed in negligible levels, while Piezo2 is expressed in A- and C-fibres (Coste et al., 2010). Piezo 1 and 2 have both been shown to produce mechanosensitive currents with cationic selective conductances, when expressed in various different cell types (Coste et al., 2010; Woo et al., 2014). In drosophila, Piezo channels are suggested to play a role in the transduction of noxious mechanical stimuli (Kim et al., 2012). However, in mammals the channel is proposed to be involved in the perception of light touch as it is localised to a subset of mechanosensory neurones which have been identified as Merkel cells (Woo et al., 2014). Recent evidence suggests that the channel could also be the main mechanotransduction channel in proprioceptors (Woo et al., 2015).

Two pore potassium domain channels

The two pore domain potassium (K2P) channel family consists of the inwardly rectifying K+ channels one and two (TWICK 1 + 2), related potassium channel one and two (TREK 1 + 2), acid-sensitive potassium channel (TASK), and TWIK-related arachidonic acid activated potassium channel (TRAAK) (Enyedi and Czirjak, 2010). The TREK and TRAAK subtypes are known to be mechanically sensitive (Kang et al., 2005). All K2P channel share a similar structure consisting of four transmembrane segments and two pore forming domains. TREK 1 and TREK 2 are outwardly rectifying potassium channels and TRAAK is a non-rectifying potassium channel (Bang et al., 2000; Fink et al., 1996; Fink et al., 1998). TREK 1, TREK 2, and TRAAK are expressed in various locations with the nervous system, including that of sensory neurons; individual channels are also found in organs with known mechanosensory complexes, such as the kidney and gastrointestinal tract (Medhurst et al., 2001; Talley et al., 2001). In primary sensory neurons, TREK 1 is located on A- and C-fibre neurons (Alloui et al., 2006). TREK 2 is strongly expressed in C-fibre neurones and weakly expressed in A-fibre neurones (Acosta et al., 2014). The TRAAK channel is only expressed upon heat

sensitive C-fibre neurones (Noel et al., 2009). As well as being sensitive to mechanical stimuli, the TREK 1, TREK2 and TRAAK channels have been shown to be temperature and pH sensitive (Kang et al., 2005). Mechanically sensitive K2P channels are likely to raise the mechanical threshold in the skin, as TREK 1, TREK 2 or TRAAK knockout mice all exhibit pronounced mechanical allodynia (Alloui et al., 2006; Noel et al., 2009; Pereira et al., 2014). It has been suggested that these channels work together with depolarising mechanically sensitive ion channels to guide the response to noxious/ non-noxious mechanical stimuli. The mechanism by which these channels open is thought to be due to membrane deformation induced disruption of a link between the C-terminus and the actin skeleton (stretch-activation). The C-terminus of TREK 1 interacts with the actin cytoskeleton and this contact represses mechano-activation of the channel (Lauritzen et al., 2005).

Ion channel	Neuronal expression	Expression in tissues involved in mechanosensation	Role in somatosensory mechanotransduction mechanisms
TRPA1	Aδ- and C-fibres	Vasculature, bladder, skin, gastrointestinal tract, inner ear	Potential noxious mechanosensor
TRPV1	Aδ- and C-fibres	Vasculature, bladder, skin, gastrointestinal tract	?
TRPV4	A- and C-fibres	Vasculature, skin, kidney, inner ear	Proposed to be involved in sensing noxious pressure
TRPC1	A-fibre	Vasculature, skin, kidney, inner ear	Proposed to be involved in detection of light touch
TRPC3	A- and C-fibre	Vasculature, skin, kidney, inner ear,	Proposed to be involved in detection of light touch
TRPC6	A- and C-fibre	Vasculature, skin, kidney, inner ear	Proposed to be involved in detection of light touch
ASIC1	A- and C-fibre	Vasculature, skin, gastrointestinal tract	?
ASIC2	A- fibre	Vasculature, skin, gastrointestinal tract	Proposed to be involved in detection of light touch
ASIC3	A- and C-fibre	Vasculature, skin, gastrointestinal tract	Reported to be involved in proprioception; unclear whether involved in low threshold touch sensation
Piezo2	A- and C-fibre	Bladder, skin, kidney, gastrointestinal tract	Proposed to be involved in detection of light touch and proprioception
TREK1	A- and C-fibre	Skin, kidney, gastrointestinal tract	Raise mechanical threshold
TREK2	Mainly C-fibre	Skin, kidney, gastrointestinal tract	Raise mechanical threshold
TRAAK	C-fibre	Skin	Raise mechanical threshold

Table 1.6 Summary of the ion channels that are proposed to be involved in mechanotransduction mechanism in the somatosensory nervous system. ASIC – Acid sensing ion channel, TREK - TWICK related potassium channel, TRAAK – TWIK-related arachidonic acid activated potassium channel, TRPA – Transient receptor potential ankyrin, TRPV – Transient receptor potential vaniloid, TRPC – Transient receptor potential canonical

1.4.2 Normal transduction properties of axons

Under normal conditions, it is assumed that most ion channels that respond to stimuli (mechanical, chemical, thermal) are destined for delivery to the peripheral terminals and therefore are not present in significant levels along the axon. However, as a proportion of axons are reported to respond to stimuli applied directly to a nerve trunk, this suggests that the ion channels responsible for transduction of this stimulus are present and functional within these axons. Detailed below are the responses of axons to different stimuli.

Mechanical

In apparently uninjured nerves, A- and C-fibre axons rarely respond to mechanical stimulation (Bove et al., 2003; Dilley and Bove, 2008a; b; Dilley et al., 2013; Hoffmann et al., 2008; Teliban et al., 2011). The proportion of C-fibre nociceptors with axonal mechanical sensitivity (AMS) in naive nerve trunks is reported to be low (0-3%) (Bove et al., 2003; Dilley et al., 2005; Dilley and Bove, 2008a; Teliban et al., 2011). In uninjured nerves, mechanically sensitive axons are not reported to have similar properties to mechanically sensitive receptive fields in the skin, i.e. stronger mechanical stimuli does not produce an increased response (Hoffmann et al., 2008). Additionally, thresholds for mechanical activation in the axons are reported to be approximately 10 times higher than in the skin.

Temperature

There have been numerous reports of axonal thermosensitivity in nerve trunks that are apparently uninjured (Hoffmann et al., 2008; 2009; Sauer et al., 2001; Teliban et al., 2011; Zimmermann et al., 1982). In rat nerves, A-fibre axons do not have axonal thermosenstivity, whereas a proportion of C-fibre axons with thermosensitive receptive fields also possess axonal thermosensitivity (See Teliban et al., 2011 for individual proportions). Axons that are thermosensitive produce a graded response to heat and cold stimuli (Hoffmann et al., 2008; Teliban et al., 2011).

Chemical

Under normal conditions, most inflammatory mediators (e.g. bradykinin, serotonin, histamine, and PG) do not excite axons when topically applied to a nerve or intraneurally injected (Govea et al., 2017; Hoffmann et al., 2008; Zimmermann et al., 1982). However, a proportion of uninjured nociceptive axons are reported to be excited by TNF (Leem and Bove, 2002; Sorkin et al., 1997). Although most inflammatory mediators do not cause excitation of axons, bradykinin and PGE2 are known to augment the responses of axons to noxious heat stimuli (Fischer and Reeh, 2007). Other chemicals, such as those that activate TRP channels, may also cause excitation when topically applied to nerve trunks. For example, the TRPV1 agonist capsaicin is reported to cause depolarisation in C-fibre axons when applied to nerve trunks (Docherty et al., 2013; Hayes et al., 1984). Furthermore, C-fibre axons respond to the application of the TRPA1 agonist cinnamaldehyde when applied to the vagal (Nassenstein et al., 2008) and sural nerves (Docherty et al., 2013).

1.5 Animal models of neuropathic pain

Much of our current understanding of the mechanisms of neuropathic pain has come from the use of animal models. Frank nerve injury models are commonly used to see how nerve trauma (crushing, stretching, constricting) causes physiological changes that lead to animals exhibiting signs of neuropathic pain (see **Table 1.7** for summary of changes that occur following different frank nerve injury models). In these models, AMS and ongoing activity are typical features indicating the increased excitability of axons. However, models of frank nerve injury are not consistent with patients who present neuropathic pain symptoms in the absence of obvious trauma to a nerve trunk. To understand the mechanisms behind the development of painful symptoms in these patients, a series of models that do not involve frank nerve injury have been developed (reviewed below).

Model	Reported changes			
	Electrophysiology	**Histology**	**Behaviour**	**References**
CCI	Reduced conduction (A- and C-fibres) & conduction slowing of A-fibres through injury site. OA – A- and C-fibres AMS – A-and C-fibres [a]	Ischemia, oedema, axonal sprouting & Wallerian degeneration at the injury site	Autonomy, heat, cold & mechanical hyperalgesia, cold & mechanical allodynia	Behaviour - (Bennett and Xie, 1988; De Vry et al., 2004; Dowdall et al., 2005; Jasmin et al., 1998; Kim et al., 1997). Histology - (Carlton et al., 1991) Electrophysiology - (Chen and Devor, 1998; Eliav and Tal, 1994; Kajander and Bennett, 1992; Laird and Bennett, 1993; Xie and Xiao, 1990)
Nerve crush	Conduction slowing in A- and C-fibres. OA – A-fibre, very few C-fibres AMS – A- and C-fibres [a]	Wallerian degeneration & axonal sprouting at the injury site	Autonomy; heat hyperalgesia, mechanical & cold allodynia (delayed onset)	Behaviour - (Bester et al., 2000) Histology - (Cragg and Thomas, 1961) Electrophysiology - (Chen and Devor, 1998; Devor, 1983; Devor and Govrin-Lippmann, 1983; Welk et al., 1990)
PNL	OA – A- and C-fibres	Oedema, Wallerian degeneration & sprouting in the ligated portion of the nerve	Mild autonomy, heat & mechanical hyperalgesia, cold & mechanical allodynia	Behaviour - (Dowdall et al., 2005; Kim et al., 1997; Seltzer et al., 1990) Histology - (Liu et al., 2000b) Electrophysiology - (Pan et al., 1999)
SNL	Conduction slowing in A- and C-fibres OA – A-fibre in injured & uninjured axons, C-fibre in uninjured axons (v. low rates) AMS – C-fibre [b]	Wallerian degeneration & axonal sprouting at the injury site	Heat, cold & mechanical hyperalgesia, cold & mechanical allodynia	Behaviour - (Allchorne et al., 2005; Choi et al., 1994; Kim and Chung, 1992) Histology - (Hu and McLachlan, 2002; Roytta et al., 1999) Electrophysiology - (Chapman et al., 1998; Dilley and Bove, 2008b; Djouhri et al., 2012; Djouhri et al., 2006; Liu et al., 2000a; Liu et al., 2000c; Wu et al., 2001)

Table 1.7 Summary of main changes that occur following frank nerve injury models typically used to study neuropathic pain. [a] typically develops at the treatment site. [b] develops at a remote location. CCI – chronic constriction injury, PNL – partial nerve ligation, SNL – spinal nerve ligation, OA – ongoing activity, AMS – axonal mechanical sensitivity.

1.5.1 Models of neuritis

Induced using complete Freund's adjuvant

The neuritis model was developed to look into the effects of localised inflammation on peripheral nerve trunks. The sciatic nerve is wrapped in a piece of Oxycel or gelfoam that is saturated in complete Freunds adjuvent (CFA) to cause the formation of an experimental neuritis (Eliav et al., 1999). The model is particularly relevant to neuropathic pain conditions that include Herpes Zoster infection and Guillain Barre syndrome (where there are immune mediated responses), but also in conditions such as CRPS-1 and NSAP injuries, in which inflammation is thought to be involved.

Behaviour

Shortly after lesion induction, heat and mechanical hyperalgesia develop rapidly (day 1 post surgery) and peak between days 2-4. After 8-9 days, changes had completely reversed. Mechanical and cold allodynia were also present and follow a similar time course (Dilley et al., 2013; Eliav et al., 1999; Pulman et al., 2013). There was no indication that animals were suffering ongoing pain. Moreover, there was no evidence for autonomy/eversion of the affected hind paw (Eliav et al., 1999).

Histology

Application of CFA causes a minimal amount of degeneration and demyelination of axons (Eliav et al., 2001; Eliav et al., 1999). At the treatment site a granuloma forms around the outside the nerve, however the nerve remains normal in size with some evidence for mild oedema. The granuloma contains increased amounts of mRNA for the pro-inflammatory cytokines TNF and chemokine (C-C motif) ligand 2 (CCL2) (Pulman et al., 2013), IL-6 and IL-1β (Eliav et al., 2009), in addition to pro-inflammatory cells such as macrophages and lymphocytes, which are concentrated around the outside of the epineurial sheath (Eliav et al., 1999). Lower levels of immune cells are present in the endoneurial compartment, but none penetrate the perineurium (Bove et al., 2003; Bove et al., 2009). Additionally, fast axonal transport is clearly disrupted on day 6 (Dilley et al., 2013).

Electrophysiology

Neuritis causes a reduction in the conduction velocity of C-fibre axons, which peaks at four weeks post-surgery but returns to a normal range by 2 months (Dilley and Bove, 2008b). Ongoing activity develops in both A- and C-fibre axons (Bove et al., 2003; Dilley et al., 2005; Eliav et al., 2001). At the peak of behavioural changes, 38% of C-fibre axons had developed ongoing activity (Richards et al., 2011). Axonal mechanical sensitivity develops in intact C- and Aδ-fibre axons, the majority of which innervated deep structures (Bove et al., 2003; Dilley et al., 2005; Eliav et al., 2001). Mechanically sensitive hotspots are typically located at the treatment site and respond to both pressure and stretching of the nerve (Bove et al., 2003; Dilley et al., 2005). Axonal mechanical sensitivity peaks between 4-7 days post-surgery and persists for 4 weeks post-surgery (Bove et al., 2003; Dilley and Bove, 2008b). Approximately 80% of nociceptive C-fibre axons develop chemical sensitivity to a combination inflammatory mediators (Govea et al., 2017). Furthermore, C-fibre axons are excited after individual application of the inflammatory mediators TNF and CCL2 (Richards et al., 2011).

Induced using zymosan

The zymosan model enables the effects of peripheral nerve inflammation to be investigated after the effects of surgery have diminished (minimising the effects of anaesthesia on the inflammatory response). Similarly to the neuritis model, gelfoam is placed around the sciatic nerve at the level of the mid-thigh. Zymosan is then delivered to the gelfoam via a catheter (stitched into the nearby muscle) 4-5 days post-surgery (Chacur et al., 2001).

Behaviour

Low doses (4ug) of zymosan induce unilateral mechanical allodynia after 3 hours post injection through the catheter. Higher doses (40-400ug) induce bilateral allodynia. These changes were dependent upon immune activation occurring close to the nerve trunk and not due to zymosan entering the systemic circulation (Chacur et al., 2001).

Histology

Zymosan application causes minimal axonal degeneration. There was evidence for mild oedema with some indication of Schwann cell activation. In the epineurium, there was increased fibroblast activity, collagen deposition and evidence for macrophage infiltration from blood vessels. Furthermore, TNF staining was found within the epineurial and endoneurial compartments (Gazda et al., 2001). Upon inspection of the gelfoam at three hours post application, there was found to be an increased number of neutrophils compared to that of the control (Gazda et al., 2001). Additionally, there is evidence that immune cells within the gelfoam release IL1, TNF and reactive oxygen species (ROS) (Gazda et al., 2001; Twining et al., 2004).

1.5.2 Model of localised axonal transport disruption

Neuritis causes the disruption to axonal transport, which is hypothesised to be an important mechanism that leads to the development of neuropathic pain like behaviours (Dilley et al., 2013). In order to examine this mechanism in isolation in the absence of potentially confounding factors caused by inflammation, axonal transport can be disrupted using anti-mitotic drugs (e.g. paclitaxel, vinblastine and colchcine) (Dilley and Bove, 2008a; Fitzgerald et al., 1984; Jackson and Diamond, 1977; LaPointe et al., 2013). These drugs disrupt the organisation of microtubule tracks that motor proteins use to transport macromolecules along the axon. For example, vinblastine inhibits assembly and promote disassembly of microtubules (Jordan and Wilson, 1990; Panda et al., 1996), whereas, paclitaxel causes stabilisation of microtubules leading to abnormal organisation (Arnal and Wade, 1995; Masurovsky et al., 1981). Experimentally axonal transport disruption can be achieved in the absence of axonal damage/degeneration through a transient exposure of a low concentration (0.1 mM) of vinblastine to the sciatic nerve (Dilley and Bove, 2008a; Fitzgerald et al., 1984).

Behaviour

Currently, there is no evidence that animals are in ongoing pain in this model. When low doses (0.1 mM) of vinblastine are applied to the nerve, mechanical allodynia develops rapidly (1-day post-surgery) and peaks on day 4. The sensitivity of animals to mechanical stimuli returns to that of baseline by 11 days post-surgery (Dilley et al., 2013). At low doses, there is currently no evidence that mechanical or heat hyperalgesia is associated with this model (Dilley et al., 2013; Fitzgerald et al., 1984).

Histology

Application of 0.1mM vinblastine to the nerve causes disruption to axonal transport (Dilley et al., 2013; Fitzgerald et al., 1984). Axonal transport disruption is assumed to be most pronounced at 2-days post-surgery, with evidence that it has recovered by day 6 (Dilley et al., 2013). At low doses (0.1mM) there is absence of any A- or C-fibre degeneration (Dilley et al., 2013; Fitzgerald et al., 1984). However at higher doses (>0.15mM) there is a decrease in the number of myelinated and unmyelinated fibres, with evidence for oedema (Fitzgerald et al., 1984). There is no evidence for the presence of macrophages at treatment site (Dilley et al., 2013).

Electrophysiology

High doses (>0.15 mM) of vinblastine cause disruption to conduction and slowing through the treatment site in A and C-fibre axons (Fitzgerald et al., 1984). Low doses (0.1 mM) of vinblastine cause both A- and C-fibre axon conduction velocities to slow through the treatment site (Dilley and Bove, 2008a). Additionally the conduction velocity of C-fibre neurons is reduced proximal to the treatment site (Dilley et al., 2013). Currently, there is no evidence that ongoing activity develops in A- or C-fibre axons in this model (Dilley et al., 2013; Govea et al., 2017; Satkeviciute et al., 2018). Axonal mechanical sensitivity develops in approximately a third of nociceptive axons between days 3-7 post-surgery (Dilley and Bove, 2008a; Dilley et al., 2013; Satkeviciute et al., 2018). The mechanically sensitive hotspots are located proximal to and at the treatment site. Furthermore, 38% of C-fibre axons develop sensitivity to inflammatory mediators at 3-4 days post-surgery (Govea et al., 2017).

1.5.3 Chemotherapy induced peripheral neuropathy model

Anti-mitotic drugs can also cause the development of neuropathic pain symptoms following repeated systemic administration (CIPN). Therefore, models of CIPN have been developed to study the underlying mechanisms. In one such model in rats, intraperitoneal administration of paclitaxel once per week, over a period of several weeks (mimicking the dosing regime in patients undergoing chemotherapy) (Cavaletti et al., 1995).The model has been adapted by other groups by using different chemotherapeutic drugs/dosing regimens. Polomano and co-workers (2001) developed a dosing regimen in which rats received four I.P. injections (2mg/kg) on alternate days. A total of 8mg/kg is thought to be the threshold for systemic toxicity in the rat (Cavaletti et al., 1995).

Behaviour

After injecting 2mg/kg paclitaxel on 4 alternate days, mechanical and cold allodynia develop shortly after the last dose was administered and peak about 1 week later. These behavioural changes persist for at least 3 weeks following the last cumulative dose. There is a little/no heat hyperalgesia that develops with this dosing regimen (Polomano et al., 2001). Mechanical hyperalgesia also develops using this regime and peaks with mechanical allodynia at about 2 weeks (Flatters and Bennett, 2006).

Histology

After repeat dose paclitaxel administration, there was no evidence for axonal degeneration in the sciatic nerve, dorsal root ganglion or spinal cord. There was some evidence for endoneurial oedema in the sciatic nerve (Polomano et al., 2001). The most notable change within the axons was an increase to the number of abnormal (swollen) mitochondria, which was seen in both A- and C-fibres. These increases were most prominent at the same time of the peak of behavioural changes in animals. There appeared to be no effect on microtubule density in A- or C-fibre axons at this time point (Flatters and Bennett, 2006).

Electrophysiology

Following cumulative paclitaxel dosing, conduction velocities remained unchanged in A- or C-fibre neurons (Xiao and Bennett, 2008). A- and C-fibre ongoing activity was recorded upon electrophysiological examination of the nerves. At the peak of behavioural symptoms (between days 28-55), 17% of the A-fibres and 20% of the C-fibres had developed ongoing activity (Xiao and Bennett, 2008).

A summary of the excitability changes that occur in axons in frank and non-frank nerve injury models is shown in **Table 1.8.**

	Model	Ongoing activity			Axonal mechanical sensitivity		
		Aβ-fibre	Aδ-fibre	C-fibre	Aβ-fibre	Aδ-fibre	C-fibre
Frank nerve injury models	Chronic constriction injury	+	+	+/- [a]	+	+	+
	Nerve crush	+	+	+/- [a]	+	+	+
	Partial nerve ligation	NR	+	+	NR	NR	NR
	Spinal nerve ligation	+	+	+/- [b]	NR	NR	+
Non-frank nerve injury models	Neuritis induced by CFA	+	+	+	-	+	+
	Neuritis induced by Zymosan	NR	NR	NR	NR	NR	NR
	Localised axonal transport disruption	-	-	-	+	+	+
	Chemotherapy induced peripheral neuropathy	+	+	+	NR	NR	NR

Table 1.8 A summary of the electrophysiological changes that occur in different models of neuropathic pain. The development of AMS and ongoing activity may occur in both the presence and absence of frank nerve injury. NR – data not reported. [a] rarely reported [b] v. low rates - uninjured only.

1.6 Summary of the mechanisms of neuropathic pain

In the following section, our current understanding of the peripheral and central mechanisms of neuropathic pain that occur following nerve injury are briefly reviewed. The major mechanisms of neuropathic pain that occur following a frank nerve injury are summarised in **Figure 1.3**.

1.6.1 Peripheral mechanisms

Frank nerve injury

Frank nerve injury (complete axotomy/crush) can cause a variety of physiological changes to the nerve. Initially, Schwann cells and macrophages break down degenerating axons distal to the injury site in a process known as Wallerian degeneration (Stoll et al., 1989). Additionally, numerous different types of inflammatory mediators and trophic factors are increased at the injury site (Heumann et al., 1987; Perrin et al., 2005; Shubayev and Myers, 2000; Zhong and Heumann, 1995). These mediators may act on ion channels and receptors (see neuro-immune interactions) located on uninjured axons in close proximity to the injured ones, causing them to become sensitised (Li et al., 2000; Wu et al., 2002). Axotomy causes the complete cessation of axonal transport and at the proximal end of the injured nerve, injured axons develop regenerating sprouts that form a neuroma (Devor and Wall, 1976; Kwon et al., 2000). Axonal sprouts are sensitive to mechanical, chemical and heat stimuli (Blenk et al., 1996; Scadding, 1981; Welk et al., 1990), which is likely to be due to the accumulation of anterogradely transported ion channels at the proximal end of injured axons (Devor and Govrin-Lippmann, 1983; Devor et al., 1993). Sodium channels have also been shown to accumulate along the length of the axon which may further contribute to the increased excitability of injured afferents (Devor et al., 1993). It is thought that regenerating sprouts contribute towards movement evoked radiating pain, as painful responses can be produced upon mechanical activation of a neuroma (Nystrom and Hagbarth, 1981).

As previously reviewed, frank nerve injury can cause the development of ongoing activity in injured A-fibre axons (Kajander and Bennett, 1992; Matzner and Devor, 1994; Scadding, 1981; Welk et al., 1990) and may also ongoing activity in uninjured C-fibre axons, although firing rates are reported to be very low (Djouhri et al., 2012; Djouhri et al., 2006; Wu et al., 2001; Wu et al., 2002). The development of ongoing activity is associated with an increased expression of sodium channels ($Na_v1.8$) (Devor et al., 1993; Gold et al., 2003; Matzner and Devor, 1994) and activation of hyperpolarization-activated cyclic nucleotide–gated (HCN) 2 channels (Emery et al., 2011). Ongoing activity is thought to be responsible for symptoms such as spontaneous pain (Arner et al., 1990; Kleggetveit et al., 2012). Moreover, it provides an afferent barrage that may lead to central changes (see section **1.5.2**) required for the development and maintenance of neuropathic pain (Campbell and Meyer, 2006; Porreca et al., 1999; Quartilho et al., 2003).

Nerve damage can also cause chemical sensitisation of sensory afferents. Injured and uninjured A- and C-fibre axons develop sensitivity to inflammatory mediators (see Neuro-immune interactions), in addition to adrenaline and noradrenaline (Devor and Govrin-Lippmann, 1983; Schafers et al., 2003; Wall and Gutnick, 1974a; b; Welk et al., 1990).

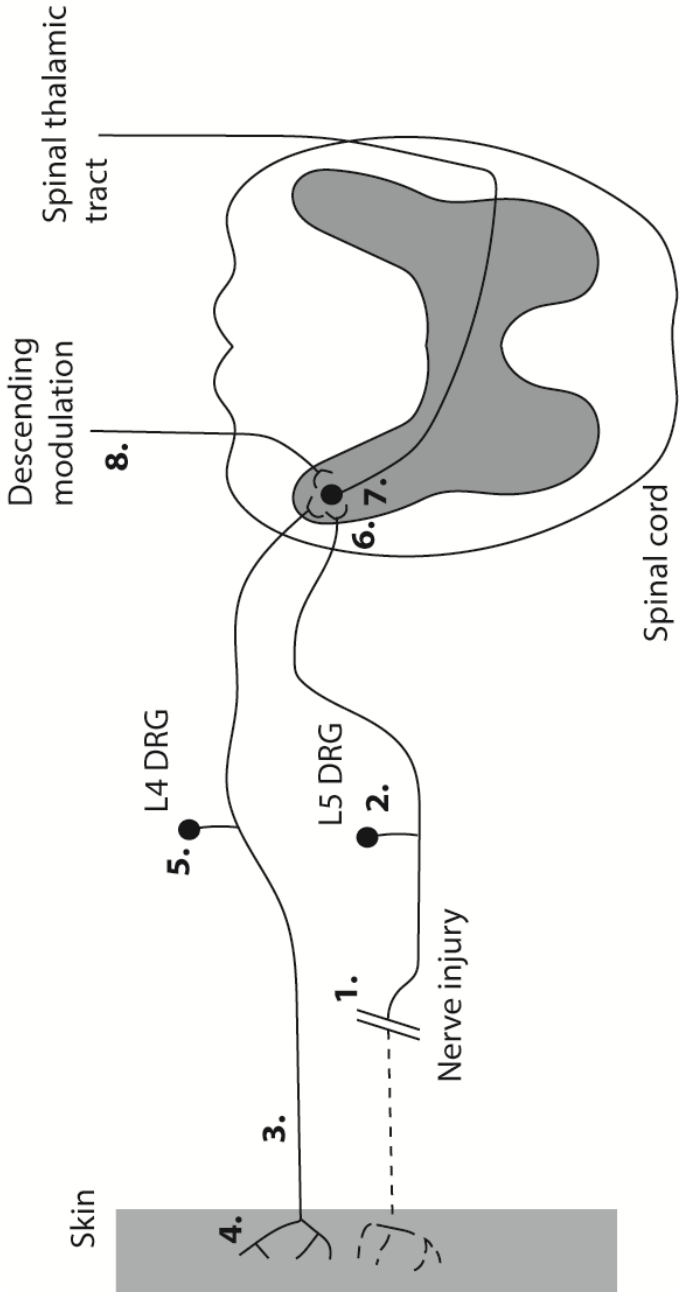

Figure 1.2 Changes to the nervous system following spinal nerve injury.
1) Nerve injury causes the development of excitability (ongoing activity, mechanical and chemical sensitivity) at the injury site. 2) The expression of different proteins is up/down regulated due to alterations in retrograde signalling. Ongoing activity can also develop in the DRG. 3) Schwann cells initiate Wallerian degeneration of the injured nerve, uninjured nerves siting close by may be affected by cytokines and growth factors. 4) Primary afferent nociceptors can also be sensitised by trophic factors and inflammatory mediators. 5) Proteins in uninjured DRGs can be up/downregulated in response to sensitisation of primary afferents in the periphery. 6) Responses to cutaneous stimuli are amplified due to sensitisation of post-synaptic dorsal horn. 7) Microglial cells may contribute to dorsal horn sensitisation 8) Changes in descending modulation may also cause increase responsiveness of dorsal horn neurons. Adapted from (Campbell and Meyer, 2006).

Neuritis

As previously reviewed, AMS develops within intact nociceptive axons following neuritis (Bove et al., 2003; Dilley and Bove, 2008b; Dilley et al., 2005). The mechanisms that lead to the development of AMS are not well understood and therefore require further investigation. It is likely that neuro-immune interactions that include the sensitisation of ion channels (see **page 49**) and the disruption of axonal transport (Amano et al., 2001; Dilley et al., 2013) contribute to the development of AMS. In normal conditions, axonal transport coordinates the delivery of sensory ion channel components, including those that are mechanically sensitive, to the peripheral terminals of neurons (Alessandri-Haber et al., 2003; Guo et al., 1999; Koschorke et al., 1994) (**Figure 1.4 A**). The components necessary for the development of AMS in C-fibre neurons are transported via axonal transport (Dilley and Bove, 2008a). It is hypothesised that axonal transport disruption causes an accumulation of mechanically sensitive ion channels, which are locally inserted into the membrane proximal to the treatment site (Dilley and Bove, 2008a; Proske and Luff, 1998) (**Figure 1.4 B**). Axonal transport disruption is also reported to cause sprout formation (Gallo and Letourneau, 1999), which, similar to sprouts in a neuroma, could also be mechanically sensitive. Axonal mechanical sensitivity may be a cause of movement evoked radiating pain in patients. Neurons with AMS respond to approximately 3% stretch, which can be generated in nerves during normal limb movements (Dilley et al., 2003; Dilley et al., 2005). Additionally, AMS may also be responsible for the nerve trunk pressure hypersensitivity seen in patients (e.g. Tinel's sign) (Greening et al., 2005; Ide et al., 2001).

Ongoing activity originates from the inflamed site in intact nociceptive axons (Bove and Dilley, 2010; Bove et al., 2003; Richards et al., 2011). Similar to the development of ongoing activity following frank nerve injury, HCN2 channels (Richards and Dilley, 2015) and sodium channels are likely to be involved. Intact nociceptive axons innervating deep tissue also develop chemosensitivity to inflammatory mediators, which provides another source of ongoing activity (Govea et al., 2017; Richards et al., 2011). Generation of ectopic activity in nociceptors innervating deep tissues is

consistent with the deep ache frequently described by patients (Birklein et al., 2001; Dilley and Greening, 2012).

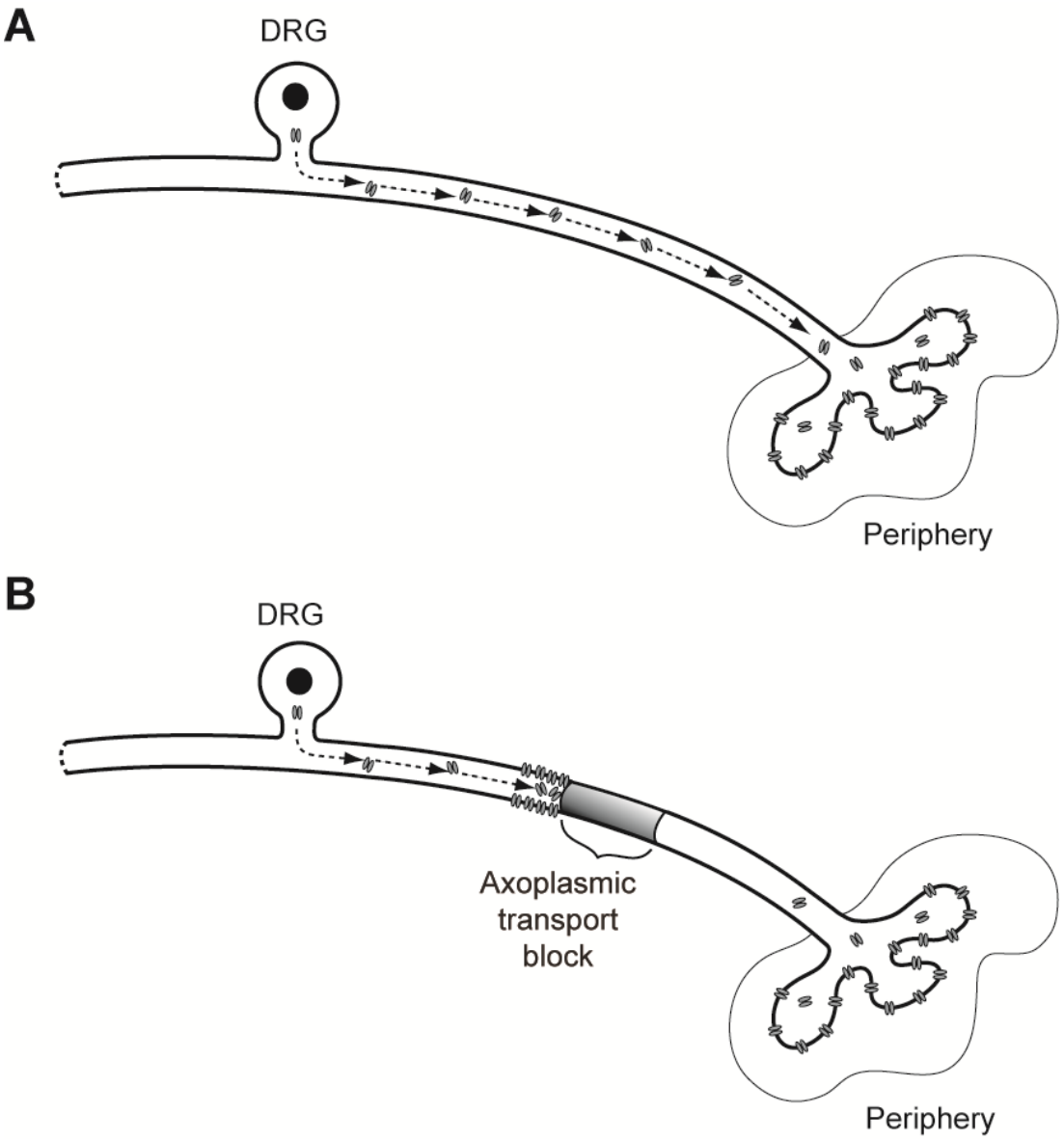

Figure 1.3 Disruption to axonal transport in sensory neurons.
Under normal conditions, sensory ion channels are transported from the cell bodies of the DRG to the peripheral terminals where they are inserted into the membrane. When axonal transport is disrupted sensory ion channels are proposed to accumulate at the site of disruption and be locally inserted into the membrane. This leads to hotspots of mechanical sensitivity, suggesting mechanically sensitive ion channels accumulate where axonal transport has been disrupted. Adapted from (Dilley and Bove, 2008a).

Neuro-immune interactions

As previously reviewed, a variety of inflammatory mediators are reported to be present at a neuritis site (see section **1.4.1**). These mediators may alter the properties of ion channels (e.g. TRPV1 and $Na_v1.8$) on nociceptive axons, thereby increasing the sensitivity of the axon. Detailed below are the mechanisms by which inflammatory mediators can sensitise/excite axons.

Nerve Growth factor

The neurotrophic factor NGF is produced in response to inflammation and causes the sensitisation of nociceptive neurons (Bennett et al., 1998a; Dmitrieva and McMahon, 1996; Koltzenburg et al., 1999; Woolf et al., 1997). This sensitisation can be mediated through a direct action of NGF on nociceptive neurons, for example, through binding to the tropomyosin A receptors (TrK A). This in turn results in the activation of downstream signalling pathways, the mechanisms of which are somewhat uncertain (see Bonnington and McNaughton, 2003; Chuang et al., 2001; Shu and Mendell, 2001; Stein et al., 2006), but involve protein kinases. Activation of protein kinases enhances the trafficking of ion channels, such as TRPV1, to the membrane (Stein et al., 2006; Zhang et al., 2005) and leads to the phosphorylation of ion channels, thereby increasing their sensitivity (Bonnington and McNaughton, 2003). Additionally, NGF is reported to enhance mechanosensitivity by causing an increase in the synthesis of mechanically sensitive ion channels (Di Castro et al., 2006).

Cytokines

During the Inflammatory response, pro-inflammatory cytokines (e.g. TNF, IL-6 and IL-1β) are released from macrophages and neutrophils and play a role in the sensitisation of primary sensory neurons (Ferreira et al., 1988; Obreja et al., 2002b; Ozaktay et al., 2002; Schafers et al., 2003). Tumour necrosis factor can bind to TNF receptors that are present on sensory neurons (Pollock et al., 2002). Through binding to TNF receptors signalling pathways are activated, which have been shown to cause the sensitisation of TRPV1 and TTX resistant sodium channels (Jin and Gereau, 2006; Nicol et al., 1997), in addition to the increased trafficking of TRPV1 and TRPA1 to the membrane (Meng et al., 2016). The receptor components required to transduce the

signal from IL-6 and IL-1β are present within sensory neurons (Gardiner et al., 2002). There is evidence to suggest that these interleukins are also involved in the sensitisation of ion channels. For example, both interleukins can sensitise the TRPV1 ion channel through a PKC dependent mechanism (Obreja et al., 2005; Obreja et al., 2002a). Interleukin-6 has been reported to sensitise unmyelinated joint afferents to mechanical stimulation, suggesting that it is involved in the modulation of mechanically sensitive ion channels (Brenn et al., 2007).

Chemokines

Macrophages and neutrophils also produce chemoattractant molecules known as chemokines, which have numerous roles in inflammation. Chemokines can bind to G-protein coupled chemokine receptors, of which there are various types of expressed in primary sensory neurons (Oh et al., 2001). Through binding to these receptors, chemokines can cause excitation in sensory neurons. For example, the chemokines CCL2 and CXCL1 promote CGRP release in primary sensory neurons and cause an increase in intracellular calcium release, an effect mediated through PKC and PLC activation (Qin et al., 2005). In vivo application of the chemokine CCL2 causes an increase in the excitability of inflamed and injured neurons (Richards et al., 2011; Sun et al., 2006; Wang et al., 2010). This effect is likely to be mediated through the activation of the TRPV1 and TRPA1 ion channels (Jung et al., 2008; Wang et al., 2010), the increase in density of TRPV1 and $Na_v1.8$ channels (Kao et al., 2012), or the inhibition of voltage gated potassium channels (Sun et al., 2006).

Bradykinin

Bradykinin is produced during the inflammatory response and can cause the sensitisation of nociceptive neurons (Ferreira et al., 1993; Franz and Mense, 1975). Bradykinin binds to B1 and B2 receptors that are coupled to G protein coupled receptors, which activate PLC. This activation results in the release in intracellular calcium from intracellular calcium stores, which in turn activates kinases, such as PKC, which is suggested to enhance TRPV1 activity (Kress et al., 1997; Premkumar and Ahern, 2000) Additionally, bradykinin can activate TRPA1 through PLC/PKA signalling pathways (Bandell et al., 2004; Wang et al., 2008).

Prostaglandins

Prostaglandins such as PGH2 are produced by the conversion of arachidonic acid by cyclooxygenase (COX) enzymes during inflammation. Prostaglandins bind to EP receptors, which are coupled to GPCRs. The prostaglandins PGI2 and PGE2 sensitise nociceptive afferents (Pitchford and Levine, 1991). For example, PGE2 sensitises C and A delta fibres to mechanical stimuli (Martin et al., 1987), most likely due to a PKA induced reduction in the sensitivity of high threshold mechanosensitive ion channels (Cho et al., 2002). PGE2 & PGI2 also augment the response of nociceptive neurons to capsaicin and can sensitise $Na_v1.8$ sodium channels present upon these neurons (Gold et al., 1996; Pitchford and Levine, 1991).

Nucleotides

Nucleotides (e.g. ATP) are important in mediating the inflammatory response (Ulmann et al., 2010). Nucleotides can bind to ionotropic P2X receptors, or the P2Y receptors that are coupled to GPCRs. Both types of receptor are present in a proportion of primary sensory neurons (Chen et al., 1995; Molliver et al., 2002). It is reported that nucleotides can sensitise nociceptors to mechanical and heat stimuli (Lechner and Lewin, 2009; Tominaga et al., 2001). Nucleotide binding to the P2Y receptor causes activation of signalling pathways, which in turn result in the modulation of potassium and sodium channels, thereby increasing the membrane excitability of neurons (Baker, 2005; Yousuf et al., 2011).

Retrograde signalling and phenotypical changes in the cell body

Frank nerve injury or neuritis may cause phenotypical changes in the cell body of the neuron, both of which are likely to be mediated via retrograde signalling pathways (Reviewed in Abe and Cavalli, 2008). Injury to axons causes the complete cessation of axonal transport. This leads to interruption of target-derived neurotrophic factors, such as glial-derived neurotrophic factor (GDNF), which can cause alterations in the levels of ion channels and receptors in the DRG (Bennett et al., 1998b; Boucher et al., 2000). In 'spared' axons that are in close proximity to the injured ones, a retrograde signal may be generated. This signal is conveyed via an importin-dynein retrograde-signalling complex, which facilitates the transport of molecules (e.g. neurotrophic factors) to the DRG (Curtis et al., 1998; Hanz et al., 2003; Perry et al., 2012). Nerve inflammation increases the levels of neurotrophic factors, such as nerve growth factor (NGF) (Obata et al., 2002), which can subsequently be retrogradely transported to the DRG. Nerve growth factor causes activation of extracellular signal related kinase (ERK) or MAPK pathways in the cell body (Delcroix et al., 2003; Obata et al., 2004), which can initiate changes to the transcription of sensory ion channels and other proteins (Obata et al., 2005; Obata et al., 2006).

1.6.2 Central mechanisms

Central sensitisation is a phenomenon that occurs within the dorsal horn of the spinal cord. The current understanding of the mechanisms that produce central sensitisation are briefly summarised below (**Figure 1.5**)

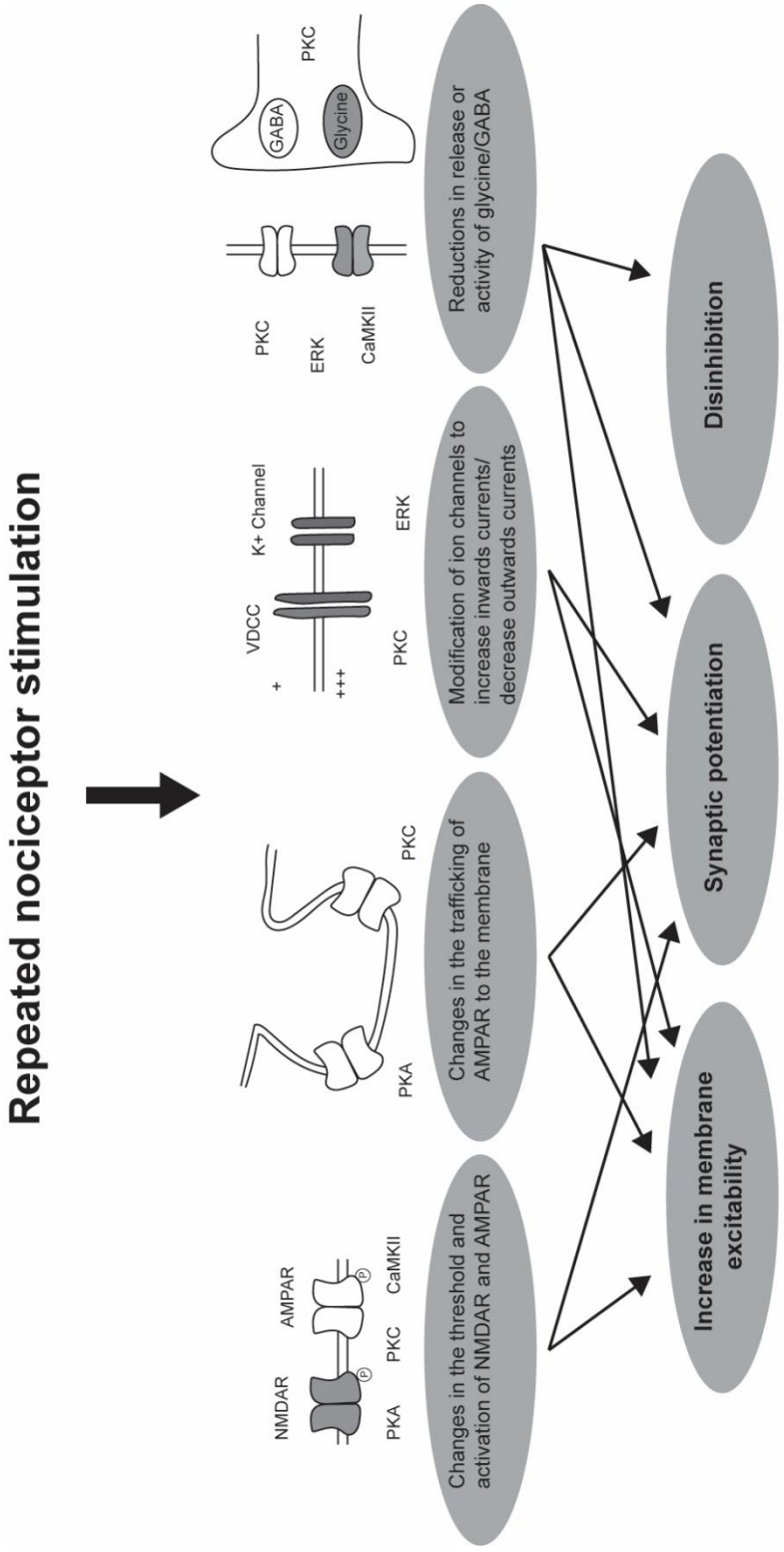

Figure 1.4. Summary of the main mechanisms that lead to the development of central sensitisation. Repeated nociceptor stimulation causes a large influx of calcium ions across the postsynaptic membrane. This causes activation of protein kinases (e.g. PKC, PKA). These kinases can phosphorylate postsynaptic proteins to modify their function. Kinases also mediate changes to receptor trafficking and cause reductions in the release and activity of glycine and GABA inhibitory pathways. Adapted from (Latremoliere and Woolf, 2009).

At the synapses between sensory neurons and dorsal horn neurons within the spinal cord, repeated stimulation of sensory neurons causes an improvement in the efficiency of this connection. Briefly, ongoing activity in nociceptors may cause release of glutamate and other neuromodulators, such as substance P, resulting in the prolonged opening of glutamate and NK1 receptors respectively. This sustained opening causes a large influx of calcium ions across the postsynaptic membrane. This in turn results in activation of kinases that phosphorylate postsynaptic NMDA and AMPA receptors, causing an increase in their currents (Chen and Huang, 1992; Esteban et al., 2003). Calcium induced activation of protein kinases can also initiate signalling (e.g. ERK), which lead to changes to transcription (Hu et al., 2007; Kawasaki et al., 2004; Wei et al., 2006). Additionally, ERK activation can modify potassium currents important in determining excitability of dorsal horn neurons (Hu et al., 2007), phosphorylate NMDA receptors to increase function (Slack et al., 2004), and increase AMPA receptor trafficking to the postsynaptic membrane (Galan et al., 2004). Together, these changes increase the excitability of the post-synaptic dorsal horn neuron. In some cases, where Aβ-fibre afferents also synapse onto pain signalling dorsal horn neurons, the postsynaptic changes described above may also improve the efficiency of this synapse. This potentiation of Aβ-fibre afferent input into the spinal cord is proposed to be a mechanism that contributes towards the development of allodynia (Klein et al., 2008; Xu et al., 2015)

A proportion of A-fibres undergo transcriptional changes after nerve injury. These fibres may start expressing neuromodulators such as substance p, CGRP and brain derived neurotrophic factor (BDNF) (Fukuoka et al., 2001; Miki et al., 1998; Noguchi et al., 1995). Through stimulation of these fibres, neuromodulators (e.g. substance P) can be released into the dorsal horn of the spinal cord (Malcangio et al., 2000). Substance P activation of NK1 receptors in the dorsal horn may 1) activate nociceptive afferents 2) cause slow synaptic potentials contributing to the development and maintenance of central sensitisation (Pitcher and Henry, 2004).

Nerve injury can cause the degeneration of GABA and Glycine inhibitory neurons in the dorsal horn of the spinal cord (Ibuki et al., 1997; Moore et al., 2002). Furthermore, GABA and glycine receptors can be desensitised through the action of

kinases (Harvey et al., 2004; Porter et al., 1990) This desensitisation reduces the level of tonic inhibition produced by these neurotransmitters and makes dorsal horn neurons more likely to fire in response to excitatory inputs (Lin et al., 1996). Changes to descending pathways may also play a role in the mechanisms of central sensitisation. For example, facilitatory pathways from higher centres such as the rostral ventromedial medulla are involved in the maintenance of central sensitisation (Burgess et al., 2002; Vera-Portocarrero et al., 2006).

1.7 Summary

Chronic pain is distressing to an individual and is a tremendous burden on our society because of costs associated with lost work days and healthcare. Origins of long-term pain that is related to a lesion or disease of the somatosensory nervous system is defined as neuropathic. In certain patients that complain of neuropathic pain like symptoms, diagnosing the cause of pain may be straightforward as they may have obvious trauma to a nerve, which may be severed, crushed or compressed. In these patients with frank nerve injuries, physiological changes to the nerve fibres at the injury site are associated with the development of painful sensory symptoms. However, many patients suffering from chronic musculoskeletal disorders, which include WAD, NSAP, fibromyalgia and CRPS-1, complain of symptoms that resemble neuropathic pain in the absence of frank nerve injury upon routine clinical examination. For example, in these patients pain can often be evoked upon normal movements, which can make day-to-day activities extremely difficult. It is unclear how such symptoms develop, but it is hypothesised that localised nerve inflammation might play an important role.

The mechanisms of neuropathic pain can be studied using animal models of nerve injury. Pain signals are normally transmitted to the central nervous system via nociceptive neurons. These sensory neurons contain ion channels at their peripheral terminals that are able to respond to noxious stimuli. Following frank nerve injury, physiological changes occur at the injury site in both nociceptive and non-nociceptive fibre types, which may lead to the development of AMS or ongoing activity. In the severed axons, the development of AMS and ongoing activity is associated with the

complete cessation of axonal transport. Axonal mechanical sensitivity is the probable cause of movement-evoked pain in patients. Ongoing activity, which can develop in injured and uninjured axons, is likely to be responsible for spontaneous pain in patients. Axonal mechanical sensitivity and ongoing activity are likely to contribute towards afferent barrage that leads to central changes, which may cause other neuropathic pain symptoms, such as allodynia.

Following neuritis, AMS and ongoing activity can also occur. However, AMS only develops in nociceptive axons. The mechanisms that lead to the development of AMS are associated with the disruption to axonal transport, which is thought to lead to the accumulation of anterogradely transported ion channels, resulting in hotspots of excitability. However, due to the potential confounding factors caused by inflammation, it is unknown what the relative contribution of axonal transport disruption is to this mechanism. To examine the effects of axonal transport disruption in intact axons in isolation, low concentrations of anti-mitotic drugs can be applied to nerve trunks. Currently, it is unknown how axonal transport disruption leads to the development of AMS and it has not been directly proven that ion channels, such as those that are mechanically sensitive, are responsible for this phenomenon.

Hypothesis

Inflammation-induced axonal transport disruption leads to an accumulation of anterogradely transported mechanically sensitive ion channels, which are locally inserted into the axonal membrane. The increased levels of ion channels at the treatment site leads to the development of mechanical sensitivity.

Aims

The ultimate aim of this project is to investigate the role of axonal transport disruption in the development of AMS in intact C-fibre neurons. Axonal transport disruption will be induced in the sciatic nerve through local application of vinblastine. Additionally, axonal transport disruption will also be examined following a localised neuritis. The development of AMS will be compared between the models.

The main aims of the project are detailed below:

1. **Investigate the profile of axonal mechanical sensitivity following localised axonal transport disruption**

   The time course of AMS following axonal transport disruption is not known. Understanding the time course will advance our understanding of how AMS correlates with the previously reported time course for axonal transport disruption and pain behaviours. Therefore, this study will use single unit in vivo electrophysiological recordings to determine the proportion of mechanically sensitive C-fibres on different days following vinblastine treatment.

2. **Examine the properties of mechanically sensitive hotspots following vinblastine-treatment and neuritis**

   The properties of AMS hotspots have not previously been reported and it has not been directly proven that mechanically sensitive ion channels contribute towards AMS. Therefore, a force-feedback controlled stimulator will be used in an ex vivo electrophysiological set up to determine the threshold of mechanically sensitive axons and whether they produce graded response to changes in force. Mechanically sensitive ion channel blockers will be applied to hotspots in order to elucidate whether mechanically sensitive ion channels contribute towards AMS.

3. **Identify the channels responsible for axonal mechanical sensitivity following vinblastine-treatment and neuritis**

   Using immunohistochemistry, determine whether the putative mechanically sensitive ion channels (TRPV1, TRPA1, ASIC3) are disrupted and accumulate at the site of axonal transport disruption. Pharmacological agents (agonists of selected sensory ion channels) will be applied to nerves to determine if they cause excitation of mechanically sensitive axons, giving indication of whether levels of these channels are increased and functional in neurons with AMS.

Chapter 2

Materials and Methods

2.1 Animals

Experiments were carried out in strict accordance with the UK Animals Scientific Procedures Act 1986. A total of 154 adult male Sprague Dawley rats (200–450 g; Charles River, Kent, UK; Harlan, Bicester, Oxon, United Kingdom) were used in this study. Rats were housed in groups of 2-4 in cages (50 x 35 x 26 cm) with sawdust, soft nesting material, soft wood blocks and plastic tubes. They had *ad libitum* access to food and water.

2.2 Surgery

All surgeries were carried out under aseptic conditions. Animals were anaesthetized and maintained on isoflurane (1.75%) in oxygen. Animals were shaved at the level of the left thigh and the surrounding skin was washed with 70% ethanol. Following this, the skin was disinfected with Videne antiseptic aqueous solution (Williams Medical Supplies, Rhymney, UK) and sterile drapes were placed on the animal. During surgical procedures, a heat mat was used to maintain body temperature. Following all surgical procedures, animals were closely monitored for adverse effects.

2.2.1 Vinblastine surgery

Vinblastine was applied to the sciatic nerve of adult rats (n = 66) as previously described (Dilley and Bove, 2008a). A two-centimetre incision was made in the skin just posterior to the femur. Following this, curved surgical scissors were used to make a blunt dissection through the myofascial plane associated with biceps femoris. A 7–8 mm length of the sciatic nerve was carefully freed from its surrounding connective tissue. A strip of Parafilm (6 mm × 20 mm; Pechiney Plastic Packaging, Menasha, WI) was positioned under the nerve to prevent leakage of the drug onto the surrounding tissue. Using curved forceps, a 5 mm × 5 mm × 10 mm piece of absorbable gelatin sponge (Spongostan; Ferrosan, Denmark) saturated in 0.1 mM vinblastine (~150 µL; diluted in filtered 0.9% w/v saline); was wrapped around the nerve. The concentration used was determined from previous studies (Dilley and Bove, 2008a; Fitzgerald et al., 1984). After 15 min, the Gelfoam and Parafilm were removed and the nerve was rinsed with saline. The location of the treatment site was carefully noted. The muscle and skin were closed using 4/0 monofilament sutures (Vicryl;

Ethicon, West Lothian, United Kingdom). The wound was rinsed with sterile saline to remove any dried blood and disinfected with betadine topical spray (Williams Medical Supplies, Rhymney, UK). The animal was allowed to recover on a heat mat and was then transferred into a clean cage. In a separate group of animals (n = 7), the same surgical procedure was followed except that gelfoam was saturated in sterile 0.9% w/v saline.

2.2.2 Neuritis surgery

An experimental neuritis was induced in adult Sprague Dawley rats (n = 38) as previously described (Dilley and Bove, 2008b). A two-centimetre incision was made in the skin just posterior to the femur. Following this, curved surgical scissors were used to make a blunt dissection through the myofascial plane associated with biceps femorus. A 7–8 mm length of the sciatic nerve was carefully freed from its surrounding connective tissue. A 5 mm × 5 mm × 10 mm piece of gelfoam saturated in CFA (~150 µL; diluted 1:2 in filtered saline) was loosely wrapped around the nerve (**Figure 2.1**). The muscle and skin were closed using Vicryl 4/0 monofilament sutures. The wound was rinsed with sterile saline to remove any dried blood and disinfected with betadine topical spray. The animal was allowed to recover on a heat mat before being transferred into a clean cage.

2.2.3 Partial ligation surgery

Partial ligation surgeries were performed to assess the disruption to the anterograde transport of sensory ion channels. A two-centimetre incision was made in the skin just posterior to the femur. Following this, a blunt dissection through the myofascial plane associated with biceps femorus and a 10 mm length of the sciatic nerve was carefully freed from its surrounding connective tissue. Using a 6-0 monofilament polyamide suture (Vicryl; Ethicon, West Lothian, United Kingdom), approximately 1/3-1/2 of the nerve was tied off, approximately 2mm proximal to the trifurcation. The suture was tied tight enough to sufficiently constrict the area whilst leaving the remaining portion of the nerve undamaged. The nerve was then treated with saline (n = 8), vinblastine (n = 8) or CFA (n = 8) (as previously described) at a position 3-5mm proximal to where the nerve has been ligated. The skin and muscle were then closed

using a Vicryl 4/0 ethilon suture. The wound was rinsed with sterile saline to remove any dried blood and disinfected with betadine topical spray. The animal was allowed to recover on a heat mat before being transferred into a clean cage.

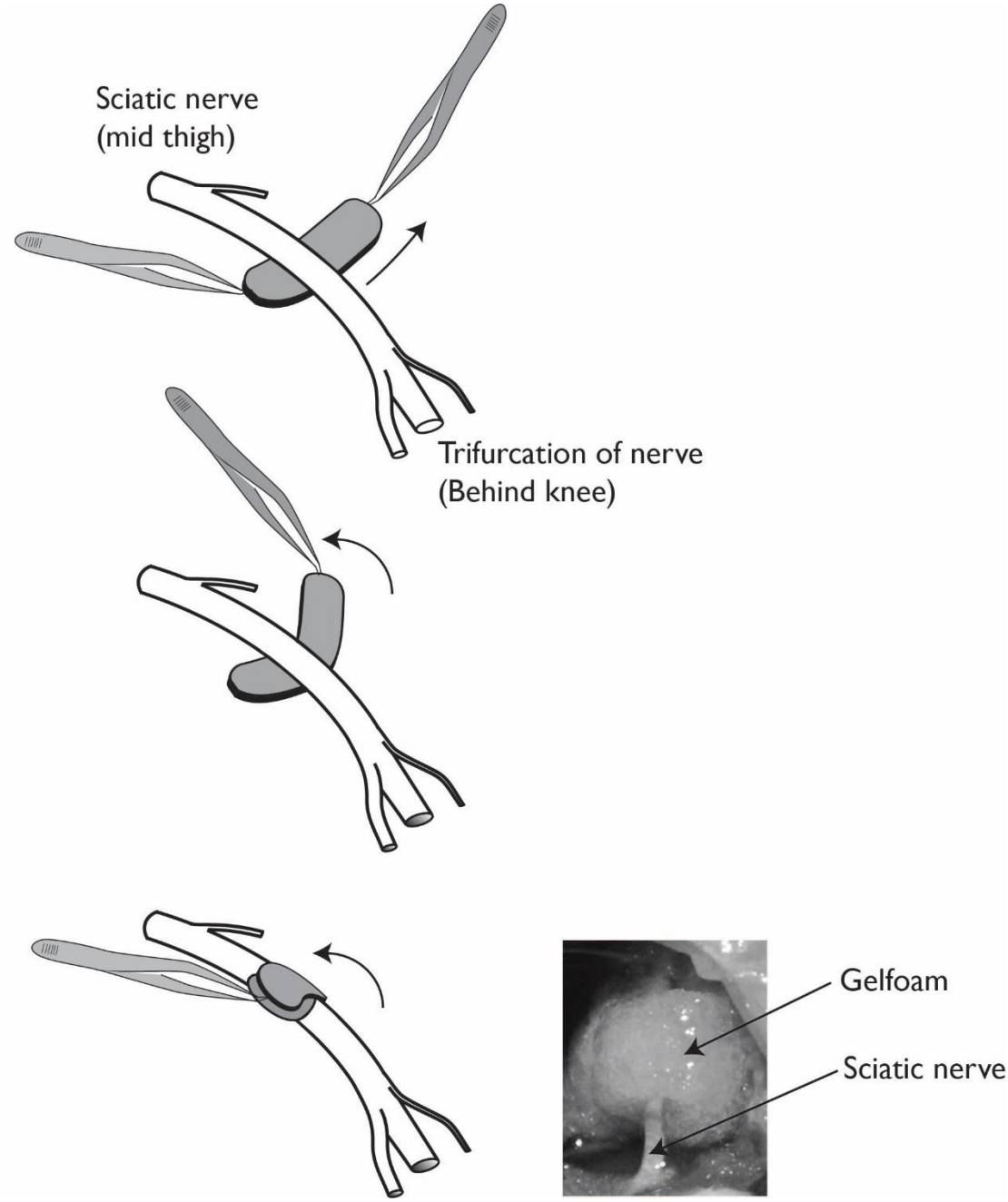

Figure 2.1 Induction of the neuritis lesion. Using curved forceps, gelfoam saturated in CFA is gently wrapped around the sciatic nerve. Image used with permission from A. Dilley

2.3 Single unit in vivo recordings

Single-unit electrophysiological recordings were made from C-fibre axons teased from the L5 dorsal root. Axons from within the L5 dorsal root were examined because many of these axons pass through the treatment site and innervate the plantar surface of the foot, which is the area of skin that was tested during previous behavioural studies (Dilley et al., 2013).

Animals were anesthetized with 1.5 g/kg 25% w/v urethane intraperitoneally. Smaller doses of urethane were given intraperitoneally as required to maintain absence of pinch withdrawal and corneal reflexes. The body temperature was monitored by a rectal thermistor probe and maintained at 37°C using a heated pad (Harvard Apparatus, Kent, United Kingdom). A lumbar laminectomy was performed from L2 to L5 to expose the spinal canal. The surrounding skin was sutured to a metal ring to form a mineral oil pool. The dura mater was opened and the L5 dorsal root was cut close to the dorsal root entry zone. The cut end of the dorsal root was placed onto a glass platform (9 mm × 5 mm).

Fine gold wire (0.075 mm diameter, Advent Research Materials Ltd, UK) electrodes that were connected to an electrode holder mounted on a micromanipulator (World Precision Instruments Inc., USA) were used to make recordings. Using finely sharpened forceps, fine filaments (6–10 μm) were teased from the cut end of the dorsal root. Filaments were split until single action potentials could be evoked using electrical stimulation of the dorsal root. Bipolar stimulating electrodes were placed under the root approximately 10-15 mm distal to where the recording electrodes were positioned (**Figure 2.2**). To identify C-fibre neurons, electrical stimulation (square wave pulses: 0.5–0.9 ms duration and 10–30 V amplitude) was applied using a constant-voltage isolated stimulator (Digitimer, Hertfordshire, United Kingdom), which was band-pass filtered (10–5,000 Hz), and monitored with an oscilloscope. Only filaments with clearly identifiable waveforms were studied. The latency of the action potential and the conduction distance were used to calculate the conduction velocity of the axon. Conduction velocities below 1.5 m s^{-1} were considered C-fibres (Harper and Lawson, 1985).

2.3.1 Receptive field characterisation

Receptive fields for isolated neurons were searched below the knee using mechanical stimuli. Most receptive fields were located by squeezing the periphery, using either fingers or forceps, or by probing the skin with blunt forceps. The loose property of the skin was exploited to carefully discriminate cutaneous *versus* deep fields (Bove et al., 2003). Cutaneous neurons had receptive fields that remained associated with the skin regardless of the skin excursion. In contrast, deep neurons were identified by moving the skin and repeating the effective stimulus to the same underlying spot. Neurons were only included for further study if they had mechanically sensitive receptive fields in the lower limb located distal to the exposed part of the sciatic nerve, indicating that their axons passed through the treatment site.

After determining the location of the receptive field, the neuron was then collided to confirm its conduction velocity. Collision involved stimulating the receptive field mechanically, whilst stimulating the dorsal root electrically. If the electrical stimulus occurred during the relative refractory period of the neuron to mechanical stimuli, the action potential was not initiated or was delayed.

2.3.2 Axonal mechanical sensitivity testing

To allow access for mechanical stimuli, the sciatic nerves were re-exposed in the thigh at the treatment site, or the equivalent area in untreated animals. In animals that underwent a neuritis surgery the gelfoam was removed prior to AMS testing. A plastic platform (9 mm × 5 mm), notched to accommodate the nerve, was positioned under the nerve with the treatment site in its centre (**Figure 2.2**). Axonal mechanical sensitivity (AMS) was tested with a tapered silicone probe. The probe used in this study was capable of delivering forces up to 400 mN pressure, although in previous studies 200 mN pressure was sufficient to activate mechanically sensitive axons (Dilley and Bove, 2008a; b). The nerve was mechanically stimulated for two seconds at different locations along the platform. Axonal mechanical sensitivity was also tested at locations proximal and distal to the platform, using a flat metal spatula placed beneath the nerve for support. If one of more action potentials were elicited within a two second stimulus, the axon was considered to be mechanically sensitive. Mechanically sensitive neurons were collided to confirm the latency of the neuron. Following mechanical stimulation, the receptive field was re-tested to ensure the neuron was still conducting through the site where the axon had been probed. To prevent the exposed tissue from drying out between mechanosensitivity testing, it was temporarily covered with gauze saturated in warmed saline.

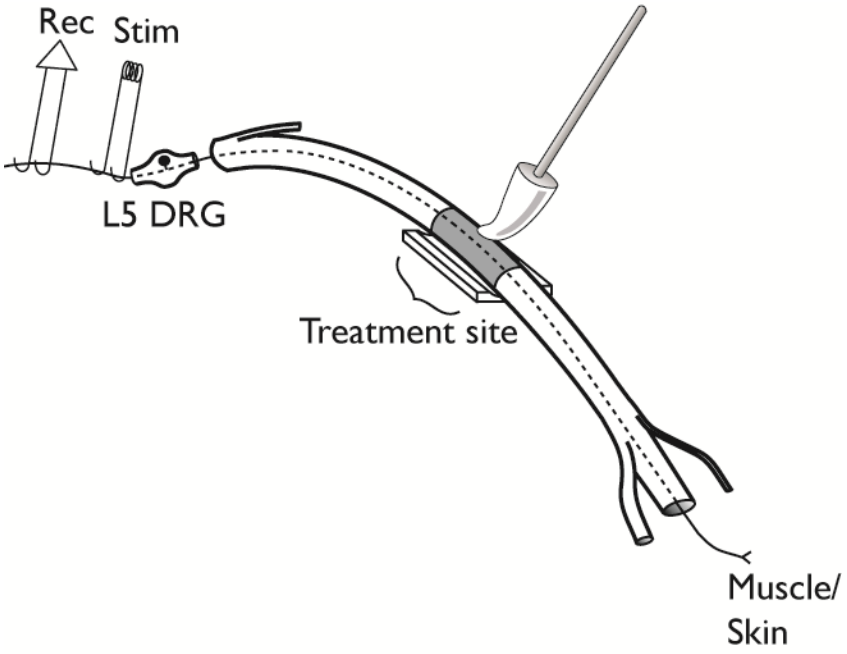

Figure 2.2 Axonal mechanical sensitivity testing. The treatment site (highlighted in grey) was placed on a grooved platform for mechanical sensitivity testing. Recordings were made from the L5 dorsal root, which contains sensory axons that pass through the treatment site and innervate the foot (Dilley and Bove, 2008a).

2.3.3 Experimental Design

Chapter 3 - Profile of axonal mechanical sensitivity in the vinblastine model

In vivo single-unit electrophysiological recordings from C-fibre neurons were carried out at 1 to 15 days following treatment with either vinblastine (n = 18), or saline (n = 3), and in untreated animals (n = 3). After a C-fibre neuron had been identified through collision and its receptive field characterised, the neuron was left for two minutes to ensure there wasn't any residual discharge. Ongoing activity was recorded for three minutes. C-fibre neurons were considered to have ongoing activity if they fired at least once per minute. The neuron was then tested for AMS at the treatment site as described above. In each experiment, approximately 5 - 8 C-fibres were characterised and tested for AMS. Neurons were typically characterised within five hours from the beginning of recording.

Chapter 6 - Electrophysiological evidence for the presence of TRPV1 and TRPA1 in mechanically sensitive axons

Receptive fields were characterised in these experiments. Mechanical receptive fields with deep locations were preferentially searched for in untreated animals. This was to ensure a similar population of C-fibre neurons was compared between groups, because neurons with AMS typically have mechanical receptive fields in deep locations (Bove et al., 2003; Dilley and Bove, 2008a).

In vivo recordings were carried out on vinblastine-treated animals (n = 13) on two to five days post-surgery and neuritis animals (n = 15) on five to eight days post-surgery. An additional set of experiments was carried out on untreated (n = 9) animals. Receptive field and AMS testing were carried out as described above. Following vinblastine treatment or neuritis, one neuron with AMS was usually recorded from in each experiment except when there was more than one neuron with AMS on the same filament (Neuritis; 2/filament, n = 4). In untreated animals, one neuron with a characterised receptive field was typically recorded from each experiment, except when there was more than one neuron with a receptive field on the same filament (2/filament, n = 2). Following characterisation of the neuron, the filament was left for 5 minutes to ensure there wasn't any residual discharge caused by mechanical

sensitivity or receptive field testing. In these experiments, C-fibres neurons were considered to have ongoing activity if they fired at least once per minute.

Perineural application of agonists to the nerve

Gelfoam was used to apply the TRPV1 agonist N-Oleoyldopamine (OLDA) (Tocris, UK) and the TRPA1 agonist Cinnamaldehyde (Sigma, UK) directly to the nerve at the treatment site. Gelfoam application of agonists was carried out on vinblastine-treated (n = 9), neuritis (n = 13) and untreated (n = 9) animals. Both OLDA (diluted in vehicle at concentrations of 10, 50, 200 µM) and cinnamaldehyde (diluted in vehicle at 100, 250, 500 µM respectively) were tested on the same nerves. The vehicle was made up of 1% Dimethyl sulfoxide (Sigma, UK), 0.5% ethanol (Sigma, UK) which was diluted in synthetic interstitial fluid (SIF); in mM: NaCl 107.8, KCl 3.5, $NaHCO_3$ 26.2, NaH_2PO_4 1.7, Na-gluconate 9.6, sucrose 7.6, glucose 5.6, $CaCl_2$ 1.5 and $MgSO_4$ 0.7 [All from Sigma, UK] (Bretag, 1969). Prior to application, all test agents were maintained at 37 ˚C. A strip of parafilm (12 x 20 mm) was initially placed under the nerve to minimise the contact of the agonists with the surrounding muscle tissue. A 15 x 10 x 3 mm piece of gelfoam saturated in the vehicle was gently wrapped around the nerve at the location of the hotspot. Following a 10-minute exposure of the vehicle, increasing concentrations of the first agonist were applied to the nerve. The protocol was then repeated with the second agonist. The individual steps were as follows (also see **Figure 2.3 A**):

1. 10 minute application of vehicle
2. 10 minute application of lowest dose of agonist
3. 10 minute application of middle dose of agonist
4. 10 minute application of highest dose of agonist
5. Receptive field and AMS testing

Nerves were washed thoroughly with SIF between each concentration of agonist. The order of which agonists were applied was alternated between experiments, except following vinblastine-treatment (See flow diagram in **Figure 2.4**). After agonists had been tested, nerves were washed thoroughly and the receptive field and AMS were checked.

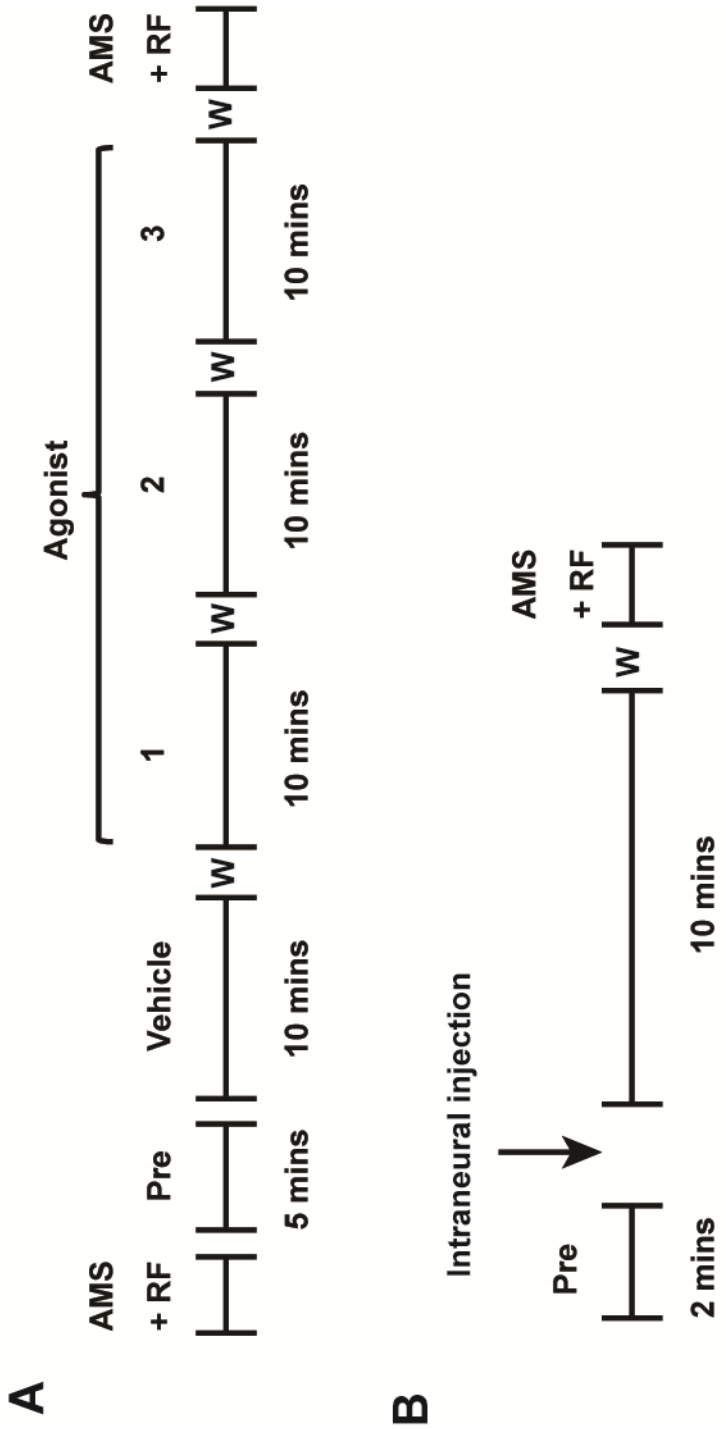

Figure 2.3 Application of agonists to the sciatic nerve. Time lines of the (A) gelfoam application and (B) intraneural injection of agonists to the sciatic nerve. A) Each agonist was applied in incrementing concentrations (1-3) before being washed off with synthetic interstitial fluid. OLDA and vehicle were intraneurally injected into nerves following gelfoam application. Cinnamaldehyde was also injected into nerves in the untreated group; however in neuritis and vinblastine groups, cinnamaldehyde was intraneurally injected alone. AMS – axonal mechanical sensitivity, testing RF – receptive fields testing.

Intraneural injection of agonists

It was apparent that perineural application of the agonists to the nerve had negligible effect on activity levels of AMS neurons (see **Chapter 6**). Therefore, agonists were also injected intraneurally into the nerves. Fifty micro molar OLDA and vehicle were injected at the vinblastine and neuritis treatment site and in untreated nerves following perineural application of agonists. Five hundred micro molar cinnamaldehyde was also injected into untreated nerves following perineural application of agonists. However, in vinblastine-treated and neuritis nerves, 500 µM cinnamaldehyde was injected into the treatment site without previous perineural application. This was to reduce the risk of experimental failure (**Figure 2.4**).

Following AMS and receptive field testing, the filament was left for a period of 2-5 minutes to ensure there was not any residual discharge. Using a 30-gauge needle bent to a 45-degree angle, 100 µL of either OLDA (50µM), cinnamaldehyde (500 µM) or vehicle was intraneurally injected onto the AMS hotspot or into the corresponding location in the nerve of untreated animals. Activity was recorded for 10 minutes before washing with SIF (**Figure 2.3 B**). The receptive field and AMS were re-tested to ensure that the intraneural injection did not cause damage to the axon.

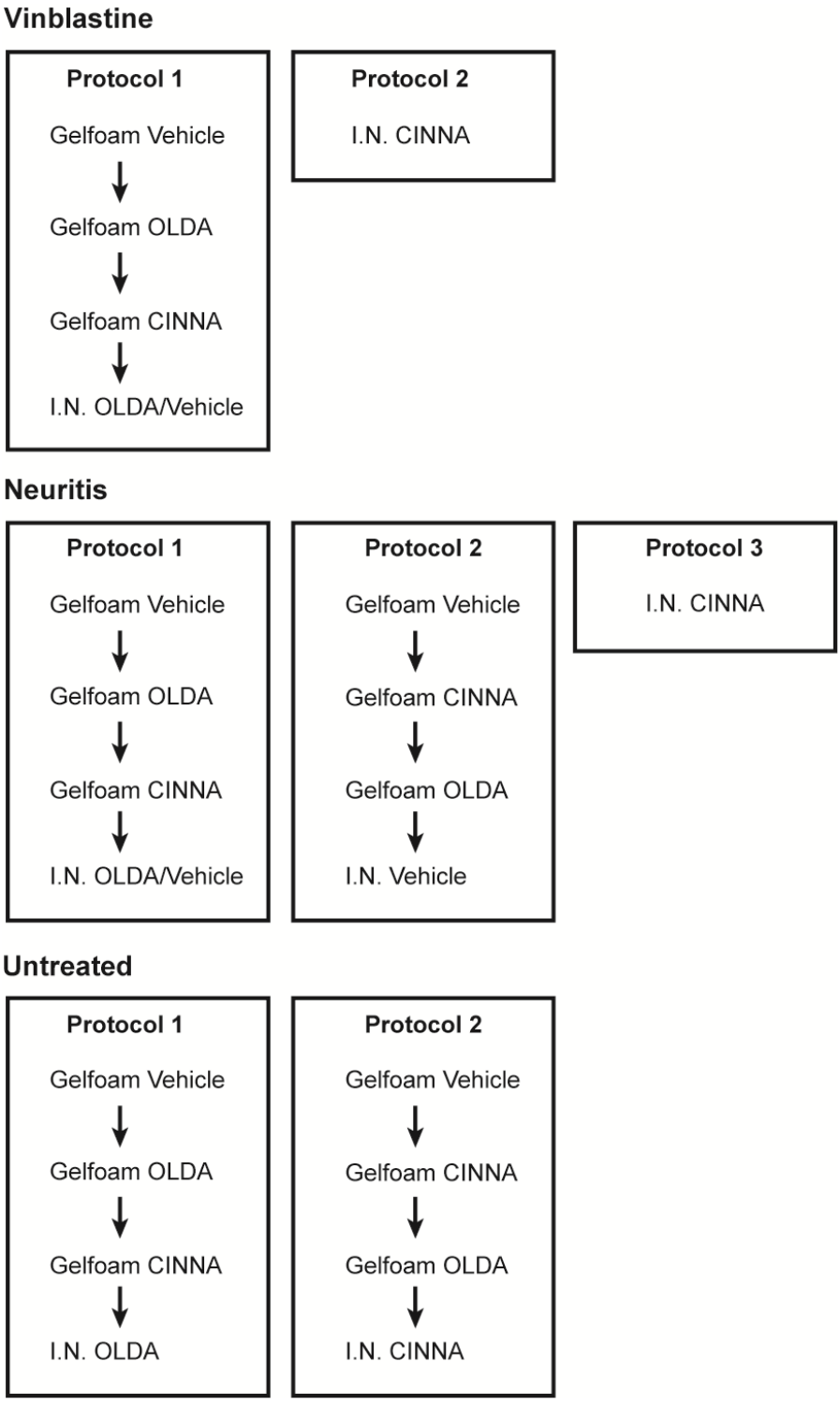

Figure 2.4 Order of agonist application in the different treatment groups.
Note that intraneural injections of cinnamaldehyde were made alone to reduce risk of experimental failure. I.N. – Intraneural, OLDA – N-Oleoyldopamine,
CINNA – Cinnamaldehyde

2.4 Ex vivo recordings

The sciatic nerve was recorded from in ex vivo recording chamber to investigate the properties of mechanically sensitive hotspots and to allow the application of mechanically sensitive ion channel blockers.

2.4.1 Ex vivo recording chamber and set up

The ex vivo recording chamber was based upon the skin-nerve chamber designed by Peter Reeh (Reeh, 1986) (**Figure 2.5**). Further modifications were made in the UK where the chamber was fully assembled. The chamber consisted of a main reservoir that had a silicone base (Sylgard 184 elastomer, Dow corning, US), which was connected to a second recording compartment. The main reservoir was perfused with carbogen buffered SIF (pH 7.4). The hydrostatic pressure of SIF was maintained using a vertical column (130 cm height) and the flow rate into the chamber was regulated through a drop chamber of an infusion set (Alaris, UK) (approximately 1 drop per sec). The chamber was heated to 32 ˚C using a HT10K foil resistive heater (Thor Labs, Germany), which was controlled and maintained with a TC200 temperature controller and a TH10K thermistor (Thor Labs, Germany). A sluice gate (6 on **Figure 2.5**) was used to control the levels of SIF within the chamber.

Experiments were carried out at two to five days following vinblastine-treatment (n = 31) and at four to eight days following neuritis (n = 19). An additional group of experiments were carried out on untreated animals (n = 7). Animals were deeply anaesthetised with euthatal and then transcardially perfused with buffered SIF. The length of the sciatic nerve was dissected from the L5 intervertebral foramen to the point of trifurcation within the popliteal fossa, and carefully transferred into the main reservoir of the ex vivo chamber. In animals that underwent a neuritis surgery the gelfoam was carefully removed. The proximal end of the nerve was passed through a hole connecting the main reservoir and the recording chamber (7 on **Figure 2.5**) using a 30-gauge needle, where it was placed onto the glass platform. The remainder of the nerve was pinned by its connective tissue using fine insect pins to a groove in the silicone floor within the main part of the chamber (5 on **Figure 2.5**). The nerve was left in SIF for one hour prior to recording, after which mineral oil was added to

recording compartment. Using the sluice gate the SIF-oil level was adjusted to ensure that the proximal end of the nerve was in mineral oil.

Fine gold wire (0.075 mm diameter, Advent Research Materials Ltd, UK) electrodes that were connected to an electrode holder mounted on a micromanipulator (World Precision Instruments Inc., USA) were used to make recordings. Recordings were made from fine filaments that were teased from the proximal end of the sciatic nerve, using finely sharpened forceps.

In the majority of experiments, bipolar stimulating electrodes were positioned distal to the treatment site (see 1 **Figure 2.5**). The anode, a tungsten needle electrode, was positioned in the nerve immediately distal to the treatment site. The shaft of the electrode was coated in resin for insulation, except for the tip, which was in contact with the nerve. The cathode, a platinum wire electrode, was positioned within the SIF close to the distal portion of the nerve. At the beginning of each experiment, a large filament was stimulated electrically using an isolated voltage stimulator (Digitimer, Hertfordshire, United Kingdom) at a strength sufficient to produce an A-fibre action potential (square wave pulses; 0.05 ms duration, 3-10 V amplitude). If an A-fibre compound was produced at a suitable threshold (< 3.5 volts) it indicated that the nerve was healthy. Following this, C-fibre recordings were made from fine filaments, which were identified by electrical stimulation as described above (see section **2.3**). Only fine filaments were examined with <15 C-fibre waveforms. The number of C-fibres was counted by gradually increasing the voltage from zero up until the maximum number of waveforms were elicited.

2.4.2 Axonal mechanical sensitivity testing

Mechanically sensitive hotspots were identified with a tapered silicone probe. To confirm the latency, action potentials were collided by stimulating the hotspot mechanically, whilst stimulating the nerve.

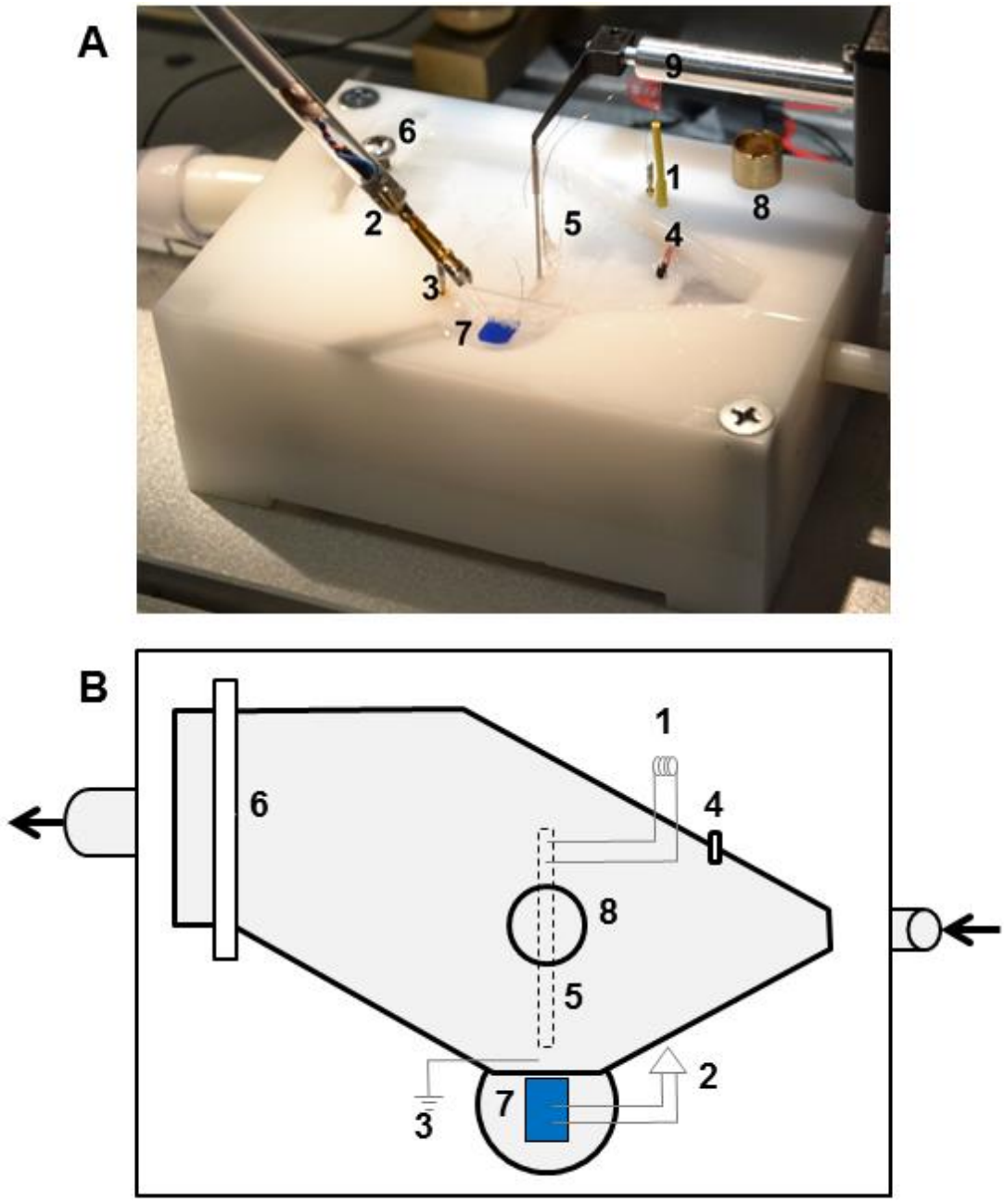

Figure 2.5 Ex vivo recording chamber. A) Photo and B) diagram of ex vivo chamber. The base of the chamber had a 5mm coating of silicone 1. Stimulating electrodes 2. Recording electrodes 3. Ground electrode (platinum wire, WPI, UK) which is positioned above the nerve just before it enters the recording chamber 4. Thermistor 5. Groove that the nerve fits into 6. Sluice gate for controlling levels of SIF 7. Recording Chamber 8. Brass well used to isolate AMS hotspot 9. Mechanical stimulator

2.4.3 Experimental design

Conduction through the treatment site

In several neuritis experiments, an A-fibre compound action potential was absent on distal stimulation, indicating conduction block. In these experiments, a C-fibre strength electrical pulse was then applied to determine whether any C-fibre axons were present. If no C-fibre axons were being identified after stimulating five teased filaments from different parts of the nerve, it was assumed that conduction was blocked distal to the treatment site. These nerves were therefore stimulated at the proximal end of the treatment site. Stimulating electrode B was carefully pinned through the side of the nerve (through the sheath) and electrode A was placed alongside it. In five experiments where conduction was thought to be affected through the treatment site, stimulation was applied proximal and distal (both up to 50 volts) to determine the percentage of through conducting axons.

Force-discharge relationships

Following the identification of a mechanically sensitive hotspot, a feedback-controlled mechanical stimulator (modified 300C-LR, Aurora Scientific) was used to apply increasing forces to the nerve (6 x 25 mN steps; duration of each stimulus: two seconds, with one second periods between steps) (**Figure 2.6 A**). The silicone probe of the stimulator (2 x 2 mm) was positioned onto the hotspot using a micromanipulator (World Precision Instruments Inc., USA) and the force was offset at a level just below the firing threshold for the unit identified. Prior to drug application, three force step protocols were carried out (**Figure 2.6 B**). Mechanical stimulation using the feedback-controlled stimulator was not carried out in untreated nerves.

Application of mechanically sensitive ion channel blockers

Following vinblastine-treatment or neuritis, a brass ring (notched to accommodate the nerve) was positioned over the nerve at each mechanically sensitive hotspot to allow the application of the mechanically sensitive ion channel blockers ruthenium red (10-50 µM) and *N*-(3-Triethylammoniumpropyl)-4-(4-(Dibutylamino) Styryl) Pyridinium Dibromide (FM1-43) (2.5-25 µM), both made up in SIF. The ring was

sealed using petroleum jelly. Both blockers were maintained at 32˚C prior to application. The blockers were only applied to neurons that had clearly defined AMS hotspots. Each concentration of drug was applied for a total of 20 minutes. After 10 minutes of drug application, five force step protocols were carried out at two-minute intervals for 10 minutes (**Figure 2.6 B**). Recovery was not assessed. The same agents were also applied to untreated nerves to assess whether the blockers affected the conduction properties of neurons. In vinblastine-treated and neuritis nerves, only one blocker was applied to the nerve. In untreated nerves, both blockers were applied individually; however, different filaments were recorded from for each blocker. All treatment groups underwent the same blocker application protocol except for two vinblastine-treated nerves, in which an additional concentration of 10 µM was applied between 2.5 and 25 µM FM1-43.

Following blocker application, the nerve was electrically stimulated and the number of C-fibres was re-counted. In vinblastine-treated and neuritis nerves, electrical stimulation of the nerve (at or distal to the hotspot) or mechanical stimulation of the hotspot with the silicone tipped applicator, were used to confirm that the mechanically sensitive axon was still conducting after the application of the blockers. In untreated nerves, electrical stimulation of the nerve distal to the blocker application site was used to assess the effects of the blockers on the conduction properties of the neurons.

To determine whether repeated mechanical stimulation caused a decrease in the responsiveness of mechanically sensitive hotspots, the same stimulation protocol was carried out without drug application following vinblastine treatment.

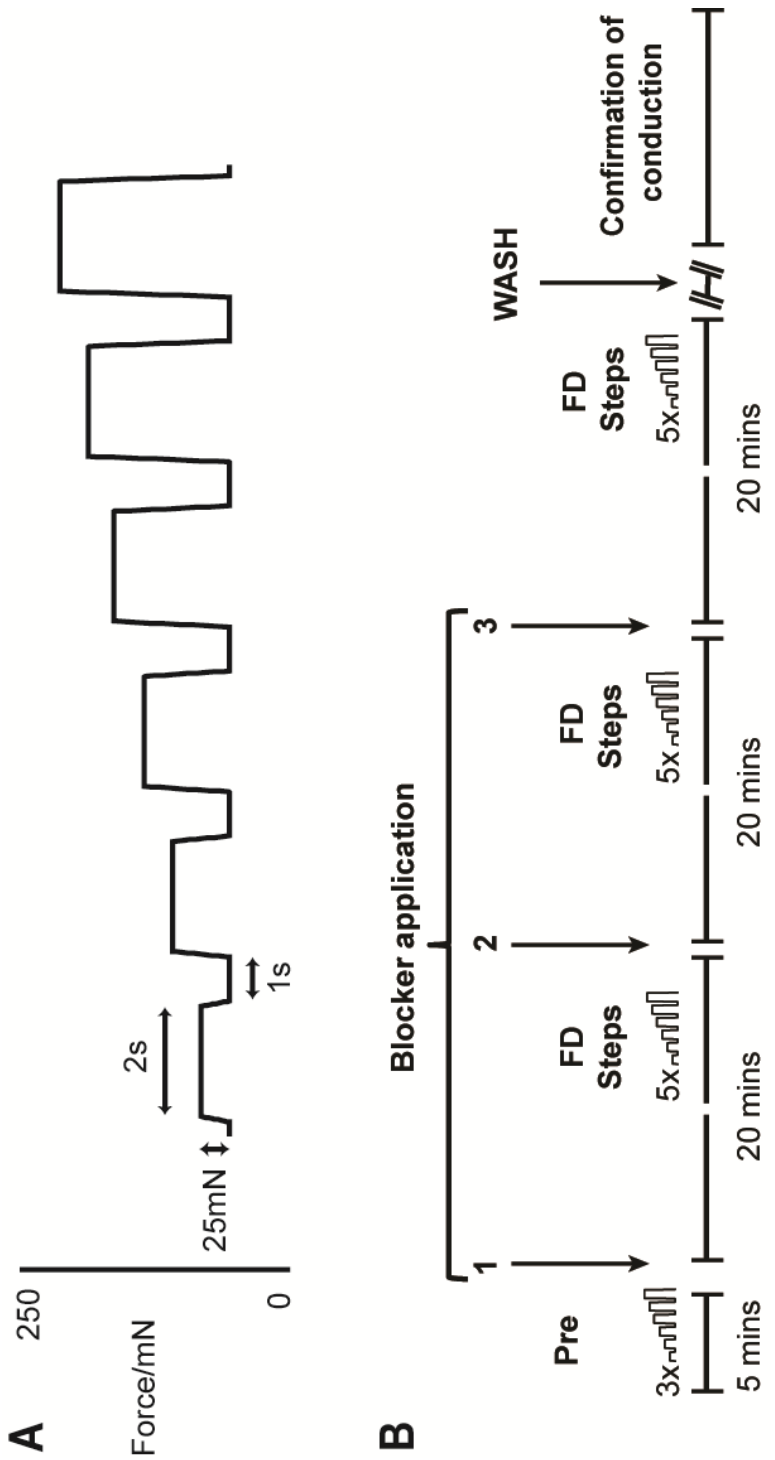

Figure 2.6 Force step protocol and mechanically sensitive ion channel blocker application timeline. A) The force was offset just below the firing threshold for the AMS unit. Six forces were applied in incrementing steps of 25mN. Duration of each stimulus was 2 seconds with a 1 second period in between. B) After baseline force discharge relationships had been established, mechanically sensitive ion channel blockers were applied in incrementing concentrations (1-3). Each concentration of drug was applied for 10 minutes, before force discharge relationships were re-assessed. After the final force discharge step protocol had been carried out at the highest concentration, the nerve was washed with SIF. Conduction was confirmed by electrical stimulation or manual mechanical stimulation of the hotspot.

2.5 Immunohistochemistry

Immunohistochemistry was used to assess staining patterns of TRPV1, TRPA1 and ASIC3 at the treatment site in the sciatic nerve and in the small to medium diameter cell bodies of the L5 dorsal root ganglia.

2.5.1 Antibodies

Table 2.1 summarises the antibodies used in the immunohistochemical procedures.

2.5.2 Immunolabeling protocol

Four days following vinblastine treatment (n = 4), neuritis (n = 4) and saline treatment (n = 4), animals were terminated by an overdose of euthatal and a 10 mm length of sciatic nerve from the treatment site and the ipsilateral L5 DRG were removed, placed in OCT embedding medium and flash frozen in isopentane (Sigma, UK) on dry ice. Tissue samples were stored at -80 ˚C overnight. On the following day, sections of both nerve and DRG were cut using a cryostat (Leica Microsystems, Wetzlar, Germany) and mounted onto gelatine-coated slides. All nerve sections were cut so that the tissue was orientated longitudinally. At least three nerve or DRG sections from each animal (vinblastine/neuritis/sham) were mounted on the same slide. DRG sections were sequentially mounted on seven consecutive slides, so that the eighth section was on the same slide as the first section. This was to avoid repeated counting of cells on the same slide. Slides were blocked using 4% normal goat serum (Vector Labs, USA) phosphate-buffered saline (PBS) (Sigma, UK) for 1 hour at room temperature. Sections were incubated overnight at 4 ˚C with either the polyclonal rabbit anti-TRPV1, anti-TRPA1 or anti-ASIC3 primary antibodies (see **Table 2.1** for dilution factors). One slide was used as a negative control, which was incubated in 4% goat serum overnight.

On day two, slides were incubated in the dark for one hour at room temperature with Alexa Fluro 488 goat anti-rabbit (Thermo Fisher Scientific), diluted 1:200, after which they were fixed for 7 minutes in 4% paraformaldehyde diluted in PBS. All slides were stained with 4',6-diamidino-2-phenylindole (DAPI, (Invitrogen, 1:2500), for 10 minutes at room temperature, before being dried and coverslipped using

glycerol/PBS mounting medium (Citifluor, London, UK). Between steps, slides were washed 3 times for 10 minutes in PBS. Slides were viewed under a fluorescence microscope (Leica Microsystems) at 488-nm and 350-nm excitation and photographed at each wavelength. Non-specific staining with secondary antibody was not found in the absence of primary antibody in any case.

In a separate set of experiments, the ligation site was removed from animals four days following vinblastine-treatment (n = 8), neuritis (n = 8) and saline treatment (n = 8) that also underwent a partial ligation distal to the treatment site. In these experiments, 16µm longitudinal nerve sections were cut using a cryostat and mounted on gelatine-coated slides. Sections were stained for TRPV1, TRPA1 or ASIC3 as described above.

Antibody target	Code	Supplier	Dilution	Previous publications
TRPV1[a]	NB100-1617	Novus Biologicals, UK	1:500	Rat brain – Immunoblotting (Liapi and Wood, 2005) Mice DRG – Immunoblotting (Stein et al., 2006) Mice brain – Immunolabeling (Sharif Naeini et al., 2006)
TRPA1	ACC-037	Alomone labs, Israel	1:300	Human urethra – Immunoblotting & immunolabeling (Gratzke et al., 2009) Rat DRG – Immunoblotting & immunolabeling (Yamamoto et al., 2015) Rat TG – Immunolabeling (Meng et al., 2015)
ASIC3	ASC-018	Alomone labs, Israel	1:400	Rat gastrointestinal tract – Immunoblotting and immunolabeling (Akiba et al., 2008) Rat TG – Immunolabeling (Yan et al., 2013) Rat TG – Immunolabeling (Meng et al., 2015)

Table 2.1 Information on the antibodies used in this study. All antibodies were diluted in 4% goat serum phosphate buffered saline [a] Same as Neuromics RA10110 TRPV1 antibody. DRG – Dorsal root ganglion, TG – trigeminal ganglia

2.6 Analysis

A Shapiro-Wilk test was used to assess whether the data sets were normally distributed to determine the appropriate analysis. GraphPad Prism (version 7) was used to analyse all data sets.

2.6.1 In vivo electrophysiology

Chapter 3 - Profile of axonal mechanical sensitivity in the vinblastine model

Characterised C-fibre neurons recorded from animals on different post-surgical days were grouped as follows: days 1-2, days 4-5, days 7-9, days 13-15. A Kruskal-Wallis test followed by Dunn's post-hoc tests was used to analyse the differences in conduction velocities and median rates of ongoing activity between the different groups. A Mann-Whitney U test was used to compare the conduction velocities and median rates of ongoing activity between the saline group and the d4-5 vinblastine group. Fisher's exact tests were used to compare the proportion of C-fibre neurons with AMS or ongoing activity at each time point. Since repeated noxious mechanical stimulation of receptive fields during an experiment leads to an increased proportion of C-fibre neurons with slow rates (<0.1 Hz) of ongoing activity (Bove and Dilley, 2010), the proportion of neurons with ongoing activity >0.1 Hz that were recorded in the first hour of the experiment were also compared using Fisher's exact tests.

Chapter 6 - Electrophysiological evidence for the presence of TRPV1 and TRPA1 in mechanically sensitive axons

Rates of activity were calculated from individual C-fibre neurons pre- and post- the application of agonists. Post-drug data for intraneural injections was split into 5 x 2 minute bins and rates of activity for each bin were calculated. A C-fibre neuron was deemed to have a positive response to an agonist if the firing rate increased by 50% above its baseline rate. However, if the increase in firing rate remained below 0.08 Hz or 0.09 Hz following gelfoam application or intraneural injection respectively, it was not considered a responder. These values were calculated from the 99% CI of the slow firing neurons (<0.1Hz) during the period immediately preceding agonist application. For neurons that were non-ongoing prior to drug application, their rate

had to increase above the 99% CI to be considered a responder. Kruskal-Wallis tests were used to compare differences in conduction velocities between the different groups. Rates of activity pre- and post-gelfoam application were compared using Kruskal-Wallis tests.

2.6.2 Ex vivo electrophysiology

A Kruskal-Wallis test followed by Dunn's post-hoc tests was used to compare differences in conduction velocities between the different groups. A Fisher's exact test was used to compare the proportion of C-fibre neurons with AMS.

The force threshold was calculated from an average of the first mechanical force that caused a response during repeated baseline testing. Data from the baseline testing (three repeats) was combined and a linear regression line was fitted to each plot, and the slope and r^2 were calculated. An unpaired Students' t-test was used to compare the slope and r^2 values between groups. The estimated response at 75 and 150 mN was calculated from the linear equation. A Mann Whitney test was used to compare the responses at 75 and 150 mN between groups. One hundred and fifty millinewtons was chosen as the sub-maximal force that produced a response in all neurons. Following the application of each concentration of drug, an average of five repeats was combined to generate linear regression lines. The change in slope and response at 150 mN were used as a measure of the effect of the mechanically sensitive ion channel blockers on AMS.

Changes in the number of spikes at 150 mN and the mechanical firing threshold following drug application were assessed using a Friedman test followed by Dunnett's post hoc tests. Changes to the slope of the force discharge relationship following drug application were assessed using a one-way repeated measures analysis of the variance (ANOVA) followed by Dunnett's post hoc tests.

2.6.3 Immunohistochemistry

DRG and sciatic nerve sections were analysed using ImageJ (Fiji) software (Fiji contributors).

Sciatic nerve

For nerve sections, a region of interest (ROI) was selected from the treatment site and an area between 3-5 mm proximal to the treatment site. The ROIs only included axonal staining avoiding any visible artefacts and blood vessels. A ratio was calculated by dividing the median intensity of antibody labelling at the treatment site by the median intensity of the nerve proximal. Ratios were averaged for each animal, which was then averaged again to give a mean ratio (from the three experimental runs).

For analysis of the sections from nerves that were partially ligated, a ROI 200 µm proximal to the ligature site (avoiding visible artefacts and blood vessels) was selected. An area covering the same distance was selected on the unligated nerves for comparison (**Figure 2.7**). A ratio was generated by dividing the median intensity of the ligated axons by the median intensity of the axons in the unligated portion of the nerve. Sections were excluded on the basis of signs of axonal damage (holes, bends or breaks) or if there were no intact axons for comparison. As a variable number of suitable nerve sections (2-10) were obtained from each animal, mean ratios were calculated. This was to ensure the data set was not biased towards one animal. Mean ratios were then averaged for each group and compared using a 1-way ANOVA followed by Dunnett's post-hoc tests

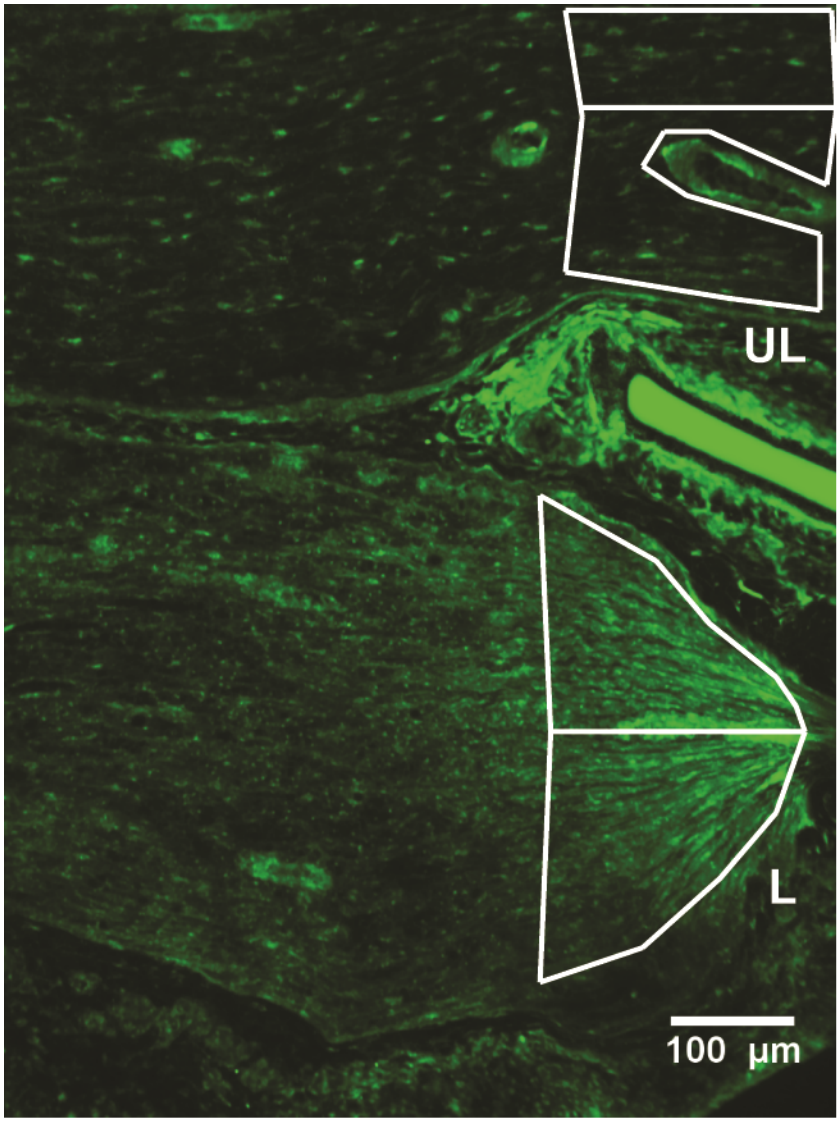

Figure 2.7 Analysis of partially ligated nerves. A region of interest 200 µm proximal to the ligation site was selected. The median intensity of this area was divided by the median intensity of the area corresponding to the unligated portion of the nerve. 10 x magnification; UL – unligated axons, L – ligated axons

Cell bodies of the dorsal route ganglion

For analysis of ion channel expression in the DRG, cell bodies were grouped into small and medium size (<32 µm, i.e. neurons with C- and Aδ-fibers) and large (>32 µm neurons with Aα/β-fibres) (Harper and Lawson, 1985). For each section, cell bodies with DAPI-positive nuclei were randomly selected using a checkerboard method (squares of grid were 40 x 40 µm). The median intensity of antibody labelling was measured in representative areas of the cell bodies, excluding the nuclei.

The intensity data was normalised to account for non-specific binding of antibodies. To normalise the intensity data, 'corrected intensity' values were calculated. To normalise antibody labelling, in each individual treatment group, the intensity of each small + medium diameter cell body was divided by the median intensity of the large diameter cell body population of that group (see **Appendix 1**). For all antibodies, between 50 - 60 small and medium diameter cell bodies were randomly selected from each experimental run. Corrected intensity values were compared using a Kruskal-Wallis test followed by Dunn's post-hoc tests.

Chapter 3

Profile of axonal mechanical sensitivity in the vinblastine model

3.1 Introduction

Axonal transport disruption can be examined in isolation (without inflammation) after application of low doses of anti-mitotic agents (such as vinblastine), in the absence of neuronal degeneration/injury (Dilley and Bove, 2008a; Fitzgerald et al., 1984). Axonal transport disruption alone can cause the development of AMS in C-fibre neurons and is thought to play a key role in the development of AMS in C-fibre neurons after induction of a neuritis (Dilley and Bove, 2008a). Mechanistically it is not known how AMS can influence the development of pain behaviours. However, it is postulated to play a role in their development, as following vinblastine treatment, there is a lack of ongoing activity in A- and C-fibre neurons (Dilley et al., 2013; Satkeviciute et al., 2018), which is widely accepted to be essential for the development and maintenance of central changes that lead to pain behaviours (Campbell and Meyer, 2006; Gracely et al., 1992; Xie et al., 2005). A previous study investigated the time course of mechanical allodynia associated with this model, which developed rapidly, peaks between days 4-5 and had completely reversed by day 11 (Dilley et al., 2013). Moreover, the time course of axonal transport disruption had also been investigated in this model, in which transport was clearly disrupted on day two, however appeared to be completely reversed by day six post-surgery (Dilley et al., 2013). It is not known how these changes relate to the development of AMS and whether AMS reverses in this model. Therefore, in this study the time course of AMS in C-fibre neurons has been investigated following vinblastine treatment. Single unit in-vivo electrophysiological recordings were carried out on different days following a vinblastine lesion. C-fibre ongoing activity was also examined and was specifically investigated within the first hour of recording (see **2.6.1**).

The primary objective was:

To determine the time course for the development of AMS and ongoing activity following vinblastine treatment.

3.2 Results

3.2.1 Effect of Surgery

All of the rats operated on made full recoveries after induction of the vinblastine surgery. Upon observation of the animals in the days following lesion induction, rats behaved normally and there was no evidence of pain or distress (e.g. hunched posture, piloerection, or vocalisation). There was no evidence that animals had difficulty weight bearing on the affected limb.

No animals showed signs of systemic infection at any time after surgery had been performed. Upon re-exposure of the sciatic nerve at the treatment site, the appearance of the nerve was normal (no evidence of a granuloma formation which is present after neuritis induction). None of the surrounding skin or muscle appeared oedematous.

3.2.2 Electrophysiology

A total of 103 filaments were recorded from 1-15 days post vinblastine lesion.

Receptive field properties

All of the mechanical receptive fields identified were deemed to be nociceptive as they were activated by strong pressure, either by squeezing the skin with forceps (cutaneous), or squeezing the muscle between the thumb and the forefinger (deep). In the untreated group of animals, 63% (12/19 neurons) of mechanical receptive fields had deep locations. A similar proportion of C-fibre neurons (74%; 86/117) had deep locations in the vinblastine group (between days 1-15); the proportion of deep neurons ranged between 66 - 82% at individual time points. In the saline treated group, 57% of C-fibre neurons had mechanical receptive fields with deep locations. Deep receptive fields were typically located within the gastrocnemius muscle or within the ankle.

Conduction velocities

Only C-fibre neurons with receptive fields were included within the analysis.

In the untreated group (n = 19 neurons), the conduction velocity of the C-fibre neurons was 0.58 m/s (IQR = 0.11), which was not significantly different to that following vinblastine treatment (Days 1-15 combined, n = 117 neurons, 0.59 m/s, IQR = 0.25; p = 0.58, Mann Whitney Test). There were no significant differences between the conduction velocities of any of the individual vinblastine time points (main effect p = 0.06, Kruskal-Wallis test; **Figure 3.1**). In the saline group (n = 26 neurons), the conduction velocity was 0.66 (IQR = 0.20), which was not significantly different to that 4-5 days following vinblastine treatment (0.64 m/s, IQR = 0.33, n = 29; p = 0.52, Mann Whitney Test; **Figure 3.1**).

The median conduction velocity of the neurons that had AMS between days 1-15 following vinblastine treatment (n = 16) was 0.55 m/s (IQR = 0.26), which was not significantly different to neurons without AMS (0.59 m/s, IQR = 0.24, n = 101; p = 0.51, Mann Whitney Test).

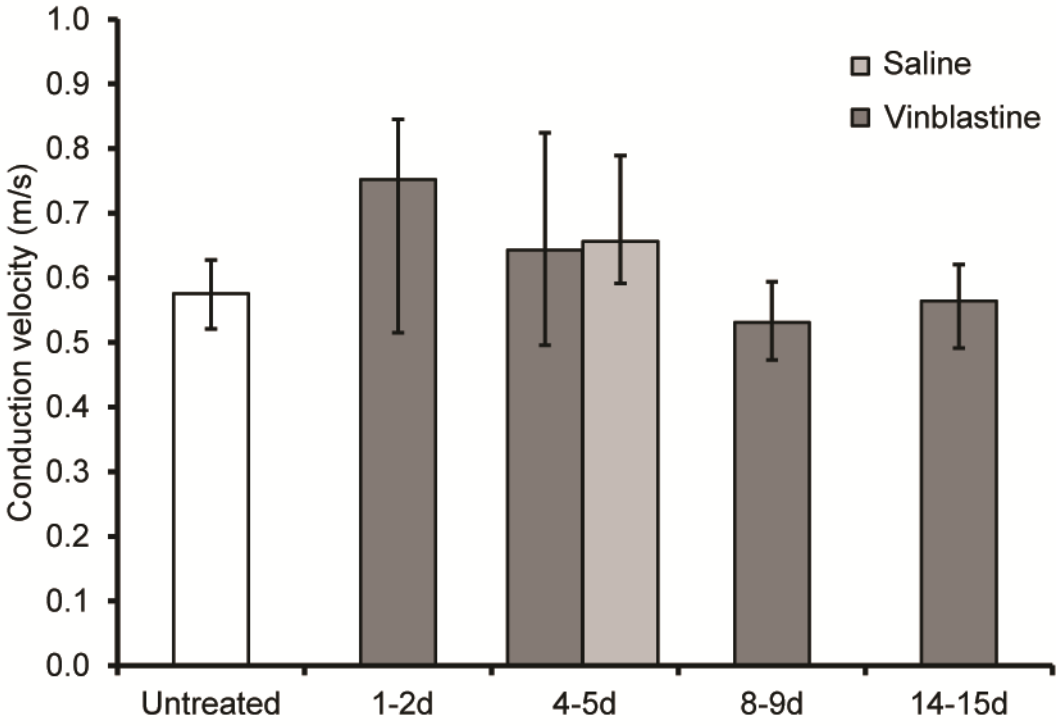

Figure 3.1 Conduction velocities in untreated, saline and vinblastine treatment groups. Number of neurons: Saline n = 26 (from 3 animals), untreated n = 19 (from 3 animals), vinblastine 1-2d n = 38 (from 6 animals), vinblastine 4-5d n = 29 (from 5 animals), vinblastine 8-9d n = 24 (from 3 animals), vinblastine 14-15d n = 26 (from 4 animals). Presented as medians. Error bars represent IQR.

Axonal mechanical sensitivity

The proportion of C-fibre neurons in each group that developed AMS is summarized in **Figure 3.2 A**. All of the neurons that developed AMS had receptive fields below the knee, and all had a relatively high mechanical threshold. Axonal mechanical sensitivity did not develop in the untreated (0/19 neurons) or saline treated groups (0/23 neurons). Following vinblastine treatment, AMS developed rapidly, with 16% (6/38) of C-fibre neurons responding to direct mechanical stimulation at the treatment site on day 1-2 post-surgery. The proportion of neurons with AMS reached a peak on day 4-5, with 28% (8/29) of all neurons responding to mechanical stimulation (both $p < 0.05$ compared to untreated and day 4-5 saline-treated groups, Fisher's exact test). By day 14, AMS was absent with 0% (0/26) of neurons being mechanically sensitive. Following vinblastine treatment, all of the C-fibre neurons that developed AMS had deep receptive fields (16/86).

Mechanically sensitive hotspots tended to be located at the treatment site or slightly proximal to the treatment site. In no instances were hotspots located distal to the treatment site. Hotspots did not produce any sustained discharge after mechanical stimulation (**Figure 3.2 B**).

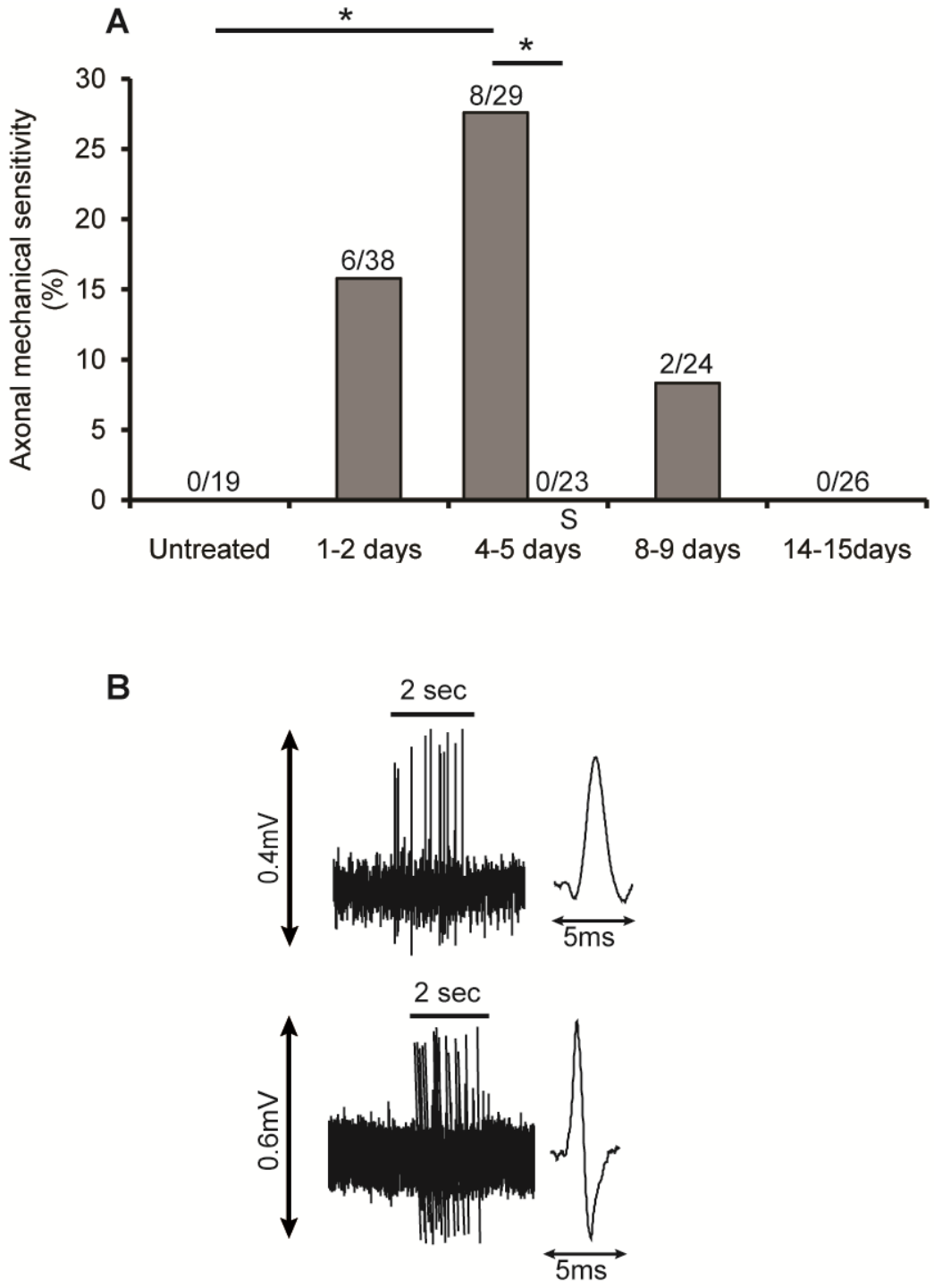

Figure 3.2 Axonal mechanical sensitivity in C-fibre neurons following vinblastine treatment. A) The proportion of C-fibre neurons with AMS on different days following vinblastine treatment. There was a significant increase in the proportion of C-fibre neurons with AMS on days 4-5 following vinblastine treatment, when compared to that of untreated and days 4-5 saline-treatment (* $p<0.05$, Fisher exact test). Number of animals: Saline n = 3, untreated n = 3, vinblastine 1-2d n = 6, vinblastine 4-5d n = 5, vinblastine 8-9d n = 3, vinblastine 14-15d n = 4. S, saline-treatment. B) Example traces of neurons with AMS responding to mechanical stimulation. Horizontal bars represent mechanical stimuli being applied to the nerve.

Ongoing activity

Figure 3.3 shows the percentage of C-fibre neurons that developed ongoing activity on different days following vinblastine treatment. The proportion of neurons with ongoing activity reached a peak on day 4-5 following vinblastine treatment, 54 % (15/29), which was not significantly different to the saline group, 43% (11/23), or to that of the untreated group, 32% (6/19) ($p = 0.37$ and $p = 0.24$ respectively, Fisher's Exact test).

The proportion of C-fibre neurons with ongoing activity found within the first hour of recording with rates lower than 0.1 Hz is shown in **Figure 3.3 B**. The proportion of ongoing neurons in the vinblastine-treated group on days 4-5 was 25% (3/12), which was not significantly different to that of saline-treated group, 33% (4/12) or to the untreated group 13% (1/8) ($p = 1.0$ and $p = 0.62$ respectively, Fisher's Exact tests).

The median firing rates of ongoing activity for all groups are shown in **Table 3.1**. There were no significant differences between the rate of ongoing activity in any of the individual vinblastine time points compared to the untreated group ($p = 0.91$, Kruskal-Wallis test). The median rate of ongoing activity in C-fibre neurons on 4-5 days following vinblastine treatment ($n = 15$) was 0.27 Hz (IQR = 0.15), which was not significantly different to the saline group (0.53 Hz, IQR = 0.95, $n = 11$; $p = 0.08$, Mann Whitney U test).

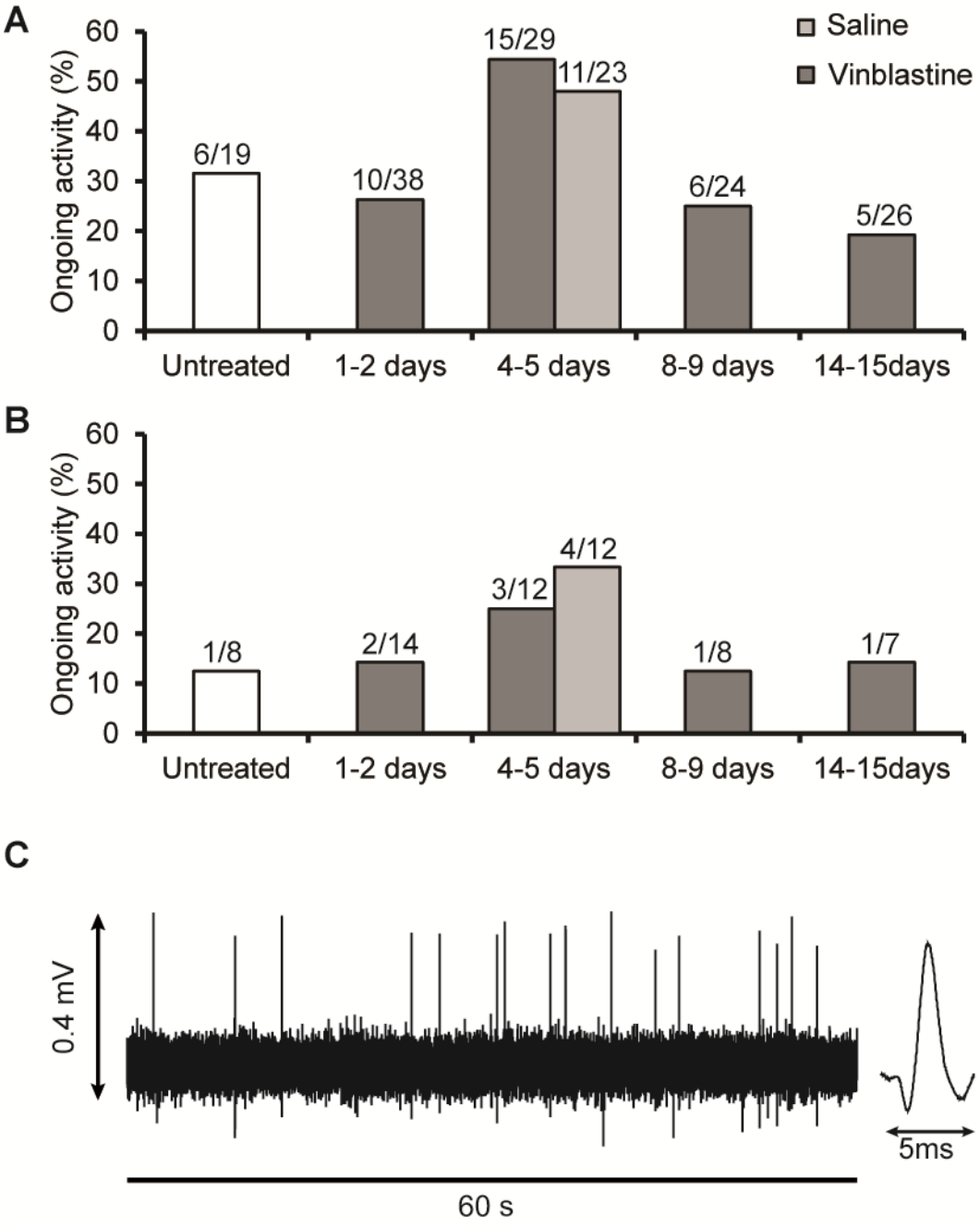

Figure 3.3 Ongoing activity in C-fibre neurons following vinblastine treatment.
A) The proportion of C-fibre neurons with ongoing activity in on different days following vinblastine treatment. B) The proportion of C-fibre neurons found within the first hour of recording with activity rates above 0.1Hz C) Example trace of an ongoing C-fibre recorded on day 4 following vinblastine treatment. Number of animals: Saline n = 3, untreated n = 3, vinblastine 1-2d n = 6, vinblastine 4-5d n = 5, vinblastine 8-9d n = 3, vinblastine 14-15d n = 4.

	Untreated	Saline	Vinblastine			
Day	-	4-5	1-2	4-5	8-9	14-15
Median rate/Hz	0.20	0.45	0.25	0.27	0.29	0.19
IQR	0.18	0.95	0.25	0.28	0.38	0.51
Number of neurons	11	11	10	15	6	5

Table 3.1 The median rates of ongoing activity in C-fibre neurons.

3.3 Main findings

- Axonal mechanical sensitivity was not present in untreated animals (0/19) or on day 4-5 in the saline-treated group (0/23).
- Following vinblastine treatment, AMS developed in 16% (6/38) of C-fibre neurons on day 1-2 and reached a maximum of 28% (8/29) on day 4-5.
- On days 4-5 following vinblastine treatment, the proportion of C-fibre neurons with AMS was significantly different compared to the saline-treated group ($p<0.05$).
- Axonal mechanical sensitivity was absent by day 14-15 following vinblastine treatment.
- Only C-fibre neurons with receptive fields located deep within tissue developed AMS.
- Following vinblastine treatment, the proportion of neurons with ongoing activity reached a peak on days 4-5, with 54 % (15/29), which was not significantly different compared to the saline group, 43% (11/23) ($p = 0.37$).

3.4 Discussion

Although the mechanisms of nerve trunk mechanical sensitivity are poorly understood, it has been proposed that localised nerve inflammation (neuritis, Dilley et al., 2011; Greening et al., 2017) may play a role in its development. Consistent with a role for inflammation, the induction of an experimental neuritis in rats causes AMS in nociceptors (Bove et al., 2003, Dilley at al., 2005). Inflammation induced axonal transport disruption is hypothesised to be an important part of the underlying mechanism that leads to the development AMS (Dilley and Bove, 2008a; Dilley et al., 2013). In this study, a model of localised axonal transport disruption, which is induced by applying low doses of vinblastine directly to the nerve trunk (Dilley and Bove, 2008a; Fitzgerald et al., 1984), was used to examine the contribution of axonal transport disruption to the development of AMS.

3.4.1 Vinblastine treatment caused the transient development of AMS

Although previous studies had examined the time course of axonal transport and mechanical allodynia following vinblastine treatment, levels of AMS were only investigated at a time point when vinblastine was considered to have its maximum effect ((Dilley and Bove, 2008a; Dilley et al., 2013). As the time course of axonal transport disruption and mechanical allodynia were transient, it was hypothesised that the development of AMS would also be short-lived. Therefore, the levels of AMS were assessed on different days following vinblastine treatment to determine a time course for its development.

The present findings have shown that vinblastine-induced disruption of axonal transport causes the rapid, yet transient, development of AMS. This pattern is consistent with the previously reported time course of axonal transport disruption, which is disrupted on day two and resolves by day six (Dilley et al., 2013). Axonal mechanical sensitivity closely correlates to the transient development of mechanical allodynia reported following vinblastine treatment (Dilley et al., 2013), which is in contrast to the chronic nature of symptoms in patients. Therefore, this indicates that there is likely to be an ongoing trigger in patients that causes persistent axonal transport disruption. This trigger may be inflammation associated with compression

of a nerve through a fibro-osseous tunnel, or inflammation associated with injury to surrounding soft tissues, such as muscle.

All of the axons that were mechanically sensitive innervated deep structures and were nociceptive, which is consistent with that of previous reports following vinblastine treatment (Dilley and Bove, 2008a; Dilley et al., 2013) and neuritis (Bove et al., 2003), and with clinical reports of deep tissue pain in patients (Bove et al., 2005; Lemming et al., 2012). This suggests that unmyelinated afferents that innervate deep structures (e.g. muscle) are particularly vulnerable to the effects of vinblastine-treatment. Such vulnerability may be related to the morphology of this population of neurons. For example, the diameters of unmyelinated axons from nerves that mainly innervate muscle are reported to be larger than that of cutaneous nerves (Schmalbruch, 1986; St John Smith et al., 2012). However, whether these morphological differences contribute to the vulnerability of deep afferents to the effects of vinblastine treatment is unknown. Alternatively, group IV afferents may have a different levels or types of sensory ion channel that are expressed in these neurons. Interestingly, a higher percentage of afferents that innervate muscle express the putative mechanically sensitive ion channels ASIC3 and TRPV1, compared to those that innervate the skin (Hu-Tsai et al., 1992; Molliver et al., 2005).

The time course for the development of AMS following vinblastine treatment contrasts from the pattern of AMS following neuritis. Although both are transient, AMS that develops following neuritis is reported to persist for up to four weeks (Dilley and Bove, 2008b). These differences might be explained by the contrasting time courses of axonal transport disruption. Axonal transport is clearly disrupted at day six following neuritis, whereas at this time point following vinblastine treatment, axonal transport disruption had resolved (Dilley et al., 2013). Axonal transport disruption has not been examined beyond day six following neuritis, and hence it is not known whether inflammation-induced axonal transport disruption is responsible for the sustained increase in mechanical sensitivity. However, inflammatory cells remain elevated at 12 weeks following neuritis (Bove et al., 2009), which suggests that inflammation persists and could trigger axonal transport disruption at later time points.

In agreement with previous findings, mechanically sensitive hotspots were located proximal to or at the site of vinblastine exposure (Dilley and Bove, 2008a; Dilley et al., 2013), which is in line with the hypothesis that anterogradely transported mechanically sensitive ion channels accumulate proximal to the site of disruption (Dilley and Bove, 2008a; Proske and Luff, 1998). Vesicles containing ion channels are assumed to have accumulated shortly after axonal transport was disrupted and, similar to that which occurs when ion channels reach the peripheral terminal, are inserted into the membrane (Ghosh et al., 2016; Meng et al., 2016). These changes are likely to result in an increase in the density of ion channels in the membrane, which leads to the development of mechanical sensitivity. The reversal of AMS on day 8-9 post-surgery, and complete recovery by day 14-15, suggests that ion channels are eventually removed from the treatment site, which is presumably due to an endocytotic mechanism. However, very little is known about the way sensory ion channels are internalised and rates at which they turnover in the membranes of excitable cells.

Although Aα- or Aβ- fibre neurons were not investigated in this study, it has been previously reported that Aδ- fibre neurons develop AMS following vinblastine treatment and neuritis (Bove et al., 2003; Dilley and Bove, 2008a). In the present study, neurons with conduction velocities that are typically associated with Aδ-fibre neurons (i.e. 2-8 m/s) were not identified. However, conduction velocities of axons are slowed along the dorsal root compared to sciatic nerve(Waddell et al., 1989), and therefore it is possible that some of the faster C-fibre neurons were in fact slow Aδ-fibre neurons.

3.4.2 Levels of ongoing activity did not increase following vinblastine treatment

The development of ongoing activity in C-fibre neurons was also examined, since such activity is likely to contribute to spontaneous pain that is reported in patients (Kleggetveit et al., 2012), and drive the mechanisms that lead to central sensitisation (Koltzenburg et al., 1992; McMahon and Wall, 1984; Wall and Woolf, 1984; Woolf, 1983). Ongoing activity has not been reported to increase following vinblastine treatment in previous studies (Dilley et al., 2013; Satkeviciute et al., 2018). As

confirmation of these findings, the levels of ongoing activity were assessed at different time points following vinblastine treatment.

In this study, the lack of a significant increase in the proportion of C-fibre neurons with ongoing activity following vinblastine treatment is in contrast to neuritis, which causes an increase in ongoing activity during the first week following surgery (Bove et al., 2003; Dilley et al., 2005; Richards et al., 2011; Satkeviciute et al., 2018). Therefore, it seems that inflammation is required for the development of such activity. Previous studies have also shown that the application of inflammatory mediators, such as TNF, can induce ongoing activity in nociceptive axons (Leem and Bove, 2002; Richards et al., 2011; Sorkin et al., 1997). Levels of TNF are raised at the neuritis site and this is likely to contribute towards the development of ongoing activity produced in this model (Pulman et al., 2013).

The absence of ongoing activity following vinblastine treatment does not exclude that ion channels involved in the generation of ongoing activity, such as HCN2 and $Na_v1.8$ (Emery et al., 2011; Richards and Dilley, 2015; Roza et al., 2003), might have accumulated at the site of axonal transport disruption. In this regard, recent evidence indicates that neurons can be excited by inflammatory mediators following vinblastine treatment (Govea et al., 2017), thus demonstrating that an additional inflammatory trigger may be required to activate these channels (Gold et al., 1996; Herrmann et al., 2017). The lack of ongoing activity following vinblastine treatment is consistent with the anti-inflammatory properties of anti-mitotic agents (Norris et al., 1977).

Ongoing activity in the C-fibres neurons of untreated animals prior to noxious stimulation is rare (Bessou and Perl, 1969; Perl et al., 1976). However, the levels of background activity from C-fibre neurons in the untreated and saline groups were relatively high. This discrepancy was most likely due to the methodology used to characterise nociceptive neurons. Repeatedly searching for noxious mechanical receptive fields causes the development of slow firing (<0.1 Hz) ongoing activity in C-fibre neurons, which is most likely due to inflammation in the periphery (Bove and Dilley, 2010; Richards et al., 2011). Accordingly, inflammatory mediators may

sensitise ion channels, such as $Na_v1.8$ (Gold et al., 1996), increasing axonal excitability sufficient to cause ongoing activity. Hence, the proportion of ongoing activity (rates greater than 0.1Hz) in C-fibre neurons that were characterised within the first hour, were also compared. In these neurons, the proportion of ongoing neurons was lower in all groups, which was similar to that reported previously (Bove and Dilley, 2010).

3.4.3 Vinblastine treatment did not cause conduction slowing in nociceptive neurons

Previous studies have reported vinblastine-induced conduction slowing in nociceptors along the dorsal root (Dilley et al., 2013) and sciatic nerve (Dilley et al, 2008). Therefore, it was hypothesised that conduction velocities would be slower following vinblastine treatment. However, in contrast to a previous finding (Dilley et al., 2013), the conduction velocity of C-fibre axons was not slowed along the dorsal root following vinblastine treatment. This discrepancy may reflect the low number of C-fibre neurons sampled in this part study.

3.4.4 Summary

Following vinblastine treatment, the development of AMS in C-fibre neurons was rapid yet transient. It is likely that the development of AMS contributes to movement-evoked radiating pain in patients. However, the transient development of AMS following vinblastine-treatment contrasts the chronic nature of symptoms that are reported in patients. This indicates that in patients, there is likely to be an inflammatory trigger that causes persistent axonal transport disruption (Dilley et al., 2011; Greening et al., 2017; Satkeviciute et al., 2018). In contrast to the development of AMS, the effects of vinblastine treatment were not sufficient to cause an increase in ongoing activity in C-fibre neurons.

Chapter 4

Ex-vivo examination of mechanically sensitive hotspots following vinblastine treatment and neuritis

4.1 Introduction

In previous studies, mechanically sensitive hotspots in C-fibre neurons from neuritis and vinblastine treated nerves have been found to fire at or below a pressure of 200 mN (Dilley and Bove, 2008a; b). However, the precise firing thresholds of mechanically sensitive hotspots are unknown and it is not known if thresholds differ between hotspots found in vinblastine-treated and neuritis nerves. Additionally, it is not known whether mechanically sensitive hotspots produce graded responses to changes in force.

It is hypothesised that fast axonal transport disruption, a feature in both vinblastine and neuritis models, causes the accumulation of mechanosensitive ion channels at the treatment site, which contributes towards the development of AMS in C-fibre neurons (Dilley et al., 2013). However, it has not been directly proven that such an accumulation of mechanosensitive channels is responsible for AMS. To determine whether mechanically sensitive channels are accumulating at the treatment site, this study has looked at the effects of mechanosensitive ion channel blockers (ruthenium red and FM1-43) on AMS. To enable AMS hotspots to be isolated so blockers could be applied, experiments were run in a modified ex-vivo recording chamber (Reeh, 1986). This also allowed for the examination of force-discharge responses of mechanically sensitive axons, generated using a force-feedback controlled mechanical stimulator, which could apply set forces to hotspots. This enabled quantification of the effects of mechanosensitive ion channel blockers and an insight into the mechanical properties of C-fibres with AMS. In addition to this, conduction through the treatment site was also investigated following neuritis.

The primary objectives were:

1. To determine whether AMS hotspots produced graded responses to changes in force.
2. To determine whether mechanically sensitive ion channel blockers attenuated AMS.

4.2 Results

4.2.1 Effect of Surgery

All animals recovered from vinblastine and neuritis surgeries without adverse effects.

Neuritis

Upon observation of the animals in the days following the neuritis surgeries, rats behaved normally and there was no evidence of pain or distress (e.g. hunched posture, piloerection, or vocalisation). There was no evidence that animals had difficulty weight bearing on the affected limb.

No animals showed signs of systemic infection at any time after surgery had been performed. Upon dissection of the nerve, there was evidence for a granuloma formation at the treatment site. Moreover, the nerve also appeared to be highly vascularised.

4.2.2 Physiology of the nerve in an ex-vivo setting

Conduction through the treatment site

In untreated nerves (n = 7) C-fibre action potentials could be evoked at a threshold between 10 - 20 volts.

Following vinblastine treatment (n = 31 nerves) C-fibre action potentials could always be evoked when the nerve was stimulated distal to the treatment site, at a threshold between 10-20 volts. As large groups of C-fibre axons (range 8 – 17 C-fibres per filament) were quickly identified in these experiments, it was assumed that there was no significant disruption to conduction through the treatment site, hence nerves were stimulated distal to the treatment site for the duration of the experiment

Following neuritis, C-fibre action potentials could be electrically evoked in 48% (9/19) of the neuritis nerves) upon distal simulation. In the 10 neuritis nerves that could not be stimulated distal to the treatment site, it was assumed that conduction was either fully or partially blocked. These nerves were stimulated at the proximal end of the treatment site for the duration of the experiment (except in 5 experiments that were initially stimulated proximally and distally – see below).

In five experiments where conduction was thought to be effected through the neuritis treatment site, 24% of C-fibres (12/49) were found to be through conducting (See **Figure 4.1 A**). In these experiments, there were no signs of conduction slowing through the treatment site (median velocity = 0.66 m/s, IQR = 0.19 and 0.68 m/s, IQR = 0.11, proximal and distal stimulation respectively; p = 0.99, Mann Whitney test; **Figure 4.1 B**).

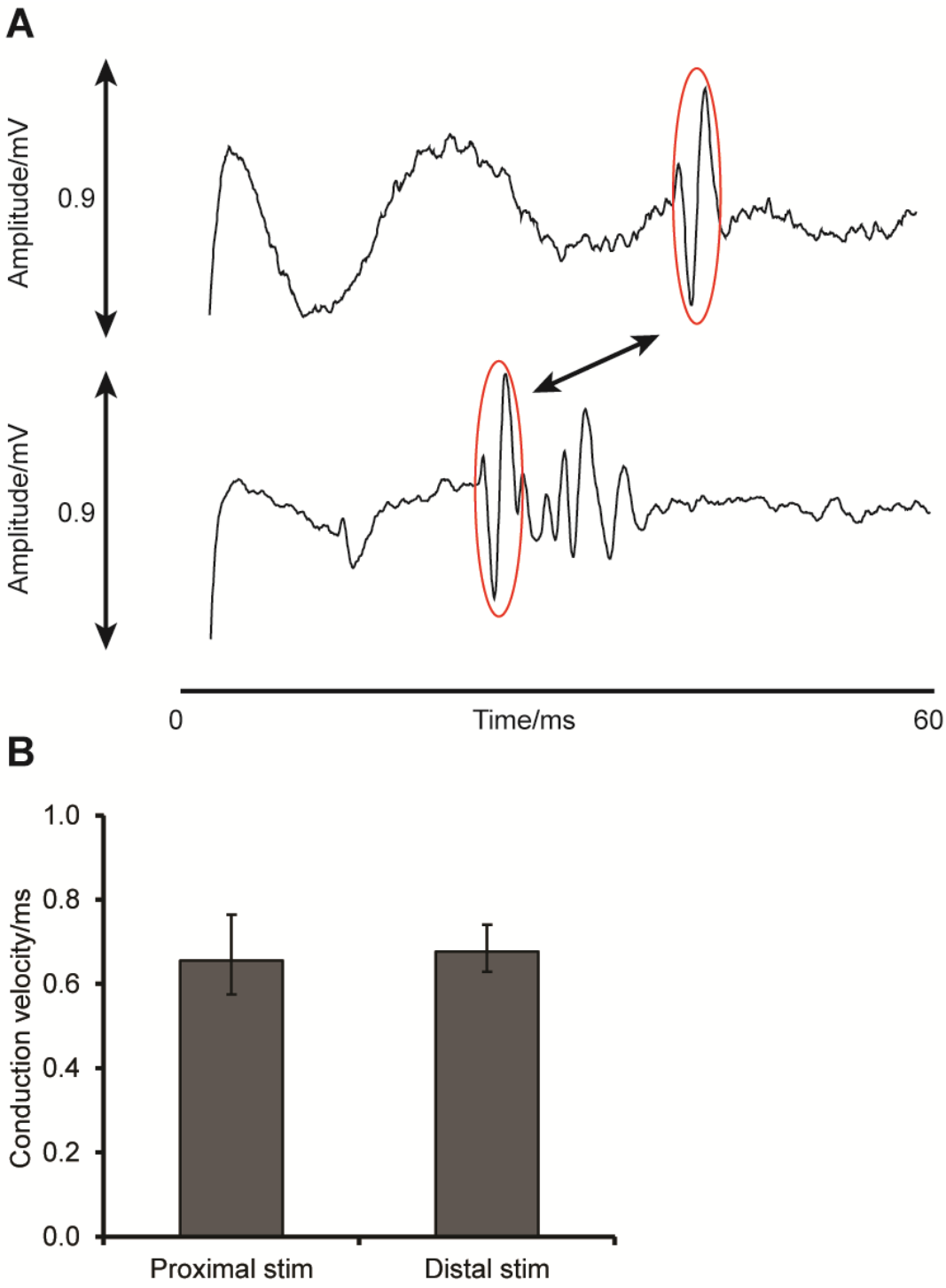

Figure 4.1 Stimulation of neuritis nerves proximal and distal to the treatment site. A) Example traces from a neuritis nerve. Top trace - Stimulation at 50 volts distal to the treatment site, three C-fibres were present. The spikes highlighted in the red circle had conduction velocities of 0.79 and 0.75 m/s. Bottom trace - Proximal stimulation at 50 volts. The highlighted spikes, which were identified to be the same as the spikes shown in the circle in the top trace, were found to have conduction velocities of 0.83 and 0.77 m/s. B) Conduction velocities of the units present on the filament when stimulating electrically proximal and distal to the neuritis site. Proximal stim n = 49, distal stim n = 12. Presented as medians, error bars represent IQR.

Conduction velocities

For vinblastine and neuritis groups, only the conduction velocities of C-fibre axons present upon filaments that had AMS were included within the analysis.

Conduction velocities of C-fibre axons stimulated distal to that of the treatment site following vinblastine treatment or neuritis (or corresponding area in untreated animals) are shown in **Figure 4.2**. In the untreated group (n = 7 animals, 89 axons), the median conduction velocity of C-fibre axons was 0.68 m/s (IQR = 0.18), which was significantly different to the vinblastine group (0.61 m/s, IQR = 0.16; n = 14 animals, 88 axons; $p < 0.001$ Dunn's post-hoc test). In the neuritis group, the median conduction velocity was 0.69 m/s (IQR = 0.16; n = 5 animals, 45 axons), which was not significantly different to the untreated group ($p = 1.0$, Dunn's post-hoc).

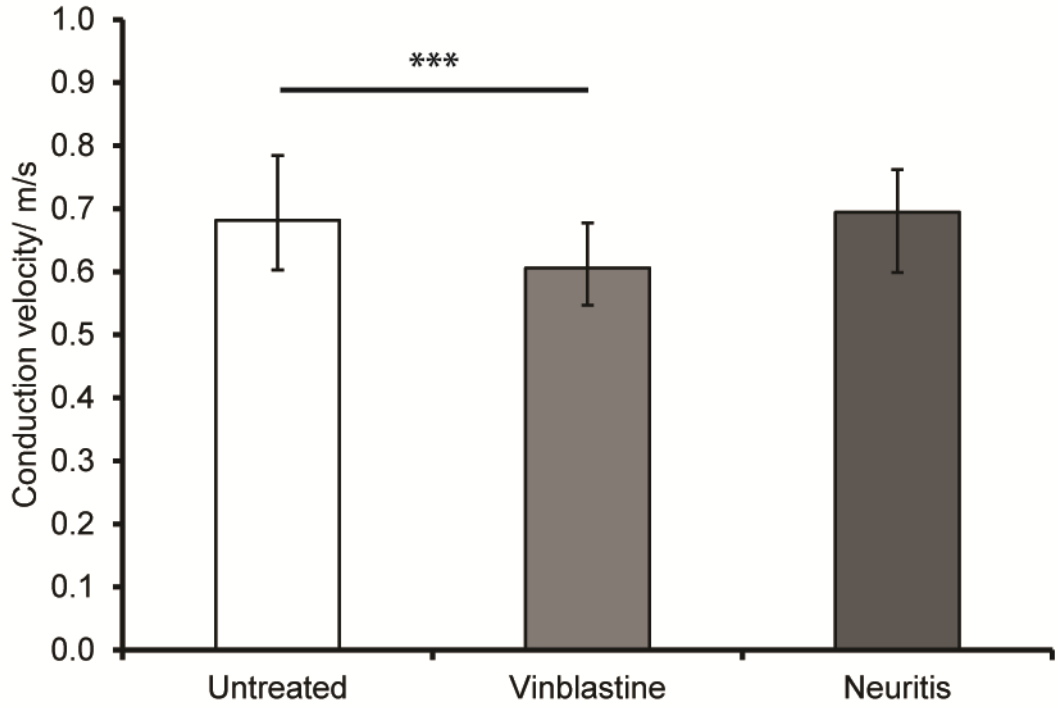

Figure 4.2 Conduction velocities of C-fibre axons in untreated, vinblastine and neuritis (distal stimulation) groups. C-fibre axons from the vinblastine group had slower conduction velocities than that of untreated group (*** $p<0.001$, Dunn's post-hoc test). Number of neurons: Untreated n = 89 (from 7 animals), vinblastine n = 88 (from 14 animals), neuritis n = 45 (from 5 animals). Data presented as medians. Error bars represent IQR.

Axonal mechanical sensitivity

Following vinblastine treatment and neuritis, the proportion of AMS ranged between 0-13 % and 2-14 % respectively. The overall proportion of AMS in C-fibre axons following vinblastine treatment and neuritis was significantly greater than that of the untreated group (both $p<0.01$, individual Fisher's exact tests; **Table 4.1**). Hotspots did not produce any sustained discharge after mechanical stimulation. Following vinblastine treatment and neuritis, mechanically sensitive hotspots were localised to a 1-2mm portion of the nerve. Following vinblastine treatment, hotspots were either located proximal to or at the treatment site. Whereas following neuritis, the majority of hotspots were located at the treatment site, with a few being located proximal to the treatment site. The AMS hotpots in the vinblastine-treated nerves were always located proximal to the stimulating electrodes. Following neuritis, all but one of the mechanically sensitive hotspots were located proximal to the stimulating electrodes; this unit was located at the neuritis treatment site.

	Untreated	Vinblastine	Neuritis
Total number of C-fibres	188	1382	878
C-fibre AMS	1	66	64
% AMS	0.5%	4.8%[a]	5.2%[b]

Table 4.1 The proportions of C-fibre axons with axonal mechanical sensitivity and ongoing activity ex-vivo. [a] Significantly different to that of untreated ($p<0.01$, Fisher's exact test) [b] Significantly different to that of untreated ($p<0.01$, Fisher's exact test). Number of animals: Untreated n = 7, vinblastine n = 31, neuritis n = 19.

4.2.3 Force-discharge relationships

Mechanically sensitive axons in both vinblastine-treated and neuritis groups produced force-discharge responses, whereby increased forces produced an increase in the number of spikes (**Figure 4.3 & 4.4**). Within the ranges of forces applied, there was a linear relationship between force and number of spikes in the majority of experiments, and therefore a linear regression line was fitted to the data (**Figure 4.5**). In one experiment, there was indication of a plateau at the highest force (**Figure 4.5 C**). In another experiment, the maximum number of spikes was elicited at the minimum applied force (see * in **Figure 4.6 B**). The r^2 value from the force-discharge relationships produced from AMS hotspots following vinblastine treatment (n = 14) was 0.58 (SEM +/- 0.05), which was not significantly different to neuritis (r^2 = 0.48, SEM +/- 0.1, n = 12; p = 0.27, unpaired Students t-test). Clear force-discharge relationships were seen in the majority of the mechanically sensitive hotspots from neuritis and vinblastine treated nerves (see **Figure 4.6**).

The mean slope of the force-discharge relationships following vinblastine treatment was 0.055 spikes.s^{-1}.mN^{-1} (SEM +/- 0.007), which was significantly greater than neuritis (0.027 spikes.s^{-1}.mN^{-1}, SEM +/- 0.008; p <0.01, unpaired Students t-test; **Figure 4.7**).

At a force of 75 mN, AMS hotspots identified following vinblastine treatment (n = 11) produced 3.0 spikes.s^{-1} (IQR = 3.1), which was not significantly different to neuritis (spikes.s^{-1} = 3.6, IQR = 2.4, n = 11; p = 0.56, Mann Whitney test). The number of spikes.s^{-1} produced at 150 mN force following vinblastine treatment (n = 14) was 7.1 (IQR = 5.9), which was greater but not significantly different to that of neuritis (spikes.s^{-1} = 5.6, IQR = 3.9, n = 12; p = 0.32, Mann Whitney test).

In the vinblastine-treated group, the median mechanical threshold for the axons that were mechanically sensitive was 48 mN (IQR = 34, n = 14), which was higher but not significantly different to that of neuritis (36 mN, IQR 13, n = 12; p = 0.076, Mann Whitney test; **Figure 4.8**).

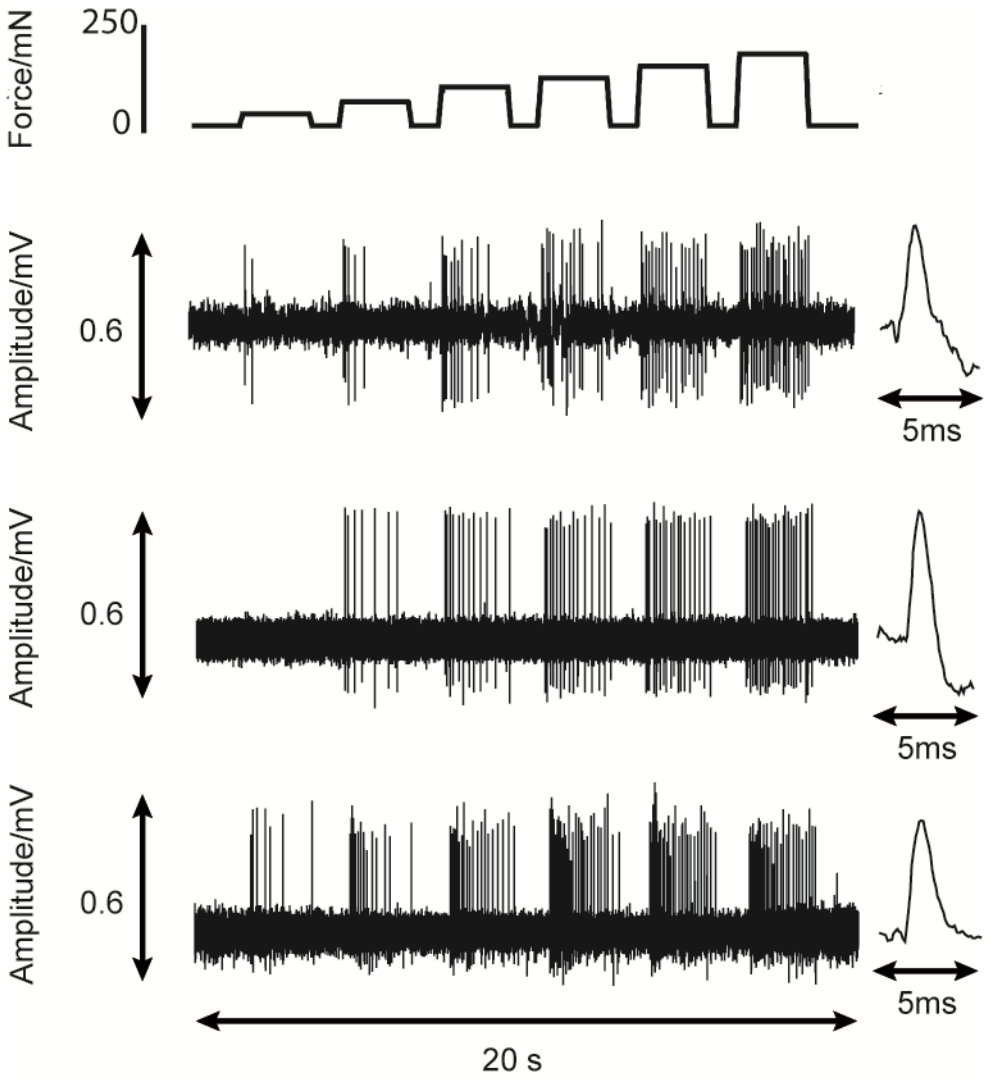

Figure 4.3 Example traces of force-discharge responses produced from mechanically sensitive hotspots following vinblastine treatment.
Top plot is the force step protocol. Hotspots produced graded response to changes in force.

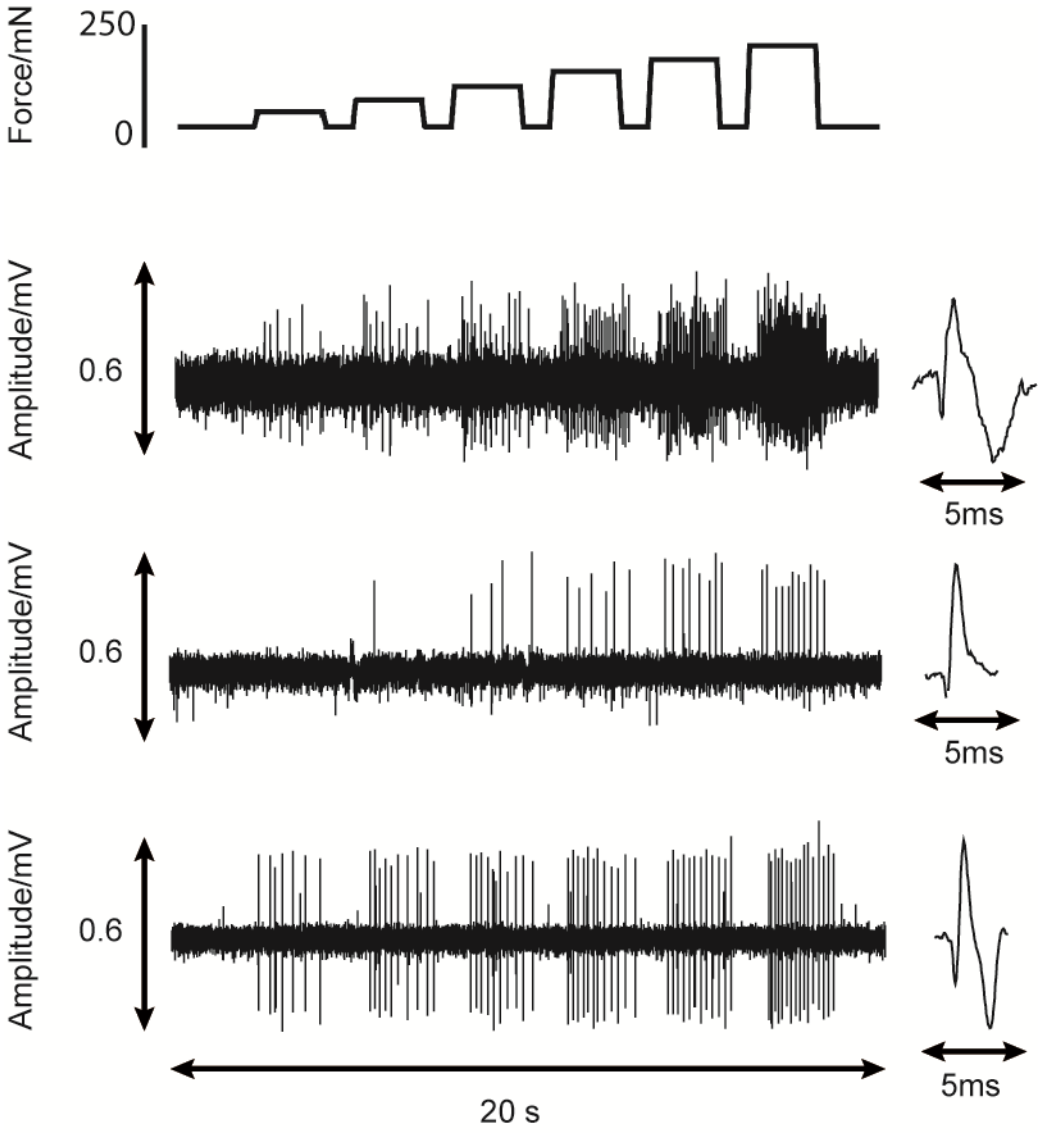

Figure 4.4 Example traces of force-discharge responses produced from mechanically sensitive hotspots following neuritis.
Top plot is the force step protocol. Hotspots produced graded response to changes in force.

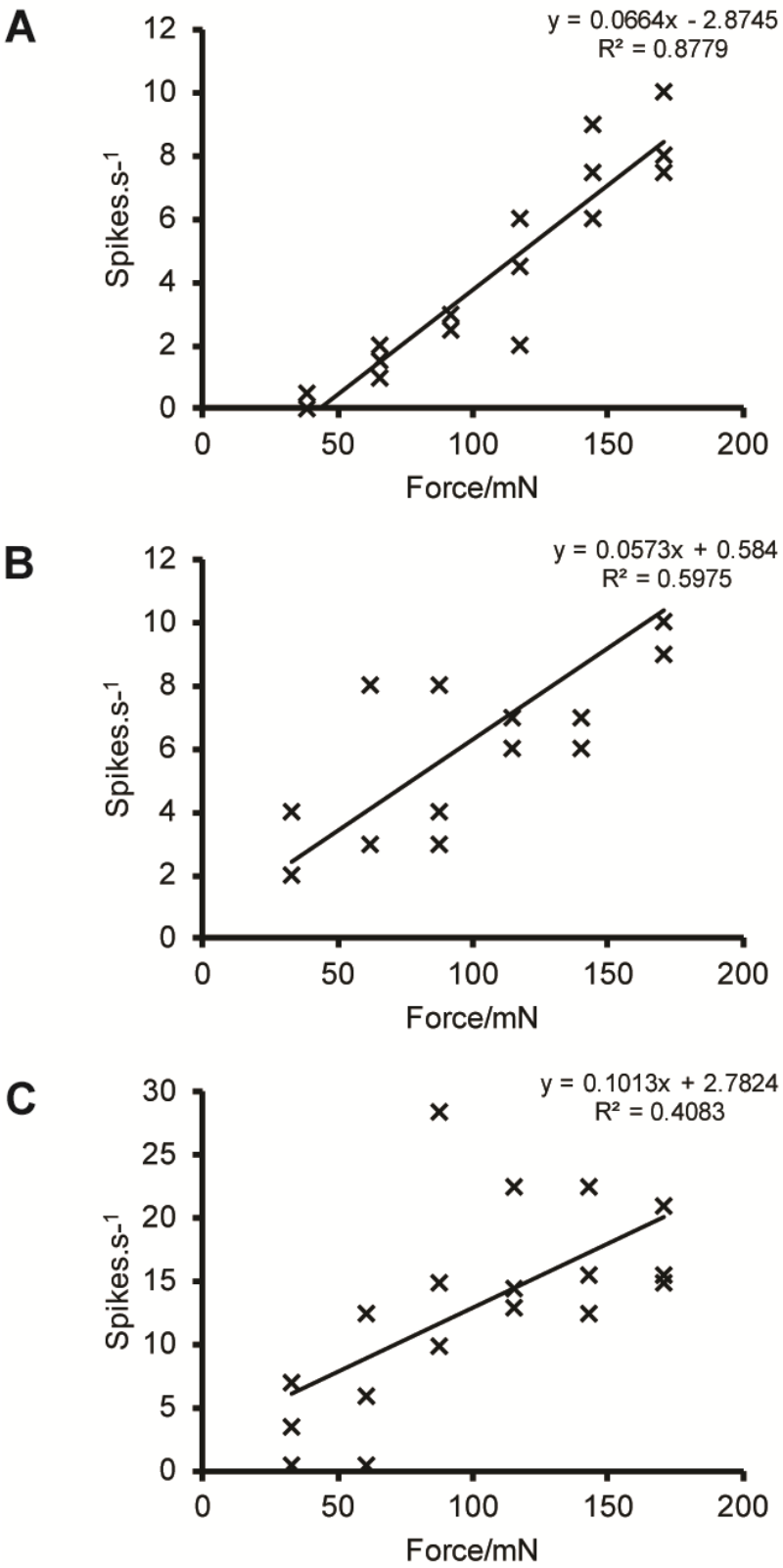

Figure 4.5 Regression lines were fitted to responses produced from mechanically sensitive hotspots. Example plots following A) vinblastine-treatment and B) neuritis. C) Hotspot following vinblastine-treatment that reached a maximum response prior to application of the top force. Each graph represents data from three trials.

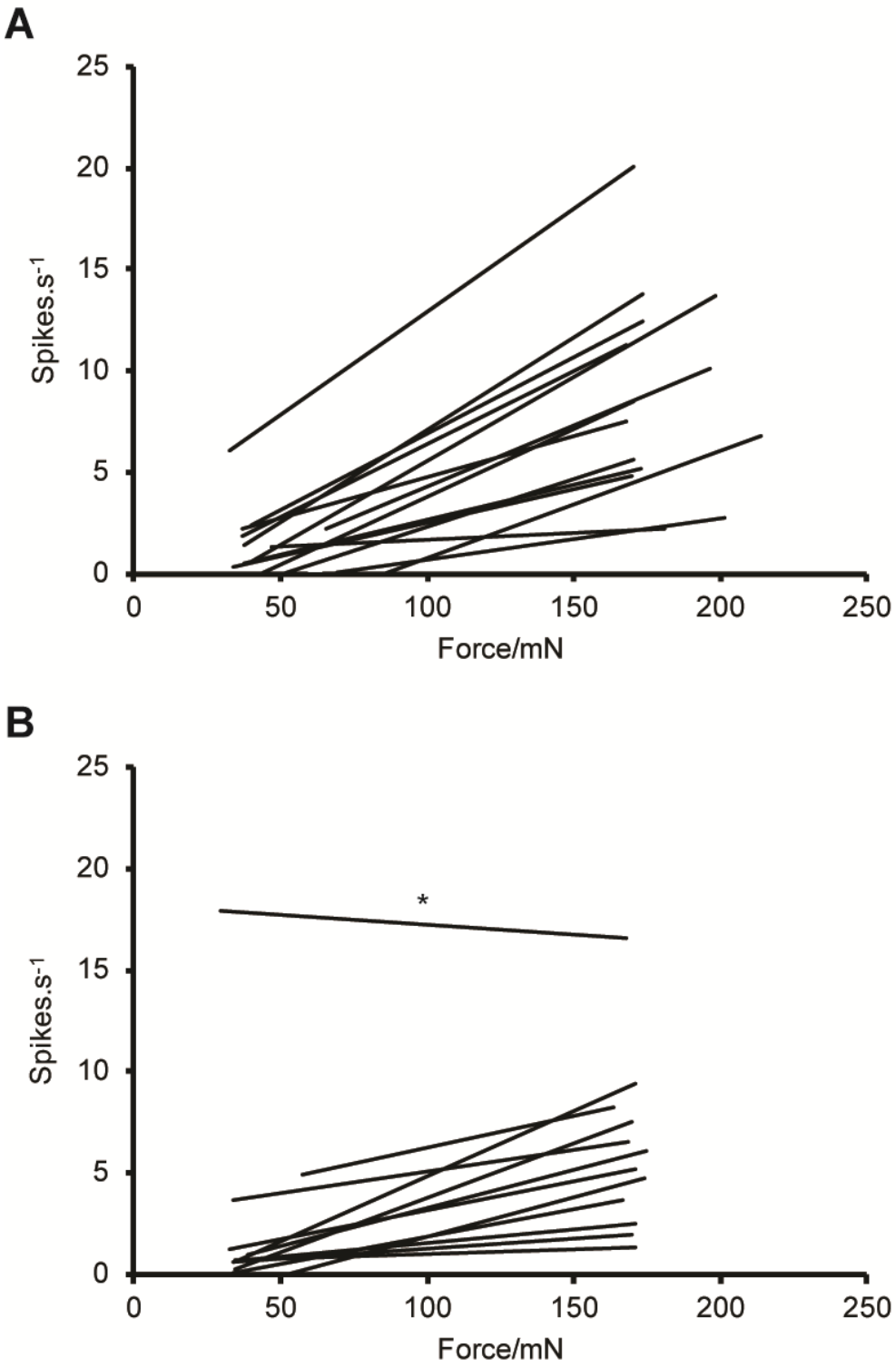

Figure 4.6 Force-discharge relationships produced from mechanically sensitive hotspots. Linear regression lines fitted to force discharge responses produced from hotspots following A) vinblastine treatment and B) neuritis. The majority of mechanically sensitive hotspots produced clear force-discharge relationships. Each line represents three repeats. * In this experiment, the minimum force elicited the maximum number of spikes. AMS hotspots: Vinblastine = 14 axons (13 nerves), neuritis n = 12 axons (10 nerves)

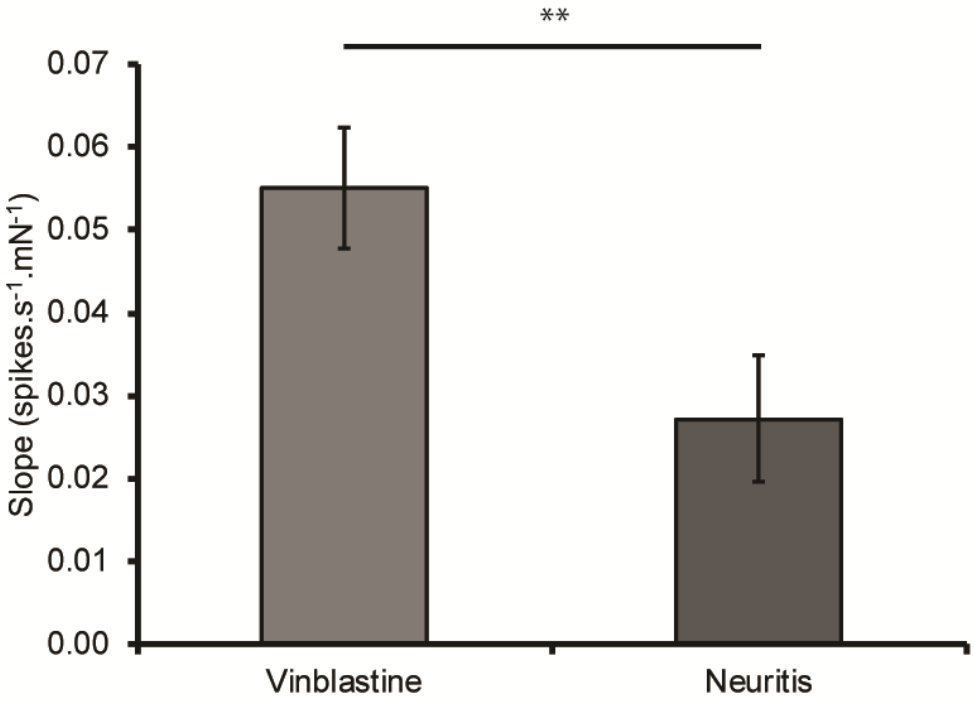

Figure 4.7 Slopes of the force-discharge relationships from mechanically sensitive hotspots Following vinblastine treatment, the slope was significantly higher than neuritis (**p<0.01, Students t-test). Data presented as means. Error bars represent SEM. AMS hotspots: Vinblastine = 14 axons (13 nerves), neuritis n = 12 axons (10 nerves)

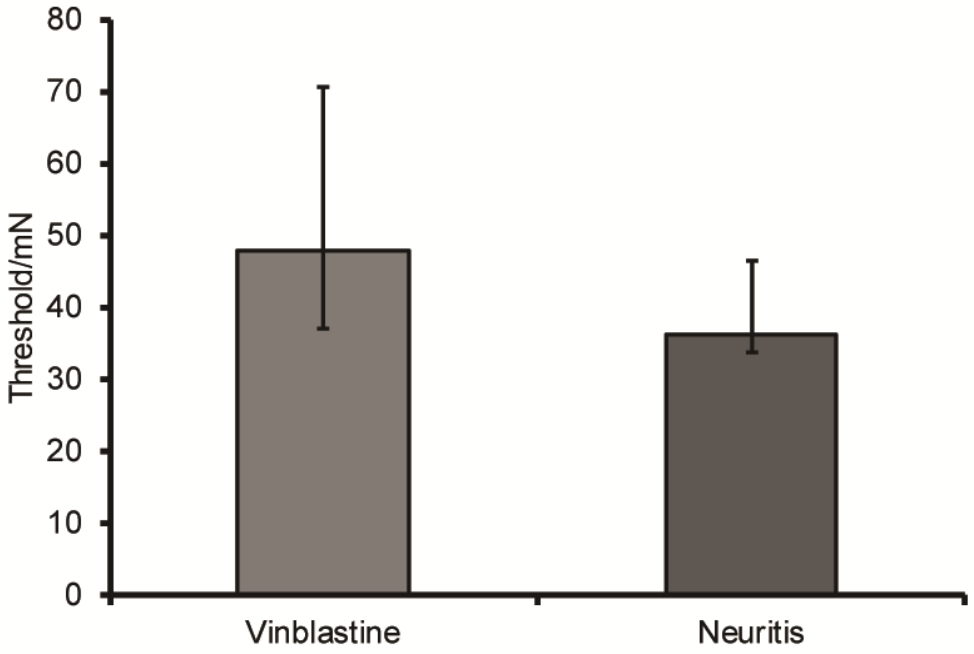

Figure 4.8 Force thresholds of mechanically sensitive hotspots
Firing thresholds were calculated from the average of the first force that caused a response from each trial. Data presented as medians. Error bars represent IQR. AMS hotspots: Vinblastine = 14 axons (13 nerves), neuritis n = 12 axons (10 nerves)

4.2.4 Control force-discharge steps

Repeated mechanical stimulation of mechanically sensitive hotspots identified following vinblastine treatment (n = 3) did not cause a reduction in the number of spikes.s^{-1} produced at 150 mN force ($p = 0.75$, Wilcoxon test), the slope of the linear line fit to force-discharge responses ($p = 0.64$, Students paired t-test) or the firing threshold ($p = 1.00$, Wilcoxon test; **Figure 4.9**).

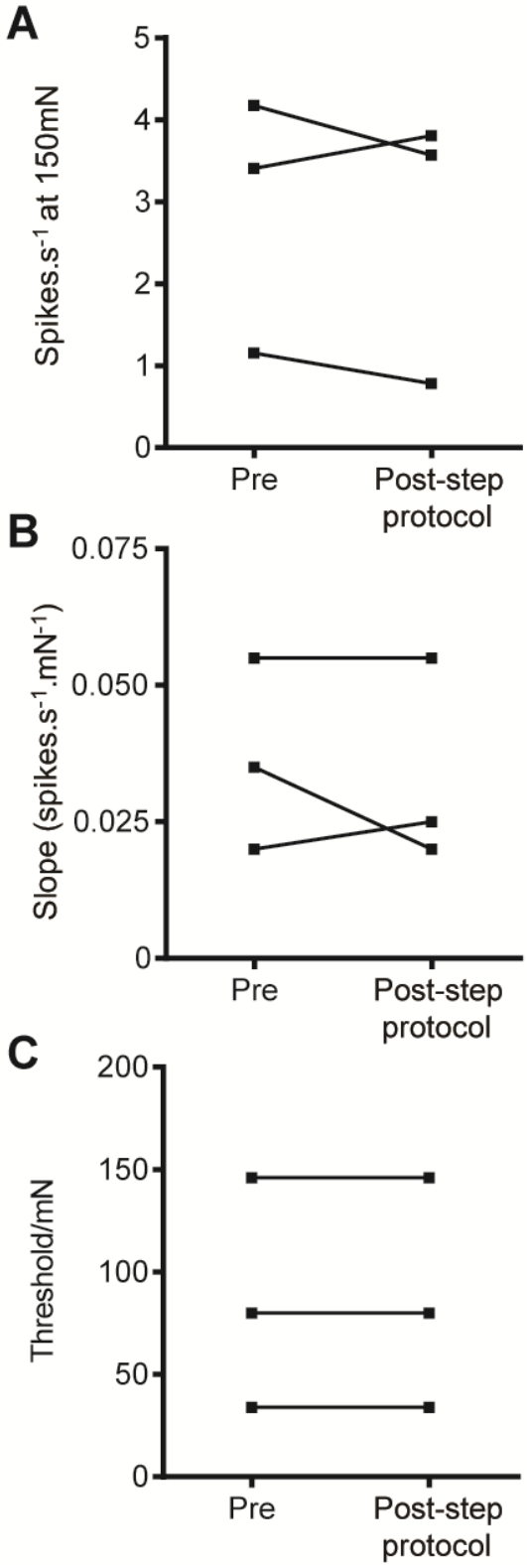

Figure 4.9 Repeated mechanical stimulation of mechanically sensitive hotspots
Application of 3 x 5 force-discharge step protocols in the absence of blockers does not affect A) the number of spikes.s^{-1} produced at 150 mN force, B) the slope of the regression line or C) the threshold of mechanically sensitive hotspots. Note that the force-discharge protocol was the same as during drug application. n = 3 mechanically sensitive hotspots from vinblastine-treated nerves.

4.2.5 Mechanosensitive ion channel blockers

Ruthenium red

All nerves were stained red at the location where ruthenium red (RR) had been applied to the nerve. Following the application of 10-50 µM RR, there was negligible block of conduction along C-fibre axons at the treatment site in untreated (87%; n = 33/38 axons), vinblastine-treated (89%; n = 32/36 axons) and neuritis nerves (88%; n = 19/21 axons).

Figure 4.10 shows example AMS responses to the force-discharge step protocol following the application of RR. Following vinblastine treatment and neuritis, ruthenium red caused a dose dependent decrease in the number of spikes.s^{-1} produced from AMS hotspots at 150 mN force (main effects: p = 0.19 and p = 0.14 respectively, Friedman test; **Figure 4.11**). Following application of 50 µM, the number of spikes.s^{-1} had reduced by 87% and 65% compared to that of baseline (vinblastine treatment and neuritis respectively).

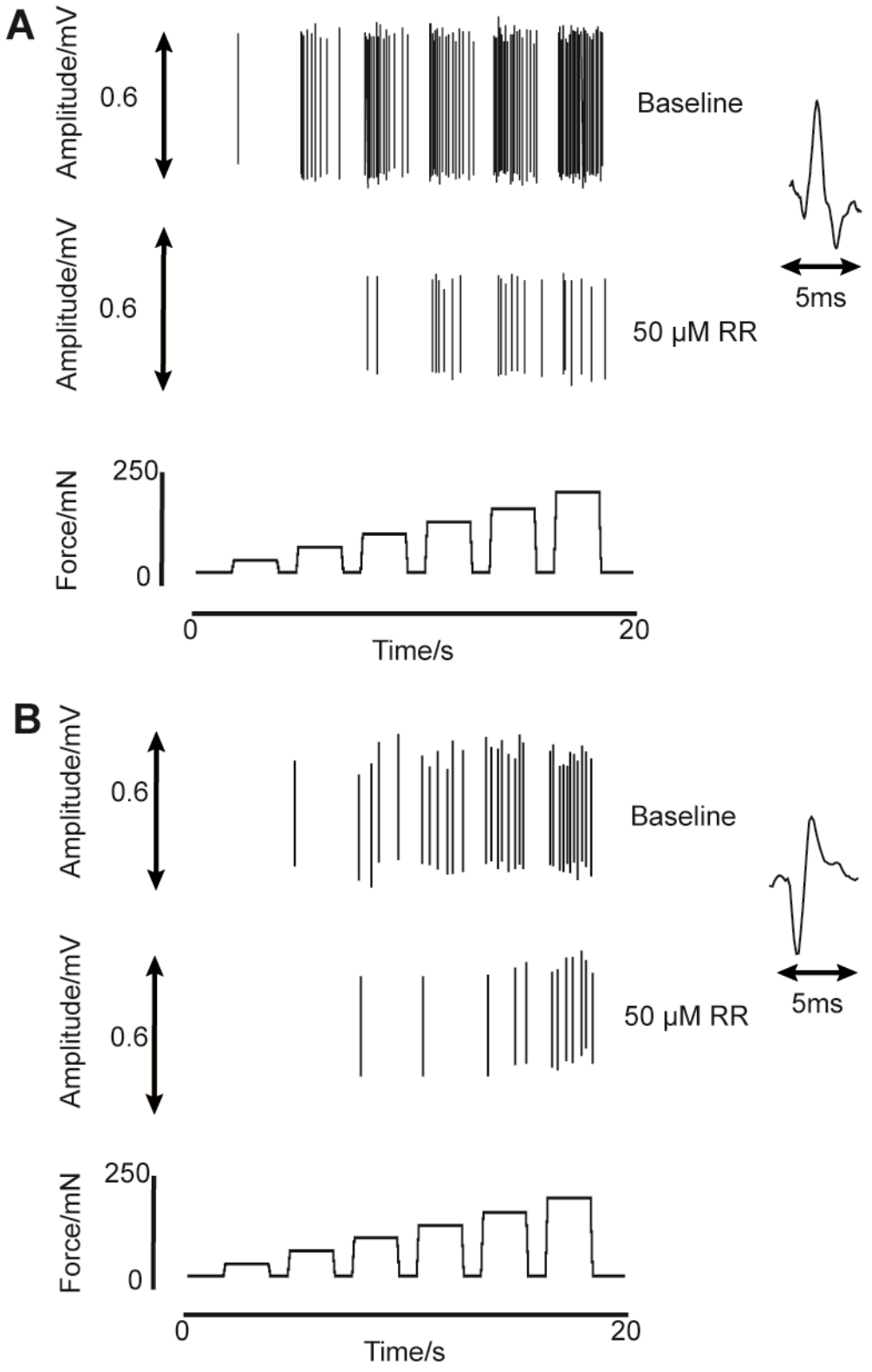

Figure 4.10 Example force-discharge responses pre and post 50µM ruthenium red. Responses from a mechanically sensitive hotspot identified in a nerve A) 4 days following vinblastine treatment and B) 5 days following neuritis. Both examples were selected from the beginning of the series of force steps that followed 50µM ruthenium red application. RR – ruthenium red.

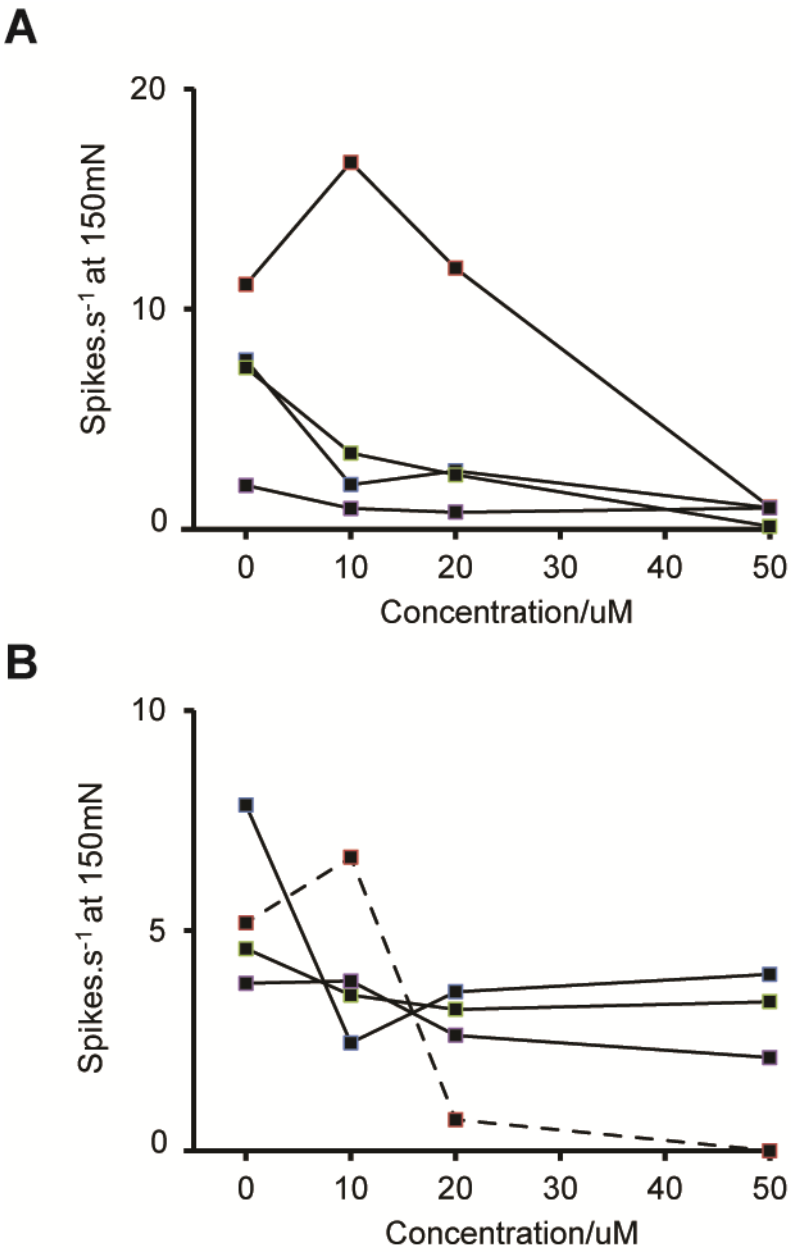

Figure 4.11 The number of spikes.s^{-1} produced from mechanically sensitive hotspots at 150 mN following application of ruthenium red. The average number of spikes.s^{-1} produced at 150 mN force from AMS hotspots ; before and after application of 10-50 µM ruthenium red following A) vinblastine treatment and B) neuritis. Hashed line represents hotspot that was distal to the stimulating electrodes. 0 = pre-drug. Vinblastine n = 4, neuritis n = 4.

Following vinblastine treatment and neuritis, ruthenium red caused a reduction in the slope of the regression line fit to force-discharge relationships from mechanically sensitive hotspots, i.e. as the concentration increased the slope decreased (main effects: p = 0.24 and p = 0.47 respectively, repeated measures one-way ANOVA**; Figure 4.12**). Following application of 50 µM, the slope decreased by 113% and 38% compared to baseline (vinblastine treatment and neuritis respectively).

Following 50 µM, at the end of the force step protocol series (force step protocol 4/5 – 5/5) the majority of mechanically sensitive hotspots in the vinblastine group did not produce positive force-discharge relationships, i.e. the slope was zero or less than zero in some cases (slopes ranged from -0.005 – +0.007 spikes.s^{-1}.mN^{-1}). This was also the case for one mechanically sensitive hotspot in the neuritis group represented by hashed line in **Figure 4.12 B** (slope -0.001spikes.s^{-1}.mN^{-1}).

Ruthenium red caused an increase in the firing threshold for AMS in all of the neurons following vinblastine treatment and two out of four neurons following neuritis (main effects: p = 0.16 and p = 0.22 respectively, Friedman test**; Figure 4.13**). Following application of 50 µM, the threshold had increased by 57% and 13% compared to that of baseline (vinblastine treatment and neuritis respectively).

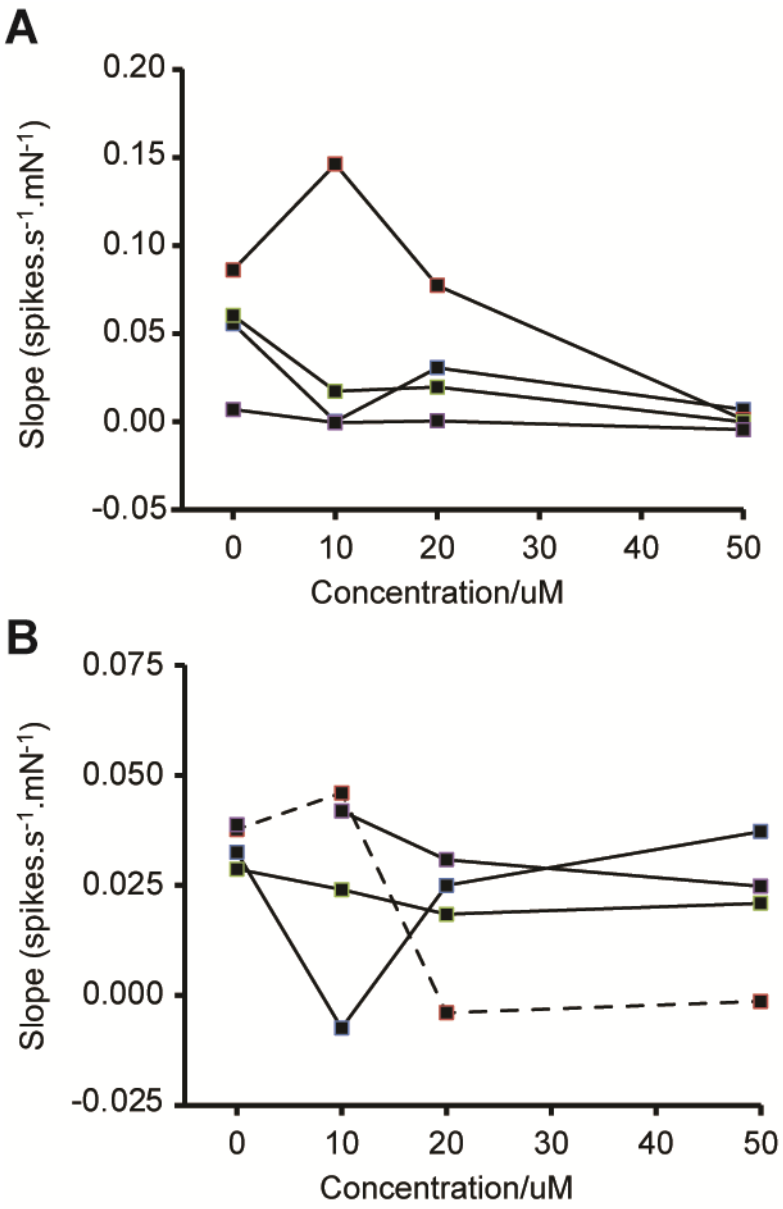

Figure 4.12 Slopes of force-discharge relationships following application of ruthenium red. The slope of force discharge relationships; before and after application of 10-50 µM ruthenium red following A) vinblastine treatment and B) neuritis. Hashed line represents hotspot that was distal to the stimulating electrodes. Vinblastine n = 4, neuritis n = 4.

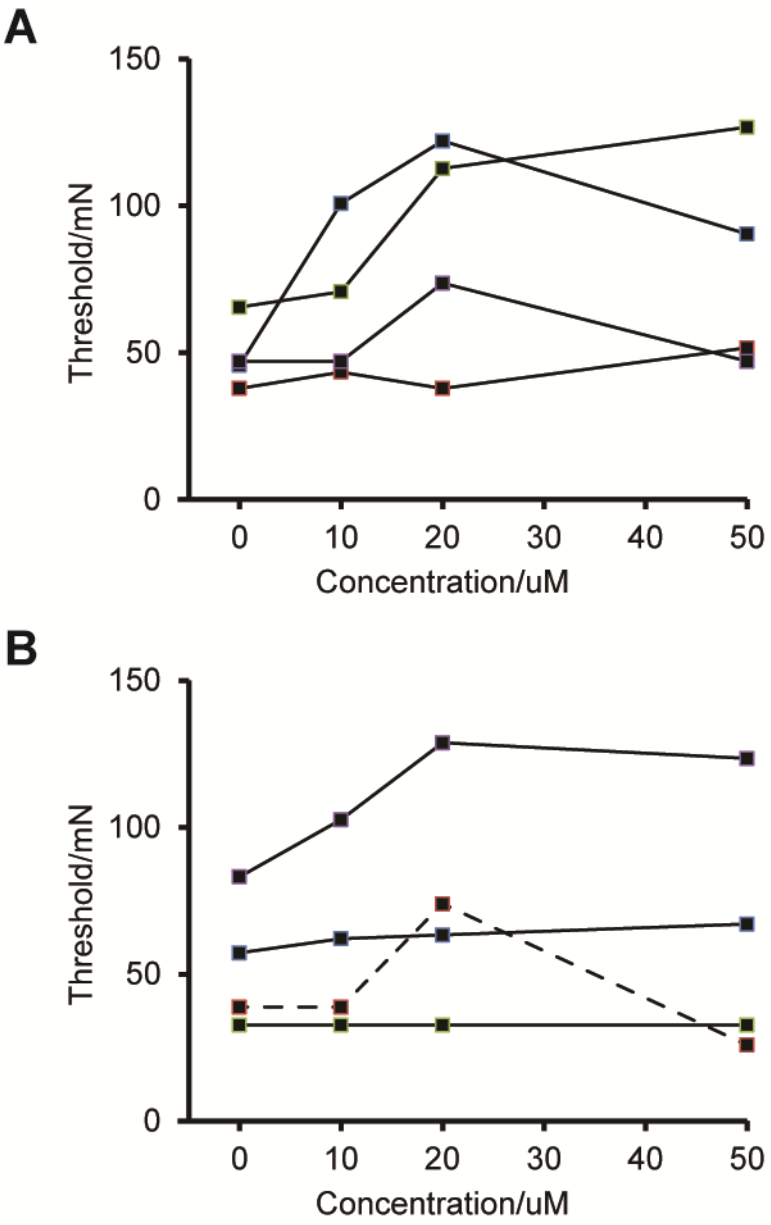

Figure 4.13 Firing thresholds following application of ruthenium red
The firing thresholds of AMS hotspots; before and after application of 10-50 µM ruthenium red following A) vinblastine treatment and B) neuritis. Hashed line represents hotspot that was distal to the stimulating electrodes. Vinblastine n = 4, neuritis n = 4.

FM1-43

All nerves were stained at the location where FM1-43 has been applied. Following the application of 2.5-25 µM FM1-43, there was negligible block of conduction along C-fibre axons at the treatment site in untreated (86%; n = 37/43 axons), vinblastine-treated (70%; n = 14/20 axons) and neuritis nerves (91%; n = 7/8 axons).

Figure 4.14 shows example AMS responses to the force-discharge step protocol following the application of FM1-43. Following both vinblastine treatment and neuritis, ruthenium red caused a dose dependent decrease in the number of spikes.s^{-1} produced from AMS hotspots at 150 mN force (main effects: both $p < 0.05$, Friedman test; **Figure 4.15**). Twenty-five micro molar FM1-43 caused a significant decrease in the number of spikes.s^{-1} produced at 150 mN force from hotspots following vinblastine treatment and neuritis (Dunn's post hoc comparisons to 0µM, both $p < 0.05$). Following application of 25 µM FM1-43, the number of spikes.s^{-1} had reduced by 70% and 58% compared to that of baseline (vinblastine treatment and neuritis respectively).

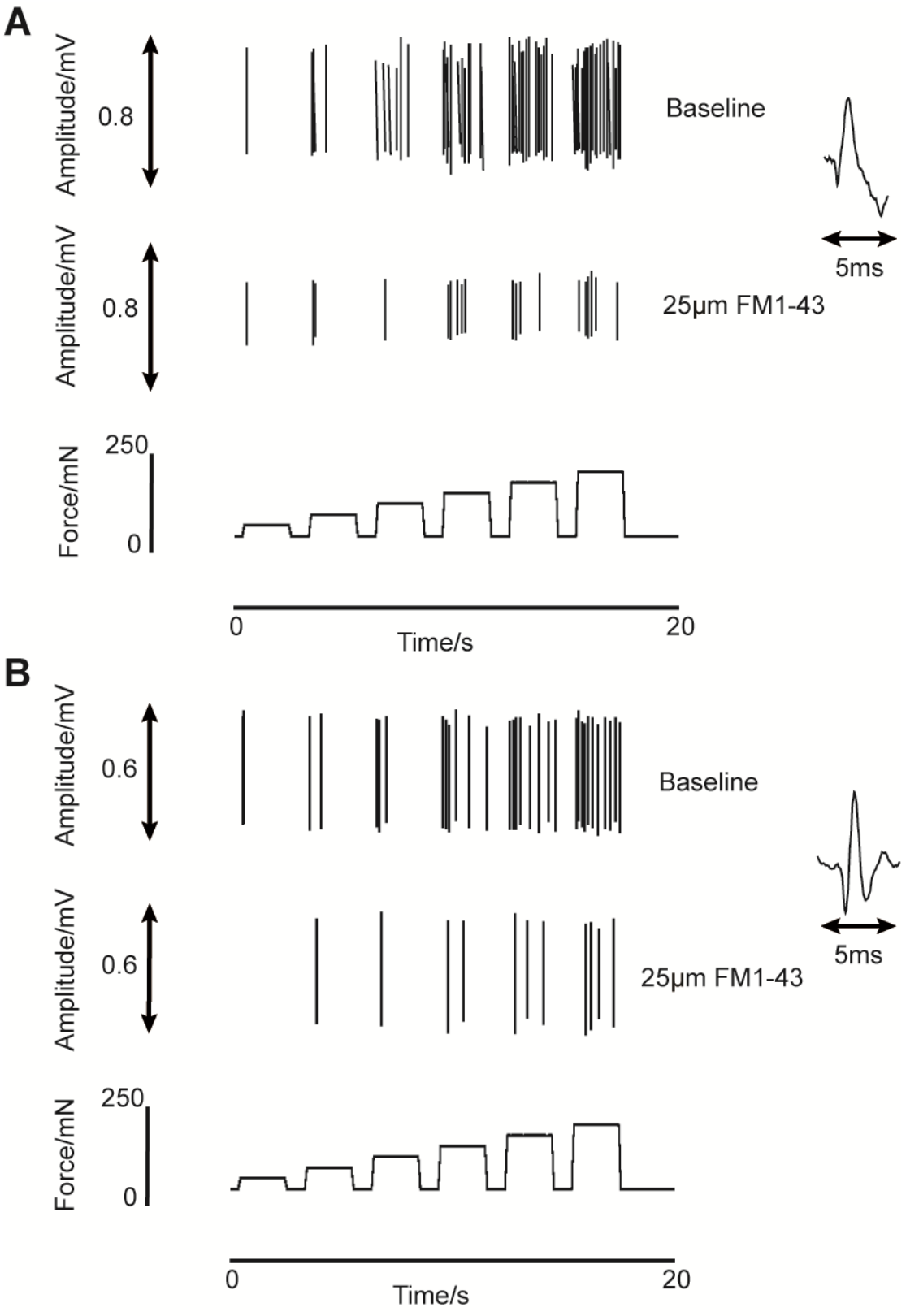

Figure 4.14 Example force-discharge responses pre and post 25µM FM1-43.
Responses from a mechanically sensitive hotspot identified in a nerve A) 4 days following vinblastine treatment and B) 6 days following neuritis.

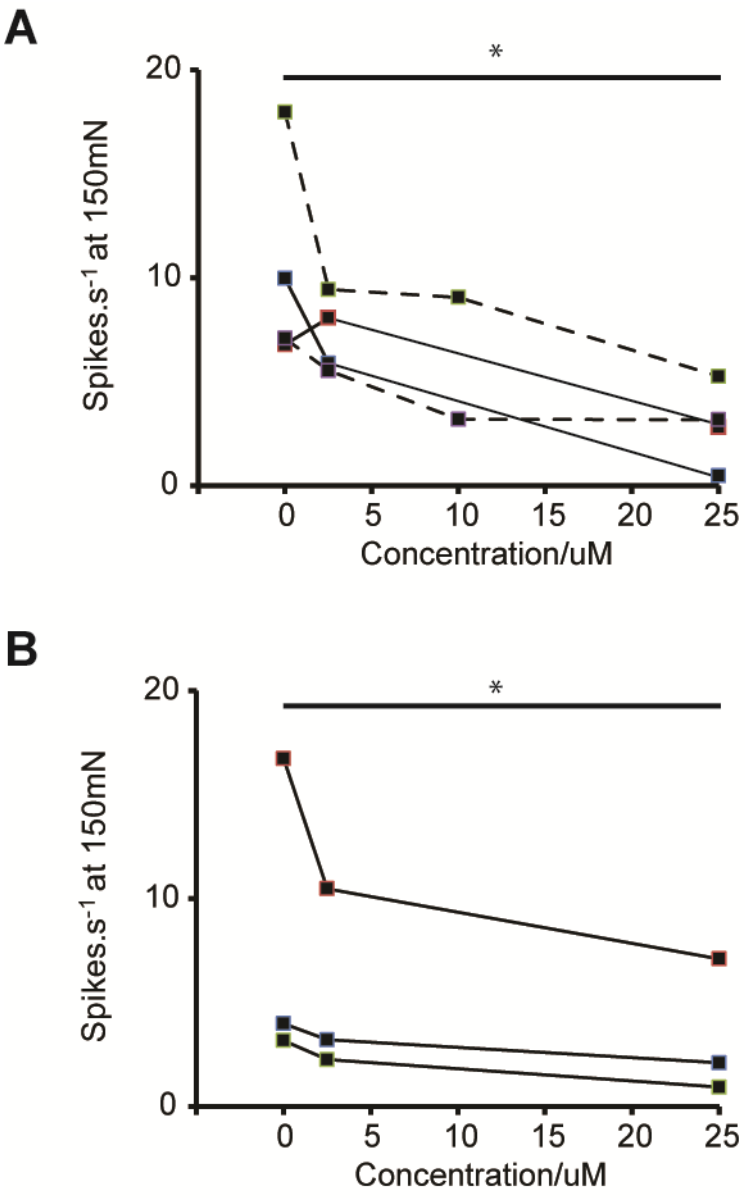

Figure 4.15 The number of spikes.s^{-1} produced from mechanically sensitive hotspots at 150 mN following application of FM1-43. The average number of spikes.s^{-1} produced at 150 mN force from AMS hotspots ; before and after application of 2.5-25µM FM1-43 following A) vinblastine treatment and B) neuritis. In two hotspots from vinblastine-treated nerves, 10 µM FM1-43 was applied between 2.5 and 25µM (hashed lines). * $p < 0.05$ Dunn's post-hoc comparison to 0 µM. Vinblastine n = 4, neuritis n = 3.

Following both vinblastine treatment and neuritis, FM1-43 caused a reduction in the slope of the linear regression line fit to force-discharge relationships from AMS hotspots (main effects: $p < 0.05$ and $p = 0.47$ respectively, repeated measures one-way ANOVA; **Figure 4.16**). Twenty-five micro molar FM1-43 caused a significant decrease in the slope of the force-discharge relationships of hotspots identified following vinblastine treatment ($p < 0.05$, Dunnett's post-hoc comparison to 0µM). Following application of 25 µM, the average slope decreased by 71% and 8% compared to baseline (vinblastine treatment and neuritis respectively).

Following both vinblastine treatment and neuritis, FM1-43 had a negligible effect on the firing threshold of mechanically sensitive hotspots (main effects: $p = 0.16$ and $p = 0.67$ respectively, Friedman test; **Figure 4.17**). Following application of 25 µM, the thresholds increased marginally by 11% and 16% compared to that of baseline (vinblastine treatment and neuritis respectively).

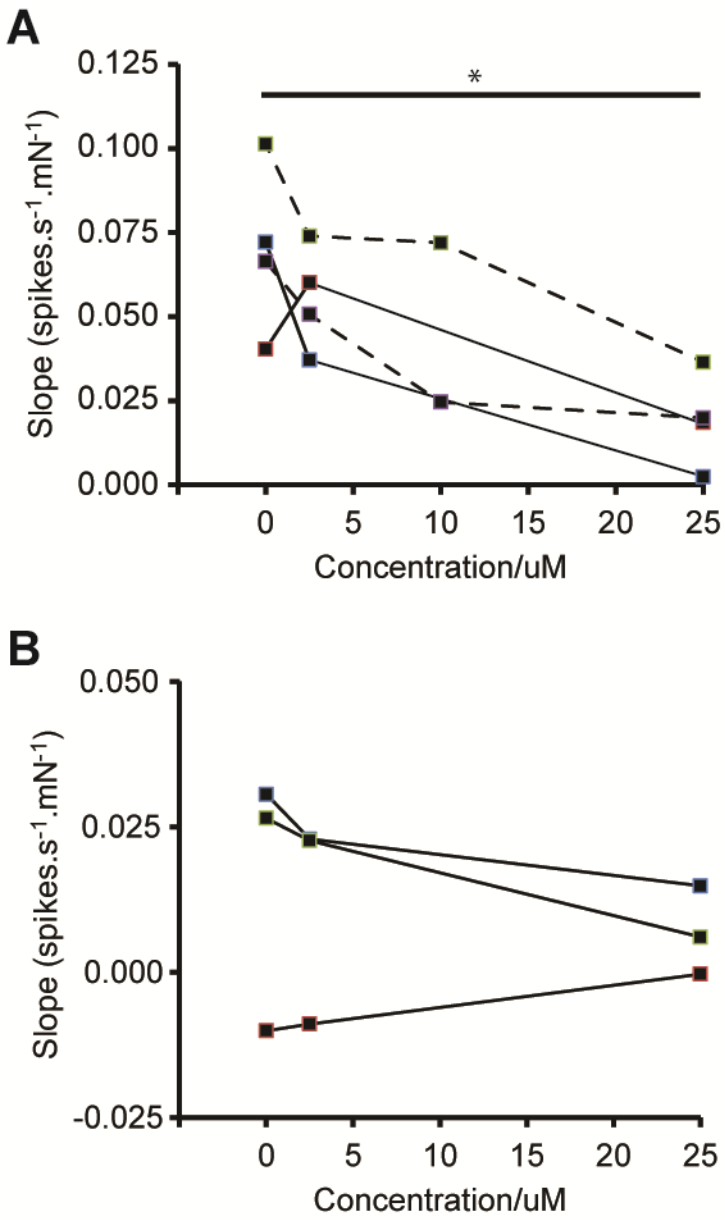

Figure 4.16 Slopes of force-discharge relationships following FM1-43 application
The slope of the force discharge relationship; before and after application of 2.5-25µM FM1-43 following A) vinblastine treatment and B) neuritis. In two hotspots from vinblastine-treated nerves, 10 µM FM1-43 was applied between 2.5 and 25 µM (hashed lines). * $p < 0.05$ Dunnett's post-hoc comparison to 0 µM. Vinblastine n = 4, neuritis n = 3.

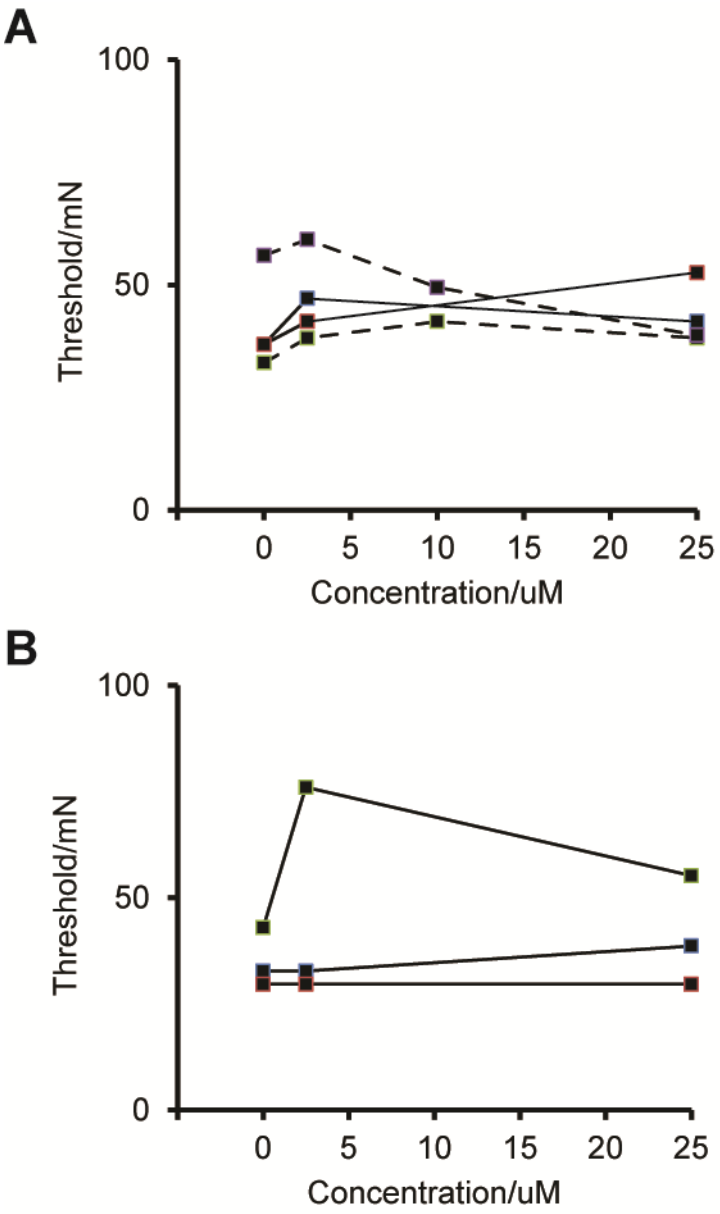

Figure 4.17 Firing thresholds following application of FM1-43
The firing thresholds of mechanically sensitive hotspots; before and after application of 2.5-25µM FM1-43 following A) vinblastine treatment and B) neuritis. In two hotspots from vinblastine-treated nerves, 10 µM FM1-43 was applied between 2.5 and 25 µM (hashed lines). Vinblastine n = 4, neuritis n = 3.

4.3 Main findings

- C-fibre axon conduction through the treatment site was disrupted in a proportion (10/19) of neuritis nerves.
- In neuritis nerves where conduction was affected, 24% (12/49) of C-fibre axons conducted across the treatment site.
- Following vinblastine treatment and neuritis, clear force-discharge relationships were produced from the majority of AMS hotspots.
- Following vinblastine treatment, the slope of the linear regression lines fitted to discharge response from AMS hotspots (0.055 spikes.s^{-1}.mN^{-1}) was significantly greater than that of the neuritis (0.027 spikes.s^{-1}.mN^{-1}; $p<0.01$).
- The firing threshold of AMS hotspots was similar following vinblastine treatment (48 mN) and neuritis (36 mN).
- Following 10-50 µM ruthenium red, there was a decrease in the number of spikes.s^{-1} produced from AMS hotspots at 150 mN force (82% and 55% decrease from baseline after 50 µM, following vinblastine treatment and neuritis respectively).
- Following 10-50 µM ruthenium red, there was an increase in the firing threshold following vinblastine treatment (57% post 50µM) and a negligible increase following neuritis (13% post 50µM).
- Following 2.5-25 µM FM1-43, there was a decrease in the number of spikes.s^{-1} produced from AMS hotspots at 150 mN force (70% and 59% decrease from baseline after 25 µM; following vinblastine treatment and neuritis respectively).
- Following 2.5-25 µM FM1-43, there were small increases in the firing thresholds (11% and 16% increase following 25 µM; following vinblastine treatment and neuritis respectively).

4.4 Discussion

Although previous studies have examined vinblastine- and neuritis-induced AMS, these studies have focused on the proportion of responding neurons rather than the characteristics of the response. It was hypothesised that mechanically sensitive ion channels are responsible for AMS, and that these channels enabled axons to encode local changes in force within the nerve. In this study, an ex-vivo recording chamber was used to record from the sciatic nerve dissected from animals following vinblastine treatment and neuritis. This facilitated the use of a force-feedback controlled stimulator to investigate the force-discharge responses produced from mechanically sensitive hotspots.

4.4.1 Mechanically stimulating hotspots produced positive force-discharge relationships

The present study set out to determine if the force-discharge relationships produced from mechanically stimulating hotspots were graded, i.e. do higher forces elicit more action potentials. At peripheral terminals, nociceptors produce graded responses (Andrew and Greenspan, 1999; Cain et al., 2001; Hoffmann et al., 2008), which allow these neurons to locally encode the rate of firing into the spinal cord. The consequence of this graded response is that increased noxious stimulation causes a greater intensity of pain. The results from this study show that mechanically sensitive hotspots also produce graded responses, which suggest that increased pressure over a nerve trunk, or increased nerve stretch, will cause increased nociceptor activation in patients with suspected neuritis. Accordingly, movements that stretch peripheral nerves may increase the afferent input into to the spinal cord, thereby contributing towards central sensitisation.

Graded responses are also reported in other excitable cells involved in mechanosensation, such as muscle spindles, hair cells and Pacinian corpuscles (Hudspeth and Corey, 1977; Ottoson and Shepherd, 1970; Tapper, 1965) where mechanically sensitive ion channels are reported to underlie mechanosensitivity (Gale et al., 2001; Woo et al., 2015). Therefore, graded responses produced from mechanically sensitive axons indicate that mechanically sensitive ion channels are

likely to underlie AMS. Interestingly, graded responses are also produced from mechanically sensitive axons following nerve crush (neuroma) (Rivera et al., 2000), which indicates that the mechanisms that cause AMS might be similar to that following vinblastine treatment and neuritis. At a neuroma site, mechanical sensitivity is likely to be due to an accumulation of mechanically sensitive ion channels subsequent to the cessation of axonal transport (Koschorke et al., 1994). This mechanism is consistent with the hypothesis that AMS is due to the disruption and subsequent accumulation of mechanically sensitive ion channels following vinblastine treatment and neuritis.

The slope of the force-discharge response was examined as a measure of the responsiveness of mechanically sensitive hotspots. There were clear differences in the slopes of the force-discharge response following vinblastine treatment compared to neuritis. The greater slopes following vinblastine treatment indicate that vinblastine hotspots were more responsive at higher forces. This difference could signify an increased density of mechanically sensitive ion channels at the treatment site following vinblastine treatment. Differences in the density of ion channels may reflect the time courses of axonal transport disruption. As the onset of axonal transport disruption is slower following neuritis compared to vinblastine treatment (Dilley et al., 2013), less channels may have accumulated at the neuritis treatment site at the time points examined in this study. Alternatively, the dissimilarity in the responsiveness between vinblastine treatment and neuritis could be due to the differences in the composition of tissue at the site where the hotspots were located. Following neuritis, a thickened granuloma forms at the treatment site due to the mass of inflammatory cells and dense fibrous tissue (Bove et al., 2003; Eliav et al., 1999). The majority of hotspots were typically located at this site. In contrast, following vinblastine treatment, the gross morphology of the nerve appears unaffected by the treatment, with no signs of a granuloma or fibrosis.

4.2.2 Firing thresholds were similar following vinblastine treatment and neuritis

The firing thresholds identified in this study are consistent with the range of forces (≤200 mN) required to initiate responses from mechanically sensitive axons in-vivo (Dilley and Bove, 2008a; b). The firing thresholds of mechanically sensitive C-fibre axons were 24 and 18 mN/mm^2 following vinblastine treatment and neuritis respectively. These values have been converted to pressures based upon the area of the probe ($2mm^2$) that was used in this study. Interestingly, firing thresholds of mechanically sensitive C-fibre axons were broadly comparable to those that developed mechanical sensitivity following nerve crush (3-11 mN/mm^2) (Janig et al., 2009; Kirillova et al., 2011; Rivera et al., 2000), which suggests that the mechanisms of mechanotransduction might be similar. As previously discussed, mechanically sensitive ion channels are likely to contribute to mechanical sensitivity following nerve crush, vinblastine treatment and neuritis. Thus, the comparable thresholds indicate that the mechanically sensitive ion channels at a neuroma site might be similar to those that have accumulated vinblastine and neuritis treatment sites. As it is likely that the firing threshold of a mechanically sensitive axon will be affected by the composition of the surrounding tissue, firing thresholds have not been compared to that of the mechanosensitive nociceptors in the skin and muscle.

4.4.3 Mechanically sensitive ion channel blockers attenuated AMS

The underlying channels that lead to AMS have yet to be identified. To verify whether mechanically sensitive ion channels are responsible for AMS in C-fibre neurons, the broad-spectrum mechanically sensitive ion channel blockers, ruthenium red and FM1-43 (Di Castro et al., 2006; Drew and Wood, 2007; Drew et al., 2002; Gale et al., 2001), were applied to AMS hotspots.

Data from this study has shown that both ruthenium red and FM1-43 cause a dose dependent attenuation of AMS following vinblastine treatment and neuritis, which is consistent with a role for mechanically sensitive ion channels. Of the putative mechanically sensitive ion channels expressed on nociceptive neurons, ruthenium red blocks the TRP channels TRPA1, TRPV1, TRPV4, and TRPC3 (Fischer et al., 2003; Nagata et al., 2005; Qu et al., 2012; Voets et al., 2002), PIEZO2 (Coste et al., 2010;

Coste et al., 2012) and tentonin 3 (Hong et al., 2016). Similar to ruthenium red, FM1-43 blocks PIEZO2 (Eijkelkamp et al., 2013), tentonin3 (Hong et al., 2016), TRPC3, but also TRPC6 (Quick et al., 2012). Of these channels, TRPA1, TRPV1 and TRPV4 are reported to be involved in mechanical nociception (Brierley et al., 2009; Brierley et al., 2008; Jones et al., 2005b; Kerstein et al., 2009; Mueller-Tribbensee et al., 2015; Rong et al., 2004; Vilceanu and Stucky, 2010) and both TRPV1 and TRPA1 are involved in inflammatory-induced mechanical sensitisation of afferents (Brederson et al., 2012; Brierley et al., 2009; De Schepper et al., 2008; DeBerry et al., 2014; Jones et al., 2005b; Kelly et al., 2015). As such, it is possible that these channels contribute towards AMS. Although TRPC3, TRPC6, PIEZO2 and tentonin3 are not reported to be involved in mechanical nociception (Hong et al., 2016; Quick et al., 2012; Woo et al., 2014), these channels may still contribute towards AMS.

Whereas the highest concentration of ruthenium red (50 µM) appeared to completely attenuate vinblastine-induced AMS, following neuritis, the same concentration produced a partial block of AMS. Interestingly, ruthenium red appeared to reach a maximum effect at 20 µM, suggesting that other mechanically sensitive ion channels that are not blocked by ruthenium red contribute towards the development of neuritis-induced AMS. Acid sensing ion channels are an example of the latter (Alvarez de la Rosa et al., 2002).

While there was a large decrease in the slope following application of 50 µM ruthenium red or 25 µM FM1-43 to hotspots in vinblastine-treated nerves, the same concentrations caused a moderate reduction in the slope following neuritis. This was probably due to a near complete block of all the channels responsible for AMS following vinblastine treatment. The reduction in the slope indicates that blockers appeared to be more effective at the highest forces that were applied to hotspots. It is not clear why this occurred. However, as ruthenium red blocks mechanically sensitive channels by binding within the channel pore (Coste et al., 2012; Voets et al., 2002), this effect might be due to use dependency. Although FM1-43 also block mechanically sensitive ion channels by binding within the channel pore (Drew and Wood, 2007; Gale et al., 2001), it is not reported to exert a use-dependent block (Gale et al., 2001).

The increase in the threshold of vinblastine-induced AMS following ruthenium red application contrasts from neuritis, where a similar response was not observed. It seems likely that the increased threshold following vinblastine treatment was due to the majority of mechanically sensitive ion channels being blocked. Accordingly, the remaining unblocked channels are likely to require higher forces to produce enough depolarisation to initiate an action potential.

4.4.4 Vinblastine treatment caused conduction slowing in nociceptive axons

Here it was found that conduction in C-fibres was slowed along the length of the sciatic nerve following vinblastine treatment, which is consistent with findings from an in-vivo study (Dilley and Bove, 2008a). Although slowing of conduction has also been reported following neuritis (Dilley and Bove, 2008b), it does not occur until later time points (1-4 weeks). Accordingly, conduction velocities were not slowed following neuritis in this study. It is not known how vinblastine treatment causes conduction slowing along axons in the sciatic nerve. However, it is possible that conduction slowing is a consequence of the reduced retrograde transport of target-derived factors, such as GDNF and NGF. Accordingly, conduction slowing following axotomy is associated with the reduced delivery of these factors to the DRG (Bennett et al., 1998b). For example, reduced NGF signalling is likely to result in a decrease in the production of neurofilaments in neurons (Verge et al., 1990), thereby causing a decrease in axonal diameter (Hoffman et al., 1987), which results in a reduction in conduction velocity (Gasser and Grundfest, 1939). Additionally, reduced target-derived factor signalling may alter the gating or expression of sodium channels, such as $Na_v1.7$ (Kim et al., 2002; Stamboulian et al., 2010), which are important in determining conduction velocity (De Col et al., 2008; Pinto et al., 2008). The reduced anterograde transport of ion channels and other molecules is also likely to contribute to conduction slowing. For instance, disrupted sodium channel transport is likely to reduce their density along the axonal membrane. Furthermore, as the transport of mitochondria is also likely to be disrupted (Shemesh and Spira, 2010), the energy deficits that probably result from this may further contribute to conduction slowing.

4.4.5 Levels of AMS are lower ex-vivo compared to in-vivo

The proportions of C-fibre axons with AMS following vinblastine treatment and neuritis were substantially lower when recording ex-vivo compared to in-vivo (Dilley and Bove, 2008a; b; Dilley et al., 2013). This suggests that neurons with AMS could be more vulnerable to damage and are particularly susceptible upon being removed from their internal environment. Mitochondria dysfunction or alterations to the distribution of mitochondria might be involved in such changes, as they are critical in supplying energy to the axon. Repeated systemic administration of anti-mitotic agents, such as paclitaxel, is known to cause an increase in the number of swollen and vacuolated mitochondria (Flatters and Bennett, 2006; Jin et al., 2008), which can lead to energy deficits in neurons (Duggett et al., 2017; Zheng et al., 2011). Inflammation can also cause damage to mitochondria (Nikic et al., 2011). However, such changes are associated with axonal degeneration (Nikic et al., 2011), which is minimal following neuritis (Eliav et al., 1999). The transport of mitochondria is disrupted following inflammation (Errea et al., 2015; Sorbara et al., 2014), and following treatment with anti-mitotic agents (Shemesh and Spira, 2010). This may lead to a decrease in the number of functional mitochondria distal to the treatment site, resulting in energy depletion.

Alternatively, temperature may have influenced the incidence of AMS, as experiments were carried out at 32˚C, rather than 37˚C. Temperature-induced changes to the properties of the membrane may alter the gating of mechanically sensitive ion channels. For example, a reduction in temperature decreases the compressibility of the membrane and increases its thickness (Heimburg, 1998), which may hinder mechanically sensitive channel opening in response to mechanical stimulation (Martinac and Hamill, 2002). Furthermore, certain ion channels are known to be gated by changes in temperature, many of which are from the TRP channel family (Vriens et al., 2014). It is important to note that several of channels that are gated by mechanical stimuli also belong to the TRP channel family. Hence, the temperature may influence the way the channel responds to mechanical stimuli, if the gating mechanisms involved are similar.

4.4.6 Conduction was partially blocked through the neuritis site

Following neuritis there was reduced conduction through the treatment site, which is in contrast to what is reported in vivo (Dilley et al., 2005). The reason for this discrepancy is unclear, but the most likely explanation is that it is due to a lack of circulation. In an in vivo preparation the nerve is likely to be sufficiently perfused with oxygen and glucose at the neuritis site due to the continuous flow of blood through intraneural blood vessels. Whereas in an ex vivo preparation, oxygen and glucose are likely to enter the axons from the cut ends or by diffusing across the epineurial and perineurial membranes. At the neuritis site the presence of a granuloma may act as a barrier that limits the supply of oxygen and glucose to the nerve, thereby causing energy depletion and hypoxic conditions, the latter of which is known to block conduction (Calcutt et al., 1991).

4.4.7 Summary

The current study has demonstrated that mechanically sensitive hotspots in C-fibre axons produce a graded response to changes in force and that mechanically sensitive ion channel blockers attenuate these responses. Taken together, this strongly suggests that mechanically sensitive ion channels are responsible for AMS. Potential mechanically sensitive ion channels that might be involved in the development of AMS include TRPA1, TRPV1 and TRPV4. However, further ex-vivo experiments investigating the effects of specific ion channel blockers were not carried out due to the technical difficulties associated with experiments (see limitations **7.3.1**). In contrast to neuritis, the conduction velocities of C-fibre axons were slowed following vinblastine treatment. Finally, a lower proportion of AMS was found ex vivo compared to that in vivo, suggesting that these axons are likely to be susceptible to changes in their internal environment.

Chapter 5

The effect of localised axonal transport disruption and neuritis on the expression of TRPV1, TRPA1 and ASIC3 in primary sensory neurons

5.1 Introduction

In a previous study from our laboratory, vinblastine treatment of the sciatic nerve and the induction of a neuritis cause the disruption to fast axonal transport (Dilley et al., 2013). Fast axonal transport is responsible for the delivery of sensory ion channels, including that of mechanically sensitive ion channels, to the periphery (Koschorke et al., 1994). However, it is not known whether the transport of sensory ion channels is disrupted as result of this axonal transport disruption and whether there is evidence for their accumulation in the nerve. Therefore, in this study, the expression of the sensory ion channels TRPV1, TRPA1 and ASIC3 were examined in the sciatic nerve following vinblastine treatment or neuritis. These ion channels were chosen based on their neuronal expression and because they are postulated to be involved in mechanical nociception and inflammatory-induced mechanical sensitivity (Brierley et al., 2011; Brierley et al., 2009; De Schepper et al., 2008; Jones et al., 2005b; Kelly et al., 2015; Kerstein et al., 2009; Page et al., 2005).

To examine the effects of axonal transport disruption on the anterograde transport of sensory ion channels, partial ligation experiments were carried out. This was carried out by assessing the build-up of TRPV1, TRPA1 and ASIC3 proximal to the point where the nerve has been partially ligated in the presence or absence of a proximal vinblastine treatment or neuritis. To determine if ion channels were accumulating in sciatic nerves following vinblastine treatment and neuritis, the expression of sensory ion channels was investigated in the sciatic nerve at the treatment site and proximal to this site. Further to this, the levels of sensory ion channel expression were also explored in the small to medium diameter cell bodies of the DRG.

The primary objectives were:

1. To determine if the anterograde transport of TRPV1, TRPA1 and ASIC3 were disrupted in the sciatic nerve.
2. To determine if there was any evidence for the accumulation of TRPV1, TRPA1 and ASIC3 at the treatment sites.

5.2 Results

5.2.1 Sensory ion channel transport disruption in the sciatic nerve.

Effect of surgery

All animals made a recovery after induction of a partial nerve ligation, including those that also had the addition of vinblastine or CFA application proximal to the site of ligation. In nerves treated with saline and vinblastine proximal to the ligation site, the nerve appeared normal apart from some evidence of oedema near to the ligation site. In nerves treated with CFA proximal to the ligation, there was evidence for a neuritis formation, which on some occasions appeared to form over the top of the ligation site. If a neuritis lesion appeared to be more distal than proximal in relation to the partial ligation site, these nerves were excluded from the final analysis, which is why n numbers are lower in the neuritis group. On observation of animals within their home cages, it appeared that animals had abnormal gait and exhibited guarding postures of the affected hind limb.

Transient receptor potential vanilloid 1

Following saline treatment, the intensity of anti-TRPV1 labelling was increased in the ligated portion of the nerve, just proximal to the site of ligation (mean ratio of the ligated vs the unligated portion was 1.70, SEM +/- 0.14, n = 5; **Figure 5.1 A**). Following vinblastine treatment, there was a significant reduction in anti-TRPV1 labelling in the ligated portion of the nerve compared to that of saline (mean ratio = 1.15, SEM +/- 0.08, n = 5; main effect $p<0.05$, one-way ANOVA; $p<0.05$, Dunnett's post hoc test; **Figure 5.1 A & B**). Following neuritis, there was a reduction in anti-TRPV1 labelling in the ligated portion of the nerve compared to that of saline treatment (mean ratio = 1.38, SEM +/- 0.2, n = 3; $p = 0.26$, Dunnett's post hoc test; **Figure 5.1 A & B**).

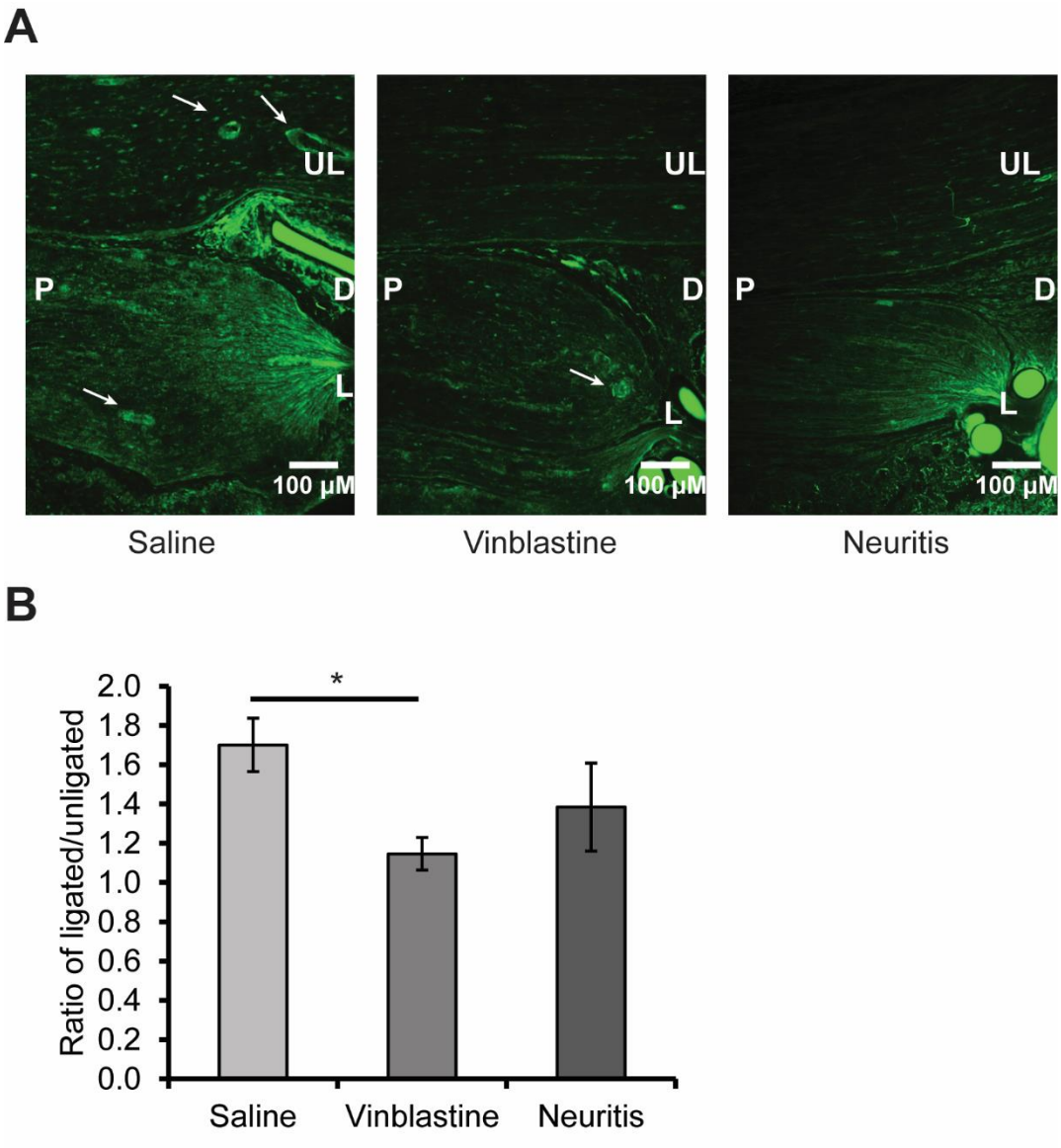

Figure 5.1 The effect of vinblastine treatment and neuritis on the anterograde transport of TRPV1 along the sciatic nerve. A) Example photographs of longitudinal sections of partially ligated nerves 4 days post-surgery treated proximally with either saline, vinblastine or CFA (neuritis). P = proximal, D = distal, L = ligated portion of the nerve, UL = unligated portion of the nerve. Taken at 10x magnification. Arrows indicate anti-TRPV1 labelling in what appeared to be blood vessel walls. B) Mean ratio of the intensities of anti-TRPV1 labelling in the ligated vs unligated portion of the nerve in animals following treatment with saline (n = 5 animals), vinblastine (n = 5 animals) or CFA (n = 3 animals) proximal to the ligation site. For each animal between 2-10 sections were analysed. Following vinblastine treatment, there was a significant reduction in the ratio of the intensity of anti-TRPV1 labelling (*p <0.05; Dunnett's post hoc comparison to saline). Error bars represent SEM.

Transient receptor potential ankyrin-1

Following saline treatment, the intensity of anti-TRPA1 labelling was increased in the ligated portion of the nerve, proximal to the site of ligation (mean ratio of the ligated vs the unligated portion was 2.44, SEM +/- 0.29, n = 4; **Figure 5.2 A**). Following vinblastine treatment, there was a significant reduction in anti-TRPA1 labelling in the ligated portion of the nerve compared to that of saline (mean ratio = 1.18, SEM +/- 0.08, n = 4; main effect $p<0.05$, one-way ANOVA; $p<0.05$, Dunnett's post hoc test; **Figure 5.2 A & B**). Following neuritis, there was a reduction in anti-TRPA1 labelling in the ligated portion of the nerve compared to that of saline treatment (mean ratio = 1.72, SEM +/- 0.37, n = 3; $p = 0.21$, Dunnett's post hoc test; **Figure 5.2 A & B**).

Acid sensing ion channel 3

Following saline treatment, there was a small increase in the intensity of anti-ASIC3 labelling proximal to where the nerve had been ligated (mean ratio of the ligated vs the unligated portion was 1.58, SEM +/- 0.18, n = 3; **Figure 5.3 A**). Following vinblastine treatment, there was a reduction in anti-ASIC3 labelling in the ligated portion of the nerve compared to that of saline treatment (mean ratio = 1.32, SEM +/- 0.01, n = 3; **Figure 5.3 A** & **B**; main effect $p = 0.36$, one-way ANOVA). Following neuritis, there was a slight reduction in anti-ASIC3 labelling in the ligated portion of the nerve compared to that of saline treatment (mean ratio = 1.40, SEM +/- 0.09, n = 3; **Figure 5.3 A** & **B**).

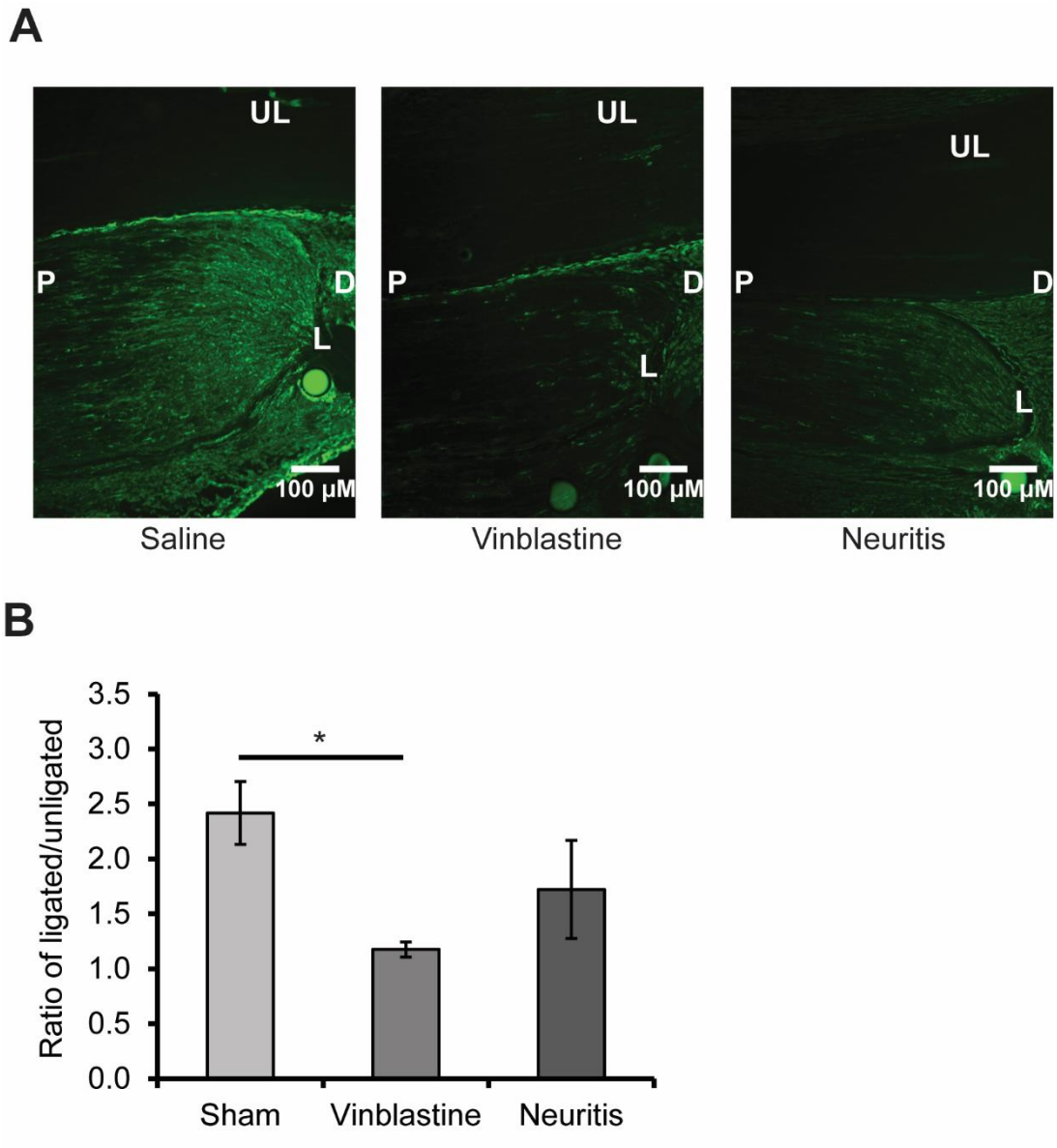

Figure 5.2 The effect of vinblastine treatment and neuritis on the anterograde transport of TRPA1 along the sciatic nerve. A) Example photographs of longitudinal sections of partially ligated nerves 4 days post-surgery treated proximally with either saline, vinblastine or CFA (neuritis). P = proximal, D = distal, L = ligated portion of the nerve, UL = unligated portion of the nerve. Taken at 10x magnification. B) Mean ratio of the intensities of anti-TRPA1 labelling in the ligated vs unligated portion of the nerve in animals following saline (n = 4), vinblastine (n = 4) or CFA (n = 4) treatment proximal to the ligation site. For each animal between 2-10 sections were analysed. Following vinblastine treatment, there was a significant reduction in the ratio of the intensity of anti-TRPA1 labelling in (*p <0.05; Dunnett's post hoc comparison to saline). Error bars represent SEM.

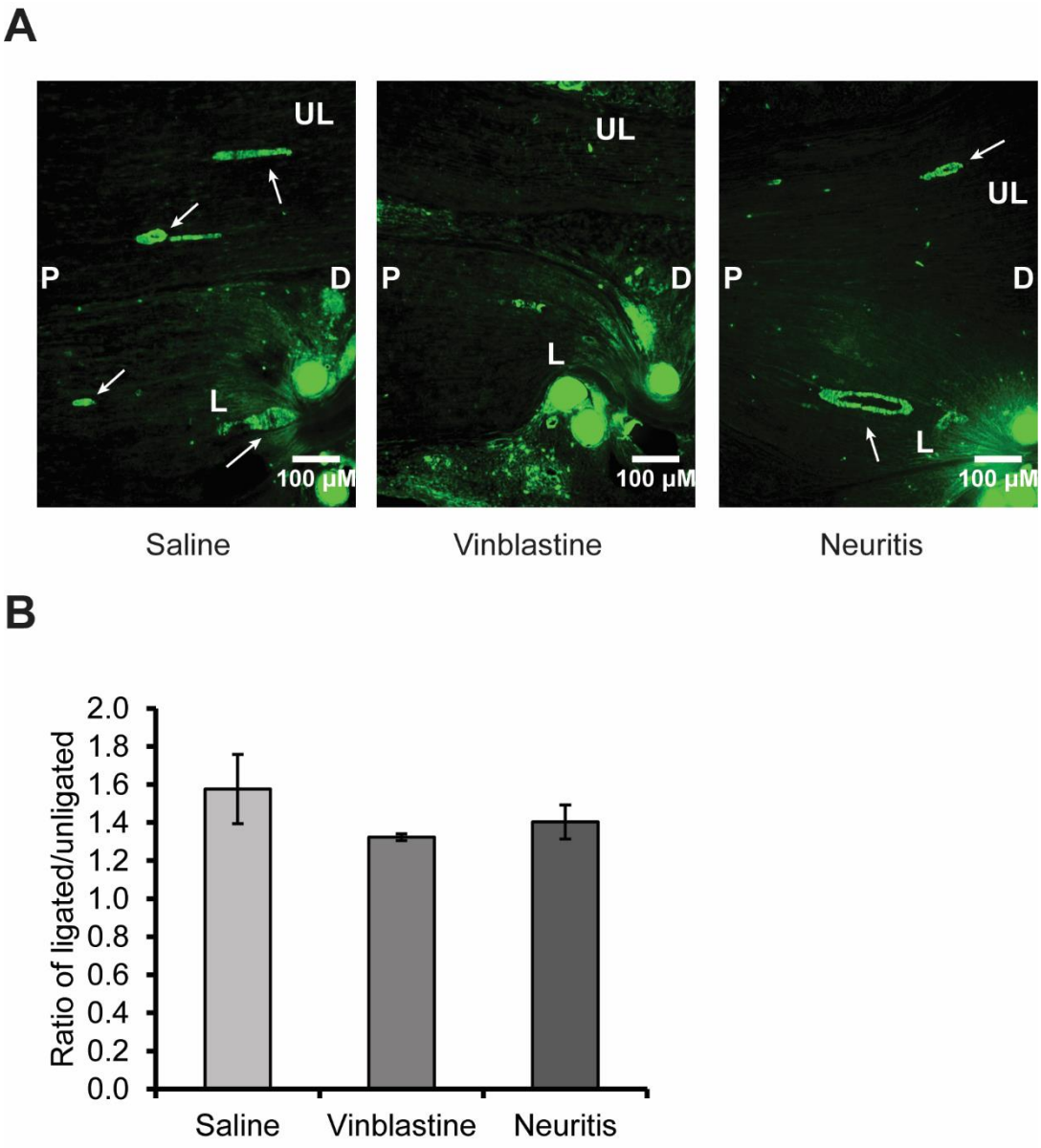

Figure 5.3 The effect of vinblastine treatment and neuritis on the anterograde transport of ASIC3 along the sciatic nerve. A) Example photographs of longitudinal sections of partially ligated nerves 4 days post lesion treated proximally with either saline, vinblastine or CFA (neuritis). P = proximal, D = distal, L = ligated portion of the nerve, UL = unligated portion of the nerve. Taken at 10x magnification. B) Mean ratio of the intensities of anti-ASIC3 labelling in the ligated vs unligated portion of the nerve in animals following saline (n = 3), vinblastine (n = 3) or CFA (n = 3) proximal to the ligation site. For each animal between 4-13 sections were analysed. Error bars represent SEM.

5.2.1 Changes to the distribution of sensory ion channels in the sciatic nerve

Effect of surgery

All of the animals that were only treated with saline, vinblastine or CFA made a recovery from their surgical procedures (no adverse effects were present in days following surgery).

Transient receptor potential vanilloid-1

The anti-TRPV1 antibody labelled structures that resembled the walls of endoneurial blood vessels (See arrow heads in **Figure 5.4 A**). Following saline and vinblastine treatment, low levels of anti-TRPV1 labelling were found at the approximate location of the treatment site in the sciatic nerve (**Figure 5.4 A**). Saline and vinblastine treatment of the nerve had no effect on the distribution of TRPV1 labelling. Following saline treatment, the mean ratio of the treatment site vs proximal anti-TRPV1 labelling intensity was 1.11 (SEM +/- 0.06, n = 3), which was not significantly different to the ratio following vinblastine treatment (mean ratio 1.11, SEM +/- 0.06, n = 3; main effect $p < 0.05$ one-way ANOVA; $p = 0.99$, Dunnett's post hoc test; **Figure 5.4 B**). Following neuritis, there was an increase in anti-TRPV1 labelling at the treatment site in comparison to that of the proximal region of nerve (**Figure 5.4 A**). The mean ratio of labelling at the treatment site vs proximal region was 1.32 (SEM +/- 0.03, n = 3), which was significantly greater than that of the ratio following saline treatment ($p < 0.05$, Dunnett's post hoc test; **Figure 5.4 B**).

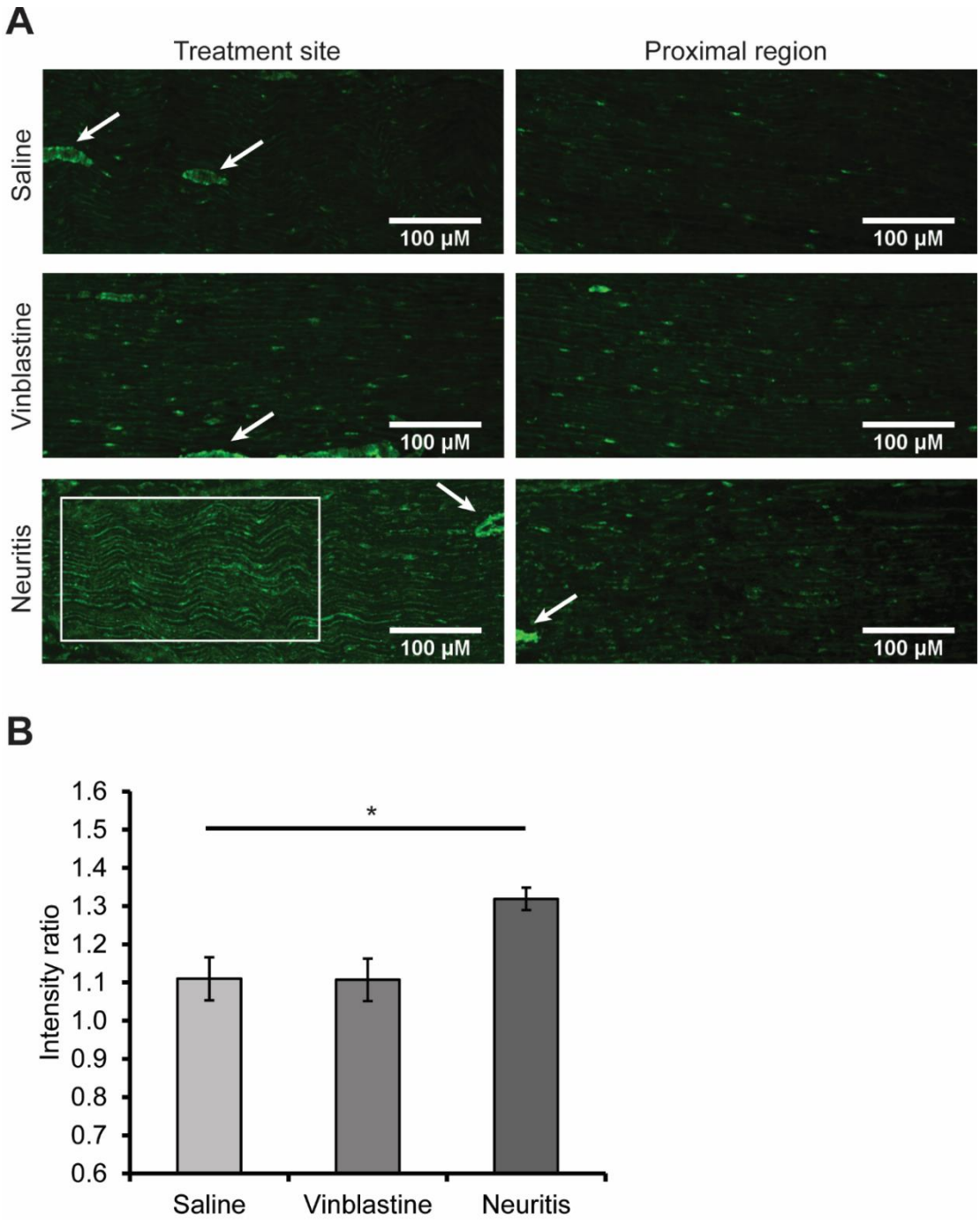

Figure 5.4 Distribution of anti-TRPV1 labelling in the sciatic nerve

A) Example photographs of longitudinal sciatic nerve sections at the approximate location of the treatment site and a region 3-5mm proximal to this region. There was an increase in anti-TRPV1 labelling at the treatment site following neuritis (highlighted in white box). Arrows indicate anti-TRPV1 labelling of blood vessel walls. Taken at 10x magnification B) Mean ratios of anti-TRPV1 labelling intensity at the treatment site vs the proximal region of nerve in saline, vinblastine and neuritis groups (all groups n = 3 animals, 2-3 sections per animal). There was a significant increase in the ratio of the intensity of anti-TRPV1 labelling in neuritis nerves (*p <0.05, Dunnett's post hoc comparison to saline). Error bars represent SEM.

Transient receptor potential ankyrin-1

The anti-TRPA1 antibody labelled structures that resembled the walls of endoneurial blood vessels (See arrow heads in **Figure 5.5 A**). Following saline treatment, vinblastine treatment and neuritis, low levels of anti-TRPA1 labelling were found at the approximate location of the treatment site. The distribution of anti-TRPA1 labelling was found to be similar in all groups (**Figure 5.5 A**). Following saline treatment, the mean ratio of the treatment site vs proximal anti-TRPA1 labelling intensity was 0.98 (SEM +/- 0.11, n = 3). Following vinblastine treatment, there was a slight increase in the ratio of labelling at the treatment site vs proximal region compared to saline, 1.22 (SEM +/- 0.19, n = 3 **Figure 5.5 B**). Following neuritis, the mean ratio of labelling at the treatment site vs proximal region was similar to that of saline, 1.08 (SEM +/- 0.09, n = 3; **Figure 5.5 B**). There were no significant differences between the treatment groups (main effect p = 0.52, one-way ANOVA).

Acid sensing ion channel 3

The anti-ASIC3 antibody labelled structures that resembled the wall of endoneurial blood vessels (See arrow heads in **Figure 5.6 A**). Following saline and vinblastine treatment, low levels of anti-ASIC3 labelling were found at the approximate location of the treatment site and the distribution of anti-ASIC3 labelling was similar in both of these treatment groups (**Figure 5.6 A**). Following saline treatment, the mean ratio of the treatment site vs proximal anti-ASIC3 labelling intensity was 0.96 (SEM +/- 0.05, n = 3), which wasn't significantly different to the ratio following vinblastine treatment (mean ratio 1.12, SEM +/- 0.06, n = 3; main effect p< 0.05, 1-way ANOVA; p = 0.14, Dunnett's post hoc test; **Figure 5.6 B**). Following neuritis, there appeared to be an increase in anti-ASIC3 labelling at the treatment site, compared to that of the region proximal to the treatment site (**Figure 5.6 A**). The mean ratio of labelling at the treatment site vs proximal region was 1.23 (SEM +/- 0.05, n = 3), which was significantly greater than the ratio of labelling following saline treatment (p < 0.05, Dunnett's post hoc test; **Figure 5.6 B**).

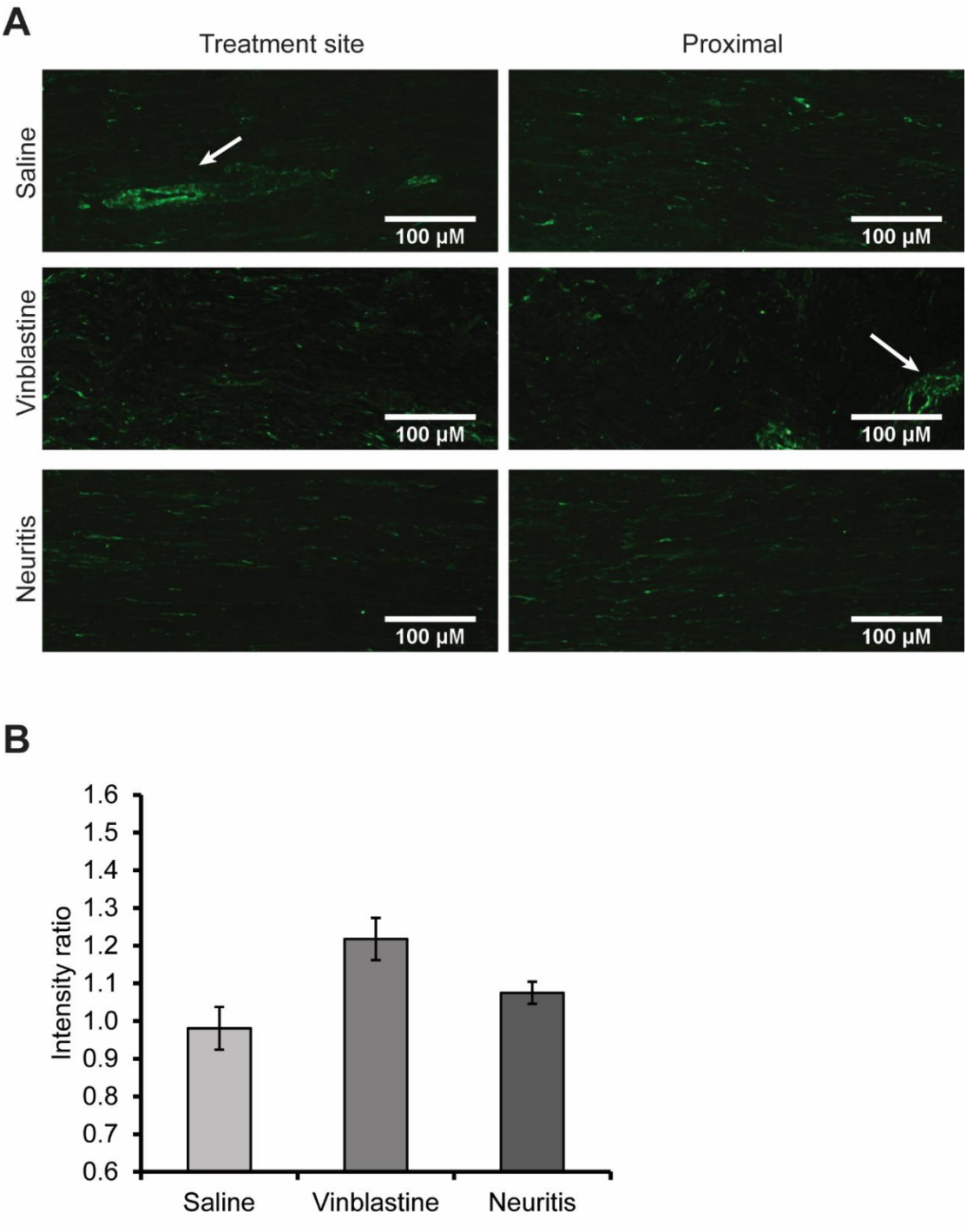

Figure 5.5 Distribution of anti-TRPA1 labelling in the sciatic nerve.
A) Example photographs of longitudinal sciatic nerve sections at the approximate location of the treatment site and a region 3-5mm proximal to this region. Arrows indicate labelling of anti-TRPA1 in what appeared to be blood vessel walls. Taken at 10x magnification. B) Mean ratios of the labelling intensity of anti-TRPA1 at the treatment site vs the proximal section of nerve in saline, vinblastine and neuritis groups (all groups n = 3 animals, 2-3 sections per animal). Error bars represent SEM.

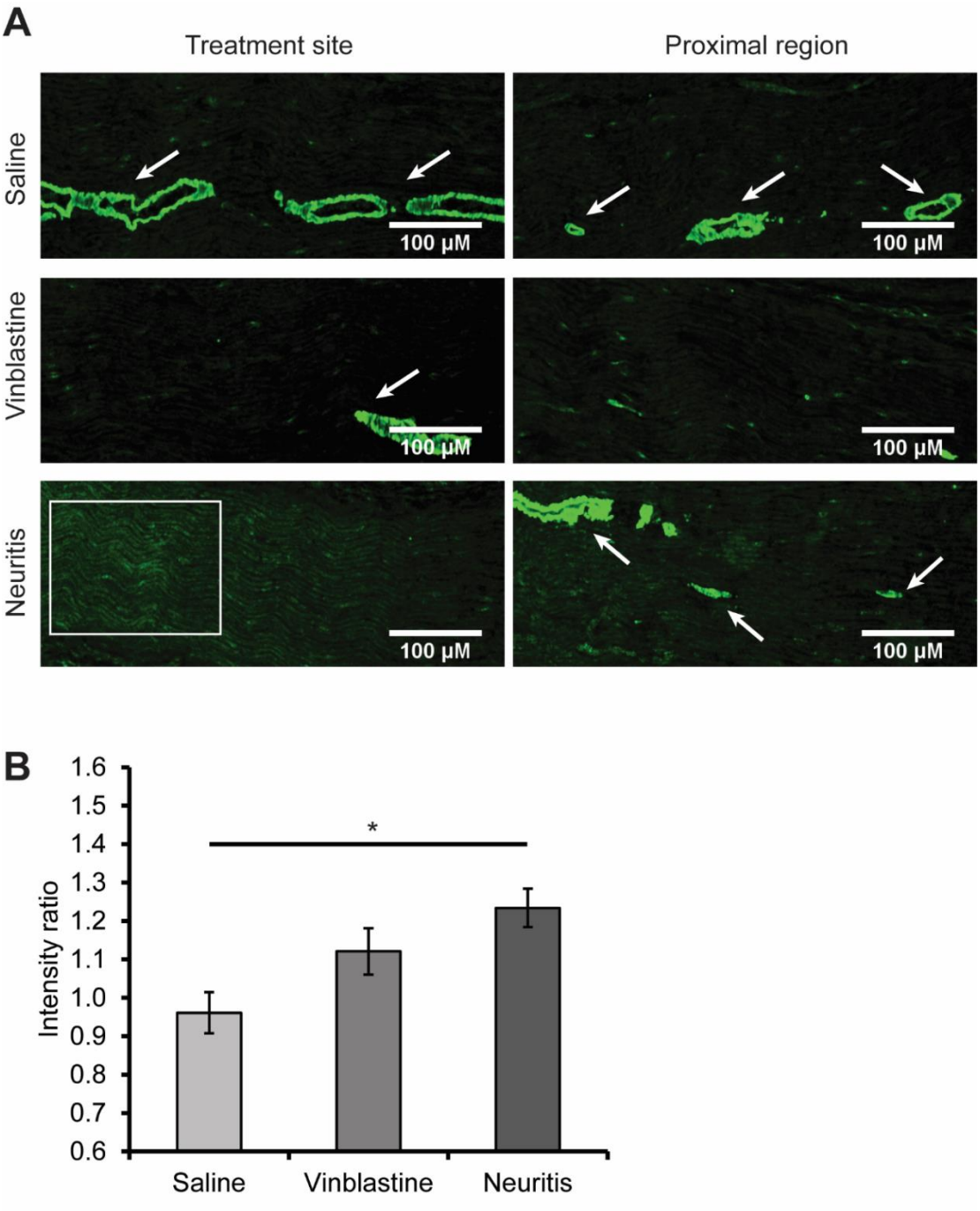

Figure 5.6 Distribution of anti-ASIC3 labelling in the sciatic nerve.
A) Example photographs of longitudinal sciatic nerve sections at the approximate location of the treatment site and a region 3-5mm proximal to this region. Following neuritis, there was an increase in anti-ASIC3 labelling at the treatment site (white box). Arrows indicate labelling of anti-ASIC3 in what appeared to be blood vessel walls. Taken at 10x magnification B) Mean ratios of the labelling intensity of anti-ASIC3 at the treatment site vs the proximal section of nerve in saline, vinblastine and neuritis groups (all groups n = 3 animals, 2-3 sections per animal). There was a significant increase in the ratio of the intensity of anti-ASIC3 labelling in neuritis nerves (*p <0.05; Dunnett's post hoc comparison to saline). Error bars represent SEM.

5.2.3 Changes in ion channel expression in the dorsal root ganglion

Transient receptor potential vanilloid 1

Anti-TRPV1 labelling was apparent within the cytosol of a proportion of small to medium diameter L5 DRG cell bodies in all treatment groups (**Figure 5.7**). Following saline treatment, the median intensity ratio of anti-TRPV1 labelling in small and medium sized diameter cell bodies was 1.57 (IQR +/- 0.73; n = 238). This was not significantly different (main effect p = 0.07; Kruskal-Wallis test) to the median intensity ratio following vinblastine treatment (1.44; IQR +/- 0.70, n = 240) or neuritis (1.57; IQR +/- 0.91, n = 240; **Figure 5.8)**

Transient receptor potential ankyrin 1

Anti-TRPA1 labelling was apparent within the cytosol of a proportion of the small to medium diameter L5 DRG cell bodies in all treatment groups and was also present in what appeared to be satellite cells (**Figure 5.9**). Following saline treatment, the median intensity ratio of anti-TRPA1 labelling in small and medium sized diameter cell bodies was 1.58 (IQR +/- 0.97, n = 240), which was not significantly different compared to vinblastine treatment (ratio = 1.59; IQR +/- 0.95, n = 232; main effect p = 0.05, Kruskal-Wallis test; p = 0.60, Dunn's post hoc test). However, following neuritis, there was a small but significant increase in the median intensity ratio (1.69; IQR +/- 0.96, n = 239) compared to saline treatment ($p < 0.05$, Dunn's post hoc test; **Figure 5.10)**

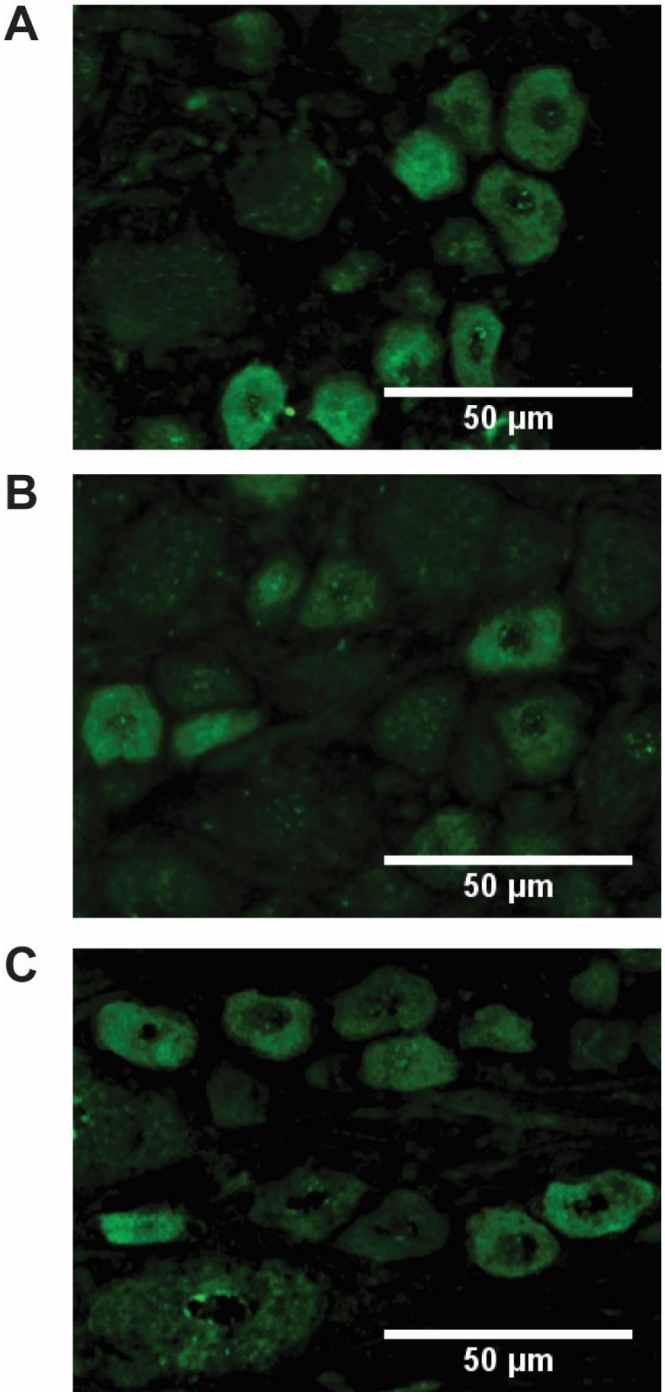

Figure 5.7 Anti-TRPV1 labelling in the L5 DRG. Anti-TRPV1 labelling in cell bodies of the L5 DRG following A) saline treatment, B) vinblastine treatment and C) neuritis. Anti-TRPV1 labelling was confined to the cytosol of a proportion of small and medium diameter cell bodies in all treatment groups. DRGs were extracted and frozen on four days post-surgery. Photographs were taken at 20x magnification

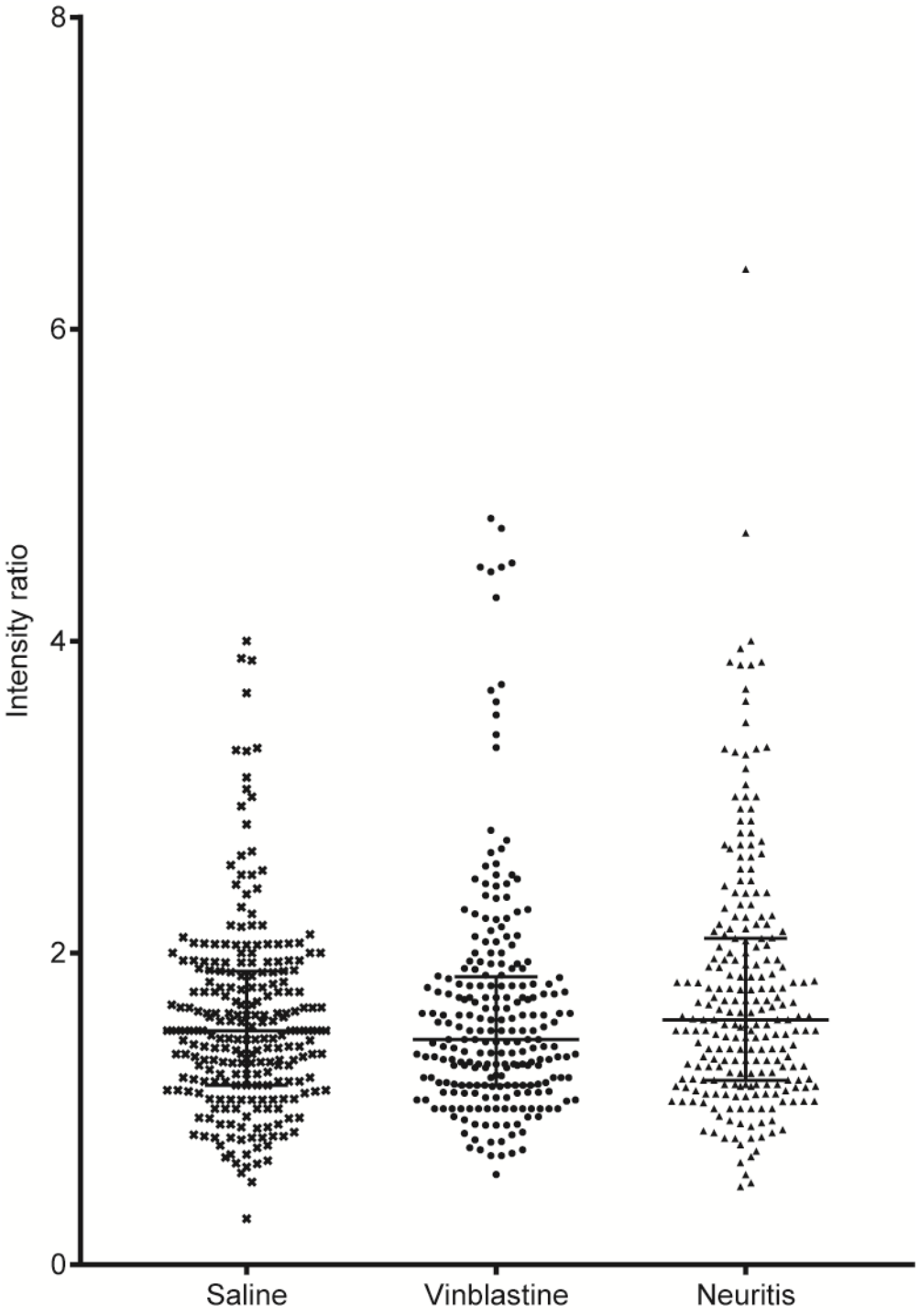

Figure 5.8 Anti-TRPV1 labelling in small and medium diameter cell bodies
Normalised intensity of anti-TRPV1 labelling in the small and medium diameter cell bodies following saline treatment, vinblastine treatment and neuritis. See Methods 2.6.3 for normalisation calculation. Data presented as medians, error bars represent IQR. Each group has an n = 238-240 cell bodies evenly selected from four animals.

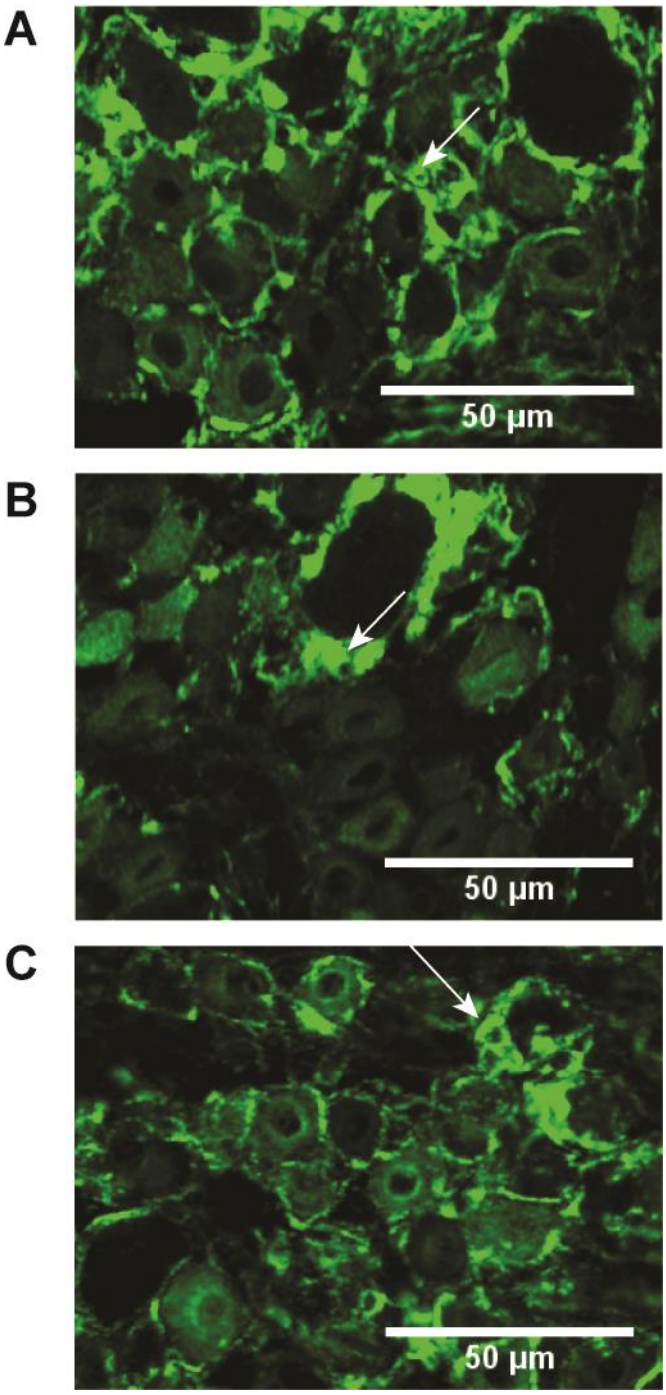

Figure 5.9 Anti-TRPA1 labelling in the L5 dorsal DRG. Anti-TRPA1 labelling in cell bodies of the L5 DRG following A) saline treatment, B) vinblastine treatment and C) neuritis. Anti-TRPA1 labelling was confined to the cytosol of a proportion of small and medium diameter cell bodies in all treatment groups. There was also intense anti-TRPA1 labelling in what appeared to be satellite cells (see arrow heads for examples). Following (C) neuritis there was an increase in labelling intensity of anti-TRPA1 within small and medium diameter cell bodies compared to that of the (A) saline treated group. DRGs were extracted on four days post-surgery. Photographs were taken at 20x magnification

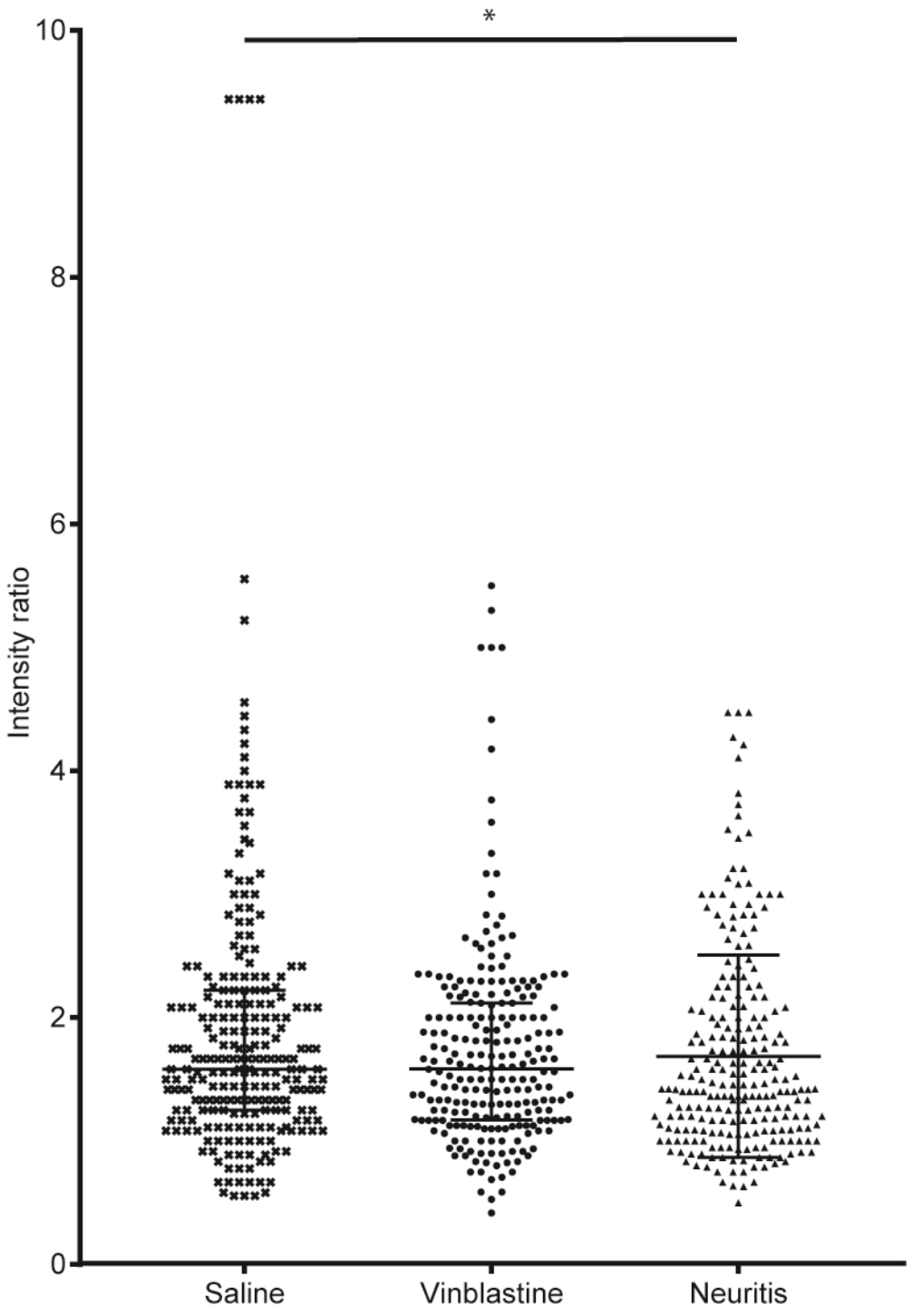

Figure 5.10 Anti-TRPA1 labelling in small and medium diameter cell bodies
Normalised intensity of anti-TRPA1 labelling in the small and medium diameter cell bodies following saline treatment, vinblastine treatment and neuritis. See Methods 2.6.3 for normalisation calculation. Data presented as medians, error bars represent IQR. Each group has an n = 232-242 cell bodies evenly selected from four animals. * P <0.05 Dunn's post hoc comparison to saline.

Acid sensing ion channel 3

Anti-ASIC3 labelling was apparent within the cytosol of a proportion of the small, medium and large diameter L5 DRG cell bodies in all treatment groups (**Figure 5.11**). Following saline treatment, the median intensity ratio of anti-ASIC3 labelling in small and medium sized diameter cell bodies was 1.82 (IQR +/- 0.88, n = 240). Following vinblastine treatment (intensity ratio = 2.0; IQR +/- 1.12, n = 237) and neuritis (intensity ratio = 1.90; IQR +/- 1.09, n = 236), the median intensity ratios were both significantly greater than that of the saline group (main effect $p < 0.01$, Kruskal-Wallis test; both $p < 0.01$, Dunn's post hoc comparisons to saline; **Figure 5.12**).

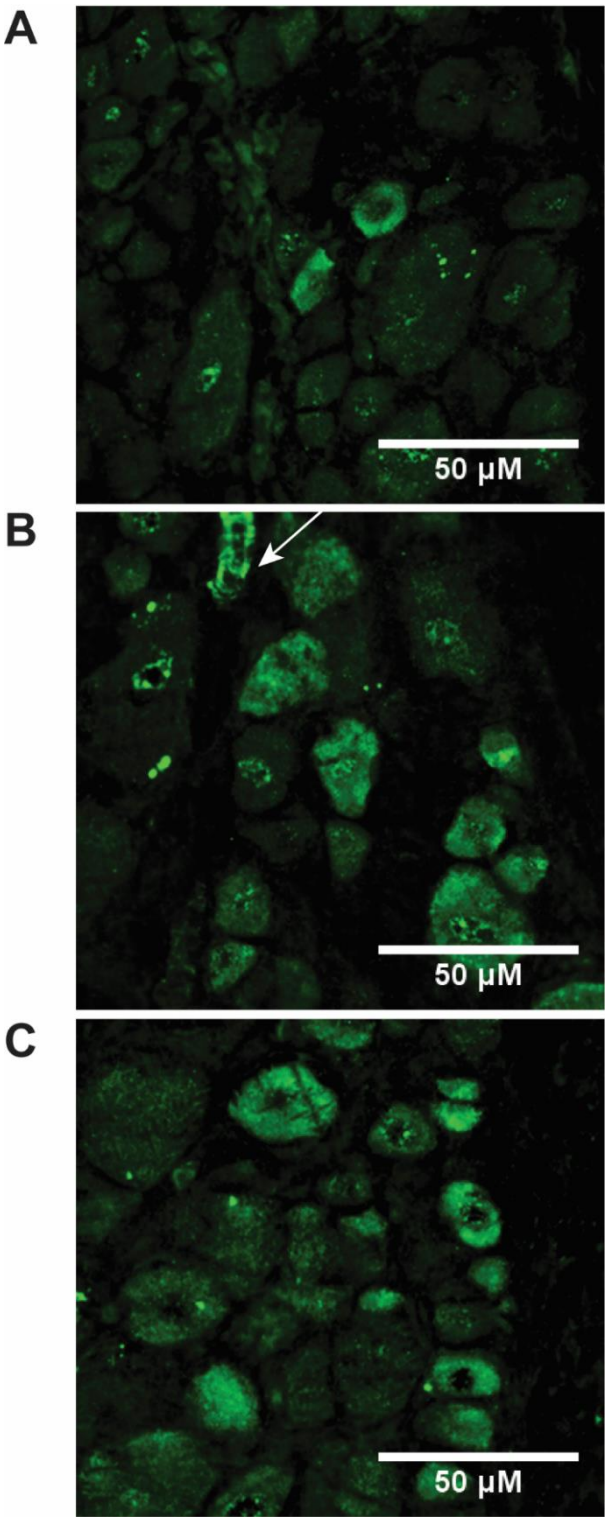

Figure 5.11 Anti-ASIC3 labelling in the L5 DRG. Anti-ASIC3 labelling in cell bodies of the L5 DRG following A) saline treatment, B) vinblastine treatment and C) neuritis. Anti-ASIC3 labelling was present in the cytosol in a proportion of all sized cell bodies in all treatment groups. Following B) vinblastine treatment and C) neuritis, there was an increase in anti-ASIC3 labelling intensity within small and medium diameter cell bodies. Arrowhead represents anti-ASIC3 blood vessel labelling. DRGs were extracted on four days post-surgery. Photographs were taken at 20x magnification.

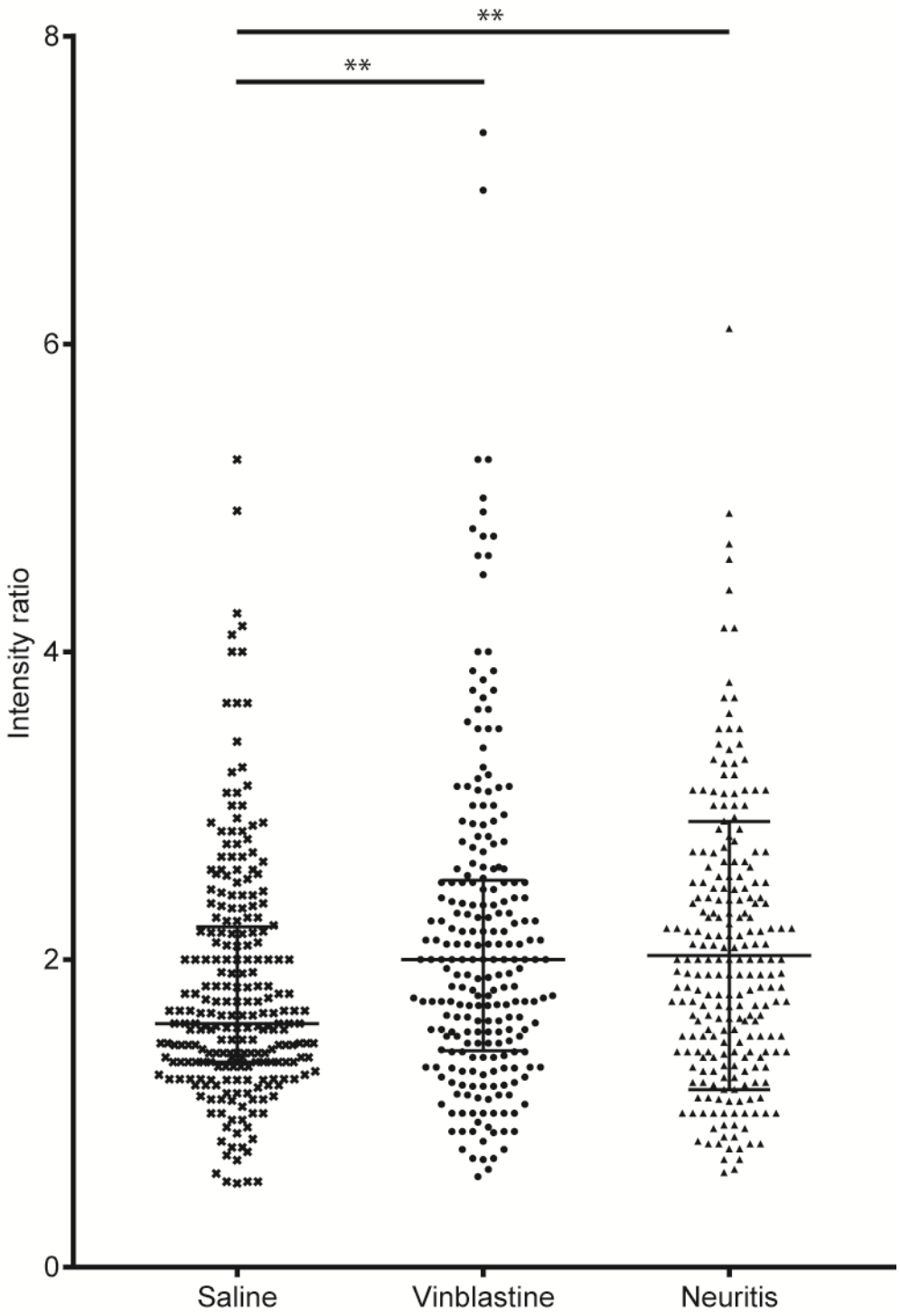

Figure 5.12 Anti-ASIC3 labelling in small and medium diameter cell bodies.
Normalised intensity of anti-ASIC3 labelling in the small and medium diameter cell bodies See Methods 2.6.3 for normalisation calculation. Data presented as medians, error bars represent IQR. Each group has an n = 236-240 cell bodies evenly selected from four animals. ** p <0.01 Dunn's post hoc comparison to saline.

5.3 Main findings

- Partially ligating a nerve caused an increase in the labelling intensity of the anti-TRPV1, anti-TRPA1 and anti-ASIC3 antibodies proximal to the ligation site (1.7, 2.4 and 1.6 fold increase respectively).
- At day four following vinblastine treatment, the transport of TRPV1 and TRPA1 was clearly disrupted. Following vinblastine treatment proximal to the partial ligation, there was a reduction in the ratio of antibody labelling in the ligated vs unligated nerve portion (TRPV1 ratio 1.7 in control, 1.2 following vinblastine; TRPA1 ratio of 2.4 in control, 1.2 following vinblastine).
- At day four following vinblastine treatment, the transport of ASIC3 was disrupted. There was a reduction in the intensity ratio of anti-ASIC3 labelling in the ligated vs unligated nerve portion (1.6 in control, 1.3 following vinblastine)
- At day four following neuritis, the transport of TRPV1 and TRPA1 was disrupted. Following neuritis proximal to the partial ligation, there was a reduction in the intensity ratio of antibody labelling in the ligated vs unligated nerve portion (TRPV1 ratio 1.7 in control, 1.4 following neuritis; TRPA1 ratio of 2.4 in control, 1.7 following neuritis).
- At day four following neuritis, the transport of ASIC3 was disrupted. Following neuritis proximal to the partial ligation, there was a slight reduction in the intensity ratio of anti-ASIC3 labelling in the ligated vs unligated nerve portion (1.6 in control, 1.4 following neuritis).
- At day four following neuritis, there was an increase in the labelling of anti-TRPV1 and anti-ASIC3 at the treatment site compared to a region 3-5 mm proximal (1.3 and 1.2 fold increases respectively).

5.4 Discussion

Data from this study suggests that the accumulation of mechanically sensitive ion channels at the site of axonal transport disruption is responsible for AMS. Although there are a considerable number of possible channels that may play a role, three possible candidates are of particular interest; namely TRPA1, TRPV1 and ASIC3. As previously stated, these channels are involved in noxious mechanical transduction and inflammatory-induced mechanical sensitivity. Therefore, as part of this study, the transport and possible accumulation of these channels at the neuritis and vinblastine treatment site was examined. As evidence of altered transcription of these channels, their protein levels have been examined in the cell bodies of sensory neurons.

5.4.1 The anterograde transport of TRPV1, TRPA1 and ASIC3 was disrupted

In the present study, nerves were partially ligated to assess the transport of sensory ion channels. This method has been successfully used to show that kinesin is disrupted following vinblastine treatment and neuritis (Dilley et al., 2013).

The increased level of immunolabeling for all three channels immediately proximal to the ligation site in saline-treated animals is consistent with the complete cessation of axonal transport at the ligation, and is consistent with the anterogradely transport of these channels. The reduction in immunolabeling of all three channels at the ligation site in vinblastine-treated and neuritis animals suggests that the transport of these channels is disrupted at a more proximal location.

The transport of these channels was examined on day four. Previous data has shown that the time courses of axonal transport disruption are different between vinblastine treatment and neuritis (Dilley et al., 2013). Following vinblastine treatment, axonal transport is clearly disrupted on day two and has resolved by day six. Whereas following neuritis, axonal transport is not clearly disrupted until day six. Therefore, it is likely that on day four axonal transport disruption may have begun to reverse following vinblastine treatment, but is beginning to be disrupted following neuritis.

The disruption to ASIC3 following vinblastine treatment and neuritis was less clear compared to that of TRPV1 and TRPA1. This may have been due to the different fibre types that the ion channels are expressed in. In comparison to TRPV1 and TRPA1, ASIC3 is expressed in both unmyelinated and myelinated fibre types (Molliver et al., 2005). The latter of which are less susceptible to the effects of anti-mitotic agents (Kingery et al., 1998) and thus axonal transport may not be disrupted in these fibres. It is unknown whether myelinated fibres are less susceptible to inflammatory-induced axonal transport disruption. However, this susceptibility seems plausible because AMS is less common in large diameter myelinated fibres following neuritis (Bove et al., 2003).

5.4.2 Evidence for TRPV1, TRPA1 and ASIC3 accumulation at the treatment site

In addition to the accumulation of TRPV1, TRPA1 and ASIC3 at the ligation site, the levels of ion channels were also examined at the treatment site and compared to a proximal section of nerve. Low levels of TRPV1 and ASIC3 were found in the sciatic nerve of saline treated animals, which is consistent with the previously reported localisation of these channels to the sciatic nerve (Alvarez de la Rosa et al., 2002; Tominaga et al., 1998). Similarly, low levels of TRPA1 were also identified in the sciatic nerve of saline treated animals.

Although the transport of ion channels appeared to be disrupted following vinblastine treatment, there was no evidence of their accumulation at the treatment site. Since the treatment site was compared to a more proximal area of nerve, this finding may indicate a more widespread accumulation following vinblastine treatment, which would be consistent with the nerve ligation data. The focal increases in ion channel levels at the neuritis site, but not proximally, might be why AMS is typically localised to this site. Whereas following vinblastine treatment, AMS hotspots were located both proximal to, and at the treatment site, which is consistent with a more widespread accumulation of ion channels.

Following neuritis, there was an increase in the levels of TRPV1 at the treatment site compared to a more proximal location, suggesting that axonal transport disruption was localised to the neuritis site. Alternatively, the focal increases in the levels of

TRPV1 following neuritis might suggest that the presence of inflammatory mediators at the neuritis site, such as TNF and NGF (Obata et al., 2002; Pulman et al., 2013), aid the trafficking and insertion of accumulated channels into the membrane. For example, TNF and NGF are reported to cause increased insertion of TRPV1 into the membrane of neurons (Camprubi-Robles et al., 2009; Meng et al., 2016; Stein et al., 2006; Zhang et al., 2005). Based upon the nerve ligation data, it was surprising that the levels of ASIC appeared to increase at the treatment site following neuritis. This suggests that there might be an alternative mechanism that causes the levels of ion channels to increase at the neuritis site (e.g. inflammatory-induced local upregulation – see **Discussion 7.1**). In contrast to TRPV1 and ASIC3, there was no increase in TRPA1 labelling at the neuritis treatment site. As TNF is reported to cause co-trafficking of vesicles containing TRPV1 and TRPA1 to the membrane (Meng et al., 2016), it was anticipated that, similar to TRPV1, TRPA1 labelling might have increased following neuritis.

5.4.3 Altered expression of TRPV1, TRPA1 and ASIC3 in the DRG

Previous studies have reported that neuritis induces an increase in the expression of activating transcription factor-3 and the ion channel, HCN2, in the DRG (Dilley et al., 2005; Richards et al., 2011). HCN2 channels are considered to contribute towards ongoing activity following neuritis (Richards and Dilley, 2015). In this study, the increased immunolabeling of anti-ASIC3 and anti-TRPA1 in the DRG following neuritis may indicate that the expression of these ion channels increased, which provides further evidence that neuritis induces phenotypical changes in sensory neurons. These findings are consistent with reports of increased TRPA1 expression in the DRG following inflammation of the joints (Dunham et al., 2008) and hind paw (da Costa et al., 2010; Obata et al., 2005), and ASIC3 mRNA expression following inflammation of joints (Ikeuchi et al., 2009), muscle (Walder et al., 2010) and hind paw (Nagae et al., 2006; Voilley et al., 2001). In contrast to TRPA1 and ASIC3, there was a lack of an increase in anti-TRPV1 immunolabeling indicating that the expression of TRPV1 did not increase, which was unexpected based on reports that the expression of TRPV1 increases in the DRG following hind paw inflammation (Amaya et al., 2003; Ji et al., 2002). The increase in anti-ASIC3 labelling within the DRG that followed vinblastine

treatment indicates that ASIC3 levels increased, which provides evidence that axonal transport disruption leads to phenotypical changes within neurons.

Although the mechanisms that cause the changes in expression were not explored in this study, it is likely that they involved retrograde signalling pathways. For example, following neuritis, NGF is produced in the inflamed nerve (Obata et al., 2002) and might be retrogradely transported to the DRG. The increased retrograde transport of NGF may result in the activation of signalling pathways, which in turn lead to the increase in the expression of ion channels (Obata et al., 2004). In both models it is possible that there is an injury-induced upregulation of importin ß1 at the treatment site, which mediates the transport of retrograde signals to the cell body (Perry et al., 2012).

5.4.4 Summary

From the present data it was clear that vinblastine treatment and neuritis disrupted the anterograde transport of TRPV1, TRPA1 and ASIC3 along axons. Whereas neuritis caused a focal increase in channel expression at the treatment site, the accumulation following vinblastine might have been more widespread. The levels of ion channels were altered in the cell bodies, suggesting that vinblastine treatment and neuritis may induce phenotypical changes within neurons.

Chapter 6

Electrophysiological evidence for the presence of TRPV1 and TRPA1 in mechanically sensitive axons

6.1 Introduction

The immunohistochemical results suggest that the transport of TRPV1, TRPA1 and ASIC3 is disrupted following vinblastine treatment and neuritis, and that TRPV1 and ASIC3 may have accumulated at the neuritis site. Thus, these ion channels may be involved in the development of AMS. To investigate the possibility that TRPV1 and TRPA1 ion channels have accumulated in neurons with AMS, pharmacological agents will be applied to nerves in an in vivo set up (not carried out ex vivo due to technical difficulties - see limitations **7.3.1**). The accumulation of ASIC3 was not investigated because previous studies have reported that ruthenium red and FM1-43, which both attenuated AMS (See **Chapter 4**), do not block ASIC channels (Alvarez de la Rosa et al., 2002; Drew and Wood, 2007).

The aim of these experiments was to examine whether TRPV1 and TRPA1 ion channels are present and functional in mechanically sensitive axons at the vinblastine and neuritis treatment sites. Therefore, N-oleoyl-dopamine (OLDA) and cinnamaldehyde, respective agonists of the TRPV1 and TRPA1 ion channels, were applied to hotspots to determine if they excited neurons with AMS. The concentrations of cinnamaldehyde and OLDA tested were selected based upon previous studies. The TRPV1 agonist OLDA activates channels at doses in the low micromolar range (EC_{50} 5-15µM in vitro) and causes thermal hyperalgesia at a concentration of 48 µM when injected subcutaneously into the rat hind paw (Chu et al., 2003; Gavva et al., 2004). The TRPA1 agonist cinnamaldehyde also activates TRPA1 channels in the low micromolar range (EC_{50} 60µM in vitro) and has shown to cause significant activity when a concentration of 300 µM was applied to the terminal of vagal nerve afferents in an ex-vivo lung prep (Bandell et al., 2004; Nassenstein et al., 2008). Agonists were directly applied to AMS hotspots by: (1) wrapping gelfoam saturated in the drug around the nerve at the treatment site and (2) injecting directly into the endoneurium.

The primary objective was:

1. To determine whether C-fibre neurons with AMS responded to application of OLDA or cinnamaldehyde.

6.2 Results

All animals recovered from vinblastine and neuritis surgeries without adverse effects.

6.2.1 Properties of neurons with identified receptive fields

In the untreated group (n = 13 neurons), the median conduction velocity of the characterised C-fibre neurons was 0.60 m/s (IQR = 0.30). Ninety two percent of the neurons had receptive fields that had deep locations. None of these neurons had AMS. Following vinblastine treatment (n = 13 neurons), the median conduction velocity of the characterised C-fibre neurons with AMS was 0.50 m/s (IQR = 0.17), which was significantly slower than that of untreated neurons (main effect $p < 0.05$, Kruskal Wallis test; $p < 0.05$, Dunn's post hoc test; **Figure 6.1**). All of the neurons had deep receptive fields that were located in the gastrocnemius muscle or the ankle joint. Following neuritis (n = 19 neurons), the median conduction velocity of neurons with AMS was 0.59 m/s (IQR = 0.22), which was not significantly different to untreated ($p = 0.74$, Dunn's post hoc test). All of the neurons had deep receptive fields that were located in the gastrocnemius muscle or the ankle joint. In all of the groups, all of the mechanical receptive fields identified were deemed to be nociceptive as they were activated by strong pressure, either by squeezing the skin with forceps (cutaneous), or squeezing the muscle between the thumb and the forefinger (deep). Axonal mechanical sensitive hotspots were always located proximal to, or at the treatment site.

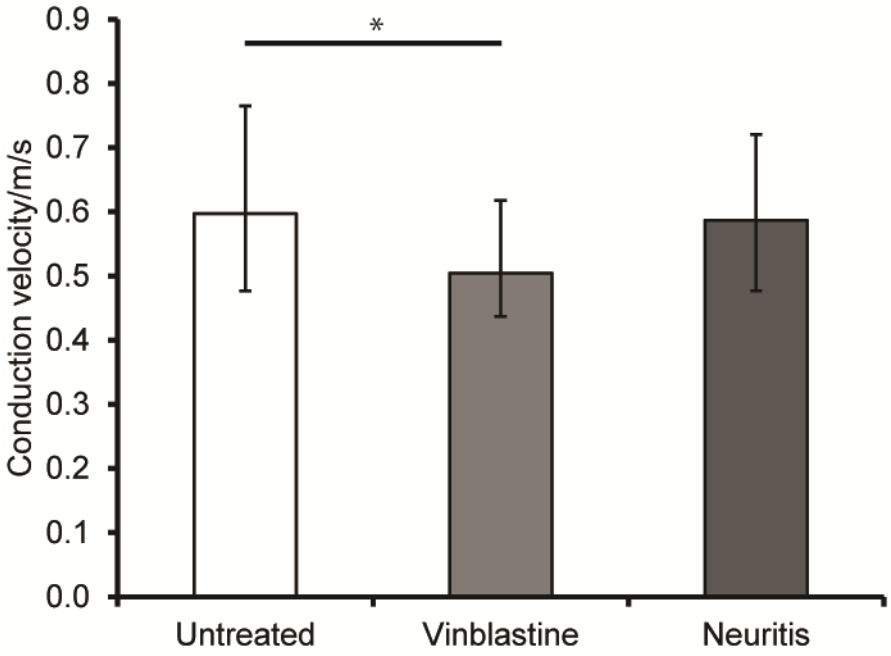

Figure 6.1 Conduction velocities of characterised C-fibre neurons.
Following vinblastine treatment, C-fibre neurons with AMS had significantly slower conduction velocities than that of untreated *P < 0.05 Dunn's post hoc test. Data presented as medians. Error bars = IQR. Untreated = 13 neurons (12 animals), vinblastine = 13 neurons (13 animals), neuritis n = 19 neurons (15 animals)

6.2.2 Perineural application of agonists to the nerve

N-oleoyl-dopamine application

In the untreated group (n = 12 animals), 31% (4/13) of C-fibre neurons with characterised receptive fields had ongoing activity at baseline (vehicle application). The baseline rates of activity in all neurons (n = 13) were low (median rate = 0.01 Hz). Perineural application of each concentration of OLDA had negligible effect on activity (p = 0.99, Kruskal-Wallis test; **Table 6.1**). Eight percent of C-fibre neurons (1/13) responded to OLDA at a concentration of 50 µM.

Following vinblastine treatment (n = 9 animals), 66% (6/9) of C-fibre neurons with AMS had ongoing activity at baseline (vehicle application). The baseline rates of activity in all neurons (n = 9) were low (median rate = 0.03 Hz). Perineural application of each concentration of OLDA had negligible effect on activity (p = 0.84, Kruskal-Wallis test; **Table 6.1**). Thirteen percent (1/9) of AMS neurons responded to OLDA at a concentration of 200 µM.

Following neuritis (n = 11 animals), 61% (8/13) of C-fibre neurons with AMS had ongoing activity at baseline (vehicle application). The baseline rates of activity in all neurons (n = 13) were low (median rate = 0.02 Hz). Perineural application of each concentration of OLDA had negligible effect on activity (p = 0.88, Kruskal-Wallis test; **Table 6.1**). At concentrations of 10 and 50 µM, eight percent (1/13) of neurons responded to OLDA.

Cinnamaldehyde application

In the untreated group (n = 12 animals), 38% (5/13) of C-fibre neurons with characterised receptive fields had ongoing activity at baseline (vehicle application). The baseline rates of activity in all neurons (n = 13) were low (median rate = 0.012 Hz). Perineural application of each concentration of cinnamaldehyde had negligible effect on activity (p = 0.80, Kruskal-Wallis test; **Table 6.2**). Fifteen percent (2/13) and 8% (1/13) of C-fibre neurons were found to respond to cinnamaldehyde at concentrations of 250 and 500 µM respectively.

Following vinblastine treatment, (n = 9 animals), 55% (5/9) of C-fibre neurons with AMS had ongoing activity at baseline (vehicle application). The baseline rates of activity in all neurons (n = 9) were low (median rate = 0.022 Hz). Perineural application of each concentration of cinnamaldehyde had negligible effect on activity (p = 0.96, Kruskal-Wallis test; **Table 6.2**). Twenty-two percent (2/9) of AMS neurons responded to cinnamaldehyde at a concentration of 500 µM.

Following neuritis, (n = 11 animals), 54% (7/13) of C-fibre neurons with AMS had ongoing activity at baseline (vehicle application). The baseline rates of activity in neurons with AMS (n = 13) were low (median rate = 0.023 Hz). Perineural application of each concentration of cinnamaldehyde had negligible effect on activity (p = 0.71, Kruskal-Wallis test; **Table 6.2**). There were no responders to any of the concentrations of cinnamaldehyde applied.

		OLDA, median rate/Hz (IQR)				p value*
Treatment	**n**	**Pre-drug**	**10 µM**	**50 µM**	**200 µM**	
Untreated	12	0.01 (0.03)	0.01 (0.03)	0.01 (0.03)	0.01 (0.03)	0.99
Vinblastine	9	0.03 (0.06)	0.02 (0.03)	0.01 (0.05)	0.02 (0.04)	0.84
Neuritis	13	0.02 (0.04)	0.02 (0.03)	0.02 (0.04)	0.02 (0.03)	0.88

Table 6.1. Activity rates of neurons with AMS at baseline (vehicle) and following perineural application of OLDA. Each concentration was topically applied to the nerve for 10 min. *Kruskal-Wallis test compared to pre-drug value

		Cinnamaldehyde, median rate/Hz (IQR)				p value*
Treatment	**n**	**Pre-drug**	**100 µM**	**250 µM**	**500 µM**	
Untreated	12	0.01 (0.02)	0.01 (0.02)	0.00 (0.01)	0.00 (0.04)	0.80
Vinblastine	9	0.02 (0.06)	0.02 (0.04)	0.04 (0.04)	0.01 (0.13)	0.96
Neuritis	13	0.02 (0.04)	0.02 (0.04)	0.01 (0.04)	0.01 (0.05)	0.71

Table 6.2. Activity rates of neurons with AMS at baseline (vehicle) and following perineural application of cinnamaldehyde. Each concentration was topically applied to the nerve for 10 min. *Kruskal-Wallis test compared to pre-drug value

6.2.3 Intraneural injection of agonists

As perineural application of agonists only initiated responses in a negligible number of neurons with AMS, agonists were intraneurally injected. In the majority of these experiments, an intraneural injection was made following the gelfoam application of each drug. An intraneural injection of 100 µL of solution into the sciatic nerve caused a brief increase in intraneural pressure at the location of the hotspot, this was normally enough to activate hotspots (see arrowheads in **Figure 6.5 B & C** for examples).

Vehicle injection

AMS and untreated neurons (with characterised receptive fields)

Following vinblastine treatment, all of C-fibre neurons with AMS (n = 3) were considered to be ongoing prior to intraneural injection of vehicle. The rates of ongoing activity ranged between 0.02 – 0.03 Hz at baseline. None (0/3) of the neurons with AMS responded to an intraneural injection of vehicle (**Figures 6.2 A & 6.3 A)**.

Following neuritis, 66% (4/6) of C-fibre neurons with AMS were considered to be ongoing prior to injection of vehicle. The rates of ongoing activity ranged between 0.03 – 0.14 Hz at baseline. None (0/6) of the neurons with AMS responded to an intraneural injection of vehicle (**Figures 6.2 B & 6.3 B)**

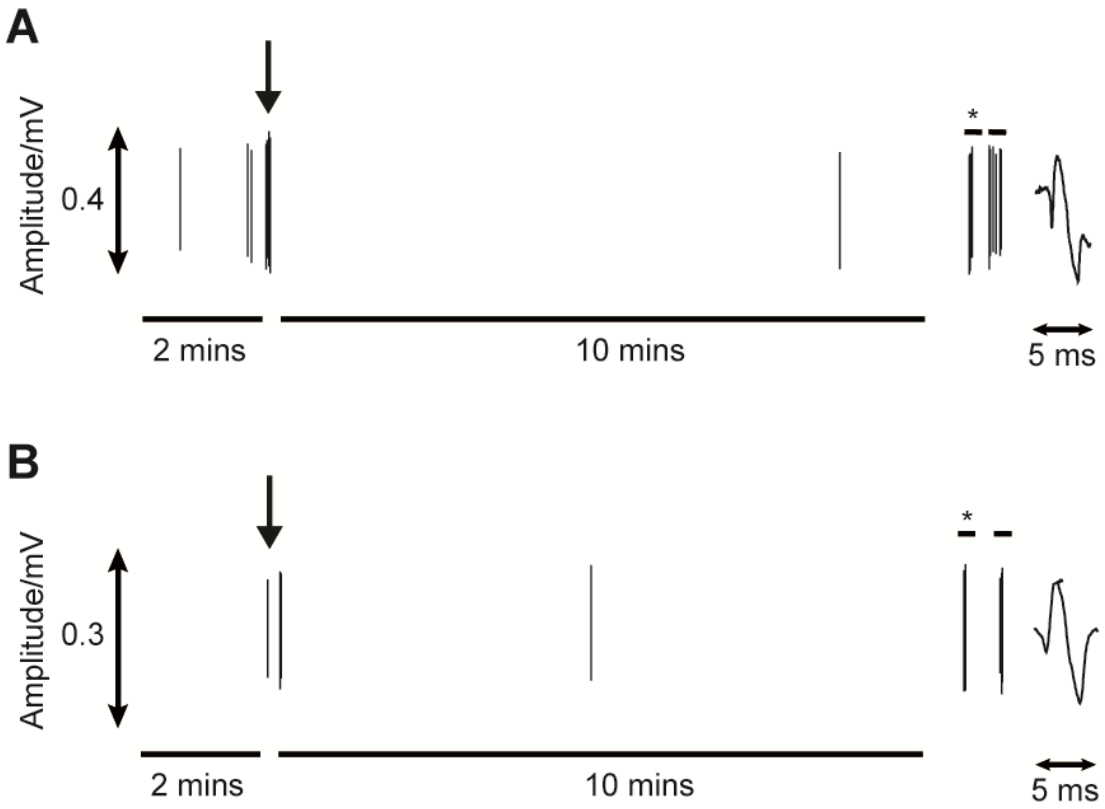

Figure 6.2 Example individual spike traces of mechanically sensitive C-fibre neurons after an intraneural injection of vehicle. Example traces show typical responses of individual C-fibre neurons to the intraneural injection of 100 µL of vehicle into the sciatic nerve in A) a vinblastine-treated and B) neuritis animal. Arrowheads correspond to time of intraneural injection. Horizontal bars represent AMS (*) and receptive field testing.

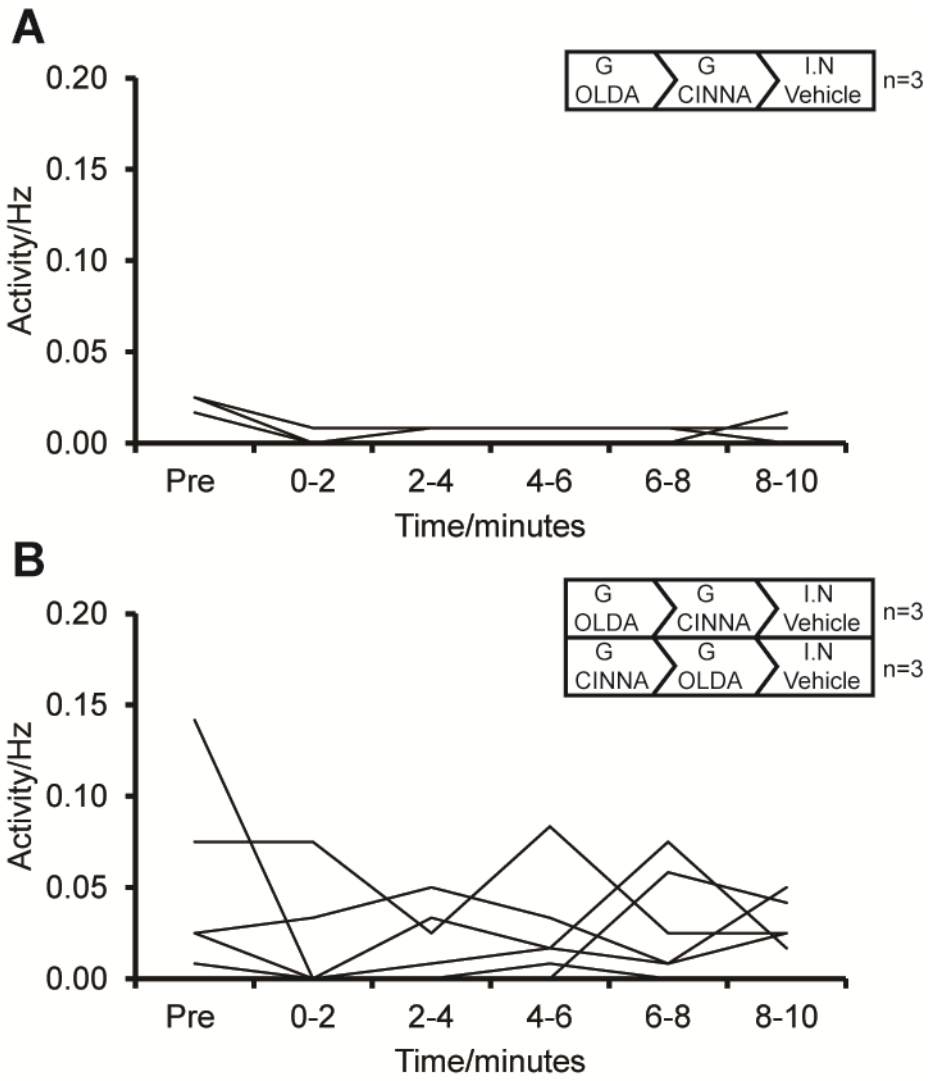

Figure 6.3 Activity rates of mechanically sensitive C-fibre neurons following the intraneural injection of vehicle. In these experiments, agonists were applied using gelfoam prior to intraneural injection. Only the intraneural injection data is presented. Each line represents the activity of an individual C-fibre neuron prior to and following intraneural injection of 100 µL of vehicle. Vehicle injection onto mechanically sensitive hotspots did not cause any activity in C-fibre neurons following A) vinblastine treatment (n = 3 neurons) and B) neuritis (n = 6 neurons). Key represents experimental protocol. G = Gelfoam, I.N = Intraneural.

Non-AMS neurons (receptive fields not identified)

Following vinblastine treatment, there were no C-fibre neurons with ongoing activity prior to intraneural injection of vehicle. None of the non-ongoing neurons (0/20) responded to injection of vehicle.

Following neuritis, 7% (2/27) of C-fibre neurons with unidentified receptive fields had ongoing activity prior to intraneural injection. The rates of ongoing activity were 0.02 and 0.05 Hz at baseline. None (0/27) of the neurons with unidentified receptive fields responded to injection of vehicle. **Figure 6.4** shows the effects of vehicle on neurons that had ongoing activity at baseline.

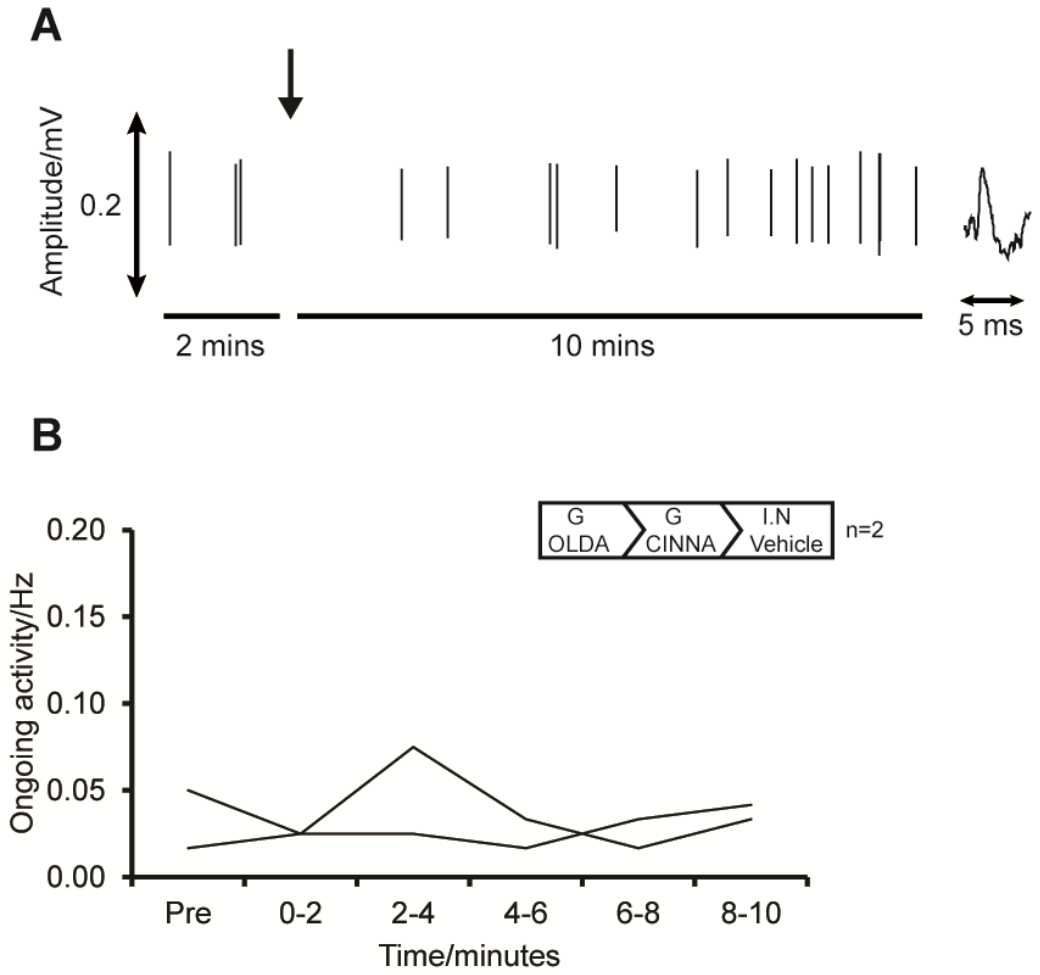

Figure 6.4 Activity rates of ongoing C-fibre neurons following the intraneural injection of vehicle. In these experiments, agonists were applied using gelfoam prior to intraneural injection. Only the intraneural injection data is presented. A) Example response of an ongoing unit after injection of 100µL of vehicle into the sciatic nerve following neuritis. Arrowhead represents time of injection. B) Each line represents the activity of an individual ongoing C-fibre neuron prior to and following intraneural injection of 100 µL of vehicle into a neuritis nerve (n = 2 neurons). Note that receptive fields were not identified in these neurons. Key represents experimental protocol. G = Gelfoam, I.N = Intraneural.

N-oleoyl-dopamine injection

AMS and untreated neurons (with characterised receptive fields)

In the untreated group, 33% (2/6) of C-fibre neurons were considered to be ongoing prior to intraneural injection of OLDA. The rates of ongoing activity were 0.02 and 0.44 Hz at baseline. No neurons (0/6) from untreated animals responded to intraneural injection of OLDA (**Figures 6.5 A & 6.6 A**).

Following vinblastine treatment, 40% (2/5) of C-fibre neurons with AMS were considered to be ongoing prior to intraneural injection of OLDA. The rates of ongoing activity were 0.05 and 0.49 Hz at baseline. Injection of OLDA onto caused a response in 20% (1/5) of neurons with AMS. However, most of the neurons with AMS didn't respond (**Figures 6.5 B & 6.6 B**). The neuron that responded was identified on day two following vinblastine-treatment.

Following neuritis, 80% (4/5) of C-fibre neurons with AMS were considered to be ongoing prior to intraneural injection of OLDA. The rates of ongoing activity were low and ranged between 0.02 – 0.06 Hz at baseline. Injection of OLDA caused a response in 60% (3/5) of neurons with AMS (an example response of a responder is shown in **Figures 6.5 C)**. Two out of the three responders had maximal responses between four to six minutes post-injection and one neuron had a maximal response within the first two minutes after injection (**Figures 6.6 C).** Two out of the three responders were ongoing prior to injection. Neurons that responded were identified between 7 - 8 days following neuritis.

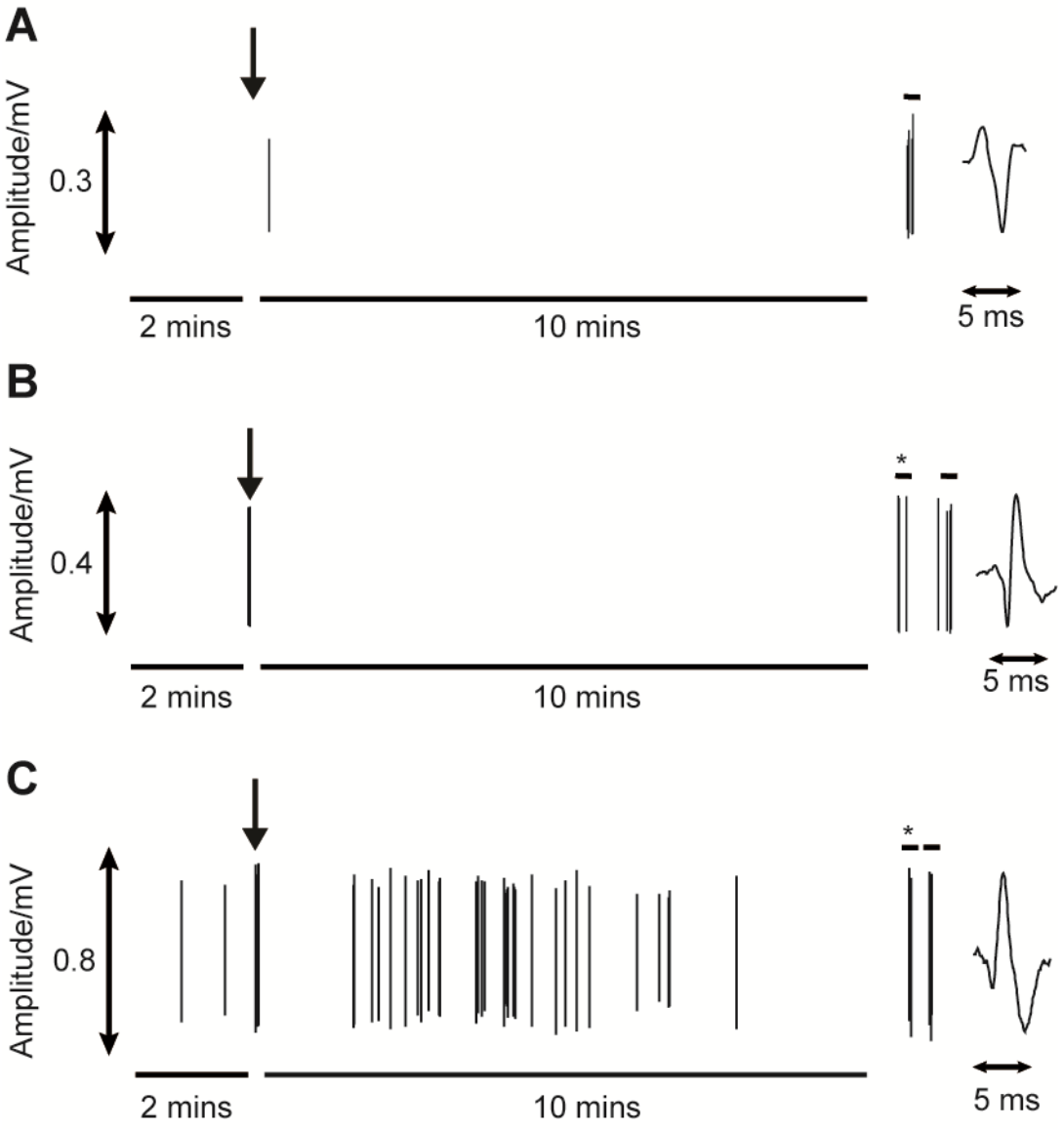

Figure 6.5 Example individual spike traces of C-fibre neurons after an intraneural injection of OLDA. Example traces show the typical responses of individual C-fibre neurons to the intraneural injection of 100 µL of 50 µM OLDA into the sciatic nerve in A) an untreated, B) vinblastine-treated and C) neuritis animal. Note that following B) vinblastine treatment and C) neuritis, neurons had AMS. Arrowheads correspond to time of intraneural injection. Horizontal bars represent AMS (*) and receptive field testing.

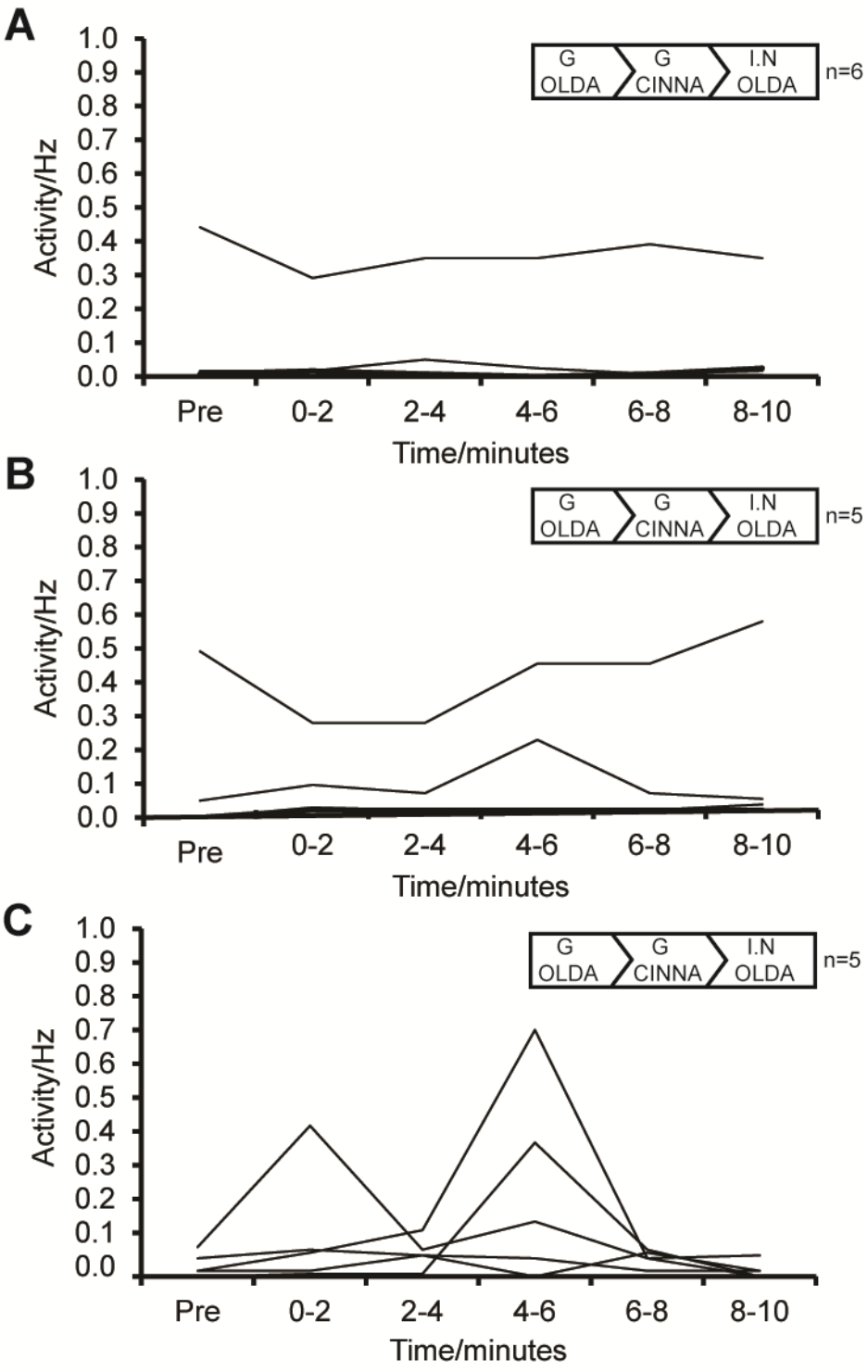

Figure 6.6 Activity rates of C-fibre neurons following the intraneural injection of OLDA. In these experiments, agonists were applied using gelfoam prior to intraneural injection. Only the intraneural injection data is presented. Each line represents the activity of an individual C-fibre neuron prior to and following intraneural injection of 100 µL of 50 µM OLDA in A) untreated (n = 6 neurons), B) vinblastine-treated (n = 5 neurons) and C) neuritis (n = 5 neurons) animals. In C) 3/5 neurons responded. Note that following B) vinblastine treatment and C) neuritis, neurons had AMS. Key represents experimental protocol. G = Gelfoam, I.N = Intraneural.

Non-AMS neurons (receptive fields not identified)

In the untreated group, 3% (1/20) of C-fibre neurons with unidentified receptive fields were ongoing prior to intraneural injection of OLDA. This neuron had a baseline firing rate of 0.22 Hz. None of the neurons (0/20) respond to an intraneural injection of OLDA. **Figures 6.7 A & 6.8 A** show the effects of OLDA on neurons that had ongoing activity at baseline.

Following vinblastine treatment, 9% (2/22) of C-fibre neurons with unidentified receptive fields had ongoing activity prior to intraneural injection of OLDA. The rates of activity were 0.04 and 0.08 Hz at baseline. None of the neurons (0/22) respond to an intraneural injection of OLDA. **Figures 6.7 B & 6.8 B** show effects of OLDA on neurons that had ongoing activity at baseline.

Following neuritis, 21% (3/14) of C-fibre neurons with unidentified receptive fields had ongoing activity prior to intraneural injection of OLDA. The rates of ongoing activity ranged between 0.06 and 0.24 Hz at baseline. None of the neurons (0/14) respond to an intraneural injection of OLDA. **Figures 6.7 C & 6.8 C** show the effects of OLDA on neurons that had ongoing activity at baseline.

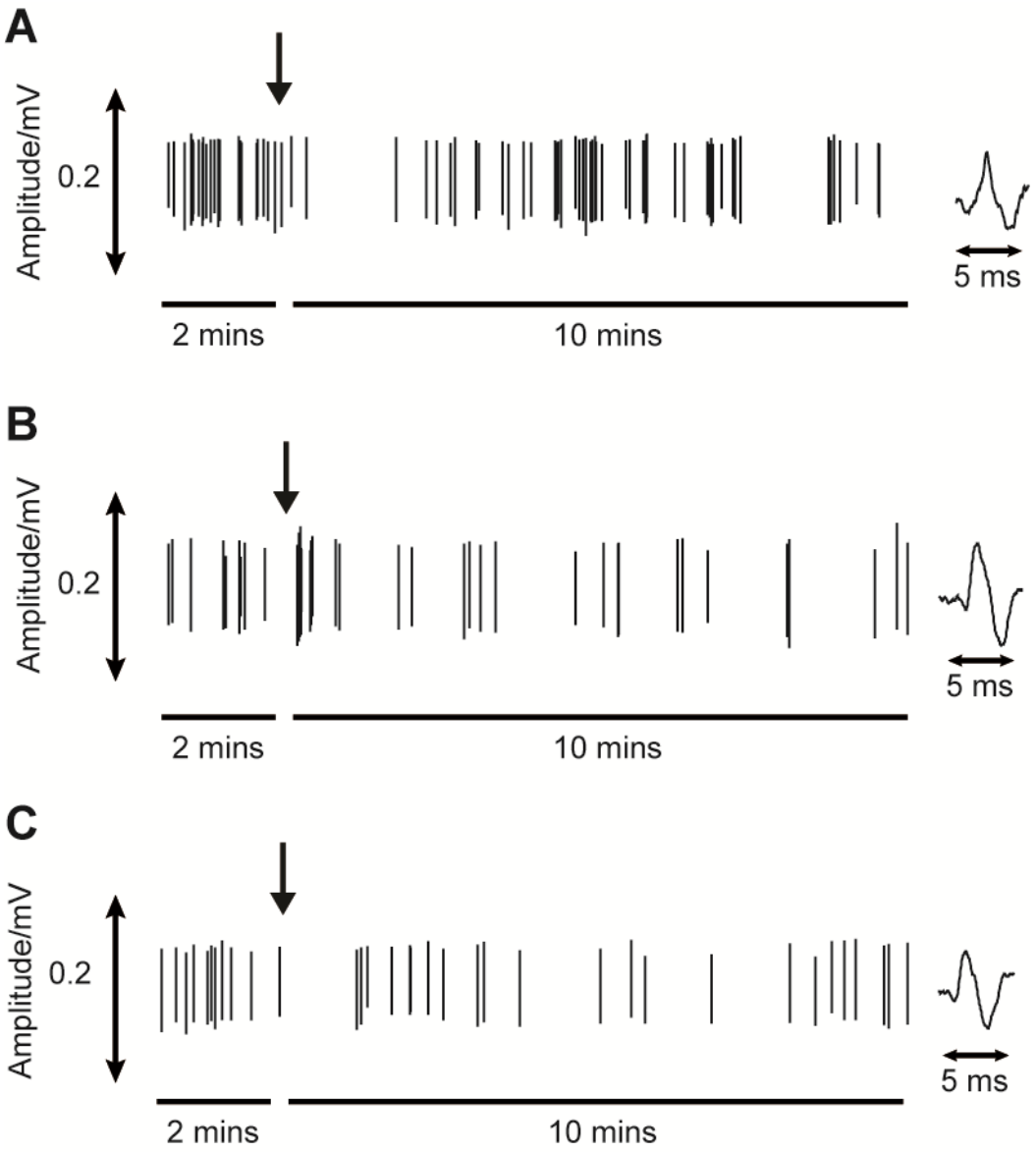

Figure 6.7 Example individual spike traces of ongoing C-fibre neurons after an intraneural injection of OLDA. Example traces show the responses of individual C-fibre neurons with ongoing activity to the intraneural injection of 100 µL of 50 µM OLDA into the sciatic nerve in A) an untreated, B) vinblastine-treated and C) neuritis animal. Note that receptive fields were not identified in these neurons. Arrowheads correspond to time of intraneural injection.

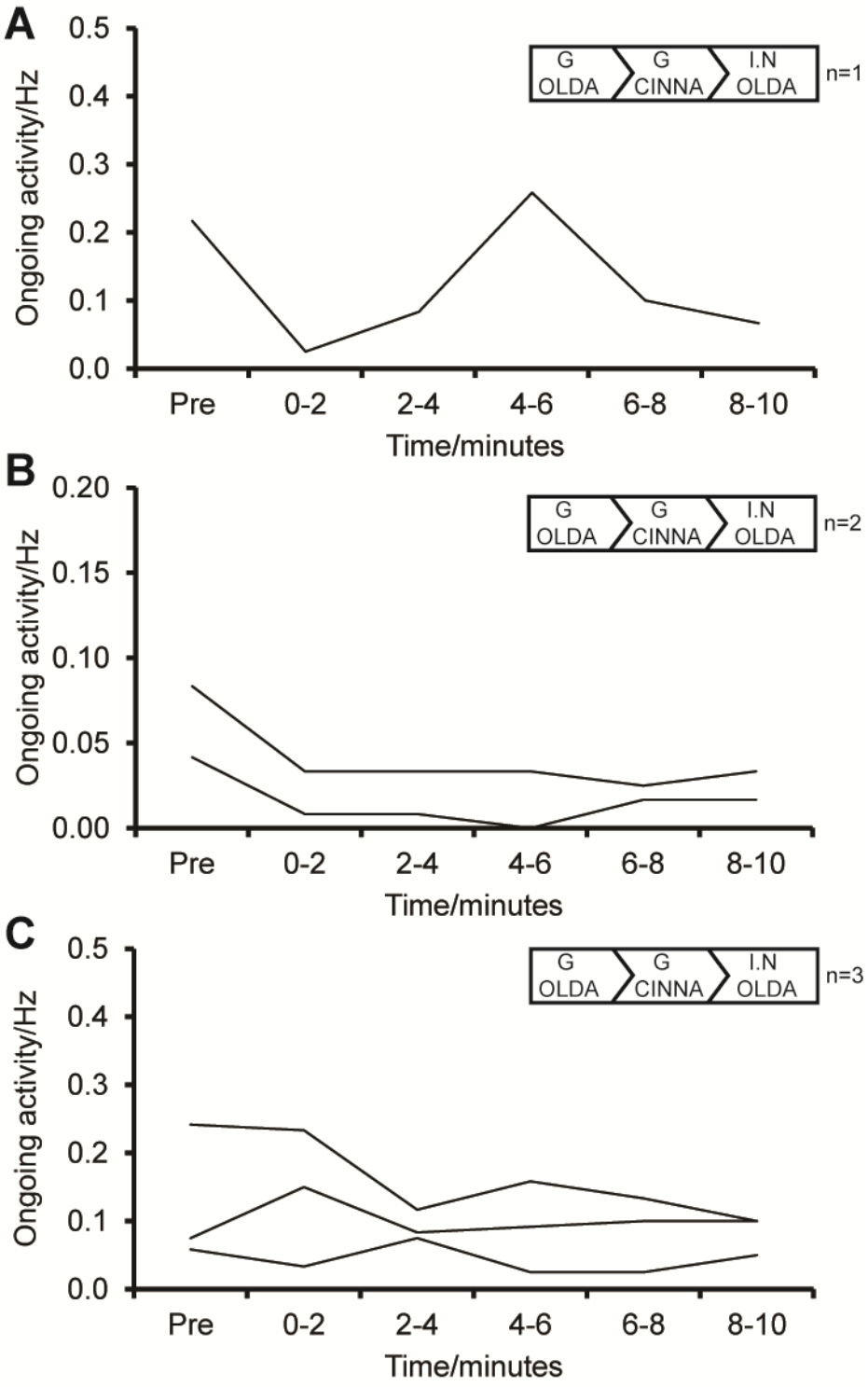

Figure 6.8 Activity rates of ongoing C-fibre neurons following the intraneural injection of OLDA. In these experiments, agonists were applied using gelfoam prior to intraneural injection. Only the intraneural injection data is presented. Each line represents the activity of an individual ongoing C-fibre neuron prior to and following intraneural injection of 100 µL of 50 µM OLDA in A) untreated (n = 1 neuron), B) vinblastine-treated (n = 2 neurons) and C) neuritis (n = 3 neurons) animals. Note that receptive fields were not identified in these neurons. Key represents experimental protocol. G = Gelfoam, I.N = Intraneural.

Cinnamaldehyde injection

AMS and untreated neurons (with characterised receptive fields)

In the untreated group, 20% (1/5) of C-fibre neurons was considered to be ongoing prior to intraneural injection of cinnamaldehyde. The rate of ongoing activity in this neuron was 0.09 Hz at baseline. None (0/5) of the neurons with AMS responded to an intraneural injection of cinnamaldehyde (**Figures 6.9 A & 6.10 A**).

Following vinblastine treatment, 25% (1/4) of C-fibre neurons with AMS was considered to be ongoing prior to intraneural injection of cinnamaldehyde. The rate of ongoing activity in this neuron was 0.03 Hz at baseline. None (0/4) of the neurons with AMS responded to an intraneural injection of cinnamaldehyde (**Figures 6.9 B & 6.10 B**).

Following neuritis, 50% (3/6) of C-fibre neurons with AMS were considered to be ongoing prior to intraneural injection of cinnamaldehyde. The rates of ongoing activity ranged between 0.04 – 0.25 Hz at baseline. Fifty percent (3/6) of C-fibre neurons with AMS responded to an intraneural injection of cinnamaldehyde (An example response of a responder is shown in **Figure 6.9 C**) and all responses peaked between zero to two minutes post-injection (**Figure 6.10 C**). The C-fibre neurons that responded were identified between 5-7 days following neuritis and were all ongoing prior to intraneural injection

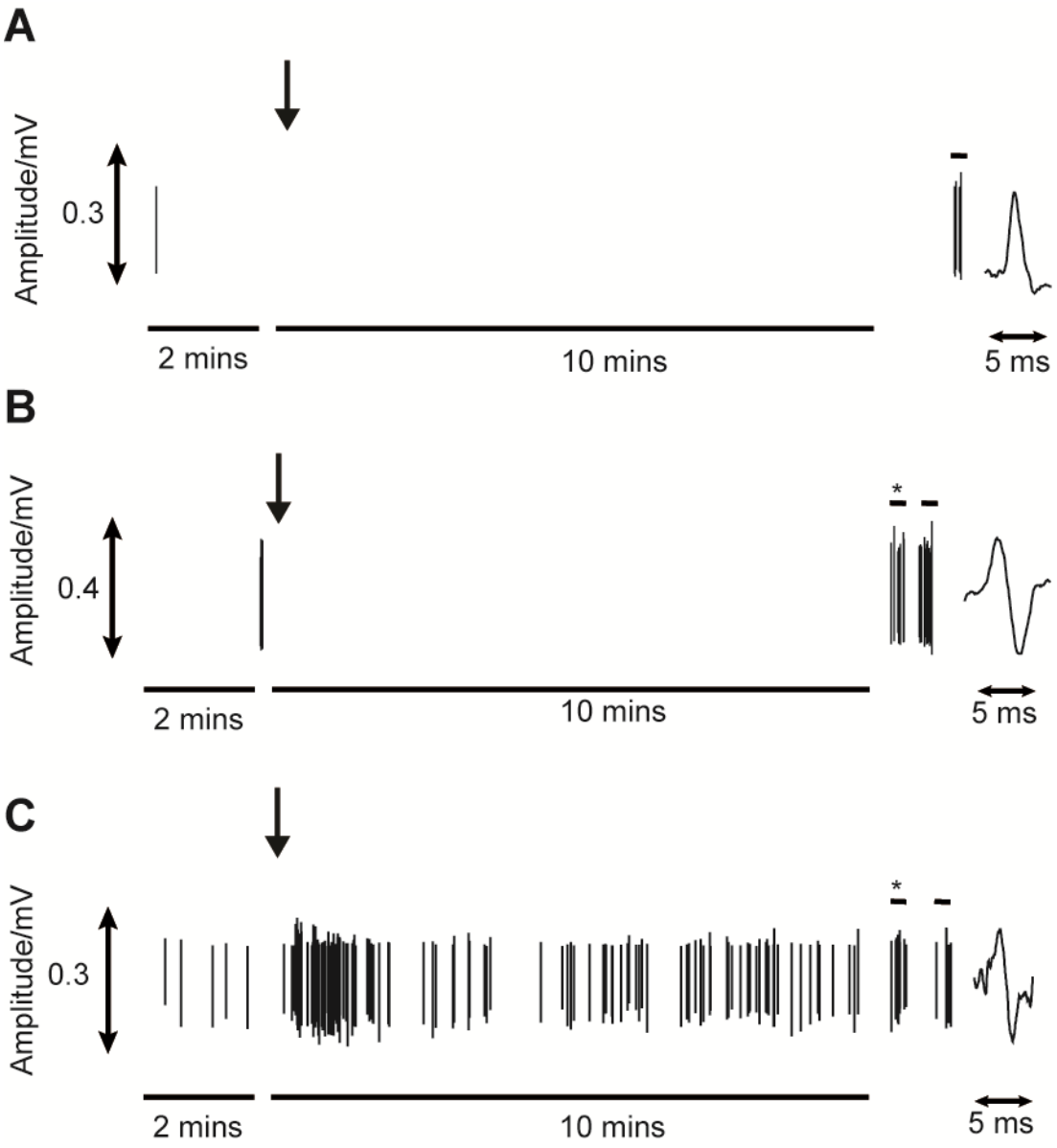

Figure 6.9 Example individual spike traces of C-fibre neurons after an intraneural injection of cinnamaldehyde. Example traces show the typical responses of individual C-fibre neurons to the intraneural injection of 100 µL of 500 µM cinnamaldehyde into the sciatic nerve in A) an untreated, B) vinblastine-treated and C) neuritis animal. Note that following B) vinblastine treatment and C) neuritis, neurons had AMS. Arrowheads correspond to time of intraneural injection Horizontal bars represent AMS (*) and receptive field testing.

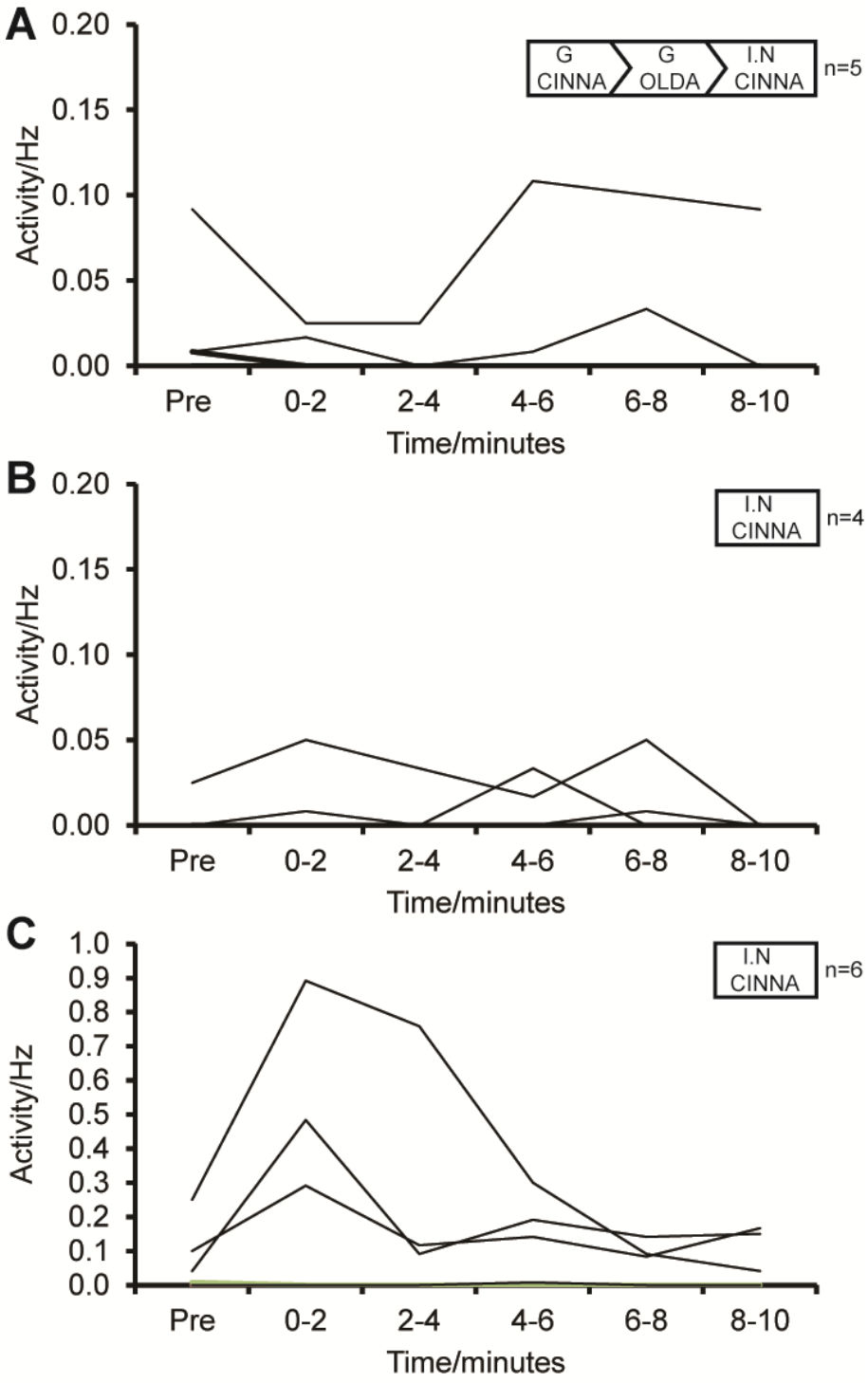

Figure 6.10 Activity rates of C-fibre neurons following the intraneural injection of cinnamaldehyde. In untreated animals, agonists were applied using gelfoam prior to intraneural injection. Only the intraneural injection data is presented. Each line represents the activity of an individual C-fibre neuron prior to and following intraneural injection of 100 µL of 500 µM cinnamaldehyde in A) untreated (n = 5 neurons), B) vinblastine-treated (n = 4 neurons) and C) neuritis (n = 6 neurons) animals. In C) 3/6 neurons responded. Note that following B) vinblastine treatment and C) neuritis, neurons had AMS. Key represents experimental protocol. G = Gelfoam, I.N = Intraneural.

Non-AMS neurons (receptive fields not identified)

In the untreated group, 4% (1/24) of C-fibre neurons with unidentified receptive fields were ongoing prior to the intraneural injection of cinnamaldehyde. This ongoing neuron had a baseline firing rate of 0.22 Hz. None of the neurons (0/24) respond to an intraneural injection of cinnamaldehyde. **Figures 6.11 A & 6.12 A** show effects of cinnamaldehyde on the neuron that had ongoing activity at baseline.

Following vinblastine treatment, 16% (4/25) of C-fibre neurons with unidentified receptive fields were ongoing prior to the intraneural injection of cinnamaldehyde. Ongoing neurons had baseline firing rates that ranged between 0.17 - 0.43 Hz. An intraneural injection of cinnamaldehyde caused a response in 4% (1/25) of neurons. The responder was ongoing at baseline. **Figures 6.11 B & 6.12 B** show effects of cinnamaldehyde on the neurons that had ongoing activity.

Following neuritis, 20% (6/30) of C-fibre neurons with unidentified receptive fields were ongoing prior to the intraneural injection of cinnamaldehyde. The majority of ongoing neurons had baseline firing rates that were high (>0.19 Hz). An intraneural injection of cinnamaldehyde caused a response in 4% (3/30) neurons. All of the responders were ongoing at baseline (**Figures 6.11 C & 6.12 C**). One neuron increased its firing rate above the response threshold in every two minute bin, reaching a peak at 6-8 minutes post-injection. Of the other two neurons, one responded between the 2-4 minutes post-injection and the other responded between 0-2 and 2-4 minutes post-injection.

For each treatment group, a summary of the responses of C-fibre neurons to the intraneural injection of vehicle, OLDA and cinnamaldehyde is shown in **Table 6.3**.

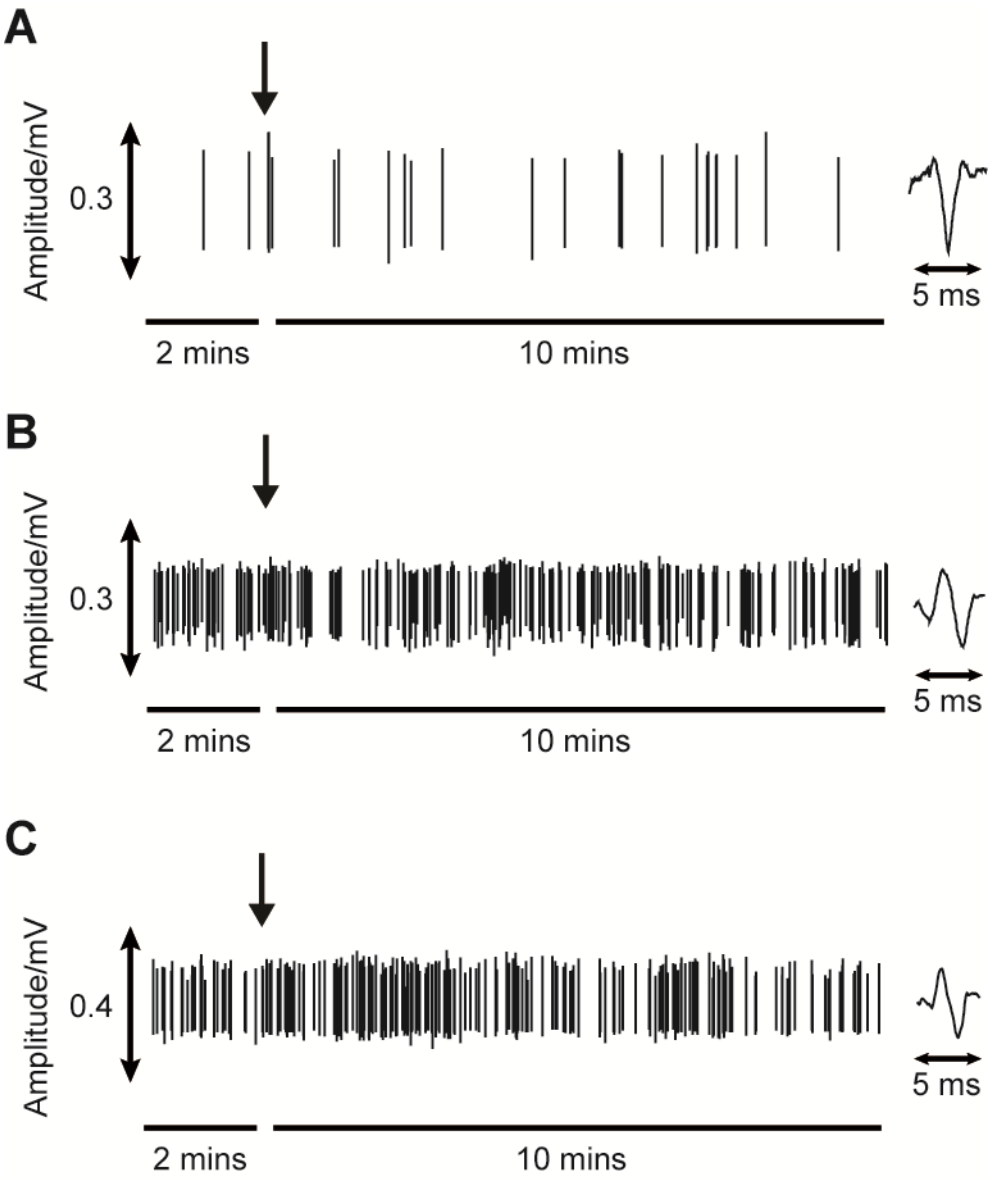

Figure 6.11 Example individual spike traces of ongoing C-fibre neurons after an intraneural injection of cinnamaldehyde. Example traces show the typical responses of individual C-fibre neurons to the intraneural injection of 100 µL of 500 µM cinnamaldehyde into the sciatic nerve in A) an untreated, B) vinblastine-treated and C) neuritis animal. Note that receptive fields were not identified in these neurons. Arrowheads correspond to time of intraneural injection.

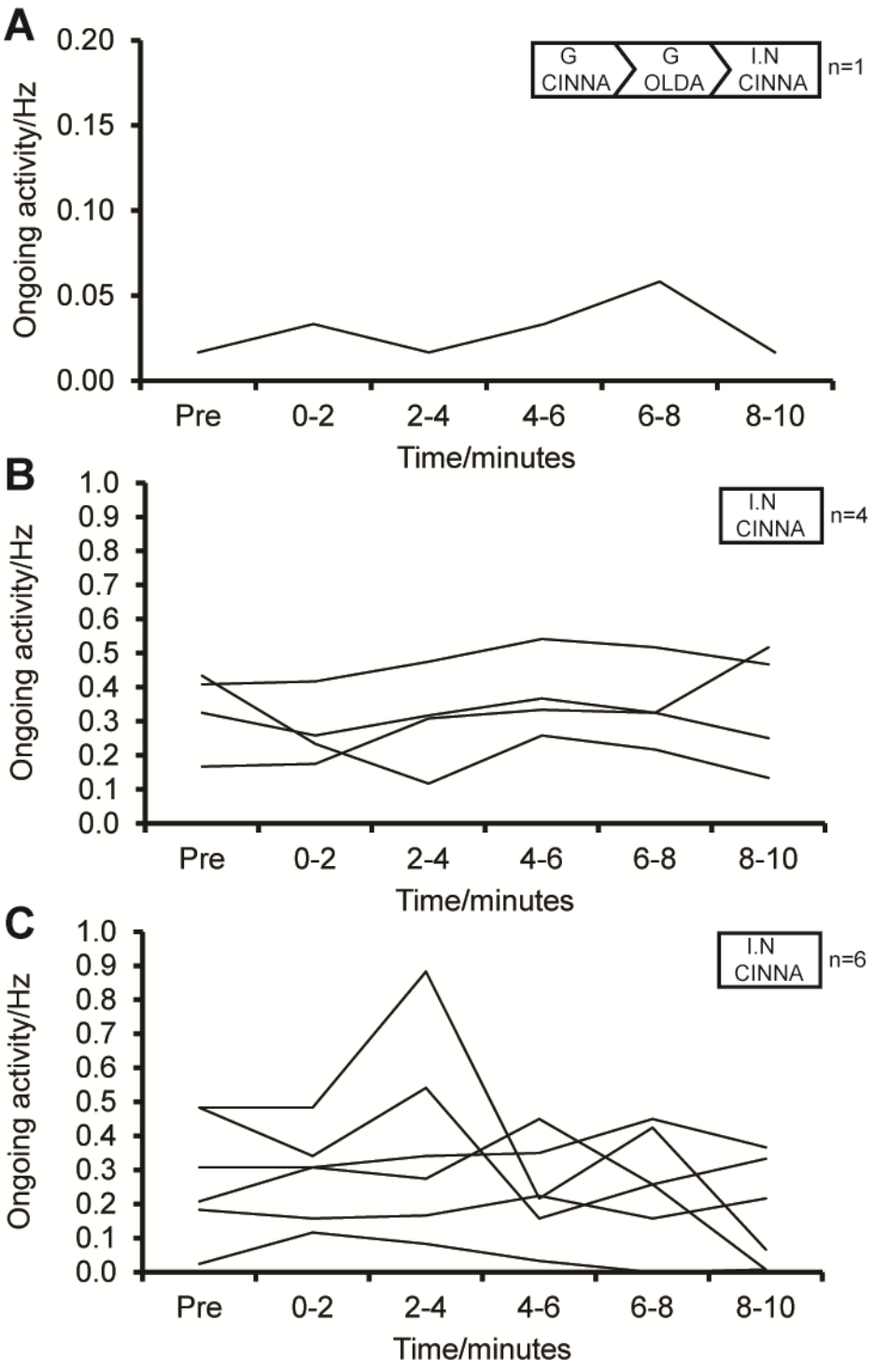

Figure 6.12 Activity rates of ongoing C-fibre neurons following the intraneural injection of cinnamaldehyde. In untreated animals, agonists were applied using gelfoam prior to intraneural injection. Only the intraneural injection data is presented. Each line represents the activity of an individual C-fibre neuron prior to and following intraneural injection of 100 µL of 500 µM cinnamaldehyde in A) untreated (n = 1), B) vinblastine-treated (n = 4 neurons) and C) neuritis (n = 6 neurons) animals. Note in B) 1/4 neurons responded and in C) 3/6 neurons responded. Receptive fields were not identified in these neurons. Key represents experimental protocol. G = Gelfoam, I.N = Intraneural.

		Vehicle	50 µM N-oleoyl-dopamine	500 µM Cinnamaldehyde
Untreated	**RF**	-	0% (0/5)	0% (0/5)
	RF not identified	-	0% (0/21)	0% (0/24)
Vinblastine	**AMS**	0% (0/3)	20% (1/5)	0% (0/4)
	RF not identified	0% (0/20)	0% (0/22)	4% (0/25)
Neuritis	**AMS**	0% (0/6)	60% (3/5)	50% (3/6)
	RF not identified	0% (0/27)	0% (0/14)	10% (3/30)

Table 6.3. A summary of the responses of C-fibre neurons to the intraneural injection of N-oleoyl-dopamine (OLDA) and cinnamaldehyde in untreated, vinblastine and neuritis groups. A neuron was considered to have responded if it increased its firing rate above threshold within any 2 minute period in the 10 minutes post-injection. RF – receptive field.

6.3 Main findings

- In untreated, vinblastine-treated and neuritis groups, a low proportion of C-fibre neurons responded to gelfoam application of 10 – 200 µM OLDA (0 - 13%) and cinnamaldehyde (0 - 22%).

- In untreated animals, an intraneural injection of 50 µM OLDA did not cause responses in C-fibre neurons with identified receptive fields (0/5) or those with unidentified receptive fields (0/21).

- Following vinblastine treatment, an intraneural injection of 50 µM OLDA caused a response in 20% (1/5) of C-fibre neurons with AMS, but did not cause responses in C-fibre neurons without AMS that had unidentified receptive fields (0/22).

- Following neuritis, intraneural injection of 50 µM OLDA caused a response in 60% (3/5) of C-fibre neurons with AMS, but did not cause responses in C-fibre neurons without AMS that had unidentified receptive fields (0/14).

- In the untreated group, an intraneural injection of 500 µM cinnamaldehyde did not cause responses in C-fibre neurons with identified receptive fields (0/5) or those with unidentified receptive fields (0/22).

- Following vinblastine treatment, an intraneural injection of 500 µM cinnamaldehyde did not cause responses in C-fibre neurons with AMS (0/4), but caused a response in 4% (1/25) of neurons without AMS that had unidentified receptive fields

- Following neuritis, intraneural injection of 500 µM caused a response in 50% (3/6) of C-fibre neurons with AMS, but only caused a response in 10% (3/30) of C-fibre neurons without AMS that had unidentified receptive fields.

6.4 Discussion

Since both TRPV1 and TRPA1 are reported to be involved in mechanical nociception (Brierley et al., 2009; Jones et al., 2005b; Kerstein et al., 2009; Rong et al., 2004; Vilceanu and Stucky, 2010), and the transport of each channel is disrupted, it is plausible that these channels contribute to AMS. As confirmation that levels of TRPV1 and TRPA1 are increased within nociceptors, and functional, agonists were applied to mechanically sensitive hotspots. In the majority of experiments, agonists were injected intraneurally following gelfoam application to ensure that the test agent crossed the epi-perineurium.

6.4.1 Perineural application of agonists had negligible effect on the excitability of C-fibre neurons

In this study, agonists were initially applied around the nerve using gelfoam, which had negligible effect on the excitability of C-fibre neurons following vinblastine treatment, neuritis and in untreated animals. It was likely that this was due to poor penetration of the agonists across the perineurium, as injection of each agonist caused responses in neurons following vinblastine treatment and neuritis. Poor penetration could have been due to the diffusion barrier of the perineurium and the positive intrafasciular pressure.

6.4.2 Intraneural injection of agonists did not initiate responses in C-fibre neurons of untreated or vinblastine-treated animals

Intraneural injection of OLDA or cinnamaldehyde did not cause responses in C-fibre neurons of untreated animals. The lack of responses indicates that, although functional TRPV1 and TRPA1 channels may be present along axons (Bernardini et al., 2004; Docherty et al., 2013), their levels are too low to initiate responses.

Following vinblastine treatment, the majority of C-fibre neurons, with and without AMS, did not respond to OLDA or cinnamaldehyde injection, suggesting that the levels of functional TRPV1 and TRPA1 are not significantly increased within these neurons. Although receptive fields of the neurons without AMS were not identified, 94% of C-fibre neurons from the L5 DRG are reported to pass through the sciatic nerve and therefore it was likely that they were exposed to agonists (Dilley et al.,

2013). Although TRPV1 and TRPA1 channels may have accumulated following axonal transport disruption, the lack of responses indicate that there is no increase in the number of functional channels in the axonal membrane. This finding suggests that other ion channels are likely to be involved in the development of AMS following vinblastine treatment, such as TRPV4, TRPC3, TRPC6, PIEZO2 and tentonin3 (see **4.4.3**).

6.4.3 OLDA and cinnamaldehyde initiated responses in a proportion of neurons with AMS following neuritis

While the majority of C-fibre neurons without AMS did not respond to an intraneural injection of OLDA following neuritis, a proportion of C-fibre neurons with AMS responded. This finding suggests that there is an increase in the levels of functional TRPV1 channels in a proportion of neurons with AMS. It is unclear why only AMS neurons were affected, but as AMS neurons typically innervate deep structures, physiological differences between muscle and cutaneous afferents might be involved. For example, TRPV1 is expressed in a greater number of afferents innervating the muscle and joints compared to the skin (Cho and Valtschanoff, 2008; Christianson et al., 2006; Hu-Tsai et al., 1992). Furthermore, as muscle afferents are reported to become more excitable than cutaneous afferents following nerve injury (Kirillova et al., 2011; Michaelis et al., 2000; Xu et al., 2010), the neurons with AMS might have been more responsive to agonists.

Similar to OLDA, injections of cinnamaldehyde also initiated responses that were generally restricted to a proportion of neurons with AMS, which suggests that there are increased levels of functional TRPA1 ion channels within these neurons. It is difficult to ascertain why levels of functional TRPA1 only appeared to increase in a proportion of neurons with AMS. As previously discussed, it is likely to reflect physiological differences between subpopulations of neurons.

Since both TRPV1 and TRPA1 are reported to be involved in mechanical nociception and the inflammatory-induced increase of mechanical sensitivity, the present data suggests that these channels might contribute towards the development of AMS following neuritis. In somatosensory neurons, TRPA1 does appear to play a role in

noxious mechanosensation under normal conditions (Brierley et al., 2011; Kerstein et al., 2009; Vilceanu and Stucky, 2010) and both TRPA1 and TRPV1 may contribute to mechanosensation under inflammatory conditions (Brederson et al., 2012; Kelly et al., 2015; Lennertz et al., 2012). However, until it has been demonstrated that these channels are mechanically gated, it not known whether they directly respond to mechanical stimulation in axons. As only a proportion of neurons with AMS appeared to have increased functional levels of TRPV1 and TRPA1, it seems likely that other ion channels, including those previously discussed, may contribute towards the development of AMS following neuritis.

In this study, neurons with ongoing activity following vinblastine treatment and neuritis were also examined to determine whether the levels of TRPV1 or TRPA1 had increased within these neurons. However, caution must be taken when interpreting this data. This is because noxious mechanical receptive field testing was likely to cause the development of ongoing activity from the terminals (Bove and Dilley, 2010), making it unclear whether ongoing activity originated at the treatment site (see limitations - **7.3.2**). In contrast to OLDA, cinnamaldehyde initiated responses in neurons that only had ongoing activity following neuritis. Additionally, all of the neurons with AMS that responded to cinnamaldehyde were ongoing at baseline. Therefore, it appears that TRPA1 levels may have increased in a proportion of neurons with ongoing activity and thus are not specific to neurons with AMS. It seems likely that increased levels of TRPA1 may in part contribute towards increased excitability in these neurons following neuritis, because the inflammatory mediator bradykinin is known to activate TRPA1 channels (Bandell et al., 2004).

6.4.4 Summary

Whereas the topical application of agonists had negligible effects on the activity of C-fibre neurons, intraneural injections initiated responses in a proportion of neurons following vinblastine treatment and neuritis. Following neuritis, a proportion of C-fibre neurons with AMS responded to OLDA and cinnamaldehyde, indicating that there are increased levels of functional TRPV1 and TRPA1 channels in these neurons. The increased presence of these ion channels suggests that they might be involved

in the development of AMS. In contrast, a low proportion of neurons with AMS responded to OLDA and cinnamaldehyde following vinblastine treatment, suggesting that there are not increased levels of functional TRPV1 and TRPA1 channels in these neurons. Therefore, TRPV1 and TRPA1 do not appear to be involved in AMS following vinblastine treatment. It is possible that there are lots of different mechanically sensitive ion channels that contribute to AMS following vinblastine treatment and neuritis, some of which may not have been identified.

Chapter 7

Discussion

7.1 Potential mechanisms of AMS

The current study has explored the relationship between axonal transport disruption and AMS in intact C-fibre neurons and has investigated the properties of mechanically sensitive hotspots following vinblastine treatment and neuritis. Additionally, it has begun to elucidate the ion channels responsible for the development of AMS. **Table 7.1** shows a summary of the characteristics of AMS that develops following vinblastine treatment and neuritis.

The main findings from this study indicate that axonal transport disruption plays an important role in the development of AMS. The transient development of AMS following vinblastine treatment is consistent with the short-lived time course of axonal transport disruption (Dilley et al., 2013). Although the development of AMS following neuritis is also reported to be transient, it is sustained for a longer period (Dilley and Bove, 2008b), which might be a consequence of a longer lasting disruption to axonal transport. Mechanistically, vinblastine disrupts axonal transport by inhibiting the growth of microtubules in addition to promoting their disassembly (Jordan and Wilson, 1990; Panda et al., 1996), which breaks down the microtubule tracks that kinesin uses to transport substances. However, the mechanisms by which inflammation disrupts kinesin-based transport are not known. It is likely that inflammatory mediators (Amano et al., 2001) and reactive oxygen species (Fang et al., 2012) are involved. Inflammatory mediators may interact with microtubule-associated proteins, such as tau, which leads to alterations in the mechanisms of motor protein interaction with microtubules (Dixit et al., 2008; Stroissnigg et al., 2007).

The outcome of these changes to kinesin-based transport leads to the disruption of anterogradely transported substances. Accordingly, the transport of TRPV1, TRPA1 and ASIC3 were clearly disrupted on day 4 following vinblastine treatment, which coincided with the time point when the levels of AMS reached a peak. Although the transport of TRPV1, TRPA1 and ASIC3 were not as clearly disrupted at this time point following neuritis, it is likely that this reflects the slower kinetics of inflammatory-induced axonal transport disruption (Dilley et al., 2013). It is proposed that

anterogradely transported ion channels subsequently accumulate and are locally inserted into the membrane, thereby causing axons to become mechanically sensitive (**Figure 7.1**). It seems possible that inflammatory mediator-induced activation of intracellular signalling cascades (e.g. PKC) might aid the insertion of mechanically sensitive ion channels into the membrane (Di Castro et al., 2006). Additionally, an inflammatory-induced upregulation of ion channels may contribute to the development of AMS. For example, hind paw inflammation is reported to increase the transport of TRPV1 mRNA to the terminals where it is locally translated, resulting in an increase in protein expression (Tohda et al., 2001).

Mechanically sensitive ion channels are shown to contribute towards AMS following vinblastine treatment and neuritis. Interestingly, the presence of mechanically sensitive ion channels enabled the axon to behave in a similar way to the terminal of a mechanosensitive nociceptor. Similarities between the properties of mechanically sensitive hotspots induced by vinblastine treatment and neuritis suggest that the mechanisms of mechanotransduction are comparable. Following neuritis, the increased levels of TRPV1 and TRPA1 in a proportion of AMS neurons indicate that these channels may contribute towards the development of AMS. However, this study has not provided evidence that TRPV1 and TRPA1 are directly involved in the mechanotransduction process. Thus, as it is still not known whether these channels can be directly gated by mechanical stimuli, other ion channels may be responsible for AMS following neuritis. In contrast to neuritis, the levels of TRPV1 and TRPA1 are not increased in neurons with AMS following vinblastine treatment, which suggests that other ion channels are involved in the development of AMS. It seems that vinblastine- and inflammation-induced axonal transport disruption will impede many of the mechanically sensitive ion channels that are transported towards the periphery. Therefore, it is possible that numerous channels expressed in C-fibre neurons will accumulate at the site of axonal transport disruption and thereby contribute towards AMS. Examples of such channels include TRPV4, TRPC3, TRPC6, PIEZO2 and tentonin3 (Alessandri-Haber et al., 2003, Coste et al., 2010; Elg et al., 2007; Hong et al., 2016).

As NGF is reported to be present at a neuritis (Obata et al., 2002) and is involved in the generation of mechanosensitivity in nociceptors (Hirth et al., 2013; Prato et al., 2017), it may also contribute towards the development of AMS. Upon NGF application, there is evidence that 'silent' nociceptors develop a novel form of mechanosensitivity, which is mediated by PIEZO 2 (Prato et al., 2017). Given that AMS typically develops in nociceptors innervating deep tissues (Bove et al., 2003), where 'silent' nociceptors are confined to (Prato et al., 2017), it is plausible that this novel form of NGF-mediated mechanosensitivity contributes towards AMS.

Another mechanism that was not investigated in this study is the potential role of axonal sprouting in the development of AMS. It has previously been reported that axonal transport disruption can lead to the formation of collateral sprouts (Gallo and Letourneau, 1999), which has been demonstrated in motor axons (Riley and Fahlman, 1985) and in larger diameter sensory axons (Guth et al., 1980) following perineural exposure of a low dose of colchicine. Such collateral sprouts may respond similar to the sprouts that form following a neuroma (Devor and Wall, 1976; Kwon et al., 2000), which are mechanically sensitive (Michaelis et al., 1995; Scadding, 1981; Welk et al., 1990).

	Vinblastine	Neuritis
Time course of AMS	Rapid induction, reaches peak at similar time point to the peak of behavioural changes, resolves by 2 weeks	Rapid induction, reaches peak at similar time point to peak of behavioural changes, persists for 4 weeks (Dilley and Bove, 2008b)
Location of hotspots	Proximal to or at the treatment site (Dilley and Bove, 2008a)	Majority at the neuritis site, some located proximally (Bove et al., 2003)
Properties of hotspots	Exhibit graded responses to changes in force, low firing thresholds	Exhibit graded responses to changes in force, low firing thresholds
Potential ion channels involved in the development of AMS	?	TRPA1, TRPV1

Table 7.1. Summary of the characteristics of AMS that develops in C-fibre neurons following vinblastine treatment and neuritis. Cells highlighted in dark grey - novel findings from this study. Cells highlighted in light grey – confirmation of previous findings.

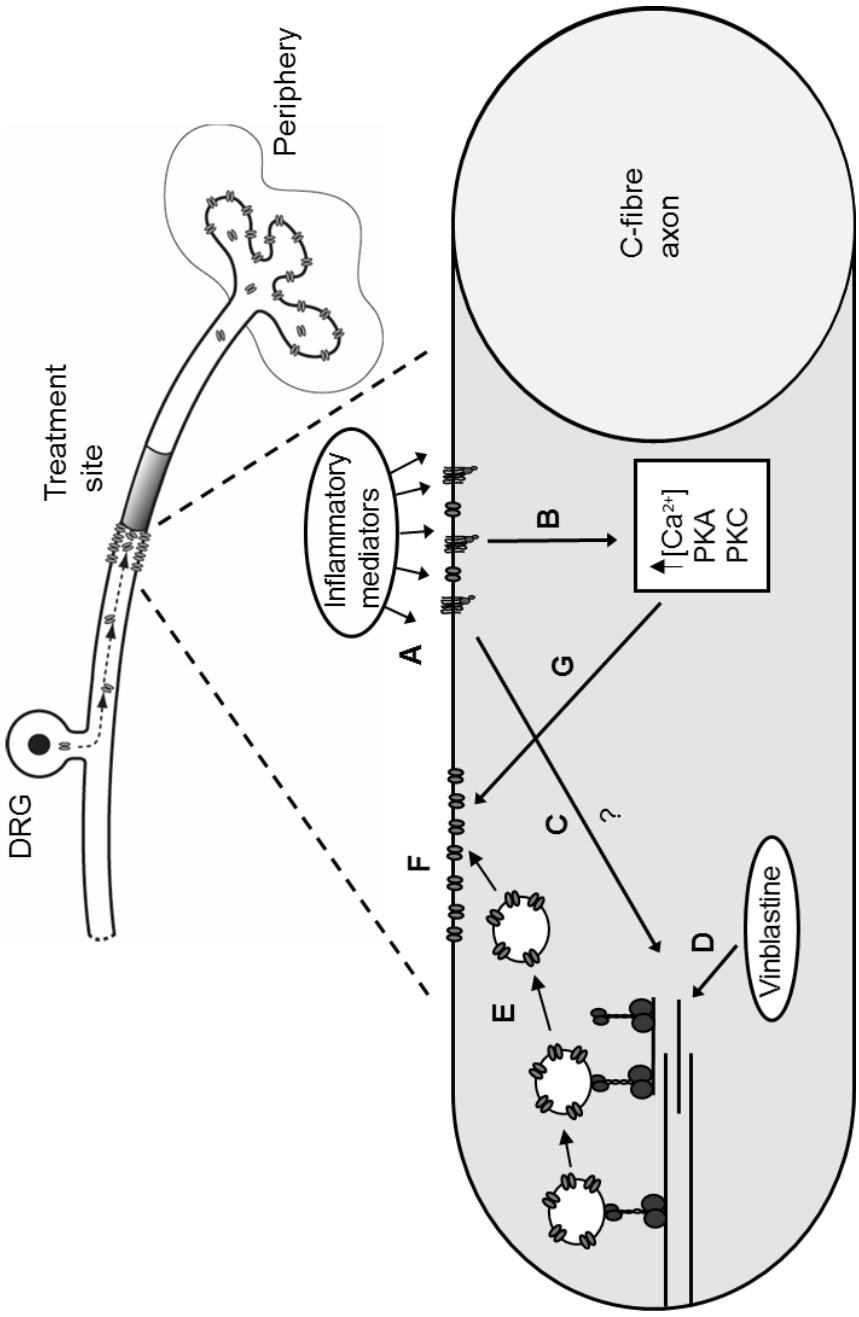

Figure 7.1 Potential mechanisms of AMS following vinblastine treatment and neuritis. Under normal conditions, sensory ion channels are transported from the dorsal root ganglion (DRG) to the periphery, where they are locally inserted into the membrane. Following neuritis, A) inflammatory mediators/growth factors may bind to ion channels and G-protein receptors causing the activation of B) intracellular signalling pathways, which results in kinase activation. C) Inflammatory mediators cause the disruption of axonal transport through an unknown mechanism. D) Vinblastine depolymerises microtubules disrupting the tracks that kinesin motor proteins use for transport. E) Axonal transport disruption leads to the accumulation of mechanically sensitive ion channels that are locally inserted into the membrane. F) Due to the increased volume of ion channels, the axon becomes mechanically sensitive. G) Inflammatory mediator induced activation of kinases may increase the trafficking of channels to the membrane and cause sensitisation of inserted channels and/or existing channels, which also may contribute towards AMS.

7.2 Clinical implications

Chronic widespread pain is extremely debilitating to an individual and is a major healthcare issue in the western world (Morales-Espinoza et al., 2016; Schaefer et al., 2016). Therefore, it is paramount that research into the underlying mechanisms that cause pain in these conditions continues. Patients with chronic widespread pain include those diagnosed with NSAP, fibromyalgia, CRPS-1 and WAD. Although many of these patients do not show signs of frank nerve injury on routine clinical examination, some may have inflamed nerves (Dilley et al., 2011; Greening et al., 2017). In these patients, it is hypothesised that inflammation-induced axonal transport disruption may play an important role in the development of painful symptoms (**Figure 7.2**).

The current study has emphasised that axonal transport disruption can cause physiological changes in nociceptive neurons. Specifically, it has focused on the development of AMS, which is likely to be the cause of nerve trunk mechanical sensitivity in patients. Inflamed nociceptors that develop AMS respond to approximately 3% stretch (Dilley et al., 2005), which may be generated in humans upon normal limb movements (Dilley et al., 2003). This suggests that daily activities, such as getting dressed, may cause activation of mechanically sensitive nociceptors, thereby causing pain. Additionally, since it is widely accepted that central mechanisms of neuropathic pain require an afferent barrage, (Campbell and Meyer, 2006; Gracely et al., 1992; Woolf, 2011; Xie et al., 2005), it is possible that activation of nociceptors with AMS may contribute to such barrage. Therefore, it is essential to understand how mechanical sensitivity arises and to elucidate the mechanically sensitive ion channels that are likely to be involved in its development. Mechanically-evoked pain is also a major impairment to patients suffering from chronic inflammatory diseases affecting the joints, such as osteoarthritis (Neogi and Zhang, 2013). Interestingly, it seems that mechanically sensitive channels are also involved in the development of mechanically-evoked pain (He et al., 2017). Hence, identification of mechanically sensitive ion channels may provide an attractive therapeutic target for the treatment of both chronic neuropathic and inflammatory pain conditions.

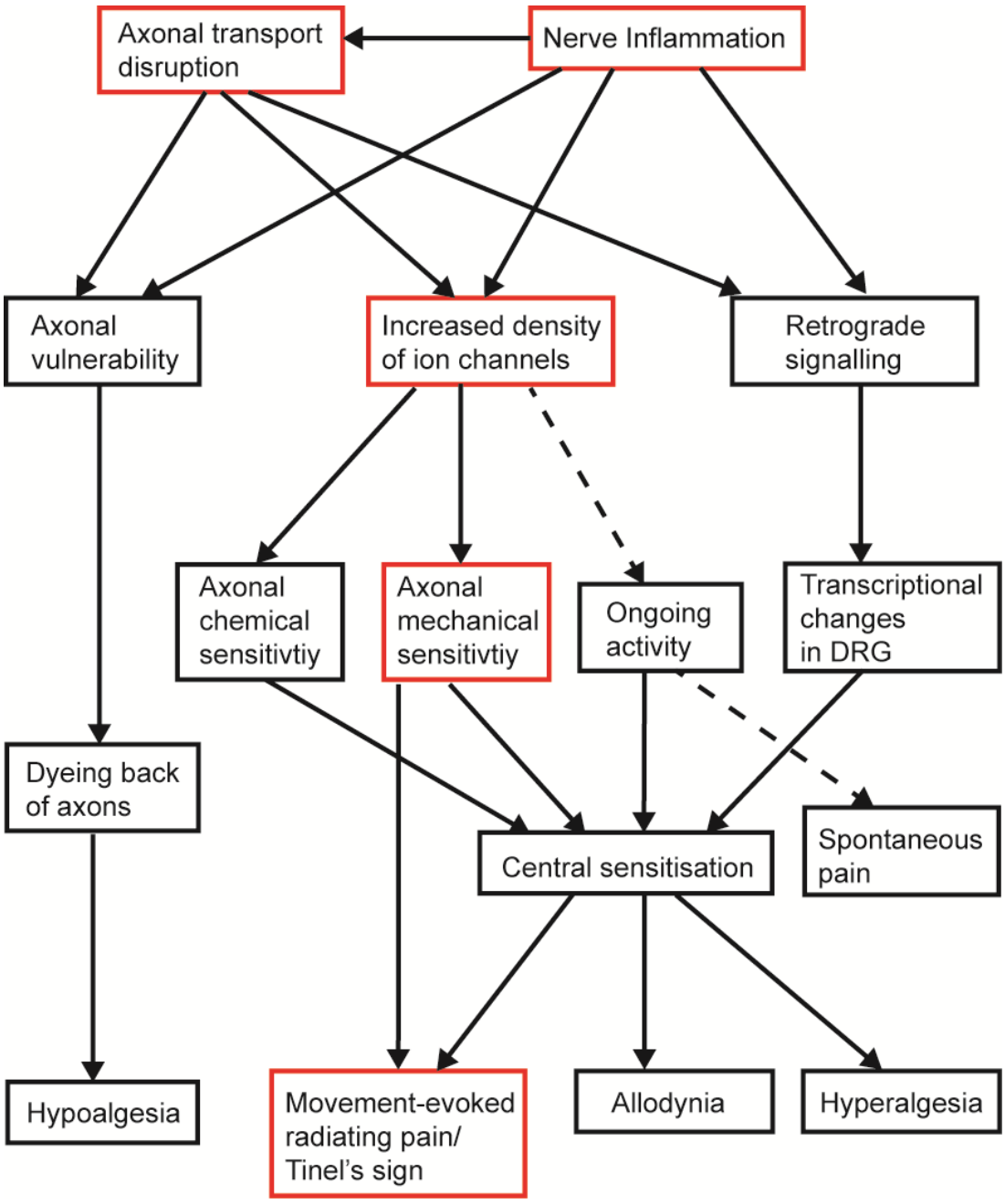

Figure 7.2 Overview of the proposed mechanisms that underlie the development of pain symptoms in patients with neuritis. Briefly, nerve inflammation induces axonal transport disruption, which in itself, and in addition to the effects of inflammatory mediators, increases the axonal density of ion channels. This leads to axons becoming mechanically and chemically sensitive and causes the generation of ongoing activity (when in the presence of inflammatory mediators). These factors may contribute to pain symptoms alone (e.g. Tinel's sign arising from mechanical sensitivity), or together to drive central sensitisation that leads neuropathic pain symptoms. Hashed line - only thought to develop in the presence of inflammatory mediators. Boxes highlighted in red - focus of this study.

7.3 Limitations

7.3.1 Ex-vivo recordings

It was not possible to generate force-discharge relationships and/or apply blockers to every mechanically sensitive hotspot identified. This was due to the fact that it was hard to pinpoint some hotspots, because they would sometimes be located on the side/ underside of the nerve. Although the stimulator was carefully positioned over the hotspot with a micromanipulator, the stimulator would sometimes slip away from the nerve, making it difficult to obtain consistent force discharge relationships.

7.3.2 In-vivo recordings

It was not possible to use the force-feedback controlled stimulator in an in vivo set-up due to technical issues (e.g. positioning of the mechanical stimulator on the nerve). For this reason, it was decided that specific channel blockers would not be tested in these experiments, as quantification of the extent of channel block was not possible. Therefore, agonists were applied to AMS hotspots.

Receptive fields were characterised in agonist experiments to ensure that a similar proportion of deep neurons were sampled from untreated animals, as neurons with AMS typically innervate deep structures. However, searching for noxious mechanical receptive fields causes inflammation that resulted in ongoing activity in C-fibre neurons (Bove and Dilley, 2010), which was reported to cause axonal sensitivity to inflammatory mediators in a previous study (Richards et al., 2011). As a consequence of this sensitisation, ongoing neurons may have been more likely to respond to agonists.

7.3.3 Immunolabeling

Antibodies were not characterised using immunoblotting in this study because this has already been performed in previous studies (See **Table 2.1**). Although labelling patterns of each antibody were consistent with previously reported expression patterns for each protein (see **Appendix 2**), the antibodies used in this study were polyclonal. Thus, there may had been an increased possibility of non-specific binding.

A more appropriate method of determining the specificity each antibody would involve a knockdown of the protein of interest in rats or mice. However, access to such knockouts was not possible in this study.

7.4 Future directions

There is unpublished evidence (communication from Geoffrey Bove) that mice nerves are better suited for ex-vivo electrophysiological recordings. Therefore, the combination of the use of ex-vivo electrophysiology with knockout mice would help to further characterise the role of TRPV1 and TRPA1 in the development of AMS. Transient receptor potential receptor ankyrin 1 knockout mice have previously been used to demonstrate that TRPA1 contributes to mechanical sensitivity in a sub-population of C-fibre neurons (Vilceanu and Stucky, 2010). Additionally, specific antagonists of the TRPV1 and TRPA1 ion channels could be employed to determine the precise role of these channels in AMS. However, due to differences in the patterns of protein expression in neurons of rats and mice (Price and Flores, 2007), caution must be taken when modelling neuritis in a different species. Hence, a series of studies validating the use of each model in-vivo and ex-vivo would need to be carried out prior to the use of mice.

Similarities between the pattern of pain behaviours and AMS might indicate that AMS is somehow involved in the development of pain behaviours. Activation of mechanically sensitive nociceptors may contribute to the afferent barrage required for the development of central changes, which may lead to the development of pain behaviours (Campbell and Meyer, 2006; Gracely et al., 1992; Woolf, 2011; Xie et al., 2005). To investigate this possibility, an implantable peristaltic mini-pump could be used to deliver agents to the treatment site (Speed and Hyndman, 2016). Following vinblastine treatment and neuritis, mechanically sensitive ion channel blockers could be delivered to the treatment site via the pump to test the hypothesis that this might reverse pain behaviours.

Concluding remarks

This study has furthered our understanding of the mechanisms that lead to the development of AMS. As AMS is likely to represent nerve trunk mechanical sensitivity in patients suffering from chronic widespread pain conditions, such as NSAP WAD and CRPS-1, it is crucial that we elucidate the ion channels involved in the development of mechanical sensitivity. Identification of such channels may facilitate the development of novel drugs to treat movement-evoked pain, ensuring that patients can perform normal day-to-day tasks in the absence of pain. Not only will this improve the patient's quality of life, but it will also reduce the socio-economic costs associated with healthcare and lost work days.

References

Abe N and Cavalli V (2008) Nerve injury signalling. *Current opinion in neurobiology* **18**:276-283.

Abraira VE and Ginty DD (2013) The sensory neurons of touch. *Neuron* **79**:618-639.

Acosta C, Djouhri L, Watkins R, Berry C, Bromage K and Lawson SN (2014) TREK2 expressed selectively in IB4-binding C-fiber nociceptors hyperpolarizes their membrane potentials and limits spontaneous pain. *The Journal of neuroscience : the official journal of the Society for Neuroscience* **34**:1494-1509.

Akiba Y, Mizumori M, Kuo M, Ham M, Guth PH, Engel E and Kaunitz JD (2008) CO2 chemosensing in rat oesophagus. *Gut* **57**:1654-1664.

Alessandri-Haber N, Yeh JJ, Boyd AE, Parada CA, Chen X, Reichling DB and Levine JD (2003) Hypotonicity induces TRPV4-mediated nociception in rat. *Neuron* **39**:497-511.

Allchorne AJ, Broom DC and Woolf CJ (2005) Detection of cold pain, cold allodynia and cold hyperalgesia in freely behaving rats. *Molecular pain* **1**:36-36.

Alloui A, Zimmermann K, Mamet J, Duprat F, Noel J, Chemin J, Guy N, Blondeau N, Voilley N, Rubat-Coudert C, Borsotto M, Romey G, Heurteaux C, Reeh P, Eschalier A and Lazdunski M (2006) TREK-1, a K+ channel involved in polymodal pain perception. *The EMBO journal* **25**:2368-2376.

Alvarez de la Rosa D, Zhang P, Shao D, White F and Canessa CM (2002) Functional implications of the localization and activity of acid-sensitive channels in rat peripheral nervous system. *Proceedings of the National Academy of Sciences of the United States of America* **99**:2326-2331.

Amano R, Hiruma H, Nishida S, Kawakami T and Shimizu K (2001) Inhibitory effect of histamine on axonal transport in cultured mouse dorsal root ganglion neurons. *NeurosciRes* **41**:201-206.

Amaya F, Oh-hashi K, Naruse Y, Iijima N, Ueda M, Shimosato G, Tominaga M, Tanaka Y and Tanaka M (2003) Local inflammation increases vanilloid receptor 1 expression within distinct subgroups of DRG neurons. *Brain research* **963**:190-196.

Anand U, Otto WR, Facer P, Zebda N, Selmer I, Gunthorpe MJ, Chessell IP, Sinisi M, Birch R and Anand P (2008) TRPA1 receptor localisation in the human peripheral nervous system and functional studies in cultured human and rat sensory neurons. *Neuroscience letters* **438**:221-227.

Anderson LE and McClure WO (1973) Differential transport of protein in axons: comparison between the sciatic nerve and dorsal columns of cats. *Proceedings of the National Academy of Sciences of the United States of America* **70**:1521-1525.

Andrew D and Greenspan JD (1999) Peripheral coding of tonic mechanical cutaneous pain: Comparison of nociceptor activity in rat and human psychophysics. *Journal of Neurophysiology* **82**:2641-2648.

Arnal I and Wade RH (1995) How does taxol stabilize microtubules? *Curr Biol* **5**:900-908.

Arner S, Lindblom U, Meyerson BA and Molander C (1990) Prolonged relief of neuralgia after regional anesthetic blocks. A call for further experimental and systematic clinical studies. *Pain* **43**:287-297.

Aubdool AA, Graepel R, Kodji X, Alawi KM, Bodkin JV, Srivastava S, Gentry C, Heads R, Grant AD, Fernandes ES, Bevan S and Brain SD (2014) TRPA1 is essential for the vascular response to environmental cold exposure. *Nature communications* **5**:5732.

Backonja MM and Stacey B (2004) Neuropathic pain symptoms relative to overall pain rating. *The journal of pain : official journal of the American Pain Society* **5**:491-497.

Baker MD (2005) Protein kinase C mediates up-regulation of tetrodotoxin-resistant, persistent Na+ current in rat and mouse sensory neurones. *The Journal of physiology* **567**:851-867.

Bandell M, Story GM, Hwang SW, Viswanath V, Eid SR, Petrus MJ, Earley TJ and Patapoutian A (2004) Noxious cold ion channel TRPA1 is activated by pungent compounds and bradykinin. *Neuron* **41**:849-857.

Bang H, Kim Y and Kim D (2000) TREK-2, a new member of the mechanosensitive tandem-pore K+ channel family. *The Journal of biological chemistry* **275**:17412-17419.

Barabas ME, Kossyreva EA and Stucky CL (2012) TRPA1 is functionally expressed primarily by IB4-binding, non-peptidergic mouse and rat sensory neurons. *PloS one* **7**:e47988.

Baron R, Binder A and Wasner G (2010) Neuropathic pain: diagnosis, pathophysiological mechanisms, and treatment. *Lancet Neurol* **9**:807-819.

Bautista DM, Jordt SE, Nikai T, Tsuruda PR, Read AJ, Poblete J, Yamoah EN, Basbaum AI and Julius D (2006) TRPA1 mediates the inflammatory actions of environmental irritants and proalgesic agents. *Cell* **124**:1269-1282.

Bautista DM, Movahed P, Hinman A, Axelsson HE, Sterner O, Högestätt ED, Julius D, Jordt S-E and Zygmunt PM (2005) Pungent products from garlic activate the sensory ion channel TRPA1. *Proceedings of the National Academy of Sciences of the United States of America* **102**:12248-12252.

Bennett DL, Koltzenburg M, Priestley JV, Shelton DL and McMahon SB (1998a) Endogenous nerve growth factor regulates the sensitivity of nociceptors in the adult rat. *EurJNeurosci* **10**:1282-1291.

Bennett DL, Michael GJ, Ramachandran N, Munson JB, Averill S, Yan Q, McMahon SB and Priestley JV (1998b) A distinct subgroup of small DRG cells express GDNF receptor components and GDNF is protective for these neurons after nerve injury. *The Journal of neuroscience : the official journal of the Society for Neuroscience* **18**:3059-3072.

Bennett GJ and Xie YK (1988) A peripheral mononeuropathy in rat that produces disorders of pain sensation like those seen in man. *Pain* **33**:87-107.

Bennett M (2001) The LANSS Pain Scale: the Leeds assessment of neuropathic symptoms and signs. *Pain* **92**:147-157.

Benson CJ, Xie J, Wemmie JA, Price MP, Henss JM, Welsh MJ and Snyder PM (2002) Heteromultimers of DEG/ENaC subunits form H+-gated channels in mouse sensory neurons. *ProcNatlAcadSciUSA* **99**:2338-2343.

Bernardini N, Neuhuber W, Reeh PW and Sauer SK (2004) Morphological evidence for functional capsaicin receptor expression and calcitonin gene-related peptide exocytosis in isolated peripheral nerve axons of the mouse. *Neuroscience* **126**:585-590.

Bessou P and Perl ER (1969) Response of cutaneous sensory units with unmyelinated fibers to noxious stimuli. *Journal of Neurophysiology* **32**:1025-1043.

Bester H, Beggs S and Woolf CJ (2000) Changes in tactile stimuli-induced behavior and c-Fos expression in the superficial dorsal horn and in parabrachial nuclei after sciatic nerve crush. *The Journal of comparative neurology* **428**:45-61.

Birder LA, Nakamura Y, Kiss S, Nealen ML, Barrick S, Kanai AJ, Wang E, Ruiz G, de Groat WC, Apodaca G, Watkins S and Caterina MJ (2002) Altered urinary bladder function in mice lacking the vanilloid receptor TRPV1. *Nature Neuroscience* **5**:856-860.

Birklein F, Riedl B, Sieweke N, Weber M and Neundorfer B (2000) Neurological findings in complex regional pain syndromes - analysis of 145 cases. *Acta Neurologica Scandinavica* **101**:262-269.

Birklein F, Schmelz M, Schifter S and Weber M (2001) The important role of neuropeptides in complex regional pain syndrome. *Neurology* **57**:2179-2184.

Black MM and Lasek RJ (1980) Slow components of axonal transport: two cytoskeletal networks. *The Journal of cell biology* **86**:616-623.

Blenk KH, Michaelis M, Vogel C and Janig W (1996) Thermosensitivity of Acutely Axotomized Sensory Nerve Fibers. *Journal of Neurophysiology* **76**:743-752.

Bohlen CJ, Chesler AT, Sharif-Naeini R, Medzihradszky KF, Zhou S, King D, Sanchez EE, Burlingame AL, Basbaum AI and Julius D (2011) A heteromeric Texas coral snake toxin targets acid-sensing ion channels to produce pain. *Nature* **479**:410-414.

Bonnington JK and McNaughton PA (2003) Signalling pathways involved in the sensitisation of mouse nociceptive neurones by nerve growth factor. *The Journal of physiology* **551**:433-446.

Boucher TJ, Okuse K, Bennett DL, Munson JB, Wood JN and McMahon SB (2000) Potent analgesic effects of GDNF in neuropathic pain states. *Science* **290**:124-127.

Bove GM and Dilley A (2010) The conundrum of sensitization when recording from nociceptors. *J Neurosci Methods* **188**:213-218.

Bove GM and Light AR (1997) The nervi nervorum: missing link for neuropathic pain? *Pain Forum* **6**:181-190.

Bove GM, Ransil BJ, Lin HC and Leem JG (2003) Inflammation induces ectopic mechanical sensitivity in axons of nociceptors innervating deep tissues. *JNeurophysiol* **90**:1949-1955.

Bove GM, Weissner W and Barbe MF (2009) Long lasting recruitment of immune cells and altered epi-perineurial thickness in focal nerve inflammation induced by complete Freund's adjuvant. *J Neuroimmunol*.

Bove GM, Zaheen A and Bajwa ZH (2005) Subjective nature of lower limb radicular pain. *JManipulative Physiol Ther* **28**:12-14.

Bradbury EJ, Burnstock G and McMahon SB (1998) The expression of P2X3 purinoreceptors in sensory neurons: effects of axotomy and glial-derived neurotrophic factor. *Molecular and cellular neurosciences* **12**:256-268.

Brederson JD, Chu KL, Reilly RM, Brown BS, Kym PR, Jarvis MF and McGaraughty S (2012) TRPV1 antagonist, A-889425, inhibits mechanotransmission in a subclass of rat primary afferent neurons following peripheral inflammation. *Synapse* **66**:187-195.

Breivik H, Collett B, Ventafridda V, Cohen R and Gallacher D (2006) Survey of chronic pain in Europe: prevalence, impact on daily life, and treatment. *European journal of pain* **10**:287-333.

Brenn D, Richter F and Schaible HG (2007) Sensitization of unmyelinated sensory fibers of the joint nerve to mechanical stimuli by interleukin-6 in the rat: an inflammatory mechanism of joint pain. *Arthritis Rheum* **56**:351-359.

Bretag AH (1969) Synthetic interstitial fluid for isolated mammalian tissue. *Life Sci* **8**:319-329.

Brierley SM, Castro J, Harrington AM, Hughes PA, Page AJ, Rychkov GY and Blackshaw LA (2011) TRPA1 contributes to specific mechanically activated currents and sensory neuron mechanical hypersensitivity. *J Physiol* **589**:3575-3593.

Brierley SM, Hughes PA, Page AJ, Kwan KY, Martin CM, O'Donnell TA, Cooper NJ, Harrington AM, Adam B, Liebregts T, Holtmann G, Corey DP, Rychkov GY and Blackshaw LA (2009) The ion channel TRPA1 is required for normal mechanosensation and is modulated by algesic stimuli. *Gastroenterology* **137**:2084-2095 e2083.

Brierley SM, Page AJ, Hughes PA, Adam B, Liebregts T, Cooper NJ, Holtmann G, Liedtke W and Blackshaw LA (2008) Selective role for TRPV4 ion channels in visceral sensory pathways. *Gastroenterology* **134**:2059-2069.

Brown AG and Iggo A (1967) A quantitative study of cutaneous receptors and afferent fibres in the cat and rabbit. *The Journal of physiology* **193**:707-733.

Burgess SE, Gardell LR, Ossipov MH, Malan TP, Jr., Vanderah TW, Lai J and Porreca F (2002) Time-dependent descending facilitation from the rostral ventromedial medulla maintains, but does not initiate, neuropathic pain. *The Journal of neuroscience : the official journal of the Society for Neuroscience* **22**:5129-5136.

Cabo R, Galvez MA, San Jose I, Laura R, Lopez-Muniz A, Garcia-Suarez O, Cobo T, Insausti R and Vega JA (2012) Immunohistochemical localization of acid-sensing ion channel 2 (ASIC2) in cutaneous Meissner and Pacinian corpuscles of Macaca fascicularis. *Neuroscience letters* **516**:197-201.

Cain DM, Khasabov SG and Simone DA (2001) Response properties of mechanoreceptors and nociceptors in mouse glabrous skin: an in vivo study. *Journal of Neurophysiology* **85**:1561-1574.

Calavia MG, Montaño JA, García-Suárez O, Feito J, Guervós MA, Germanà A, del Valle M, Pérez-Piñera P, Cobo J and Vega JA (2010) Differential Localization of Acid-Sensing Ion Channels 1 and 2 in Human Cutaneus Pacinian Corpuscles. *Cellular and Molecular Neurobiology* **30**:841-848.

Calcutt NA, Ettlinger CB, Carrington AL, Diemel L and Tomlinson DR (1991) Resistance to hypoxic conduction block in sciatic nerves of rats with streptozotocin-induced diabetes mellitus. *Journal of the neurological sciences* **103**:116-123.

Campbell JN and Meyer RA (2006) Mechanisms of neuropathic pain. *Neuron* **52**:77-92.

Camprubi-Robles M, Planells-Cases R and Ferrer-Montiel A (2009) Differential contribution of SNARE-dependent exocytosis to inflammatory potentiation of TRPV1 in nociceptors. *FASEB J* **23**:3722-3733.

Carlton SM, Dougherty PM, Pover CM and Coggeshall RE (1991) Neuroma formation and numbers of axons in a rat model of experimental peripheral neuropathy. *Neuroscience Letters* **131**:88-92.

Carp SJ, Barbe MF, Winter KA, Amin M and Barr AE (2007) Inflammatory biomarkers increase with severity of upper-extremity overuse disorders. *Clin Sci (Lond)* **112**:305-314.

Caterina MJ, Leffler A, Malmberg AB, Martin WJ, Trafton J, PetersenZeitz KR, Koltzenburg M, Basbaum AI and Julius D (2000) Impaired nociception and pain sensation in mice lacking the capsaicin receptor. *Science* **288**:306-313.

Caterina MJ, Schumacher MA, Tominaga M, Rosen TA, Levine JD and Julius D (1997) The capsaicin receptor: a heat-activated ion channel in the pain pathway. *Nature* **389**:816-824.

Cavaletti G, Tredici G, Braga M and Tazzari S (1995) Experimental peripheral neuropathy induced in adult rats by repeated intraperitoneal administration of taxol. *Exp Neurol* **133**:64-72.

Cavanaugh DJ, Chesler AT, Jackson AC, Sigal YM, Yamanaka H, Grant R, O'Donnell D, Nicoll RA, Shah NM, Julius D and Basbaum AI (2011) Trpv1 reporter mice reveal highly restricted brain distribution and functional expression in arteriolar smooth muscle cells. *The Journal of neuroscience : the official journal of the Society for Neuroscience* **31**:5067-5077.

Chacur M, Milligan ED, Gazda LS, Armstrong C, Wang HC, Tracey KJ, Maier SF and Watkins LR (2001) A new model of sciatic inflammatory neuritis (SIN): induction of unilateral and bilateral mechanical allodynia following acute unilateral peri-sciatic immune activation in rats. *Pain* **94**:231-244.

Chambers MR, Andres KH, von Duering M and Iggo A (1972) The structure and function of the slowly adapting type II mechanoreceptor in hairy skin. *Q J Exp Physiol Cogn Med Sci* **57**:417-445.

Chapman V, Suzuki R and Dickenson AH (1998) Electrophysiological characterization of spinal neuronal response properties in anaesthetized rats after ligation of spinal nerves L5-L6. *The Journal of physiology* **507 (Pt 3)**:881-894.

Chen CC, Akopian AN, Sivilotti L, Colquhoun D, Burnstock G and Wood JN (1995) A P2X purinoceptor expressed by a subset of sensory neurons. *Nature* **377**:428-431.

Chen CC, England S, Akopian AN and Wood JN (1998) A sensory neuron-specific, proton-gated ion channel. *ProcNatlAcadSciUSA* **95**:10240-10245.

Chen L and Huang LY (1992) Protein kinase C reduces Mg2+ block of NMDA-receptor channels as a mechanism of modulation. *Nature* **356**:521-523.

Chen Y and Devor M (1998) Ectopic mechanosensitivity in injured sensory axons arises from the site of spontaneous electrogenesis. *Eur J Pain* **2**:165-178.

Chien LY, Cheng JK, Chu D, Cheng CF and Tsaur ML (2007) Reduced expression of A-type potassium channels in primary sensory neurons induces mechanical hypersensitivity. *The Journal of neuroscience : the official journal of the Society for Neuroscience* **27**:9855-9865.

Cho H, Shin J, Shin CY, Lee SY and Oh U (2002) Mechanosensitive ion channels in cultured sensory neurons of neonatal rats. *JNeurosci* **22**:1238-1247.

Cho WG and Valtschanoff JG (2008) Vanilloid receptor TRPV1-positive sensory afferents in the mouse ankle and knee joints. *Brain research* **1219**:59-65.

Choi JY, Kang CH, Kim BJ, Park KW and Yu SW (2009) Brachial plexopathy following herpes zoster infection: two cases with MRI findings. *Journal of the neurological sciences* **285**:224-226.

Choi Y, Yoon YW, Na HS, Kim SH and Chung JM (1994) Behavioral signs of ongoing pain and cold allodynia in a rat model of neuropathic pain. *Pain* **59**:369-376.

Chowdary PD, Che DL and Cui B (2012) Neurotrophin signaling via long-distance axonal transport. *Annu Rev Phys Chem* **63**:571-594.

Christianson JA, McIlwrath SL, Koerber HR and Davis BM (2006) Transient receptor potential vanilloid 1-immunopositive neurons in the mouse are more prevalent within colon afferents compared to skin and muscle afferents. *Neuroscience* **140**:247-257.

Chu CJ, Huang SM, De Petrocellis L, Bisogno T, Ewing SA, Miller JD, Zipkin RE, Daddario N, Appendino G, Di Marzo V and Walker JM (2003) N-oleoyldopamine, a novel endogenous capsaicin-like lipid that produces hyperalgesia. *J Biol Chem* **278**:13633-13639.

Chuang HH, Prescott ED, Kong H, Shields S, Jordt SE, Basbaum AI, Chao MV and Julius D (2001) Bradykinin and nerve growth factor release the capsaicin receptor from PtdIns(4,5)P2-mediated inhibition. *Nature* **411**:957-962.

Coleman GT, Bahramali H, Zhang HQ and Rowe MJ (2001) Characterization of tactile afferent fibers in the hand of the marmoset monkey. *Journal of neurophysiology* **85**:1793-1804.

Corey DP, Garcia-Anoveros J, Holt JR, Kwan KY, Lin SY, Vollrath MA, Amalfitano A, Cheung EL, Derfler BH, Duggan A, Geleoc GS, Gray PA, Hoffman MP, Rehm HL, Tamasauskas D and Zhang DS (2004) TRPA1 is a candidate for the mechanosensitive transduction channel of vertebrate hair cells. *Nature* **432**:723-730.

Corrow K, Girard BM and Vizzard MA (2010) Expression and response of acid-sensing ion channels in urinary bladder to cyclophosphamide-induced cystitis. *Am J Physiol Renal Physiol* **298**:F1130-1139.

Coste B, Mathur J, Schmidt M, Earley TJ, Ranade S, Petrus MJ, Dubin AE and Patapoutian A (2010) Piezo1 and Piezo2 are essential components of distinct mechanically activated cation channels. *Science* **330**:55-60.

Coste B, Xiao B, Santos JS, Syeda R, Grandl J, Spencer KS, Kim SE, Schmidt M, Mathur J, Dubin AE, Montal M and Patapoutian A (2012) Piezo proteins are pore-forming subunits of mechanically activated channels. *Nature* **483**:176-181.

Cragg BG and Thomas PK (1961) Changes in conduction velocity and fibre size proximal to peripheral nerve lesions. *The Journal of physiology* **157**:315-327.

Curtis R, Tonra JR, Stark JL, Adryan KM, Park JS, Cliffer KD, Lindsay RM and DiStefano PS (1998) Neuronal injury increases retrograde axonal transport of the neurotrophins to spinal sensory neurons and motor neurons via multiple receptor mechanisms. *Molecular and cellular neurosciences* **12**:105-118.

da Costa DS, Meotti FC, Andrade EL, Leal PC, Motta EM and Calixto JB (2010) The involvement of the transient receptor potential A1 (TRPA1) in the

maintenance of mechanical and cold hyperalgesia in persistent inflammation. *Pain* **148**:431-437.

Dagenais S, Caro J and Haldeman S (2008) A systematic review of low back pain cost of illness studies in the United States and internationally. *Spine J* **8**:8-20.

De Col R, Messlinger K and Carr RW (2008) Conduction velocity is regulated by sodium channel inactivation in unmyelinated axons innervating the rat cranial meninges. *J Physiol* **586**:1089-1103.

De Schepper HU, De Winter BY, Van Nassauw L, Timmermans JP, Herman AG, Pelckmans PA and De Man JG (2008) TRPV1 receptors on unmyelinated C-fibres mediate colitis-induced sensitization of pelvic afferent nerve fibres in rats. *J Physiol* **586**:5247-5258.

De Vry J, Kuhl E, Franken-Kunkel P and Eckel G (2004) Pharmacological characterization of the chronic constriction injury model of neuropathic pain. *Eur J Pharmacol* **491**:137-148.

DeAngelis LM, Gnecco C, Taylor L and Warrell RP, Jr. (1991) Evolution of neuropathy and myopathy during intensive vincristine/corticosteroid chemotherapy for non-Hodgkin's lymphoma. *Cancer* **67**:2241-2246.

DeBerry JJ, Schwartz ES and Davis BM (2014) TRPA1 mediates bladder hyperalgesia in a mouse model of cystitis. *Pain* **155**:1280-1287.

Deering-Rice CE, Johansen ME, Roberts JK, Thomas KC, Romero EG, Lee J, Yost GS, Veranth JM and Reilly CA (2012) Transient receptor potential vanilloid-1 (TRPV1) is a mediator of lung toxicity for coal fly ash particulate material. *Molecular pharmacology* **81**:411-419.

Delcroix JD, Valletta JS, Wu C, Hunt SJ, Kowal AS and Mobley WC (2003) NGF signaling in sensory neurons: evidence that early endosomes carry NGF retrograde signals. *Neuron* **39**:69-84.

Deval E, Noel J, Lay N, Alloui A, Diochot S, Friend V, Jodar M, Lazdunski M and Lingueglia E (2008) ASIC3, a sensor of acidic and primary inflammatory pain. *The EMBO journal* **27**:3047-3055.

Devor M (1983) Nerve pathophysiology and mechanisms of pain in causalgia. *J Auton Nerv Syst* **7**:371-384.

Devor M and Govrin-Lippmann R (1983) Axoplasmic transport block reduces ectopic impulse generation in injured peripheral nerves. *Pain* **16**:73-85.

Devor M, Govrin-Lippmann R and Angelides K (1993) Na+ channel immunolocalization in peripheral mammalian axons and changes following nerve injury and neuroma formation. *JNeurosci* **13**:1976-1992.

Devor M and Wall PD (1976) Type of sensory nerve fibre sprouting to form a neuroma. *Nature* **262**:705-708.

Di Castro A, Drew LJ, Wood JN and Cesare P (2006) Modulation of sensory neuron mechanotransduction by PKC- and nerve growth factor-dependent pathways. *ProcNatlAcadSciUSA* **103**:4699-4704.

Dilley A and Bove GM (2008a) Disruption of axoplasmic transport induces mechanical sensitivity in intact rat C-fibre nociceptor axons. *J Physiol* **586**:593-604.

Dilley A and Bove GM (2008b) Resolution of inflammation-induced axonal mechanical sensitivity and conduction slowing in C-fiber nociceptors. *J Pain* **9**:185-192.

Dilley A and Greening J (2012) Non-Specific Arm Pain, in *Wall and Melzack's Textbook of Pain* (McMahon S and Koltzenburg M eds), Elsevier.

Dilley A, Greening J, Walker-Bone K and Good C (2011) Magnetic resonance imaging signal hyperintensity of neural tissues in diffuse chronic pain syndromes: a pilot study. *Muscle Nerve* **44**:981-984.

Dilley A, Lynn B, Greening J and DeLeon N (2003) Quantitative in vivo studies of median nerve sliding in response to wrist, elbow, shoulder and neck movements. *ClinBiomech(Bristol, Avon)* **18**:899-907.

Dilley A, Lynn B and Pang SJ (2005) Pressure and stretch mechanosensitivity of peripheral nerve fibres following local inflammation of the nerve trunk. *Pain* **117**:462-472.

Dilley A, Richards N, Pulman KG and Bove GM (2013) Disruption of fast axonal transport in the rat induces behavioral changes consistent with neuropathic pain. *J Pain* **14**:1437-1449.

Dixit R, Ross JL, Goldman YE and Holzbaur EL (2008) Differential regulation of dynein and kinesin motor proteins by tau. *Science* **319**:1086-1089.

Djouhri L, Fang X, Koutsikou S and Lawson SN (2012) Partial nerve injury induces electrophysiological changes in conducting (uninjured) nociceptive and nonnociceptive DRG neurons: Possible relationships to aspects of peripheral neuropathic pain and paresthesias. *Pain* **153**:1824-1836.

Djouhri L, Fang X, Okuse K, Wood JN, Berry CM and Lawson SN (2003) The TTX-resistant sodium channel Nav1.8 (SNS/PN3): expression and correlation with membrane properties in rat nociceptive primary afferent neurons. *Journal of Physiology* **550**:3-52.

Djouhri L, Koutsikou S, Fang X, McMullan S and Lawson SN (2006) Spontaneous pain, both neuropathic and inflammatory, is related to frequency of spontaneous firing in intact C-fiber nociceptors. *J Neurosci* **26**:1281-1292.

Dmitrieva N and McMahon SB (1996) Sensitisation of visceral afferents by nerve growth factor in the adult rat. *Pain* **66**:87-97.

Docherty RJ, Ginsberg L, Jadoon S, Orrell RW and Bhattacharjee A (2013) TRPA1 insensitivity of human sural nerve axons after exposure to lidocaine. Pain 154:1569-1577.

Dougherty PM, Cata JP, Cordella JV, Burton A and Weng HR (2004) Taxol-induced sensory disturbance is characterized by preferential impairment of myelinated fiber function in cancer patients. *Pain* **109**:132-142.

Dowdall T, Robinson I and Meert TF (2005) Comparison of five different rat models of peripheral nerve injury. *Pharmacol Biochem Behav* **80**:93-108.

Drew LJ, Rohrer DK, Price MP, Blaver KE, Cockayne DA, Cesare P and Wood JN (2004) Acid-sensing ion channels ASIC2 and ASIC3 do not contribute to mechanically activated currents in mammalian sensory neurones. *The Journal of physiology* **556**:691-710.

Drew LJ and Wood JN (2007) FM1-43 is a permeant blocker of mechanosensitive ion channels in sensory neurons and inhibits behavioural responses to mechanical stimuli. *Mol Pain* **3**:1.

Drew LJ, Wood JN and Cesare P (2002) Distinct mechanosensitive properties of capsaicin-sensitive and -insensitive sensory neurons. *JNeurosci* **22**:RC228.

Du X and Gamper N (2013) Potassium channels in peripheral pain pathways: expression, function and therapeutic potential. *Curr Neuropharmacol* **11**:621-640.

Dube GR, Lehto SG, Breese NM, Baker SJ, Wang X, Matulenko MA, Honore P, Stewart AO, Moreland RB and Brioni JD (2005) Electrophysiological and in vivo characterization of A-317567, a novel blocker of acid sensing ion channels. *Pain* **117**:88-96.

Duggett NA, Griffiths LA and Flatters SJL (2017) Paclitaxel-induced painful neuropathy is associated with changes in mitochondrial bioenergetics, glycolysis, and an energy deficit in dorsal root ganglia neurons. *Pain* **158**:1499-1508.

Dunham JP, Kelly S and Donaldson LF (2008) Inflammation reduces mechanical thresholds in a population of transient receptor potential channel A1-expressing nociceptors in the rat. *Eur J Neurosci* **27**:3151-3160.

Earley S, Gonzales AL and Crnich R (2009) Endothelium-dependent cerebral artery dilation mediated by TRPA1 and Ca2+-Activated K+ channels. *Circ Res* **104**:987-994.

Eijkelkamp N, Linley JE, Torres JM, Bee L, Dickenson AH, Gringhuis M, Minett MS, Hong GS, Lee E, Oh U, Ishikawa Y, Zwartkuis FJ, Cox JJ and Wood JN (2013) A role for Piezo2 in EPAC1-dependent mechanical allodynia. *Nature communications* **4**:1682.

Elg S, Marmigere F, Mattsson JP and Ernfors P (2007) Cellular subtype distribution and developmental regulation of TRPC channel members in the mouse dorsal root ganglion. *The Journal of comparative neurology* **503**:35-46.

Eliav E, Benoliel R, Herzberg U, Kalladka M and Tal M (2009) The Role of IL-6 and IL-1beta in Painful Perineural Inflammatory Neuritis. *Brain Behav Immun*.

Eliav E, Benoliel R and Tal M (2001) Inflammation with no axonal damage of the rat saphenous nerve trunk induces ectopic discharge and mechanosensitivity in myelinated axons. *NeurosciLett* **311**:49-52.

Eliav E, Herzberg U, Ruda MA and Bennett GJ (1999) Neuropathic pain from an experimental neuritis of the rat sciatic nerve. *Pain* **83**:169-182.

Eliav E and Tal M (1994) Electrophysiological properties of experimental neuropathy (CCI) in rats. *SocNeurosciAbstr* **20**:761.

Elliott TE, Renier CM and Palcher JA (2003) Chronic pain, depression, and quality of life: correlations and predictive value of the SF-36. *Pain Med* **4**:331-339.

Elvey R and Idczak R (1979) Brachial plexus tension tests and the pathoanatomical origin of arm pain, in *Aspects of Manipulative Therapy* pp 105-110, Lincoln Institute of Health Sciences, Melbourne.

Emery EC, Young GT, Berrocoso EM, Chen L and McNaughton PA (2011) HCN2 ion channels play a central role in inflammatory and neuropathic pain. *Science* **333**:1462-1466.

Enyedi P and Czirjak G (2010) Molecular background of leak K+ currents: two-pore domain potassium channels. *Physiol Rev* **90**:559-605.

Errea O, Moreno B, Gonzalez-Franquesa A, Garcia-Roves PM and Villoslada P (2015) The disruption of mitochondrial axonal transport is an early event in neuroinflammation. *J Neuroinflammation* **12**:152.

Esteban JA, Shi SH, Wilson C, Nuriya M, Huganir RL and Malinow R (2003) PKA phosphorylation of AMPA receptor subunits controls synaptic trafficking underlying plasticity. *Nature neuroscience* **6**:136-143.

Fang C, Bourdette D and Banker G (2012) Oxidative stress inhibits axonal transport: implications for neurodegenerative diseases. *Mol Neurodegener* **7**:29.

Fang X, Djouhri L, Black JA, Dib-Hajj SD, Waxman SG and Lawson SN (2002) The presence and role of the tetrodotoxin-resistant sodium channel Na(v)1.9 (NaN) in nociceptive primary afferent neurons. *JNeurosci* **22**:7425-7433.

Fang X, Djouhri L, McMullan S, Berry C, Okuse K, Waxman SG and Lawson SN (2005) trkA is expressed in nociceptive neurons and influences electrophysiological properties via Nav1.8 expression in rapidly conducting nociceptors. *J Neurosci* **25**:4868-4878.

Ferreira SH, Lorenzetti BB, Bristow AF and Poole S (1988) Interleukin-1 beta as a potent hyperalgesic agent antagonized by a tripeptide analogue. *Nature* **334**:698-700.

Ferreira SH, Lorenzetti BB and Poole S (1993) Bradykinin initiates cytokine-mediated inflammatory hyperalgesia. *British Journal of Pharmacology* **110**:1227-1231.

Fink M, Duprat F, Lesage F, Reyes R, Romey G, Heurteaux C and Lazdunski M (1996) Cloning, functional expression and brain localization of a novel unconventional outward rectifier K+ channel. *The EMBO journal* **15**:6854-6862.

Fink M, Lesage F, Duprat F, Heurteaux C, Reyes R, Fosset M and Lazdunski M (1998) A neuronal two P domain K+ channel stimulated by arachidonic acid and polyunsaturated fatty acids. *The EMBO journal* **17**:3297-3308.

Finnerup NB, Otto M, McQuay HJ, Jensen TS and Sindrup SH (2005) Algorithm for neuropathic pain treatment: an evidence based proposal. *Pain* **118**:289-305.

Finnerup NB, Sindrup SH and Jensen TS (2010) The evidence for pharmacological treatment of neuropathic pain. *Pain* **150**:573-581.

Fischer MJ and Reeh PW (2007) Sensitization to heat through G-protein-coupled receptor pathways in the isolated sciatic mouse nerve. *The European journal of neuroscience* **25**:3570-3575.

Fischer MJ, Reeh PW and Sauer SK (2003) Proton-induced calcitonin gene-related peptide release from rat sciatic nerve axons, in vitro, involving TRPV1. *Eur J Neurosci* **18**:803-810.

Fitzgerald M, Woolf CJ, Gibson SJ and Mallaburn PS (1984) Alterations in the structure, function, and chemistry of C fibers following local application of vinblastine to the sciatic nerve of the rat. *JNeurosci* **4**:430-441.

Flatters SJ and Bennett GJ (2006) Studies of peripheral sensory nerves in paclitaxel-induced painful peripheral neuropathy: evidence for mitochondrial dysfunction. *Pain* **122**:245-257.

Fogleman M and Brogmus G (1995) Computer mouse use and cumulative trauma disorders of the upper extremities. *Ergonomics* **38**:2465-2475.

Forman DS, Padjen AL and Siggins GR (1977) Effect of temperature on the rapid retrograde transport of microscopically visible intra-axonal organelles. *Brain research* **136**:215-226.

Forsyth PA, Balmaceda C, Peterson K, Seidman AD, Brasher P and DeAngelis LM (1997) Prospective study of paclitaxel-induced peripheral neuropathy with quantitative sensory testing. *J Neurooncol* **35**:47-53.

Franz M and Mense S (1975) Muscle receptors with group IV afferent fibres responding to application of bradykinin. *Brain Research* **92**:369-383.

Fukuoka T, Kondo E, Dai Y, Hashimoto N and Noguchi K (2001) Brain-derived neurotrophic factor increases in the uninjured dorsal root ganglion neurons in selective spinal nerve ligation model. *The Journal of neuroscience : the official journal of the Society for Neuroscience* **21**:4891-4900.

Galan A, Laird JM and Cervero F (2004) In vivo recruitment by painful stimuli of AMPA receptor subunits to the plasma membrane of spinal cord neurons. *Pain* **112**:315-323.

Gale JE, Marcotti W, Kennedy HJ, Kros CJ and Richardson GP (2001) FM1-43 dye behaves as a permeant blocker of the hair-cell mechanotransducer channel. *The Journal of neuroscience : the official journal of the Society for Neuroscience* **21**:7013-7025.

Gallo G and Letourneau PC (1999) Different contributions of microtubule dynamics and transport to the growth of axons and collateral sprouts. *The Journal of neuroscience : the official journal of the Society for Neuroscience* **19**:3860-3873.

Garcia-Anoveros J, Derfler B, Neville-Golden J, Hyman BT and Corey DP (1997) BNaC1 and BNaC2 constitute a new family of human neuronal sodium channels related to degenerins and epithelial sodium channels. *ProcNatlAcadSciUSA* **94**:1459-1464.

Garcia-Anoveros J, Samad TA, Woolf CJ and Corey DP (2001) Transport and localization of the DEG/ENaC ion channel BNaC1alpha to peripheral mechanosensory terminals of dorsal root ganglia neurons. *Journal of Neuroscience* **21**:2678-2686.

Gardiner NJ, Cafferty WB, Slack SE and Thompson SW (2002) Expression of gp130 and leukaemia inhibitory factor receptor subunits in adult rat sensory neurones: regulation by nerve injury. *Journal of neurochemistry* **83**:100-109.

Garewal HS, Brooks RJ, Jones SE and Miller TP (1983) Treatment of advanced breast cancer with mitomycin C combined with vinblastine or vindesine. *Journal of clinical oncology : official journal of the American Society of Clinical Oncology* **1**:772-775.

Gargan MF and Bannister GC (1994) The rate of recovery following whiplash injury. *European spine journal : official publication of the European Spine Society, the European Spinal Deformity Society, and the European Section of the Cervical Spine Research Society* **3**:162-164.

Garrison SR, Dietrich A and Stucky CL (2012) TRPC1 contributes to light-touch sensation and mechanical responses in low-threshold cutaneous sensory neurons. *Journal of neurophysiology* **107**:913-922.

Gasser HS and Grundfest H (1939) Axon diameters in relation to the spike dimensions and the conduction velocity in mammalian A fibers. *AmJPhysiol* **127**:393-414.

Gavva NR, Klionsky L, Qu Y, Shi L, Tamir R, Edenson S, Zhang TJ, Viswanadhan VN, Toth A, Pearce LV, Vanderah TW, Porreca F, Blumberg PM, Lile J, Sun Y, Wild

K, Louis JC and Treanor JJ (2004) Molecular determinants of vanilloid sensitivity in TRPV1. *The Journal of biological chemistry* **279**:20283-20295.

Gazda LS, Milligan ED, Hansen MK, Twining CM, Poulos NM, Chacur M, O'Connor KA, Armstrong C, Maier SF, Watkins LR and Myers RR (2001) Sciatic inflammatory neuritis (SIN): behavioral allodynia is paralleled by peri-sciatic proinflammatory cytokine and superoxide production. *Journal of the Peripheral Nervous System* **6**:111-129.

Georgopoulos AP (1976) Functional properties of primary afferent units probably related to pain mechanisms in primate glabrous skin. *Journal of neurophysiology* **39**:71-83.

Gerdle B, Lemming D, Kristiansen J, Larsson B, Peolsson M and Rosendal L (2008) Biochemical alterations in the trapezius muscle of patients with chronic whiplash associated disorders (WAD)--a microdialysis study. *Eur J Pain* **12**:82-93.

Ghosh D, Pinto S, Danglot L, Vandewauw I, Segal A, Van Ranst N, Benoit M, Janssens A, Vennekens R, Vanden Berghe P, Galli T, Vriens J and Voets T (2016) VAMP7 regulates constitutive membrane incorporation of the cold-activated channel TRPM8. *Nature communications* **7**:10489.

Gilbert RF, Emson PC, Fahrenkrug J, Lee CM, Penman E and Wass J (1980) Axonal transport of neuropeptides in the cervical vagus nerve of the rat. *Journal of neurochemistry* **34**:108-113.

Gold MS, Reichling DB, Shuster MJ and Levine JD (1996) Hyperalgesic agents increase a tetrodotoxin-resistant Na+ current in nociceptors. *Proc Natl Acad Sci U S A* **93**:1108-1112.

Gold MS, Weinreich D, Kim CS, Wang R, Treanor J, Porreca F and Lai J (2003) Redistribution of Na(V)1.8 in uninjured axons enables neuropathic pain. *JNeurosci* **23**:158-166.

Golech SA, McCarron RM, Chen Y, Bembry J, Lenz F, Mechoulam R, Shohami E and Spatz M (2004) Human brain endothelium: coexpression and function of vanilloid and endocannabinoid receptors. *Brain research Molecular brain research* **132**:87-92.

Govea RM, Barbe MF and Bove GM (2017) Group IV nociceptors develop axonal chemical sensitivity during neuritis and following treatment of the sciatic nerve with vinblastine. *J Neurophysiol* **118**:2103-2109.

Gower DJ and Tytell M (1987) Axonal transport of clathrin-associated proteins. *Brain research* **407**:1-8.

Gracely RH, Lynch SA and Bennett GJ (1992) Painful neuropathy: altered central processing maintained dynamically by peripheral input. *Pain* **51**:175-194.

Grafstein B, Miller JA, Ledeen RW, Haley J and Specht SC (1975) Axonal transport of phospholipid in goldfish optic system. *Experimental neurology* **46**:261-281.

Gratzke C, Streng T, Waldkirch E, Sigl K, Stief C, Andersson KE and Hedlund P (2009) Transient receptor potential A1 (TRPA1) activity in the human urethra--evidence for a functional role for TRPA1 in the outflow region. *Eur Urol* **55**:696-704.

Greening J, Anantharaman K, Young R and Dilley A (2017) Evidence for increased MRI signal intensity and morphological changes in the brachial plexus and median

nerves of patients with chronic arm and neck pain following whiplash injury. *Journal of Orthopaedic & Sports Physical Therapy* **In Press**.

Greening J, Dilley A and Lynn B (2005) In vivo study of nerve movement and mechanosensitivity of the median nerve in whiplash and non-specific arm pain patients. *Pain* **115**:248-253.

Grunder S, Geissler HS, Bassler EL and Ruppersberg JP (2000) A new member of acid-sensing ion channels from pituitary gland. *Neuroreport* **11**:1607-1611.

Guler AD, Lee H, Iida T, Shimizu I, Tominaga M and Caterina M (2002) Heat-evoked activation of the ion channel, TRPV4. *Journal of Neuroscience* **22**:6408-6414.

Guo A, Vulchanova L, Wang J, Li X and Elde R (1999) Immunocytochemical localization of the vanilloid receptor 1 (VR1): relationship to neuropeptides, the P2X(3) purinoceptor and IB4 binding sites. *EurJNeurosci* **11**:946-958.

Guth L, Smith S, Donati EJ and Albuquerque EX (1980) Induction of intramuscular collateral nerve sprouting by neurally applied colchicine. *Experimental neurology* **67**:513-523.

Hamill OP and Maroto R (2007) Chapter 9 - TRPCs as MS Channels, in *Current Topics in Membranes* (Hamill OP ed) pp 191-231, Academic Press.

Hanz S, Perlson E, Willis D, Zheng JQ, Massarwa R, Huerta J, Koltzenburg M, Kohler M, van-Minnen J, Twiss JL and Fainzilber M (2003) Axoplasmic importins enable retrograde injury signaling in lesioned nerve. *Neuron* **40**:1095-1104.

Harper AA and Lawson SN (1985) Conduction velocity is related to morphological cell type in rat dorsal root ganglion neurones. *JPhysiolLond* **359**:31-46.

Harvey RJ, Depner UB, Wassle H, Ahmadi S, Heindl C, Reinold H, Smart TG, Harvey K, Schutz B, Abo-Salem OM, Zimmer A, Poisbeau P, Welzl H, Wolfer DP, Betz H, Zeilhofer HU and Muller U (2004) GlyR alpha3: an essential target for spinal PGE2-mediated inflammatory pain sensitization. *Science* **304**:884-887.

Hayes AG, Hawcock AB and Hill RG (1984) The depolarizing effect of capsaicin on rat isolated sciatic nerve. Life Sci 35:1561-1568.

He BH, Christin M, Mouchbahani-Constance S, Davidova A and Sharif-Naeini R (2017) Mechanosensitive ion channels in articular nociceptors drive mechanical allodynia in osteoarthritis. *Osteoarthritis Cartilage* **25**:2091-2099.

Heimburg T (1998) Mechanical aspects of membrane thermodynamics. Estimation of the mechanical properties of lipid membranes close to the chain melting transition from calorimetry. *Biochimica et Biophysica Acta (BBA) - Biomembranes* **1415**:147-162.

Herrmann S, Rajab H, Christ I, Schirdewahn C, Hofler D, Fischer MJM, Bruno A, Fenske S, Gruner C, Kramer F, Wachsmann T, Wahl-Schott C, Stieber J, Biel M and Ludwig A (2017) Protein kinase A regulates inflammatory pain sensitization by modulating HCN2 channel activity in nociceptive sensory neurons. *Pain* **158**:2012-2024.

Heumann R, Korsching S, Bandtlow C and Thoenen H (1987) Changes of nerve growth factor synthesis in nonneuronal cells in response to sciatic nerve transection. *Journal of Cell Biology* **104**:1623-1631.

Hirokawa N, Sato-Yoshitake R, Kobayashi N, Pfister KK, Bloom GS and Brady ST (1991) Kinesin associates with anterogradely transported membranous organelles in vivo. *The Journal of cell biology* **114**:295-302.

Hirth M, Rukwied R, Gromann A, Turnquist B, Weinkauf B, Francke K, Albrecht P, Rice F, Hagglof B, Ringkamp M, Engelhardt M, Schultz C, Schmelz M and Obreja O (2013) Nerve growth factor induces sensitization of nociceptors without evidence for increased intraepidermal nerve fiber density. Pain 154:2500-2511.

Hoffman PN, Cleveland DW, Griffin JW, Landes PW, Cowan NJ and Price DL (1987) Neurofilament gene expression: a major determinant of axonal caliber. *Proceedings of the National Academy of Sciences of the United States of America* **84**:3472-3476.

Hoffman PN and Lasek RJ (1975) The slow component of axonal transport. Identification of major structural polypeptides of the axon and their generality among mammalian neurons. *The Journal of cell biology* **66**:351-366.

Hoffmann P, Buck-Gramcko D and Lubahn JD (1993) The Hoffmann-Tinel sign. 1915. *J Hand Surg Br* **18**:800-805.

Hoffmann T, Sauer SK, Horch RE and Reeh PW (2008) Sensory transduction in peripheral nerve axons elicits ectopic action potentials. *J Neurosci* **28**:6281-6284.

Hoffmann T, Sauer SK, Horch RE and Reeh PW (2009) Projected pain from noxious heat stimulation of an exposed peripheral nerve--a case report. *European journal of pain* **13**:35-37.

Holland JF, Scharlau C, Gailani S, Krant MJ, Olson KB, Horton J, Shnider BI, Lynch JJ, Owens A, Carbone PP, Colsky J, Grob D, Miller SP and Hall TC (1973) Vincristine treatment of advanced cancer: a cooperative study of 392 cases. *Cancer research* **33**:1258-1264.

Hollenbeck PJ (1993) Products of endocytosis and autophagy are retrieved from axons by regulated retrograde organelle transport. *The Journal of cell biology* **121**:305-315.

Hong GS, Lee B, Wee J, Chun H, Kim H, Jung J, Cha JY, Riew TR, Kim GH, Kim IB and Oh U (2016) Tentonin 3/TMEM150c Confers Distinct Mechanosensitive Currents in Dorsal-Root Ganglion Neurons with Proprioceptive Function. *Neuron* **91**:107-118.

Hu-Tsai M-i, Winter J and Woolf CJ (1992) Regional differences in the distribution of capsaicin-sensitive target-identified adult rat dorsal root ganglion neurons. *Neuroscience letters* **143**:251-254.

Hu HJ, Alter BJ, Carrasquillo Y, Qiu CS and Gereau RWt (2007) Metabotropic glutamate receptor 5 modulates nociceptive plasticity via extracellular signal-regulated kinase-Kv4.2 signaling in spinal cord dorsal horn neurons. *The Journal of neuroscience : the official journal of the Society for Neuroscience* **27**:13181-13191.

Hu P and McLachlan EM (2002) Macrophage and lymphocyte invasion of dorsal root ganglia after peripheral nerve lesions in the rat. *Neuroscience* **112**:23-38.

Huber TB, Schermer B, Müller RU, Höhne M, Bartram M, Calixto A, Hagmann H, Reinhardt C, Koos F, Kunzelmann K, Shirokova E, Krautwurst D, Harteneck C, Simons M, Pavenstädt H, Kerjaschki D, Thiele C, Walz G, Chalfie M and Benzing T (2006) Podocin and MEC-2 bind cholesterol to regulate the activity of

associated ion channels. *Proceedings of the National Academy of Sciences of the United States of America* **103**:17079-17086.

Hudspeth AJ and Corey DP (1977) Sensitivity, polarity, and conductance change in the response of vertebrate hair cells to controlled mechanical stimuli. *Proceedings of the National Academy of Sciences of the United States of America* **74**:2407-2411.

Huygen FJ, De Bruijn AG, De Bruin MT, Groeneweg JG, Klein J and Zijlstra FJ (2002) Evidence for local inflammation in complex regional pain syndrome type 1. *Mediators of inflammation* **11**:47-51.

IASP (1986) Classification of chronic pain. Descriptions of chronic pain syndromes and definitions of pain terms. Prepared by the International Association for the Study of Pain, Subcommittee on Taxonomy. *Pain Suppl* **3**:S1-226.

Ibuki T, Hama AT, Wang XT, Pappas GD and Sagen J (1997) Loss of GABA-immunoreactivity in the spinal dorsal horn of rats with peripheral nerve injury and promotion of recovery by adrenal medullary grafts. *Neuroscience* **76**:845-858.

Ide M, Ide J, Yamaga M and Takagi K (2001) Symptoms and signs of irritation of the brachial plexus in whiplash injuries. *J Bone Joint Surg Br* **83**:226-229.

Ikeuchi M, Kolker SJ and Sluka KA (2009) Acid-sensing ion channel 3 expression in mouse knee joint afferents and effects of carrageenan-induced arthritis. *The journal of pain : official journal of the American Pain Society* **10**:336-342.

Inoue K, Koizumi S, Fuziwara S, Denda S, Inoue K and Denda M (2002) Functional vanilloid receptors in cultured normal human epidermal keratinocytes. *Biochemical and biophysical research communications* **291**:124-129.

Jackson P and Diamond J (1977) Colchicine block of cholinesterase transport in rabbit sensory nerves without interference with the long-term viability of the axons. *Brain Res* **130**:579-584.

Janig W, Grossmann L and Gorodetskaya N (2009) Mechano- and thermosensitivity of regenerating cutaneous afferent nerve fibers. *Experimental brain research* **196**:101-114.

Jasmin L, Kohan L, Franssen M, Janni G and Goff JR (1998) The cold plate as a test of nociceptive behaviors: description and application to the study of chronic neuropathic and inflammatory pain models. *Pain* **75**:367-382.

Jasti J, Furukawa H, Gonzales EB and Gouaux E (2007) Structure of acid-sensing ion channel 1 at 1.9 A resolution and low pH. *Nature* **449**:316-323.

Jelliffe AM (1969) Vinblastine in the treatment of Hodgkin's disease. *Br J Cancer* **23**:44-48.

Ji RR, Samad TA, Jin SX, Schmoll R and Woolf CJ (2002) p38 MAPK activation by NGF in primary sensory neurons after inflammation increases TRPV1 levels and maintains heat hyperalgesia. *Neuron* **36**:57-68.

Jin HW, Flatters SJ, Xiao WH, Mulhern HL and Bennett GJ (2008) Prevention of paclitaxel-evoked painful peripheral neuropathy by acetyl-L-carnitine: effects on axonal mitochondria, sensory nerve fiber terminal arbors, and cutaneous Langerhans cells. *Exp Neurol* **210**:229-237.

Jin X and Gereau RWt (2006) Acute p38-mediated modulation of tetrodotoxin-resistant sodium channels in mouse sensory neurons by tumor necrosis factor-alpha. *J Neurosci* **26**:246-255.

Jones G, Zhu Y, Silva C, Tsutsui S, Pardo CA, Keppler OT, McArthur JC and Power C (2005a) Peripheral nerve-derived HIV-1 is predominantly CCR5-dependent and causes neuronal degeneration and neuroinflammation. *Virology* **334**:178-193.

Jones RC, 3rd, Xu L and Gebhart GF (2005b) The mechanosensitivity of mouse colon afferent fibers and their sensitization by inflammatory mediators require transient receptor potential vanilloid 1 and acid-sensing ion channel 3. *The Journal of neuroscience : the official journal of the Society for Neuroscience* **25**:10981-10989.

Jordan MA and Wilson L (1990) Kinetic analysis of tubulin exchange at microtubule ends at low vinblastine concentrations. *Biochemistry* **29**:2730-2739.

Jordt SE, Bautista DM, Chuang HH, McKemy DD, Zygmunt PM, Hogestatt ED, Meng ID and Julius D (2004) Mustard oils and cannabinoids excite sensory nerve fibres through the TRP channel ANKTM1. *Nature* **427**:260-265.

Jung H, Toth PT, White FA and Miller RJ (2008) Monocyte chemoattractant protein-1 functions as a neuromodulator in dorsal root ganglia neurons. *J Neurochem* **104**:254-263.

Juniper M, Le TK and Mladsi D (2009) The epidemiology, economic burden, and pharmacological treatment of chronic low back pain in France, Germany, Italy, Spain and the UK: a literature-based review. *Expert Opin Pharmacother* **10**:2581-2592.

Kajander KC and Bennett GJ (1992) Onset of a painful peripheral neuropathy in rat: a partial and differential deafferentation and spontaneous discharge in A beta and A delta primary afferent neurons. *JNeurophysiol* **68**:734-744.

Kang D, Choe C and Kim D (2005) Thermosensitivity of the two-pore domain K+ channels TREK-2 and TRAAK. *The Journal of physiology* **564**:103-116.

Kao DJ, Li AH, Chen JC, Luo RS, Chen YL, Lu JC and Wang HL (2012) CC chemokine ligand 2 upregulates the current density and expression of TRPV1 channels and Nav1.8 sodium channels in dorsal root ganglion neurons. *J Neuroinflammation* **9**:189.

Karcher RL, Deacon SW and Gelfand VI (2002) Motor-cargo interactions: the key to transport specificity. *Trends Cell Biol* **12**:21-27.

Kark T, Bagi Z, Lizanecz E, Pasztor ET, Erdei N, Czikora A, Papp Z, Edes I, Porszasz R and Toth A (2008) Tissue-specific regulation of microvascular diameter: opposite functional roles of neuronal and smooth muscle located vanilloid receptor-1. *Molecular pharmacology* **73**:1405-1412.

Kawasaki Y, Kohno T, Zhuang ZY, Brenner GJ, Wang H, Van Der MC, Befort K, Woolf CJ and Ji RR (2004) Ionotropic and metabotropic receptors, protein kinase A, protein kinase C, and Src contribute to C-fiber-induced ERK activation and cAMP response element-binding protein phosphorylation in dorsal horn neurons, leading to central sensitization. *J Neurosci* **24**:8310-8321.

Kelly S, Chapman RJ, Woodhams S, Sagar DR, Turner J, Burston JJ, Bullock C, Paton K, Huang J, Wong A, McWilliams DF, Okine BN, Barrett DA, Hathway GJ, Walsh DA and Chapman V (2015) Increased function of pronociceptive TRPV1 at the level of the joint in a rat model of osteoarthritis pain. *Annals of the Rheumatic Diseases* **74**:252-259.

Kerstein PC, del Camino D, Moran MM and Stucky CL (2009) Pharmacological blockade of TRPA1 inhibits mechanical firing in nociceptors. *Mol Pain* **5**:19.

Kim CH, Oh Y, Chung JM and Chung K (2002) Changes in three subtypes of tetrodotoxin sensitive sodium channel expression in the axotomized dorsal root ganglion in the rat. *Neuroscience Letters* **323**:125-128.

Kim KJ, Yoon YW and Chung JM (1997) Comparison of three rodent neuropathic pain models. *Experimental Brain Research* **113**:200-206.

Kim SE, Coste B, Chadha A, Cook B and Patapoutian A (2012) The role of Drosophila Piezo in mechanical nociception. *Nature* **483**:209-212.

Kim SH and Chung JM (1992) An experimental model for peripheral neuropathy produced by segmental spinal nerve ligation in the rat. *Pain* **50**:355-363.

Kingery WS (1997) A critical review of controlled clinical trials for peripheral neuropathic pain and complex regional pain syndromes. *Pain* **73**:123-139.

Kingery WS, Guo TZ, Poree LR and Maze M (1998) Colchicine treatment of the sciatic nerve reduces neurogenic extravasation, but does not affect nociceptive thresholds or collateral sprouting in neuropathic or normal rats. *Pain* **74**:11-20.

Kirillova I, Rausch VH, Tode J, Baron R and Janig W (2011) Mechano- and thermosensitivity of injured muscle afferents. *Journal of neurophysiology* **105**:2058-2073.

Kivioja J, Ozenci V, Rinaldi L, Kouwenhoven M, Lindgren U and Link H (2001) Systemic immune response in whiplash injury and ankle sprain: elevated IL-6 and IL-10. *Clin Immunol* **101**:106-112.

Kleggetveit IP, Namer B, Schmidt R, Helas T, Ruckel M, Orstavik K, Schmelz M and Jorum E (2012) High spontaneous activity of C-nociceptors in painful polyneuropathy. *Pain* **153**:2040-2047.

Klein T, Stahn S, Magerl W and Treede RD (2008) The role of heterosynaptic facilitation in long-term potentiation (LTP) of human pain sensation. Pain 139:507-519.

Koltzenburg M, Bennett DL, Shelton DL and McMahon SB (1999) Neutralization of endogenous NGF prevents the sensitization of nociceptors supplying inflamed skin. *EurJNeurosci* **11**:1698-1704.

Koltzenburg M, Lundberg LE and Torebjork HE (1992) Dynamic and static components of mechanical hyperalgesia in human hairy skin. *Pain* **51**:207-219.

Koschorke GM, Meyer RA and Campbell JN (1994) Cellular components necessary for mechanoelectrical transduction are conveyed to primary afferent terminals by fast axonal transport. *Brain Res* **641**:99-104.

Kress M, Karasek J, Ferrer-Montiel AV, Scherbakov N and Haberberger RV (2008) TRPC channels and diacylglycerol dependent calcium signaling in rat sensory neurons. *Histochem Cell Biol* **130**:655-667.

Kress M, Reeh PW and Vyklicky L (1997) An interaction of inflammatory mediators and protons in small diameter dorsal root ganglion neurons of the rat. *Neuroscience letters* **224**:37-40.

Krishtal OA and Pidoplichko VI (1980) A receptor for protons in the nerve cell membrane. *Neuroscience* **5**:2325-2327.

Kung C (2005) A possible unifying principle for mechanosensation. *Nature* **436**:647-654.

Kuzhikandathil EV, Wang H, Szabo T, Morozova N, Blumberg PM and Oxford GS (2001) Functional analysis of capsaicin receptor (vanilloid receptor subtype 1) multimerization and agonist responsiveness using a dominant negative mutation. *The Journal of neuroscience : the official journal of the Society for Neuroscience* **21**:8697-8706.

Kwan KY, Allchorne AJ, Vollrath MA, Christensen AP, Zhang DS, Woolf CJ and Corey DP (2006) TRPA1 contributes to cold, mechanical, and chemical nociception but is not essential for hair-cell transduction. *Neuron* **50**:277-289.

Kwan KY, Glazer JM, Corey DP, Rice FL and Stucky CL (2009) TRPA1 modulates mechanotransduction in cutaneous sensory neurons. *J Neurosci* **29**:4808-4819.

Kwon KB, Kim JS and Chang BJ (2000) Translocational changes of localization of synapsin in axonal sprouts of regenerating rat sciatic nerves after ligation crush injury. *Journal of veterinary science* **1**:1-9.

Laird JM and Bennett GJ (1993) An electrophysiological study of dorsal horn neurons in the spinal cord of rats with an experimental peripheral neuropathy. *J Neurophysiol* **69**:2072-2085.

LaPointe NE, Morfini G, Brady ST, Feinstein SC, Wilson L and Jordan MA (2013) Effects of eribulin, vincristine, paclitaxel and ixabepilone on fast axonal transport and kinesin-1 driven microtubule gliding: Implications for chemotherapy-induced peripheral neuropathy. *Neurotoxicology* **37**:231-239.

Latremoliere A and Woolf CJ (2009) Central sensitization: a generator of pain hypersensitivity by central neural plasticity. *J Pain* **10**:895-926.

Lauritzen I, Chemin J, Honore E, Jodar M, Guy N, Lazdunski M and Jane Patel A (2005) Cross-talk between the mechano-gated K2P channel TREK-1 and the actin cytoskeleton. *EMBO reports* **6**:642-648.

Lazarevic L (1880) Ischias postica cotunnii and its differential diagnosis. . *Srp Arh Celok Lek* **7**:23–35.

Lechner SG and Lewin GR (2009) Peripheral sensitisation of nociceptors via G-protein-dependent potentiation of mechanotransduction currents. *The Journal of physiology* **587**:3493-3503.

Lee CH, Sun SH, Lin SH and Chen CC (2011) Role of the acid-sensing ion channel 3 in blood volume control. *Circ J* **75**:874-883.

Leem JG and Bove GM (2002) Mid-axonal tumor necrosis factor-alpha induces ectopic activity in a subset of slowly conducting cutaneous and deep afferent neurons. *J Pain* **3**:45-49.

LeMasurier M and Gillespie PG (2005) Hair-cell mechanotransduction and cochlear amplification. *Neuron* **48**:403-415.

Lemming D, Graven-Nielsen T, Sorensen J, Arendt-Nielsen L and Gerdle B (2012) Widespread pain hypersensitivity and facilitated temporal summation of deep tissue pain in whiplash associated disorder: an explorative study of women. *J Rehabil Med* **44**:648-657.

Levine J and Willard M (1981) Fodrin: axonally transported polypeptides associated with the internal periphery of many cells. *The Journal of cell biology* **90**:631-642.

Li YB, Dorsi MJ, Meyer RA and Belzberg AJ (2000) Mechanical hyperalgesia after an L5 spinal nerve lesion in the rat is not dependent on input from injured nerve fibers. *Pain* **85**:493-502.

Liao M, Cao E, Julius D and Cheng Y (2013) Structure of the TRPV1 ion channel determined by electron cryo-microscopy. *Nature* **504**:107-112.

Liapi A and Wood JN (2005) Extensive co-localization and heteromultimer formation of the vanilloid receptor-like protein TRPV2 and the capsaicin receptor TRPV1 in the adult rat cerebral cortex. *The European journal of neuroscience* **22**:825-834.

Liedtke W, Choe Y, Marti-Renom MA, Bell AM, Denis CS, Sali A, Hudspeth AJ, Friedman JM and Heller S (2000) Vanilloid receptor-related osmotically activated channel (VR-OAC), a candidate vertebrate osmoreceptor. *Cell* **103**:525-535.

Liedtke W, Tobin DM, Bargmann CI and Friedman JM (2003) Mammalian TRPV4 (VR-OAC) directs behavioral responses to osmotic and mechanical stimuli in Caenorhabditis elegans. *Proceedings of the National Academy of Sciences of the United States of America* **100 Suppl 2**:14531-14536.

Lin Q, Peng YB and Willis WD (1996) Inhibition of primate spinothalamic tract neurons by spinal glycine and GABA is reduced during central sensitization. *Journal of neurophysiology* **76**:1005-1014.

Lin S-H, Cheng Y-R, Banks RW, Min M-Y, Bewick GS and Chen C-C (2016) Evidence for the involvement of ASIC3 in sensory mechanotransduction in proprioceptors. Nature Communications 7:11460.

Lin SY and Corey DP (2005) TRP channels in mechanosensation. *Current opinion in neurobiology* **15**:350-357.

Lingueglia E, de Weille JR, Bassilana F, Heurteaux C, Sakai H, Waldmann R and Lazdunski M (1997) A modulatory subunit of acid sensing ion channels in brain and dorsal root ganglion cells. *The Journal of biological chemistry* **272**:29778-29783.

Liu C-N, Wall PD, Ben-Dor E, Michaelis M, Amir R and Devor M (2000a) Tactile allodynia in the absence of C-fiber activation: altered firing properties of DRG neurons following spinal nerve injury. *Pain* **85**:503-521.

Liu T, van Rooijen N and Tracey DJ (2000b) Depletion of macrophages reduces axonal degeneration and hyperalgesia following nerve injury. *Pain* **86**:25-32.

Liu XG, Eschenfelder S, Blenk KH, Janig W and Habler HJ (2000c) Spontaneous activity of axotomized afferent neurons after L5 spinal nerve injury in rats. *Pain* **84**:309-318.

Lizanecz E, Bagi Z, Pasztor ET, Papp Z, Edes I, Kedei N, Blumberg PM and Toth A (2006) Phosphorylation-dependent desensitization by anandamide of vanilloid receptor-1 (TRPV1) function in rat skeletal muscle arterioles and in Chinese hamster ovary cells expressing TRPV1. *Molecular pharmacology* **69**:1015-1023.

Loeb GE (1981) Somatosensory unit input to the spinal cord during normal walking. *Can J Physiol Pharmacol* **59**:627-635.

Lorenz T and Willard M (1978) Subcellular fractionation of intra-axonally transport polypeptides in the rabbit visual system. *Proceedings of the National Academy of Sciences of the United States of America* **75**:505-509.

Lu Y, Ma X, Sabharwal R, Snitsarev V, Morgan D, Rahmouni K, Drummond HA, Whiteis CA, Costa V, Price M, Benson C, Welsh MJ, Chapleau MW and Abboud FM (2009) The ion channel ASIC2 is required for baroreceptor and autonomic control of the circulation. *Neuron* **64**:885-897.

Lussier MP, Cayouette S, Lepage PK, Bernier CL, Francoeur N, St-Hilaire M, Pinard M and Boulay G (2005) MxA, a member of the dynamin superfamily, interacts with the ankyrin-like repeat domain of TRPC. *The Journal of biological chemistry* **280**:19393-19400.

Lynn B (1971) The form and distribution of the receptive fields of Pacinian corpuscles found in and around the cat's large foot pad. *The Journal of physiology* **217**:755-771.

Maihofner C, Handwerker HO, Neundorfer B and Birklein F (2005) Mechanical hyperalgesia in complex regional pain syndrome: a role for TNF-alpha? *Neurology* **65**:311-313.

Malcangio M, Ramer MS, Jones MG and McMahon SB (2000) Abnormal substance P release from the spinal cord following injury to primary sensory neurons. *EurJNeurosci* **12**:397-399.

Maroto R, Raso A, Wood TG, Kurosky A, Martinac B and Hamill OP (2005) TRPC1 forms the stretch-activated cation channel in vertebrate cells. *Nature cell biology* **7**:179-185.

Martin HA, Basbaum AI, Kwiat GC, Goetzl EJ and Levine JD (1987) Leukotriene and prostaglandin sensitization of cutaneous high- threshold C- and A-delta mechanonociceptors in the hairy skin of rat hindlimbs. *Neuroscience* **22**:651-659.

Martinac B and Hamill OP (2002) Gramicidin A channels switch between stretch activation and stretch inactivation depending on bilayer thickness. *Proceedings of the National Academy of Sciences of the United States of America* **99**:4308-4312.

Masurovsky EB, Peterson ER, Crain SM and Horwitz SB (1981) Microtubule arrays in taxol-treated mouse dorsal root ganglion-spinal cord cultures. *Brain research* **217**:392-398.

Matzner O and Devor M (1994) Hyperexcitability at sites of nerve injury depends on voltage-sensitive Na+ channels. *Journal of Neurophysiology* **72**:349-359.

McCloskey DI (1978) Kinesthetic sensibility. *Physiol Rev* **58**:763-820.

McMahon SB and Wall PD (1984) Receptive fields of rat lamina 1 projection cells move to incorporate a nearby region of injury. *Pain* **19**:235-247.

Medhurst AD, Rennie G, Chapman CG, Meadows H, Duckworth MD, Kelsell RE, Gloger, II and Pangalos MN (2001) Distribution analysis of human two pore domain potassium channels in tissues of the central nervous system and periphery. *Brain research Molecular brain research* **86**:101-114.

Mendelson M and Lowenstein WR (1964) Mechanisms of Receptor Adaptation. *Science* **144**:554-555.

Meng J, Wang J, Steinhoff M and Dolly JO (2016) TNFalpha induces co-trafficking of TRPV1/TRPA1 in VAMP1-containing vesicles to the plasmalemma via Munc18-1/syntaxin1/SNAP-25 mediated fusion. *Sci Rep* **6**:21226.

Meng Q, Fang P, Hu Z, Ling Y and Liu H (2015) Mechanotransduction of trigeminal ganglion neurons innervating inner walls of rat anterior eye chambers. *Am J Physiol Cell Physiol* **309**:C1-10.

Meyers JR, MacDonald RB, Duggan A, Lenzi D, Standaert DG, Corwin JT and Corey DP (2003) Lighting up the senses: FM1-43 loading of sensory cells through nonselective ion channels. *Journal of Neuroscience* **23**:4054-4065.

Michaelis M, Blenk KH, Janig W and Vogel C (1995) Development of spontaneous activity and mechanosensitivity in axotomized afferent nerve fibers during the first hours after nerve transection in rats. *JNeurophysiol* **74**:1020-1027.

Michaelis M, Liu XG and Janig W (2000) Axotomized and intact muscle afferents but no skin afferents develop ongoing discharges of dorsal root ganglion origin after peripheral nerve lesion. *Journal of Neuroscience* **20**:2742-2748.

Miki K, Fukuoka T, Tokunaga A and Noguchi K (1998) Calcitonin gene-related peptide increase in the rat spinal dorsal horn and dorsal column nucleus following peripheral nerve injury: up-regulation in a subpopulation of primary afferent sensory neurons. *Neuroscience* **82**:1243-1252.

Millard CL and Woolf CJ (1988) Sensory innervation of the hairs of the rat hindlimb: a light microscopic analysis. *The Journal of comparative neurology* **277**:183-194.

Molliver DC, Cook SP, Carlsten JA, Wright DE and McCleskey EW (2002) ATP and UTP excite sensory neurons and induce CREB phosphorylation through the metabotropic receptor, P2Y2. *The European journal of neuroscience* **16**:1850-1860.

Molliver DC, Immke DC, Fierro L, Pare M, Rice FL and McCleskey EW (2005) ASIC3, an acid-sensing ion channel, is expressed in metaboreceptive sensory neurons. *Molecular pain* **1**:35.

Moloney N, Hall T and Doody C (2010) An investigation of somatosensory profiles in work related upper limb disorders: a case-control observational study protocol. *BMC Musculoskelet Disord* **11**:22.

Montell C (2005) The TRP superfamily of cation channels. *Sci STKE* **2005**:re3.

Moore KA, Kohno T, Karchewski LA, Scholz J, Baba H and Woolf CJ (2002) Partial peripheral nerve injury promotes a selective loss of GABAergic inhibition in the superficial dorsal horn of the spinal cord. *Journal of Neuroscience* **22**:6724-6731.

Morales-Espinoza EM, Kostov B, Salami DC, Perez ZH, Rosalen AP, Molina JO, Gonzalez-de Paz L, Momblona JM, Areu JB, Brito-Zeron P, Ramos-Casals M, Siso-Almirall A and Group CS (2016) Complexity, comorbidity, and health care costs associated with chronic widespread pain in primary care. *Pain* **157**:818-826.

Moshourab RA, Wetzel C, Martinez-Salgado C and Lewin GR (2013) Stomatin-domain protein interactions with acid-sensing ion channels modulate nociceptor mechanosensitivity. *The Journal of physiology* **591**:5555-5574.

Mueller-Tribbensee SM, Karna M, Khalil M, Neurath MF, Reeh PW and Engel MA (2015) Differential Contribution of TRPA1, TRPV4 and TRPM8 to Colonic Nociception in Mice. *PloS one* **10**:e0128242.

Nagae M, Hiraga T, Wakabayashi H, Wang L, Iwata K and Yoneda T (2006) Osteoclasts play a part in pain due to the inflammation adjacent to bone. *Bone* **39**:1107-1115.

Nagano I, Shapshak P, Yoshioka M, Xin K, Nakamura S and Bradley WG (1996) Increased NADPH-diaphorase reactivity and cytokine expression in dorsal root ganglia in acquired immunodeficiency syndrome. *Journal of the neurological sciences* **136**:117-128.

Nagata K, Duggan A, Kumar G and Garcia-Anoveros J (2005) Nociceptor and hair cell transducer properties of TRPA1, a channel for pain and hearing. *J Neurosci* **25**:4052-4061.

Nagy JI and Hunt SP (1982) Fluoride-resistant acid phosphatase-containing neurones in dorsal root ganglia are separate from those containing substance P or somatostatin. *Neuroscience* **7**:89-97.

Nassenstein C, Kwong K, Taylor-Clark T, Kollarik M, Macglashan DM, Braun A and Undem BJ (2008) Expression and function of the ion channel TRPA1 in vagal afferent nerves innervating mouse lungs. *The Journal of physiology* **586**:1595-1604.

Neogi T and Zhang Y (2013) Epidemiology of osteoarthritis. *Rheum Dis Clin North Am* **39**:1-19.

Nicol GD, Lopshire JC and Pafford CM (1997) Tumor necrosis factor enhances the capsaicin sensitivity of rat sensory neurons. *Journal of Neuroscience* **17**:975-982.

Nikic I, Merkler D, Sorbara C, Brinkoetter M, Kreutzfeldt M, Bareyre FM, Bruck W, Bishop D, Misgeld T and Kerschensteiner M (2011) A reversible form of axon damage in experimental autoimmune encephalomyelitis and multiple sclerosis. *Nat Med* **17**:495-499.

Noel J, Zimmermann K, Busserolles J, Deval E, Alloui A, Diochot S, Guy N, Borsotto M, Reeh P, Eschalier A and Lazdunski M (2009) The mechano-activated K+ channels TRAAK and TREK-1 control both warm and cold perception. *The EMBO journal* **28**:1308-1318.

Noguchi K, Kawai Y, Fukuoka T, Senba E and Miki K (1995) Substance P induced by peripheral nerve injury in primary afferent sensory neurons and its effect on dorsal column nucleus neurons. *Journal of Neuroscience* **15**:7633-7643.

Norris DA, Weston WL and Sams WM, Jr. (1977) The effect of immunosuppressive and anti-inflammatory drugs on monocyte function in vitro. *J Lab Clin Med* **90**:569-580.

Nozawa K, Kawabata-Shoda E, Doihara H, Kojima R, Okada H, Mochizuki S, Sano Y, Inamura K, Matsushime H, Koizumi T, Yokoyama T and Ito H (2009) TRPA1 regulates gastrointestinal motility through serotonin release from enterochromaffin cells. *Proceedings of the National Academy of Sciences of the United States of America* **106**:3408-3413.

Nystrom B and Hagbarth KE (1981) Microelectrode recordings from transected nerves in amputees with phantom limb pain. *Neuroscience letters* **27**:211-216.

Obata K, Katsura H, Mizushima T, Yamanaka H, Kobayashi K, Dai Y, Fukuoka T, Tokunaga A, Tominaga M and Noguchi K (2005) TRPA1 induced in sensory

neurons contributes to cold hyperalgesia after inflammation and nerve injury. *J Clin Invest* **115**:2393-2401.

Obata K, Katsura H, Sakurai J, Kobayashi K, Yamanaka H, Dai Y, Fukuoka T and Noguchi K (2006) Suppression of the p75 neurotrophin receptor in uninjured sensory neurons reduces neuropathic pain after nerve injury. *The Journal of neuroscience : the official journal of the Society for Neuroscience* **26**:11974-11986.

Obata K, Tsujino H, Yamanaka H, Yi D, Fukuoka T, Hashimoto N, Yonenobu K, Yoshikawa H and Noguchi K (2002) Expression of neurotrophic factors in the dorsal root ganglion in a rat model of lumbar disc herniation. *Pain* **99**:121-132.

Obata K, Yamanaka H, Dai Y, Mizushima T, Fukuoka T, Tokunaga A and Noguchi K (2004) Activation of extracellular signal-regulated protein kinase in the dorsal root ganglion following inflammation near the nerve cell body. *Neuroscience* **126**:1011-1021.

Obreja O, Biasio W, Andratsch M, Lips KS, Rathee PK, Ludwig A, Rose-John S and Kress M (2005) Fast modulation of heat-activated ionic current by proinflammatory interleukin 6 in rat sensory neurons. *Brain* **128**:1634-1641.

Obreja O, Rathee PK, Lips KS, Distler C and Kress M (2002a) IL-1 beta potentiates heat-activated currents in rat sensory neurons: involvement of IL-1RI, tyrosine kinase, and protein kinase C. *Faseb J* **16**:1497-1503.

Obreja O, Schmelz M, Poole S and Kress M (2002b) Interleukin-6 in combination with its soluble IL-6 receptor sensitises rat skin nociceptors to heat, in vivo. *Pain* **96**:57-62.

Ochs S (1972) Rate of fast axoplasmic transport in mammalian nerve fibres. *The Journal of physiology* **227**:627-645.

Oh SB, Tran PB, Gillard SE, Hurley RW, Hammond DL and Miller RJ (2001) Chemokines and glycoprotein120 produce pain hypersensitivity by directly exciting primary nociceptive neurons. *J Neurosci* **21**:5027-5035.

Ottoson D and Shepherd GM (1970) Steps in impulse generation in the isolated muscle spindle. *Acta Physiol Scand* **79**:423-430.

Owsianik G, Talavera K, Voets T and Nilius B (2006) Permeation and selectivity of TRP channels. *Annu Rev Physiol* **68**:685-717.

Ozaktay AC, Cavanaugh JM, Asik I, DeLeo JA and Weinstein JN (2002) Dorsal root sensitivity to interleukin-1 beta, interleukin-6 and tumor necrosis factor in rats. *European Spine Journal* **11**:467-475.

Page AJ, Brierley SM, Martin CM, Martinez-Salgado C, Wemmie JA, Brennan TJ, Symonds E, Omari T, Lewin GR, Welsh MJ and Blackshaw LA (2004) The ion channel ASIC1 contributes to visceral but not cutaneous mechanoreceptor function. *Gastroenterology* **127**:1739-1747.

Page AJ, Brierley SM, Martin CM, Price MP, Symonds E, Butler R, Wemmie JA and Blackshaw LA (2005) Different contributions of ASIC channels 1a, 2, and 3 in gastrointestinal mechanosensory function. *Gut* **54**:1408-1415.

Pan HL, Eisenach JC and Chen SR (1999) Gabapentin suppresses ectopic nerve discharges and reverses allodynia in neuropathic rats. *J PharmacolExpTher* **288**:1026-1030.

Panda D, Jordan MA, Chu KC and Wilson L (1996) Differential effects of vinblastine on polymerization and dynamics at opposite microtubule ends. *The Journal of biological chemistry* **271**:29807-29812.

Pare M, Smith AM and Rice FL (2002) Distribution and terminal arborizations of cutaneous mechanoreceptors in the glabrous finger pads of the monkey. *The Journal of comparative neurology* **445**:347-359.

Paulsen CE, Armache JP, Gao Y, Cheng Y and Julius D (2015) Structure of the TRPA1 ion channel suggests regulatory mechanisms. *Nature* **520**:511-517.

Pereira V, Busserolles J, Christin M, Devilliers M, Poupon L, Legha W, Alloui A, Aissouni Y, Bourinet E, Lesage F, Eschalier A, Lazdunski M and Noel J (2014) Role of the TREK2 potassium channel in cold and warm thermosensation and in pain perception. *Pain*.

Perl ER, Kumazawa T, Lynn B and Kenins P (1976) Sensitization of high threshold receptors with unmyelinated (C) afferent fibers. *ProgBrain Res* **43**:263-277.

Perozo E, Kloda A, Cortes DM and Martinac B (2002) Physical principles underlying the transduction of bilayer deformation forces during mechanosensitive channel gating. *Nature structural biology* **9**:696-703.

Perrin FE, Lacroix S, Aviles-Trigueros M and David S (2005) Involvement of monocyte chemoattractant protein-1, macrophage inflammatory protein-1alpha and interleukin-1beta in Wallerian degeneration. *Brain* **128**:854-866.

Perry RB, Doron-Mandel E, Iavnilovitch E, Rishal I, Dagan SY, Tsoory M, Coppola G, McDonald MK, Gomes C, Geschwind DH, Twiss JL, Yaron A and Fainzilber M (2012) Subcellular knockout of importin beta1 perturbs axonal retrograde signaling. *Neuron* **75**:294-305.

Pinto V, Derkach VA and Safronov BV (2008) Role of TTX-sensitive and TTX-resistant sodium channels in Adelta- and C-fiber conduction and synaptic transmission. *Journal of neurophysiology* **99**:617-628.

Pitcher GM and Henry JL (2004) Nociceptive response to innocuous mechanical stimulation is mediated via myelinated afferents and NK-1 receptor activation in a rat model of neuropathic pain. *Exp Neurol* **186**:173-197.

Pitchford S and Levine JD (1991) Prostaglandins sensitize nociceptors in cell culture. *Neuroscience letters* **132**:105-108.

Pollock J, McFarlane SM, Connell MC, Zehavi U, Vandenabeele P, MacEwan DJ and Scott RH (2002) TNF-alpha receptors simultaneously activate Ca2+ mobilisation and stress kinases in cultured sensory neurones. *Neuropharmacology* **42**:93-106.

Polomano RC, Mannes AJ, Clark US and Bennett GJ (2001) A painful peripheral neuropathy in the rat produced by the chemotherapeutic drug, paclitaxel. *Pain* **94**:293-304.

Porreca F, Lai J, Bian D, Wegert S, Ossipov MH, Eglen RM, Kassotakis L, Novakovic S, Rabert DK, Sangameswaran L and Hunter JC (1999) A comparison of the potential role,of the tetrodotoxin-insensitive sodium channels, PN3/SNS and NaN/SNS2, in rat models of chronic pain. *ProcNatAcadSciUsa* **96**:7640-7644.

Porter NM, Twyman RE, Uhler MD and Macdonald RL (1990) Cyclic AMP-dependent protein kinase decreases GABAA receptor current in mouse spinal neurons. *Neuron* **5**:789-796.

Prato V, Taberner FJ, Hockley JRF, Callejo G, Arcourt A, Tazir B, Hammer L, Schad P, Heppenstall PA, St. John Smith E and Lechner SG (2017) "Genetic identification of mechanoinsensitive 'silent' nociceptors". Cell reports 21:3102-3115.

Premkumar LS and Ahern GP (2000) Induction of vanilloid receptor channel activity by protein kinase C. *BritJAnaesth* **408**:985-990.

Press R, Deretzi G, Zou LP, Zhu J, Fredman P, Lycke J and Link H (2001) IL-10 and IFN-gamma in Guillain-Barre syndrome. Network Members of the Swedish Epidemiological Study Group. *Journal of neuroimmunology* **112**:129-138.

Price MP, Lewin GR, McIlwrath SL, Cheng C, Xie J, Heppenstall PA, Stucky CL, Mannsfeldt AG, Brennan TJ, Drummond HA, Qiao J, Benson CJ, Tarr DE, Hrstka RF, Yang B, Williamson RA and Welsh MJ (2000) The mammalian sodium channel BNC1 is required for normal touch sensation. *Nature* **407**:1007-1011.

Price MP, McIlwrath SL, Xie J, Cheng C, Qiao J, Tarr DE, Sluka KA, Brennan TJ, Lewin GR and Welsh MJ (2001) The DRASIC Cation Channel Contributes to the Detection of Cutaneous Touch and Acid Stimuli in Mice. *Neuron* **32**:1071-1083.

Price TJ and Flores CM (2007) Critical Evaluation of the Colocalization Between Calcitonin Gene-Related Peptide, Substance P, Transient Receptor Potential Vanilloid Subfamily Type 1 Immunoreactivities, and Isolectin B4 Binding in Primary Afferent Neurons of the Rat and Mouse. *The Journal of Pain* **8**:263-272.

Pritchard J and Hughes RA (2004) Guillain-Barre syndrome. *Lancet* **363**:2186-2188.

Proske U and Luff AR (1998) Mechanical sensitivity of muscle afferents in a nerve treated with colchicine. *Experimental Brain Research* **119**:391-398.

Pulman KG, Smith M, Mengozzi M, Ghezzi P and Dilley A (2013) The erythropoietin-derived peptide ARA290 reverses mechanical allodynia in the neuritis model. *Neuroscience* **233**:174-183.

Qin X, Wan Y and Wang X (2005) CCL2 and CXCL1 trigger calcitonin gene-related peptide release by exciting primary nociceptive neurons. *J Neurosci Res* **82**:51-62.

Qu L, Li Y, Pan X, Zhang P, LaMotte RH and Ma C (2012) Transient receptor potential canonical 3 (TRPC3) is required for IgG immune complex-induced excitation of the rat dorsal root ganglion neurons. *The Journal of neuroscience : the official journal of the Society for Neuroscience* **32**:9554-9562.

Quartilho A, Mata HP, Ibrahim MM, Vanderah TW, Porreca F, Makriyannis A and Malan TP, Jr. (2003) Inhibition of inflammatory hyperalgesia by activation of peripheral CB2 cannabinoid receptors. *Anesthesiology* **99**:955-960.

Quick K, Zhao J, Eijkelkamp N, Linley JE, Rugiero F, Cox JJ, Raouf R, Gringhuis M, Sexton JE, Abramowitz J, Taylor R, Forge A, Ashmore J, Kirkwood N, Kros CJ, Richardson GP, Freichel M, Flockerzi V, Birnbaumer L and Wood JN (2012) TRPC3 and TRPC6 are essential for normal mechanotransduction in subsets of sensory neurons and cochlear hair cells. *Open Biol* **2**:120068.

Quintner JL (1989) A study of upper limb pain and paraesthesiae following neck injury in motor vehicle accidents: assessment of the brachial plexus tension test of Elvey. *BrJ Rheumatol* **28**:528-533.

Rasband MN, Park EW, Vanderah TW, Lai J, Porreca F and Trimmer JS (2001) Distinct potassium channels on pain-sensing neurons. *Proceedings of the National Academy of Sciences of the United States of America* **98**:13373-13378.

Reading SA, Earley S, Waldron BJ, Welsh DG and Brayden JE (2005) TRPC3 mediates pyrimidine receptor-induced depolarization of cerebral arteries. *Am J Physiol Heart Circ Physiol* **288**:H2055-2061.

Reeh PW (1986) Sensory receptors in mammalian skin in an in vitro preparation. *Neuroscience Letters* **66**:141-146.

Reis GF, Yang G, Szpankowski L, Weaver C, Shah SB, Robinson JT, Hays TS, Danuser G and Goldstein LS (2012) Molecular motor function in axonal transport in vivo probed by genetic and computational analysis in Drosophila. *Molecular biology of the cell* **23**:1700-1714.

Riccio A, Medhurst AD, Mattei C, Kelsell RE, Calver AR, Randall AD, Benham CD and Pangalos MN (2002) mRNA distribution analysis of human TRPC family in CNS and peripheral tissues. *Brain research Molecular brain research* **109**:95-104.

Richards N, Batty T and Dilley A (2011) CCL2 has similar excitatory effects to TNF-alpha in a subgroup of inflamed C-fiber axons. *J Neurophysiol* **106**:2838-2848.

Richards N and Dilley A (2015) Contribution of hyperpolarization-activated channels to heat hypersensitivity and ongoing activity in the neuritis model. *Neuroscience* **284**:87-98.

Riley DA and Fahlman CS (1985) Colchicine-induced differential sprouting of the endplates on fast and slow muscle fibers in rat extensor digitorum longus, soleus and tibialis anterior muscles. *Brain research* **329**:83-95.

Rivera L, Gallar J, Pozo MA and Belmonte C (2000) Responses of nerve fibres of the rat saphenous nerve neuroma to mechanical and chemical stimulation: an in vitro study. *J Physiol* **527 Pt 2**:305-313.

Rong W, Hillsley K, Davis JB, Hicks G, Winchester WJ and Grundy D (2004) Jejunal afferent nerve sensitivity in wild-type and TRPV1 knockout mice. *The Journal of physiology* **560**:867-881.

Roytta M, Wei H and Pertovaara A (1999) Spinal nerve ligation-induced neuropathy in the rat: sensory disorders and correlation between histology of the peripheral nerves. *Pain* **80**:161-170.

Roza C, Laird JM, Souslova V, Wood JN and Cervero F (2003) The tetrodotoxin-resistant Na+ channel Nav1.8 is essential for the expression of spontaneous activity in damaged sensory axons of mice. *JPhysiol* **550**:921-926.

Rush AM, Cummins TR and Waxman SG (2007) Multiple sodium channels and their roles in electrogenesis within dorsal root ganglion neurons. *J Physiol* **579**:1-14.

Rutter AR, Ma QP, Leveridge M and Bonnert TP (2005) Heteromerization and colocalization of TrpV1 and TrpV2 in mammalian cell lines and rat dorsal root ganglia. *Neuroreport* **16**:1735-1739.

Satkeviciute I, Goodwin G, Bove GM and Dilley A (2018) The time course of ongoing activity during neuritis and following axonal transport disruption. *J Neurophysiol*. **119**:1993-2000.

Sauer SK, Reeh PW and Bove GM (2001) Noxious heat-induced CGRP release from rat sciatic nerve axons in vitro. *EurJNeurosci* **14**:1203-1208.

Scadding JW (1981) Development of ongoing activity, mechanosensitivity, and adrenaline sensitivity in severed peripheral nerve axons. *ExpNeurol* **73**:345-364.

Schaefer C, Mann R, Masters ET, Cappelleri JC, Daniel SR, Zlateva G, McElroy HJ, Chandran AB, Adams EH, Assaf AR, McNett M, Mease P, Silverman S and Staud R (2016) The Comparative Burden of Chronic Widespread Pain and Fibromyalgia in the United States. *Pain Pract* **16**:565-579.

Schafers M, Lee DH, Brors D, Yaksh TL and Sorkin LS (2003) Increased sensitivity of injured and adjacent uninjured rat primary sensory neurons to exogenous tumor necrosis factor-alpha after spinal nerve ligation. *Journal of Neuroscience* **23**:3028-3038.

Schinkel C, Gaertner A, Zaspel J, Zedler S, Faist E and Schuermann M (2006) Inflammatory mediators are altered in the acute phase of posttraumatic complex regional pain syndrome. *Clin J Pain* **22**:235-239.

Schmalbruch H (1986) Fiber composition of the rat sciatic nerve. *AnatRec* **215**:71-81.

Schmidt R, Schmelz M, Forster C, Ringkamp M, Torebjork E and Handwerker H (1995) Novel classes of responsive and unresponsive C nociceptors in human skin. *Journal of Neuroscience* **15**:333-341.

Schnapp BJ and Reese TS (1989) Dynein is the motor for retrograde axonal transport of organelles. *Proceedings of the National Academy of Sciences of the United States of America* **86**:1548-1552.

Scholz J and Woolf CJ (2002) Can we conquer pain? *Nature neuroscience* **5 Suppl**:1062-1067.

Schonback J and Cuenod M (1971) Axoplasmic migration of protein. A light microscopic autoradiographic study in the avian retino-tectal pathway. *Experimental brain research* **12**:275-282.

Seltzer Z, Dubner R and Shir Y (1990) A novel behavioral model of neuropathic pain disorders produced in rats by partial sciatic nerve injury. *Pain* **43**:205-218.

Sexton JE, Desmonds T, Quick K, Taylor R, Abramowitz J, Forge A, Kros CJ, Birnbaumer L and Wood JN (2016) The contribution of TRPC1, TRPC3, TRPC5 and TRPC6 to touch and hearing. *Neurosci Lett* **610**:36-42.

Sharif Naeini R, Witty MF, Seguela P and Bourque CW (2006) An N-terminal variant of Trpv1 channel is required for osmosensory transduction. *Nature neuroscience* **9**:93-98.

Shemesh OA and Spira ME (2010) Paclitaxel induces axonal microtubules polar reconfiguration and impaired organelle transport: implications for the pathogenesis of paclitaxel-induced polyneuropathy. *Acta Neuropathol* **119**:235-248.

Shigematsu H, Sokabe T, Danev R, Tominaga M and Nagayama K (2010) A 3.5-nm structure of rat TRPV4 cation channel revealed by Zernike phase-contrast cryoelectron microscopy. *The Journal of biological chemistry* **285**:11210-11218.

Shu X and Mendell LM (2001) Acute sensitization by NGF of the response of small-diameter sensory neurons to capsaicin. *J Neurophysiol* **86**:2931-2938.

Shubayev VI and Myers RR (2000) Upregulation and interaction of TNF alpha and gelatinases A and B in painful peripheral nerve injury. *Brain Research* **855**:83-89.

Silverman JD and Kruger L (1990) Selective neuronal glycoconjugate expression in sensory and autonomic ganglia: relation of lectin reactivity to peptide and enzyme markers. *JNeurocytol* **19**:789-801.

Silverstein B, Welp E, Nelson N and Kalat J (1998) Claims incidence of work-related disorders of the upper extremities: Washington state, 1987 through 1995. *Am J Public Health* **88**:1827-1833.

Simone DA and Kajander KC (1997) Responses of cutaneous A-fiber nociceptors to noxious cold. *Journal of neurophysiology* **77**:2049-2060.

Slack SE, Pezet S, McMahon SB, Thompson SW and Malcangio M (2004) Brain-derived neurotrophic factor induces NMDA receptor subunit one phosphorylation via ERK and PKC in the rat spinal cord. *The European journal of neuroscience* **20**:1769-1778.

Sorbara CD, Wagner NE, Ladwig A, Nikic I, Merkler D, Kleele T, Marinkovic P, Naumann R, Godinho L, Bareyre FM, Bishop D, Misgeld T and Kerschensteiner M (2014) Pervasive axonal transport deficits in multiple sclerosis models. *Neuron* **84**:1183-1190.

Sorkin LS, Xiao WH, Wagner R and Myers RR (1997) Tumour necrosis factor-alpha induces ectopic activity in nociceptive primary afferent fibres. *Neuroscience* **81**:255-262.

Spassova MA, Hewavitharana T, Xu W, Soboloff J and Gill DL (2006) A common mechanism underlies stretch activation and receptor activation of TRPC6 channels. *Proceedings of the National Academy of Sciences of the United States of America* **103**:16586-16591.

Speed JS and Hyndman KA (2016) In vivo organ specific drug delivery with implantable peristaltic pumps. *Scientific reports* **6**:26251.

St John Smith E, Purfurst B, Grigoryan T, Park TJ, Bennett NC and Lewin GR (2012) Specific paucity of unmyelinated C-fibers in cutaneous peripheral nerves of the African naked-mole rat: comparative analysis using six species of Bathyergidae. *The Journal of comparative neurology* **520**:2785-2803.

Stamboulian S, Choi JS, Ahn HS, Chang YW, Tyrrell L, Black JA, Waxman SG and Dib-Hajj SD (2010) ERK1/2 mitogen-activated protein kinase phosphorylates sodium channel Na(v)1.7 and alters its gating properties. *The Journal of neuroscience : the official journal of the Society for Neuroscience* **30**:1637-1647.

Staniland AA and McMahon SB (2009) Mice lacking acid-sensing ion channels (ASIC) 1 or 2, but not ASIC3, show increased pain behaviour in the formalin test. *European journal of pain* **13**:554-563.

Stein AT, Ufret-Vincenty CA, Hua L, Santana LF and Gordon SE (2006) Phosphoinositide 3-kinase binds to TRPV1 and mediates NGF-stimulated TRPV1 trafficking to the plasma membrane. *J Gen Physiol* **128**:509-522.

Sterling M, Treleaven J, Edwards S and Jull G (2002) Pressure Pain Thresholds in Chronic Whiplash Associated Disorder: Further Evidence of Altered Central Pain Processing. *Journal of Musculoskeletal Pain* **10**:69-81.

Stockel K, Schwab M and Thoenen H (1975) Comparison between the retrograde axonal transport of nerve growth factor and tetanus toxin in motor, sensory and adrenergic neurons. *Brain research* **99**:1-16.

Stoll G, Griffin JW, Li CY and Trapp BD (1989) Wallerian degeneration in the peripheral nervous system: participation of both Schwann cells and macrophages in myelin degradation. *Journal of Neurocytology* **18**:671-683.

Story GM, Peier AM, Reeve AJ, Eid SR, Mosbacher J, Hricik TR, Earley TJ, Hergarden AC, Andersson DA, Hwang SW, McIntyre P, Jegla T, Bevan S and Patapoutian A (2003) ANKTM1, a TRP-like channel expressed in nociceptive neurons, is activated by cold temperatures. *Cell* **112**:819-829.

Stoter G, Vendrik CP, Struyvenberg A, Sleyfer DT, Vriesendorp R, Schraffordt Koops H, van Oosterom AT, ten Bokkel Huinink WW and Pinedo HM (1984) Five-year survival of patients with disseminated nonseminomatous testicular cancer treated with cisplatin, vinblastine, and bleomycin. *Cancer* **54**:1521-1524.

Streng T, Axelsson HE, Hedlund P, Andersson DA, Jordt SE, Bevan S, Andersson KE, Hogestatt ED and Zygmunt PM (2008) Distribution and function of the hydrogen sulfide-sensitive TRPA1 ion channel in rat urinary bladder. *Eur Urol* **53**:391-399.

Stroissnigg H, Trancikova A, Descovich L, Fuhrmann J, Kutschera W, Kostan J, Meixner A, Nothias F and Propst F (2007) S-nitrosylation of microtubule-associated protein 1B mediates nitric-oxide-induced axon retraction. *Nature cell biology* **9**:1035-1045.

Strotmann R, Harteneck C, Nunnenmacher K, Schultz G and Plant TD (2000) OTRPC4, a nonselective cation channel that confers sensitivity to extracellular osmolarity. *Nature cell biology* **2**:695-702.

Suh YS, Chung K and Coggeshall RE (1984) A study of axonal diameters and areas in lumbosacral roots and nerves in the rat. *The Journal of comparative neurology* **222**:473-481.

Sun JH, Yang B, Donnelly DF, Ma C and LaMotte RH (2006) MCP-1 enhances excitability of nociceptive neurons in chronically compressed dorsal root ganglia. *Journal of Neurophysiology* **96**:2189-2199.

Suzuki M, Mizuno A, Kodaira K and Imai M (2003) Impaired pressure sensation in mice lacking TRPV4. *The Journal of biological chemistry* **278**:22664-22668.

Talley EM, Solorzano G, Lei Q, Kim D and Bayliss DA (2001) Cns distribution of members of the two-pore-domain (KCNK) potassium channel family. *The Journal of neuroscience : the official journal of the Society for Neuroscience* **21**:7491-7505.

Tang J, Lin Y, Zhang Z, Tikunova S, Birnbaumer L and Zhu MX (2001) Identification of common binding sites for calmodulin and inositol 1,4,5-trisphosphate receptors on the carboxyl termini of trp channels. *The Journal of biological chemistry* **276**:21303-21310.

Tapper DN (1965) Stimulus-response relationships in the cutaneous slowly-adapting mechanoreceptor in hairy skin of the cat. *Experimental neurology* **13**:364-385.

Teliban A, Bartsch F, Struck M, Baron R and Janig W (2011) Axonal thermosensitivity and mechanosensitivity of cutaneous afferent neurons. *Eur J Neurosci* **33**:110-118.

Tobin DM, Madsen DM, Kahn-Kirby A, Peckol EL, Moulder G, Barstead R, Maricq AV and Bargmann CI (2002) Combinatorial expression of TRPV channel proteins

defines their sensory functions and subcellular localization in C. elegans neurons. *Neuron* **35**:307-318.

Tohda C, Sasaki M, Konemura T, Sasamura T, Itoh M and Kuraishi Y (2001) Axonal transport of VR1 capsaicin receptor mRNA in primary afferents and its participation in inflammation-induced increase in capsaicin sensitivity. *JNeurochem* **76**:1628-1635.

Tominaga M, Caterina MJ, Malmberg AB, Rosen TA, Gilbert H, Skinner K, Raumann BE, Basbaum AI and Julius D (1998) The cloned capsaicin receptor integrates multiple pain-producing stimuli. *Neuron* **21**:531-543.

Tominaga M, Wada M and Masu M (2001) Potentiation of capsaicin receptor activity by metabotropic ATP receptors as a possible mechanism for ATP-evoked pain and hyperalgesia. *Proceedings of the National Academy of Sciences of the United States of America* **98**:6951-6956.

Torebjork HE and Ochoa JL (1980) Specific sensations evoked by activity in single identified sensory units in man. *Acta Physiol Scand* **110**:445-447.

Tracey WD, Jr., Wilson RI, Laurent G and Benzer S (2003) painless, a Drosophila gene essential for nociception. *Cell* **113**:261-273.

Twining CM, Sloane EM, Milligan ED, Chacur M, Martin D, Poole S, Marsh H, Maier SF and Watkins LR (2004) Peri-sciatic proinflammatory cytokines, reactive oxygen species, and complement induce mirror-image neuropathic pain in rats. *Pain* **110**:299-309.

Ugawa S, Ueda T, Yamamura H and Shimada S (2005) In situ hybridization evidence for the coexistence of ASIC and TRPV1 within rat single sensory neurons. *Molecular Brain Research* **136**:125-133.

Ulmann L, Hirbec H and Rassendren F (2010) P2X4 receptors mediate PGE2 release by tissue-resident macrophages and initiate inflammatory pain. *EMBO J* **29**:2290-2300.

Vallbo A, Olausson H, Wessberg J and Norrsell U (1993) A system of unmyelinated afferents for innocuous mechanoreception in the human skin. *Brain research* **628**:301-304.

van Hecke O, Torrance N and Smith BH (2013) Chronic pain epidemiology and its clinical relevance. *Br J Anaesth* **111**:13-18.

Vazquez G, Wedel BJ, Aziz O, Trebak M and Putney JW (2004) The mammalian TRPC cation channels. *Biochimica et Biophysica Acta (BBA) - Molecular Cell Research* **1742**:21-36.

Vejsada R, Paleček J, Hník P and Soukup T (1985) Postnatal development of conduction velocity and fibre size in the rat tibial nerve. International Journal of Developmental Neuroscience 3:583-595.

Vera-Portocarrero LP, Zhang ET, Ossipov MH, Xie JY, King T, Lai J and Porreca F (2006) Descending facilitation from the rostral ventromedial medulla maintains nerve injury-induced central sensitization. *Neuroscience* **140**:1311-1320.

Verge VM, Tetzlaff W, Bisby MA and Richardson PM (1990) Influence of nerve growth factor on neurofilament gene expression in mature primary sensory neurons. *The Journal of neuroscience : the official journal of the Society for Neuroscience* **10**:2018-2025.

Vilceanu D and Stucky CL (2010) TRPA1 mediates mechanical currents in the plasma membrane of mouse sensory neurons. *PloS one* **5**:e12177.

Voets T, Prenen J, Vriens J, Watanabe H, Janssens A, Wissenbach U, Bodding M, Droogmans G and Nilius B (2002) Molecular determinants of permeation through the cation channel TRPV4. *The Journal of biological chemistry* **277**:33704-33710.

Voilley N, de Weille J, Mamet J and Lazdunski M (2001) Nonsteroid anti-inflammatory drugs inhibit both the activity and the inflammation-induced expression of acid-sensing ion channels in nociceptors. *JNeurosci* **21**:8026-8033.

Vriens J, Nilius B and Voets T (2014) Peripheral thermosensation in mammals. *Nat Rev Neurosci* **15**:573-589.

Vriens J, Watanabe H, Janssens A, Droogmans G, Voets T and Nilius B (2004) Cell swelling, heat, and chemical agonists use distinct pathways for the activation of the cation channel TRPV4. *Proceedings of the National Academy of Sciences of the United States of America* **101**:396-401.

Waddell PJ, Lawson SN and McCarthy PW (1989) Conduction velocity changes along the processes of rat primary sensory neurons. *Neuroscience* **30**:577-584.

Walder RY, Rasmussen LA, Rainier JD, Light AR, Wemmie JA and Sluka KA (2010) ASIC1 and ASIC3 play different roles in the development of Hyperalgesia after inflammatory muscle injury. *The journal of pain : official journal of the American Pain Society* **11**:210-218.

Waldmann R, Bassilana F, de Weille J, Champigny G, Heurteaux C and Lazdunski M (1997a) Molecular cloning of a non-inactivating proton-gated Na+ channel specific for sensory neurons. *The Journal of biological chemistry* **272**:20975-20978.

Waldmann R, Champigny G, Bassilana F, Heurteaux C and Lazdunski M (1997b) A proton-gated cation channel involved in acid-sensing. *Nature* **386**:173-177.

Wall PD and Gutnick M (1974a) Ongoing activity in peripheral nerves: the physiology and pharmacology of impulses originating from a neuroma. *Exp Neurol* **43**:580-593.

Wall PD and Gutnick M (1974b) Properties of afferent nerve impulses originating from a neuroma. *Nature* **248**:740-743.

Wall PD and Woolf CJ (1984) Muscle but not cutaneous C-afferent input produces prolonged increases in the excitability of the flexion reflex in the rat. *JPhysiolLond* **356**:443-458.

Wang CH, Zou LJ, Zhang YL, Jiao YF and Sun JH (2010) The excitatory effects of the chemokine CCL2 on DRG somata are greater after an injury of the ganglion than after an injury of the spinal or peripheral nerve. *Neuroscience letters* **475**:48-52.

Wang S, Dai Y, Fukuoka T, Yamanaka H, Kobayashi K, Obata K, Cui X, Tominaga M and Noguchi K (2008) Phospholipase C and protein kinase A mediate bradykinin sensitization of TRPA1: a molecular mechanism of inflammatory pain. *Brain* **131**:1241-1251.

Watson CP, Deck JH, Morshead C, Van der Kooy D and Evans RJ (1991) Post-herpetic neuralgia: further post-mortem studies of cases with and without pain. *Pain* **44**:105-117.

Wedel BJ, Vazquez G, McKay RR, St JBG and Putney JW, Jr. (2003) A calmodulin/inositol 1,4,5-trisphosphate (IP3) receptor-binding region targets

TRPC3 to the plasma membrane in a calmodulin/IP3 receptor-independent process. *The Journal of biological chemistry* **278**:25758-25765.

Wei F, Vadakkan KI, Toyoda H, Wu LJ, Zhao MG, Xu H, Shum FW, Jia YH and Zhuo M (2006) Calcium calmodulin-stimulated adenylyl cyclases contribute to activation of extracellular signal-regulated kinase in spinal dorsal horn neurons in adult rats and mice. *The Journal of neuroscience : the official journal of the Society for Neuroscience* **26**:851-861.

Welk E, Leah JD and Zimmermann M (1990) Characteristics of A- and C-fibers ending in a sensory nerve neuroma in the rat. *J Neurophysiol* **63**:759-766.

Windebank AJ and Grisold W (2008) Chemotherapy-induced neuropathy. *J Peripher Nerv Syst* **13**:27-46.

Woo SH, Lukacs V, de Nooij JC, Zaytseva D, Criddle CR, Francisco A, Jessell TM, Wilkinson KA and Patapoutian A (2015) Piezo2 is the principal mechanotransduction channel for proprioception. *Nat Neurosci* **18**:1756-1762.

Woo SH, Ranade S, Weyer AD, Dubin AE, Baba Y, Qiu Z, Petrus M, Miyamoto T, Reddy K, Lumpkin EA, Stucky CL and Patapoutian A (2014) Piezo2 is required for Merkel-cell mechanotransduction. *Nature* **509**:622-626.

Woolf CJ (1983) Evidence for a central component of post-injury pain hypersensitivity. *Nature* **306**:686-688.

Woolf CJ (2011) Central sensitization: implications for the diagnosis and treatment of pain. *Pain* **152**:S2-15.

Woolf CJ, Allchorne A, Safieh-Garabedian B and Poole S (1997) Cytokines, nerve growth factor and inflammatory hyperalgesia: the contribution of tumour necrosis factor alpha. *British Journal of Pharmacology* **121**:417-424.

Wu G, Ringkamp M, Hartke TV, Murinson BB, Campbell JN, Griffin JW and Meyer RA (2001) Early onset of spontaneous activity in uninjured C-fiber nociceptors after injury to neighboring nerve fibers. *JNeurosci* **21**:RC140.

Wu G, Ringkamp M, Murinson BB, Pogatzki EM, Hartke TV, Weerahandi HM, Campbell JN, Griffin JW and Meyer RA (2002) Degeneration of myelinated efferent fibers induces spontaneous activity in uninjured C-fiber afferents. *JNeurosci* **22**:7746-7753.

Xiao WH and Bennett GJ (2008) Chemotherapy-evoked neuropathic pain: Abnormal spontaneous discharge in A-fiber and C-fiber primary afferent neurons and its suppression by acetyl-L-carnitine. *Pain* **135**:262-270.

Xie W, Strong JA, Meij JT, Zhang JM and Yu L (2005) Neuropathic pain: early spontaneous afferent activity is the trigger. *Pain* **116**:243-256.

Xie YK and Xiao WH (1990) Electrophysiological evidence for hyperalgesia in the peripheral neuropathy. *Sci China B* **33**:663-672.

Xu J, Gu H and Brennan TJ (2010) Increased sensitivity of group III and group IV afferents from incised muscle in vitro. *Pain* **151**:744-755.

Xu ZZ, Kim YH, Bang S, Zhang Y, Berta T, Wang F, Oh SB and Ji RR (2015) Inhibition of mechanical allodynia in neuropathic pain by TLR5-mediated A-fiber blockade. Nat Med 21:1326-1331.

Yamamoto K, Chiba N, Chiba T, Kambe T, Abe K, Kawakami K, Utsunomiya I and Taguchi K (2015) Transient receptor potential ankyrin 1 that is induced in

dorsal root ganglion neurons contributes to acute cold hypersensitivity after oxaliplatin administration. *Mol Pain* **11**:69.

Yan J, Wei X, Bischoff C, Edelmayer RM and Dussor G (2013) pH-evoked dural afferent signaling is mediated by ASIC3 and is sensitized by mast cell mediators. *Headache* **53**:1250-1261.

Yen YT, Tu PH, Chen CJ, Lin YW, Hsieh ST and Chen CC (2009) Role of acid-sensing ion channel 3 in sub-acute-phase inflammation. *Molecular pain* **5**:1.

Yousuf A, Klinger F, Schicker K and Boehm S (2011) Nucleotides control the excitability of sensory neurons via two P2Y receptors and a bifurcated signaling cascade. *Pain* **152**:1899-1908.

Yu L, Yang F, Luo H, Liu FY, Han JS, Xing GG and Wan Y (2008) The role of TRPV1 in different subtypes of dorsal root ganglion neurons in rat chronic inflammatory nociception induced by complete Freund's adjuvant. *Molecular pain* **4**:61.

Zhang X, Huang J and McNaughton PA (2005) NGF rapidly increases membrane expression of TRPV1 heat-gated ion channels. *Embo J* **24**:4211-4223.

Zheng H, Xiao WH and Bennett GJ (2011) Functional deficits in peripheral nerve mitochondria in rats with paclitaxel- and oxaliplatin-evoked painful peripheral neuropathy. *Experimental neurology* **232**:154-161.

Zhong J and Heumann R (1995) Lesion-induced interleukin-6 mRNA expression in rat sciatic nerve. *Annals of the New York Academy of Sciences* **762**:488-490.

Zimmermann M, Sanders K, Culp WJ and Ochoa J (1982) Responses of nerve axons and receptor endings to heat, ischemia, and algesic substances. Abnormal excitability of regenerating nerve endings, in *Abnormal Nerves and Muscles as Impulse Generators* pp 513-532, Oxford University Press, New York.

Appendices

Appendix I: Normalisation of antibody labelling in the dorsal root ganglion

For the TRPV1, TRPA1 and ASIC3 antibodies, it was noticed that there were observable differences in the labelling intensities of large diameter cell bodies between the treatment groups, which were not thought to be a result of treatment. This was due to the order the tissue was cut. DRG sections were always cut and mounted in the same order (saline > vinblastine > neuritis); reversing the cutting order resulted in the intensity of large diameter cell bodies in the saline group being greater than that of the other two groups, indicating that the later cuts sections had higher levels of background staining. As confirmation of this artefact, a series of additional experiments were performed on the L5 DRG from untreated animals (n = 3). Sections were cut and mounted on slides, which were left at room temperature. After 45 minutes, a second series of sections were cut and mounted on the same slides. The immunohistochemistry procedure (described in methods) was performed with the TRPV1 antibody. Median intensities of TRPV1 cell body labelling were increased in both small to medium and large diameter cell bodies in the later compared to the earlier cut sections (**Figures 8.1 & 8.2**). This confirmed that the artefact affected cell bodies of all diameter for the TRPV1 antibody. It was assumed that similar artefacts occurred with the other two antibodies.

Since it is the small to medium diameter cell bodies that are of interest, the intensity data from this population has been normalised to the large diameter population. It was deemed suitable to do this because there is minimal expression of the TRPV1 and TRPA1 in large diameter cell bodies under normal conditions (Amaya et al., 2003; Barabas et al., 2012; Caterina et al., 1997; Nagata et al., 2005; Story et al., 2003; Yu et al., 2008), and both vinblastine-treatment and neuritis did not effect the level of ion channel expression, as antibody labelling was always confined to single population (one cluster) of cells. It was not possible to follow this same method of normalisation for ASIC3 as there were a proportion of large diameter cell bodies which clearly had positive labelling of the ion channel, in agreement with previous findings (Molliver et al., 2005). The two populations (deemed ASIC3 positive and ASIC3 negative) of large diameter cell body cells were separated by the median of the entire population. A median of the larger diameter cell bodies that were not

deemed to express ASIC3 (< median of the entire population) was calculated, and used to normalise the intensity of small and medium diameter cell bodies.

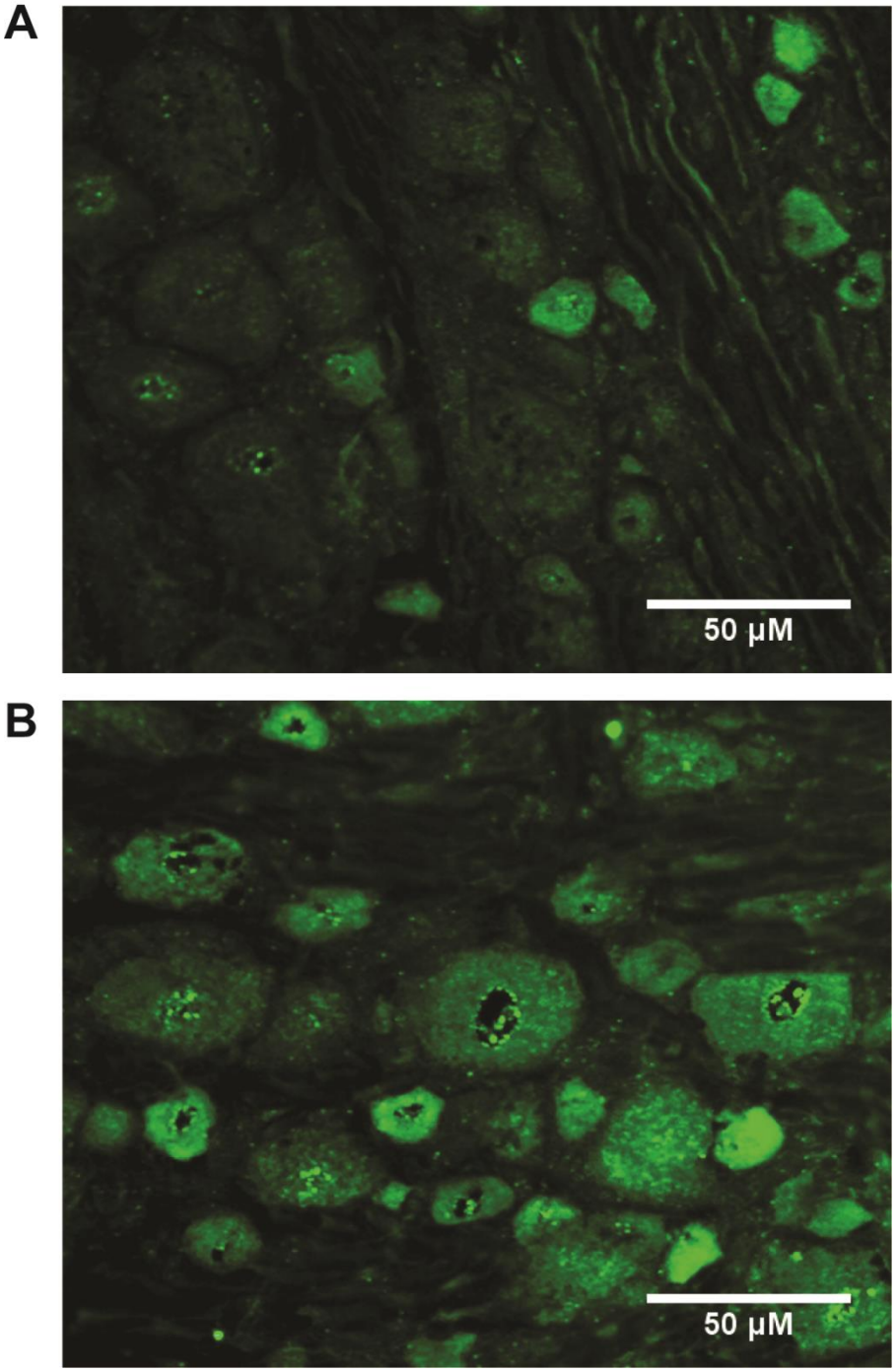

Figure 8.1 Differences in the labelling of TRPV1 in the untreated dorsal route ganglion (DRG) of an untreated animal. TRPV1 labelling in the DRG of an untreated animal cut first (A) and that of the same DRG (B) which was cut 45 minutes later. The amount of time in which a section is sat unfixed upon a slide affects the amount of non-specific labelling of TRPV1.

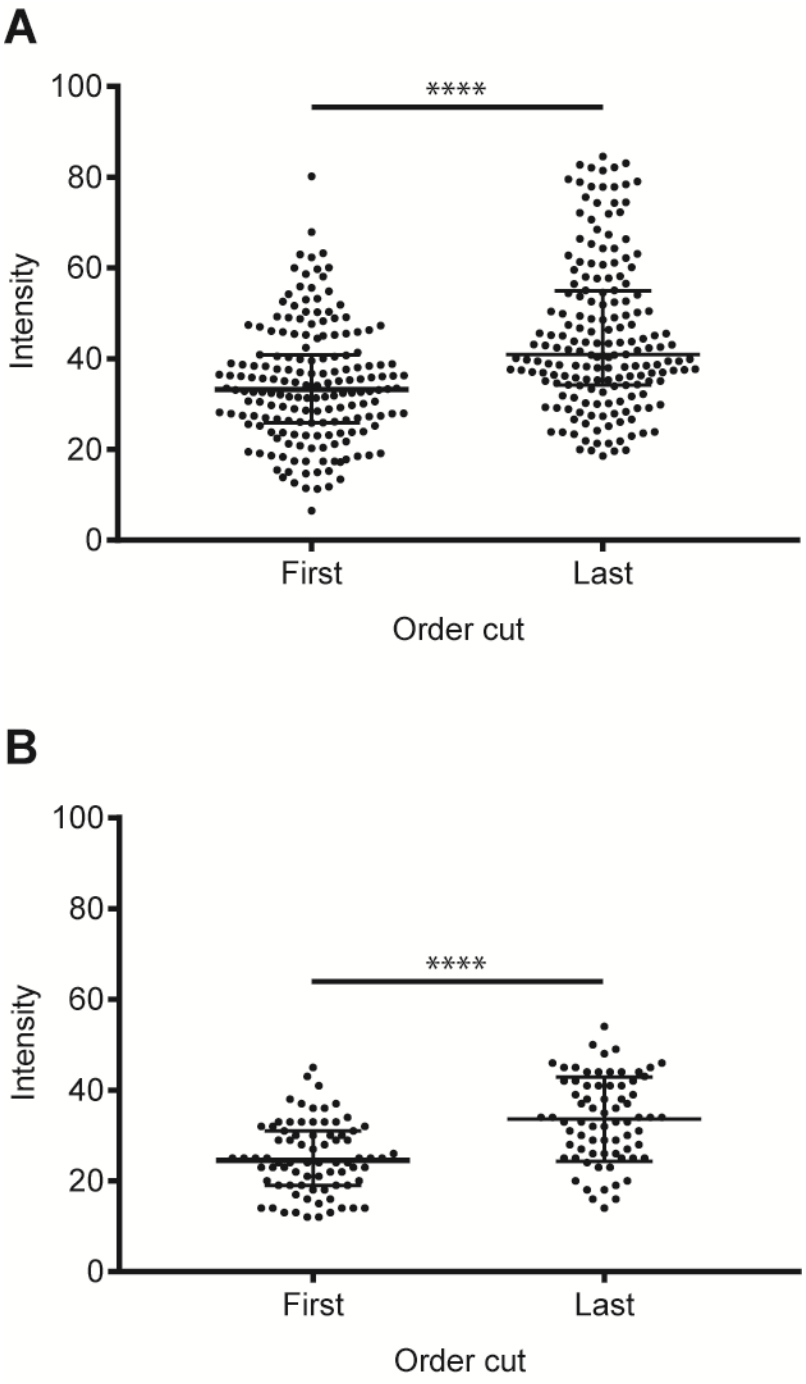

Figure 8.2 Effect of the cutting order on the labelling of TRPV1 in cell bodies of the dorsal route ganglion (DRG). There was a significant increase in the intensity of TRPV1 labelling in small to medium and large diameter cell bodies (**** p <0.0001; Mann Whitney test)

Appendix II: Antibody labelling profiles

The anti-TRPV1 antibody used in this study labelled small to medium diameter neuronal cell bodies in the L5 DRG, axons in the sciatic nerve and the walls of blood vessels, which is consistent with the localisation of TRPV1 (Bernardini et al., 2004; Caterina et al., 1997; Cavanaugh et al., 2011; Guo et al., 1999; Kark et al., 2008; Lizanecz et al., 2006; Tominaga et al., 1998; Yu et al., 2008).

The anti-TRPA1 antibody used in this study labelled small to medium diameter neuronal cell bodies in the L5 DRG and the walls of blood vessels, which is consistent with the localisation of TRPA1 (Aubdool et al., 2014; Bautista et al., 2006; Earley et al., 2009; Story et al., 2003). TRPA1 labelling was also found to be present in what appeared to be satellite cells in the DRG, which was an unexpected finding. In previous studies, TRPA1 does not appear to label satellite cells (Bautista et al., 2005; Story et al., 2003).

The anti-ASIC3 antibody used in this study labelled small, medium and large diameter neuronal cell bodies in the L5 DRG, the sciatic nerve and the walls of blood vessels, which is consistent with the localisation of ASIC3. (Alvarez de la Rosa et al., 2002; Molliver et al., 2005; Price et al., 2001; Ugawa et al., 2005; Yen et al., 2009).

Appendix III: Publications

Paper published in Journal of Neurophysiology, 2018.

Satkeviciute I, Goodwin G, Bove GM and Dilley A (2018) The time course of ongoing activity during neuritis and following axonal transport disruption. *Journal of neurophysiology.*

Local nerve inflammation (neuritis) leads to ongoing activity and axonal mechanical sensitivity (AMS) along intact nociceptor axons, and disrupts axonal transport. This phenomenon forms the most feasible cause of radiating pain, such as sciatica. We have previously shown that axonal transport disruption without inflammation or degeneration also leads to AMS, but does not cause ongoing activity at the time point when AMS occurs, despite causing cutaneous hypersensitivity. However, there have been no systematic studies of ongoing activity during neuritis or non-inflammatory axonal transport disruption. In this study, we present the time course of ongoing activity from primary sensory neurons following neuritis and vinblastine-induced axonal transport disruption. Whereas 24% of C/slow Aδ-fiber neurons had ongoing activity during neuritis, few (<10%) A- and C-fiber neurons showed ongoing activity 1-15 days following vinblastine treatment. In contrast, AMS increased transiently at the vinblastine treatment site, peaking on day 4-5 (28% of C/slow Aδ-fiber neurons) and resolved by day 15. Conduction velocities were slowed in all groups. In summary, the disruption of axonal transport without inflammation does not lead to ongoing activity in sensory neurons, including nociceptors, but does cause a rapid and transient development of AMS. Since it is proposed that AMS underlies mechanically-induced radiating pain, and a transient disruption of axonal transport (as previously reported) leads to transient AMS, it follows that processes that disrupt axonal transport, such as neuritis, must persist to maintain AMS and the associated symptoms.